Mechanisms of graft-versus-host-disease: a role for Langerhans cells in regulating skin GVHD

By

Thomas Joseph Conlan

Thesis submitted for the degree of Doctor of Philosophy at

University College London

Research Department of Haematology

Cancer Institute

Royal Free Campus

September 2014

Declaration

I, Thomas Joseph Conlan confirm that the work presented in this thesis is my own. Where information has been derived from other sources, I confirm that this has been indicated in the thesis.

The microarray study was carried out in conjunction with Dr Pedro Ascensao Santos E Sousa. I designed and executed the experiments, while Dr Sousa kindly analysed and annotated the data.

Signed: Date:

Abstract

Allogeneic bone marrow transplantation (BMT) is an important and commonly used treatment for a variety of haematological malignancies. Central to the therapeutic benefits of allogeneic BMT is the role of donor T cells, which mediate a potent anti-neoplastic effect against tumours in the recipient. However, the presence of donor T cells is also tightly associated with the development of the life-threatening condition graft-versus-host-disease (GVHD), a disorder where alloreactive donor T cells recognise the recipient as 'non-self' and elicit a potent anti-host immune response. Antigen presenting cells (APC) are critical to the induction of acute GVHD. However, recent studies have questioned whether any particular subset of APC has a non-redundant role in the priming of an alloreactive donor T cell response.

One of the most commonly affected organs in acute GVHD is the skin, which contains a diverse array of professional APC subsets capable of initiating potent immune responses. One such subset is Langerhans cells (LC), a population of radioresistant dendritic cells (DC) that form a dense interlacing network within the epidermis. Using an *in vivo* mouse model of acute GVHD where host LC can be conditionally depleted, LC were found to play an important role in the development of acute GVHD in the skin. The depletion of host LC significantly reduced the severity of cutaneous GVHD that developed following allogeneic BMT. Host LC were required *in situ* in the epidermis for both the accumulation and function of alloreactive donor CD8 T cells in the skin. A role for host Langerin^{+} dDC, a population shown to be critical for CD8-mediated T cell responses in the skin, was also ruled out. These findings describe a novel role for host LC in the regulation of cutaneous GVHD *in situ,* which could identify a novel target for organ specific immunosuppression following allogeneic BMT.

Table of Contents

List of Figures

List of Tables

Acknowledgements

First and foremost, I would like to thank my supervisors Professor Ronjon Chakraverty and Dr Clare Bennett for their guidance and support throughout the project. I am very grateful to have had the opportunity to work as part of their group. They have always been receptive to my ideas and suggestions, while keeping my bad ones in check.

I would like to particularly acknowledge Dr Pedro Sousa for all his assistance throughout the project. It was greatly appreciated. My gratitude goes out to everyone in the Chakraverty/Bennett group, especially: Lei Zhang, Hugh Goold and Cara Lomas for their help with experiments; Farnaz Fallah-Arani and Barry Flutter for their valued guidance; Janani Sivakumaran, Pedro Velica, James Griffin, Sophie Ward and Alastair Hotblack for their friendship and support during the project; and finally Mathias Zech for the very competitive games of squash.

I would also like to thank my collaborators Dr Elisa Gomez Perdiguero, Dr Terry Means and Professor Frederic Geissman for their assistance during my project. In particular Elisa for her continued patience helping me to sort cells from the skin. I am also grateful to the Medical Research Council for funding my PhD through the “Bench to Bedside” program.

I would like to give my most heartfelt thank you to Nicola who has been with me every step of the way. Nicola has always been there, through the late nights in the lab to the late nights in writing this thesis up. She really has been amazing. Finally, I would like to thank my mother, for always believing in me. Providing support and encouragement along the way.

Abbreviation List

Acronym	Definition
AEMT	Antigen Exposed MataHari T cells
ALL	Acute Lymphoblastic Leukaemia
AML	Acute Myeloid Leukaemia
ANOVA	Analysis of Variance
APC	Antigen Presenting Cell
ATP	Adenosine-5'-triphosphate
β_2m	β_2-microglobulin
BL/6	C57BL/6
BM	Bone Marrow
BMT	Bone Marrow Transplantation
C	Celsius
CD	Cluster of differentiation
cDC	Conventional Dendritic Cell
CHS	Contact Hypersensitivity
CML	Chronic Myeloid Leukaemia
CSA	Ciclosporin
CTL	Cytotoxic T Lymphocyte
D	Dimension
DAMPs	Danger-associated molecular patterns
DC	Dendritic Cell
dDC	Dermal Dendritic Cell
DISC	Death-inducing signalling complex
DLI	Donor Leukocyte Infusion
DT	Diphtheria Toxin
DTR	Diphtheria Toxin Receptor
DLA	Dog Leukocyte Antigen
dLN	Draining Lymph Node
EGFP	Enhanced Green Fluorescent Protein
EpCAM	Epithelial Cell Adhesion Molecule
FACS	Fluorescence-activated Cell Sorting
FBS	Fetal Bovine Serum
FDR	False Discovery Rate
Flt3	fms-like Tyrosine Kinase 3 Ligand
FSC	Forward Scatter
GSEA	Gene Set Enrichment Analysis
Gy	Gray (SI Unit)
GVHD	Graft-versus-host-disease
GVL	Graft-versus-leukemia
H	Histocompatibility
hr	Hour
HBV	Hepatitis B Virus
HEV	High Endothelial Venule

HLA	Human Leukocyte Antigen
HSCT	Haematopoietic Stem Cell Transplantation
HSV	Herpes Simplex Virus
IA	Influenza A
i.d.	Intradermal
IL	Interleukin
Imiq	Imiquimod
i.n.	Intranasally
iNOS	Inducible Nitric Oxide Synthase
i.p.	Intraperitoneal
i.v.	Intravenous
KO	Knockout
LP	Lamina Propria
LC	Langerhans Cell
LCMV	Lymphocytic Choriomeningitis Virus
LFC	Linear Fold Change
LN	Lymph Node
MC	Mixed Chimera
Mh	MataHari
MHC	Major Histocompatibility Complex
ml	Millilitre
MSD	Matched Sibling Donor
ng	Nanogram
NK	Natural Killer
NLR	Nod-like receptor
OVA	Ovalbumin
PAMPs	Pathogen-associated molecular patterns
PBMC	Peripheral Blood Mononuclear Cells
PBS	Phosphate Buffered Saline
PBSC	Peripheral Blood Stem Cells
PP	Peyer's Patches
PI	Propidium Iodide
pLN	Peripheral Lymph Nodes
PRR	Pattern Recognition Receptors
PSGL	P-selecting glycoprotein ligand
PVCA	Principal Variance Component Analysis
qPCR	Quantitative Polymerase Chain Reaction
R	Receptor
rDC	Respiratory DC
RLR	Rig-I-like receptors
RMA	Robust multi-array average
SC	Splenocytes
SSC	Side Scatter
Siglec	Sialic acid–binding immunoglobulin-like lectin
TBI	Total Body Irradiation
TCD	T cell depleted

TCR	T cell receptor
Teff	Effector T cells
Tg	Transgenic
TLR	Toll-like-receptor
TNF	Tumor necrosis factor
TRAIL	TNF-related apoptosis inducing ligand
Treg	Regulatory T cell
Trm	T resident memory
TRM	Transplant Related Mortality
TWEAK	TNF-like weak inducers of apoptosis
U	Units
vs	Versus

1 Introduction

1.1 Bone marrow transplantation as a therapy in the clinic

1.1.1 Autologous versus allogeneic BMT in the clinic today

Bone marrow transplantation (BMT), or haematopoietic stem cell transplantation (HSCT), is a commonly used treatment in the clinic whereby the haematopoietic system of a patient is reconstituted (or replaced) by the intravenous (i.v.) injection of *ex vivo* haematopoietic stem cells derived from a suitable donor. Used to treat a variety of congenital and acquired haematological conditions (Figure 1), there are two forms of transplant predominantly used in the clinic today: autologous (self) and allogeneic (non-self) transplants[1].

Autologous transplantation involves the collection and cryopreservation of a patient's own stem cells before they receive myeloablative treatments such as high-dose chemotherapy or radiation. The harvested stem cells are subsequently infused back into the patient to reconstitute haematopoiesis. It accounts for around 60% of all transplants in the clinic and is mainly used to treat haematological malignancies that are sensitive to treatment, with multiple myeloma and non-Hodgkin lymphoma the most common indications for an autologous transplant[1]. The primary advantage of this form of transplant is the absence of any form of alloimmune responses against the recipient as the cells come from the patient. There is no need for immunosuppression or histocompatibility matching. However, this can also be a disadvantage in some instances as autologous transplants rely solely on the conditioning regime and chemotherapy as a therapeutic modality, limiting its use to certain clinical indications. In addition, neoplastic cells can also be collected when the stem cells are harvested, causing patients to relapse post transplant[2].

Allogeneic transplantation differs in that it involves the transplant of haematopoietic stem cells from a healthy donor other than the recipient (Figure 2). The use of allogeneic BMT as a therapy was initially developed for two reasons. Firstly, it provided clinicians with a way to treat patients with congenital or acquired diseases that affect the function of bone marrow or bone marrow derived cells, by replacing the abnormal haematopoietic system of the patient with one from a healthy donor. Secondly, it allowed the delivery of myeloablative doses of radiation and/or chemotherapy to treat aggressive haematological malignancies while harnessing the potent anti-neoplastic graft-versus-leukemia (GVL) effect, associated with lower rates of malignant relapse[2].

Since the first allogeneic BMT in 1956[3], improvements in our understanding of the biology of transplantation has seen the number of transplants rapidly rise. Today, over 60,000 transplants are carried out worldwide each year as a frontline treatment for a variety of life-threatening conditions that were previously considered incurable. However, significant challenges remain as BMT continues to be associated with a high rate of morbidity and mortality in the clinic with disease relapse, infection due to pancytopenia and the development of graft-versus-host-disease (GVHD) remaining problematic (Figure 3). To gain further insight into the challenges faced in the clinic today, we will first explore the series of observations and discoveries over the last 5 decades that led to the development of the treatments we see today.

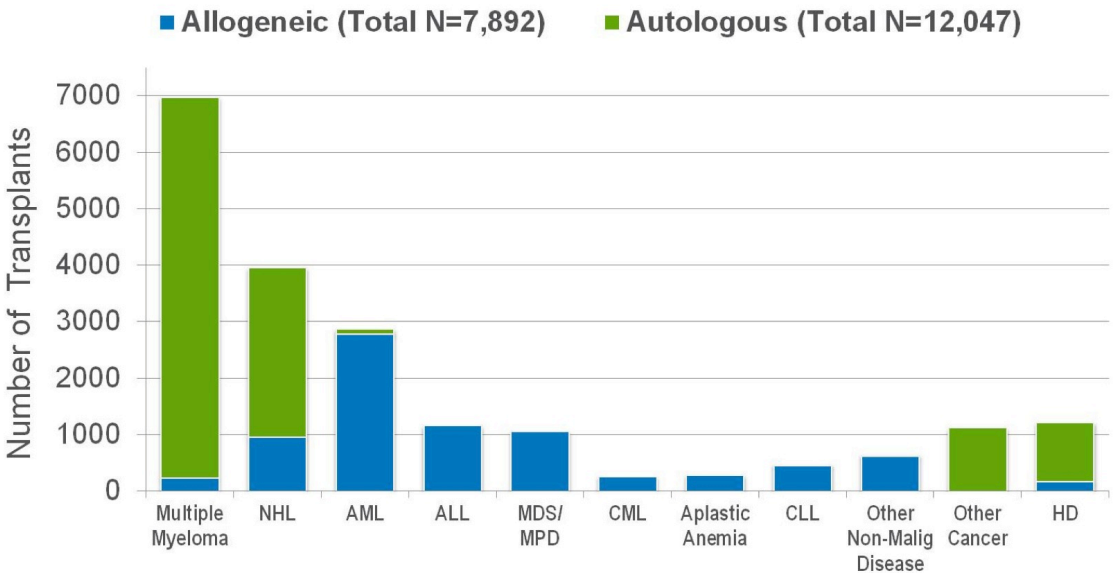

Figure 1: Clinical indications for HSCT in the United States in 2011. Autologous transplants accounted for around 60% of all transplants in the US and were primarily used to treat multiple myeloma and non-Hodgkin lymphoma (NHL). Allogeneic transplants were mainly used to treat acute myeloid leukemia (AML) and acute lymphoblastic leukaemia (ALL). Reprinted with permission from the Center for International Bone Marrow Transplant Research (www.cibmtr.org)[1].

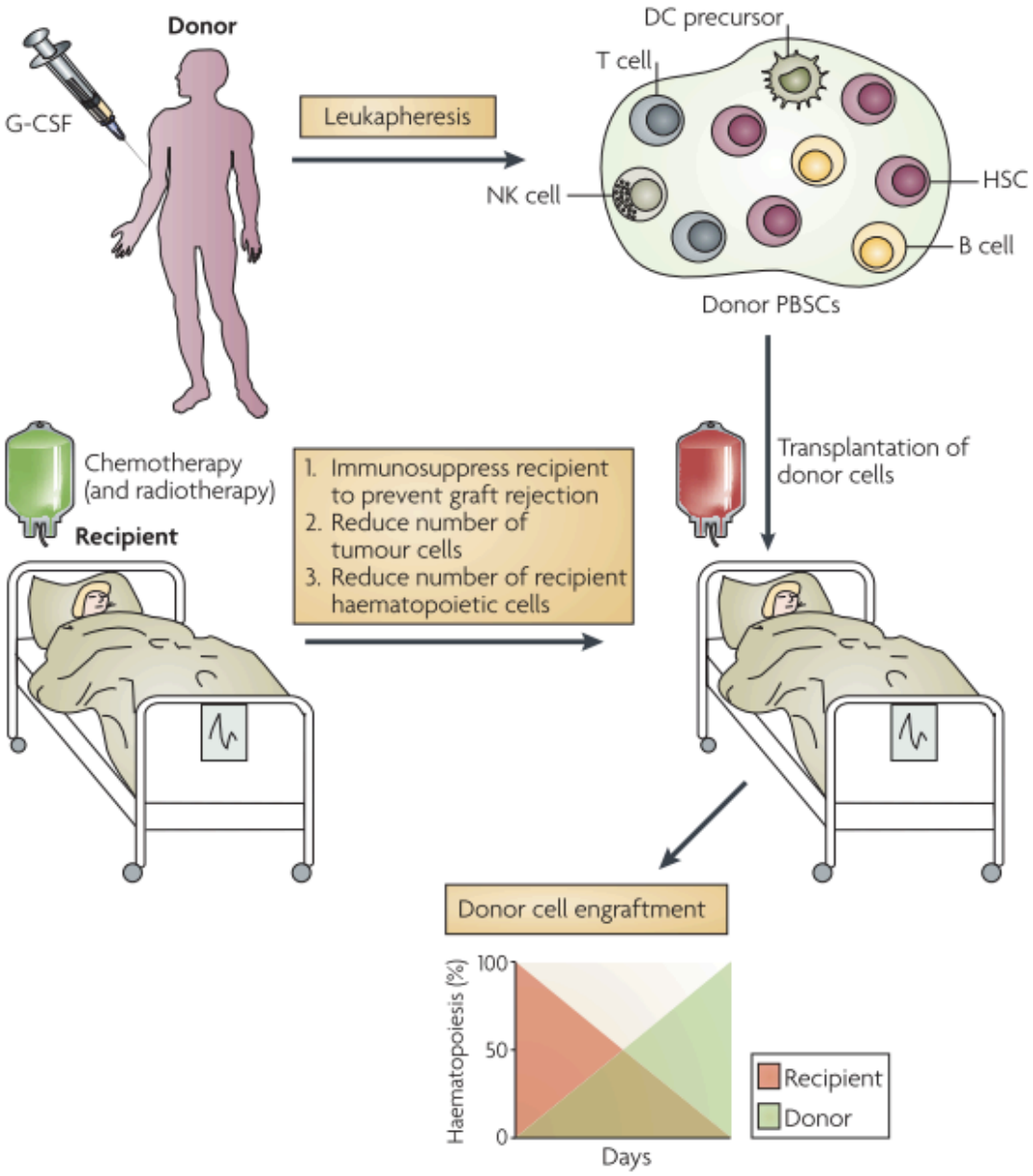

Figure 2: Overview of an allogeneic haematopoietic stem cell transplant in the clinic today. A healthy donor, matched for histocompatibility, is injected with granulocyte colony-stimulating factor to stimulate the bone marrow to release stem cells into the peripheral blood. These cells are then harvested by leukapheresis. The recipient is conditioned with chemotherapy and/or radiotherapy to enhance stem cell engraftment, treat the haematological malignancy (if present) and to create a niche for the newly grafted haematopoietic stem cells. The recipient is then transfused with donor peripheral blood mononuclear cells (PBMCs) where the donor cells engraft over a period of time replacing the recipients own haematopoietic system. Reprinted with permission from the Nature Publishing Group[4].

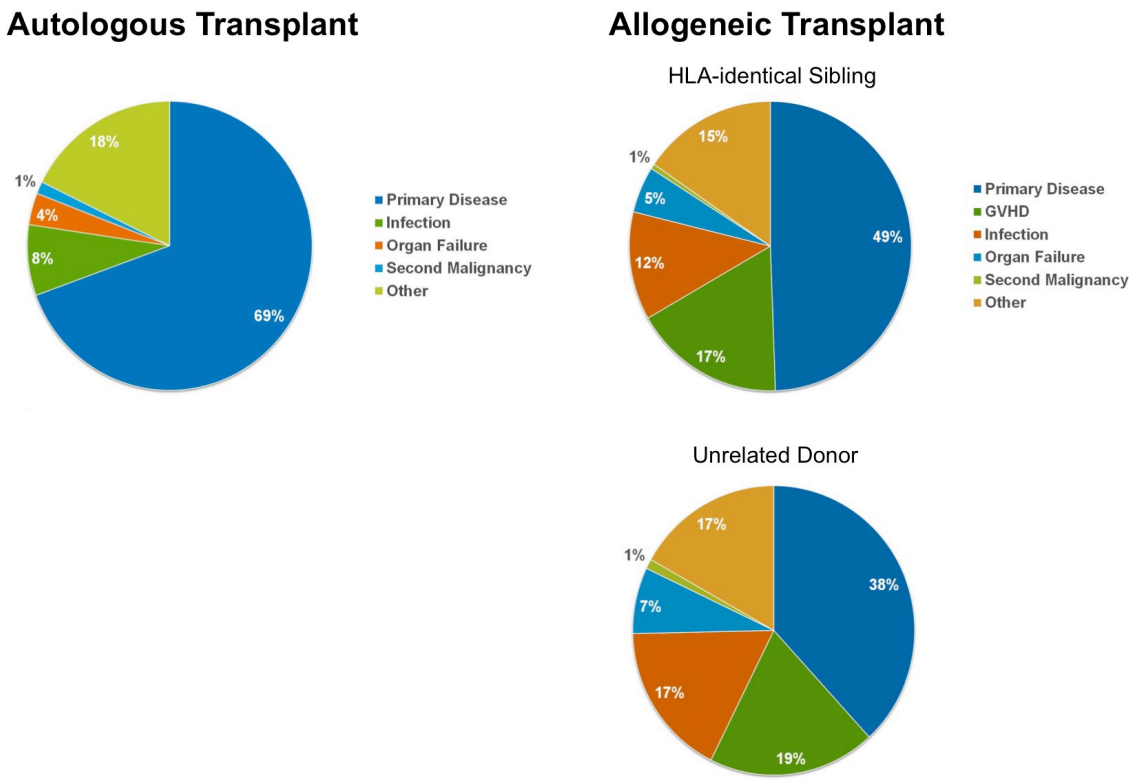

Figure 3: Transplant-related mortality between 2010-2011. For both autologous and allogeneic transplants, disease relapse remains the primary cause of mortality in the clinic. This is particularly problematic in autologous BMT, accounting for 70% of transplant-related mortality (TRM). The development of GVHD remains a major problem for allogeneic BMT using grafts from HLA-matched sibling and unrelated donors (HLA allelic identity at the HLA-A, HLA-B, HLA-C and HLA-ADRB1 loci, 8/8 match[5]) accounting for 17% and 19% of TRM respectively. Infection is also a major cause of mortality in the clinic. The type of infection is usually related to the time after transplant (pre-engraftment and post-engraftment). Infections commonly seen after BMT include the bacteria *Pseudomonas aeruginosa* and *Costridium difficile,* fungal species such as *Aspergillus* and *Candida* and viral infections with cytomegalovirus and Epstein-Barr virus. Reprinted with permission from the Center for International Bone Marrow Transplant Research (www.cibmtr.org)[1].

1.1.2 The dawn of the haematopoietic stem cell

The concept of a hematopoietic stem cell capable of reconstituting haematopoiesis *in vivo* dates back to the 1940's when the US government allocated substantial funds to counter the effects of high-dose radiation exposure in humans, in particular bone marrow failure, after the detonation of nuclear weapons in Japan[6]. This surge of research led to the landmark observation by Jacobsen and colleagues in 1949, that mice could be protected from the lethal effects of ionizing radiation by shielding their spleens with lead[7]. Following on from his initial observations, Jacobsen demonstrated that mice could also be rescued from the lethal effects of radiation by the intraperitoneal injection of splenocytes (SC) from healthy donors immediately after radiation exposure[8]. This led to the belief by many investigators at the time of the 'humoral' hypothesis; that an as yet unidentified "substance of non-cellular nature" in the spleen was responsible for stimulating recovery or that a toxin produced upon exposure to radiation was somehow neutralised by the shielded spleen (Figure 4)[9].

However, doubts surrounding the existence of a 'humoral' factor in the spleen soon began to emerge in the early 1950's when Lorenz and colleagues demonstrated that protection against radiation induced bone marrow aplasia in mice and guinea pigs could also be conferred by the infusion of bone marrow cells from a healthy donor[10]. Support for a 'cellular hypothesis' gained momentum when Main and Prehn observed that skin grafts from different strains survived indefinitely on allogeneic chimeras that received marrow from the corresponding strain[11]. Shortly thereafter, the 'humoral hypothesis' was replaced by the 'cellular hypothesis' when firm evidence began to emerge from a number of studies that protection from radiation lethality was mediated entirely by haematopoietic stem cells found in the bone marrow[6,12,13]. In one prominent study, Ford et al. were able to demonstrate, using cytogenetically marked chromosomes in donor bone marrow, that recovery of the hematopoietic system in

lethally irradiated mice was entirely derived from donor bone marrow, thus confirming the 'cellular hypothesis'[12].

Taken together, the idea that the haematopoietic system could be destroyed using ionizing radiation and subsequently reconstituted using pluripotent haematopoietic stem cells excited scientists and clinicians alike for its potential both in the lab and as a therapy in the clinic. It became possible for the first time to remove an abnormal haematopoietic system or cure patients with bone marrow aplasia, replacing diseased or dying bone marrow with a haematopoietic system from a healthy donor. It also provided oncologists with an opportunity to increase the dose of cytotoxic anti-cancer drugs beyond their normal non-myeloablative range, increasing their potential efficacy against tumour cells.

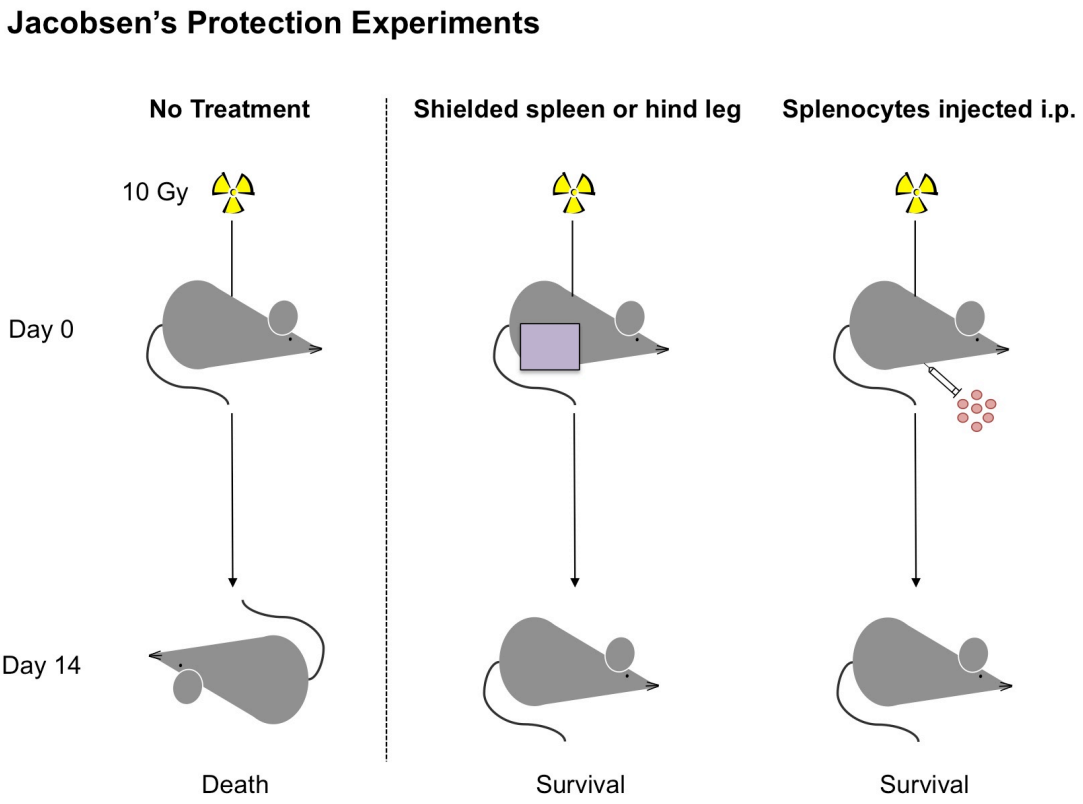

Figure 4: Summary of Jacobsen's observations from his radiation protection experiments. CF-1 mice lethally irradiated with 10 Gy would die from bone marrow aplasia between 7 and 14 days after radiation exposure. However, if either the spleen or hind leg of CF-1 mice was shielded from x-rays using lead, a significant cohort of mice would survive. Similarly, if CF-1 mice exposed to x-rays were injected with splenocytes from a healthy CF-1 donor immediately afterwards, a significant cohort would survive. These experiments led to the widespread adoption of the 'humoral hypothesis' at the time[9].

1.1.3 First steps into the clinic

Despite promising results in mouse models, the initial use of BMT as a therapy in the clinic was largely disappointing with allograft failure, infection due to leukopenia and disease relapse hampering efforts[14].

First attempted by E Donnall Thomas in the United States in 1956, 5 adult patients with end stage malignancies were transplanted with allogeneic (non-self) bone marrow derived from foetuses and adults. From a therapeutic standpoint, the results were disastrous with all patients dying a short time later from either allograft failure or a relapse of leukemia. However, the study did prove that high doses of donor bone marrow prepared properly could be safely transfused into humans, providing clinicians with a baseline for future studies[3].

By 1959, a number of new studies were published in patients with leukemia and victims of radiation exposure yielding only slightly better results[15–17]. Following on from their initial work, Thomas and colleagues treated two patients with acute lymphoblastic leukemia (ALL) with a lethal dose of total body irradiation (TBI) and subsequently transplanted them with bone marrow from identical twin siblings (syngeneic transplant)[15]. Although both patients died after their leukemia relapsed a number of months later, it was the first reported case where patients receiving a lethal dose of radiation showed prompt clinical and haematological recovery upon transplantation, validating the observations made in mice. More importantly, it also indicated that TBI alone would not be sufficient to destroy all leukemic cells and future treatments would need to be developed in combination with chemotherapy[15]. In another study of note published in 1959, McGovern et al. tried a different approach. Using cryopreserved stem cells harvested from an ALL patient in remission, they described the first instant of an autologous (self) transplant in humans, transplanting the harvested stem cells back into the patient after a myeloablative conditioning regime[16]. Despite the patient going into remission for a second time, the leukemia relapsed and the patient died.

In addition, in the absence of any detailed knowledge of histocompatibility for human leukocyte antigens (HLA), a lethal and often fatal new side effect began to emerge in patients shortly after the successful engraftment of a donor haematopoietic system. They developed a painful maculopapular skin rash, severe diarrhoea and jaundice in what became known as 'secondary syndrome' at the time[17]. The potential for a graft-versus-host response after BMT was first described by Barnes and Loutit in mice in 1957[18]. They noted that lethally irradiated mice transfused with bone marrow from a different strain would survive the initial radiation induced bone marrow aplasia (primary disease) but develop a lethal and debilitating 'secondary disease' that caused weight loss and diarrhoea 2-3 weeks after transplant (Figure 5). For a number of years it was unclear whether this 'secondary disease' was a host-versus-graft or a graft-versus-host response until van Bekkum demonstrated that the severity of disease was directly related to the number of splenic lymphocytes grafted, providing firm evidence that cells from the donor graft were mounting an immune response against the host[19]. Similarly, when donor lymphocytes were depleted from the graft, mice failed to develop 'secondary disease' across major histocompatibility complex-mismatched (MHC-mismatched) donor-recipient combinations. Thus 'secondary disease' became known as graft-versus-host-disease (GVHD), and remains a major cause of morbidity and mortality in the clinic to this day.

Despite the initial promise of BMT as a therapy in the clinic, enthusiasm for the therapy had waned tremendously by the mid-1960s[20]. The number of transplants performed sharply declined as clinicians realised the treatment was simply not working. In 1967, the concept of an allogeneic transplant in the clinic was declared dead when van Bekkum and de Vries noted that "the clinical applications were undertaken too soon, most of them before even the minimum of basic knowledge required to bridge the gap between mouse and patient had been obtained"[21]. This was brought to the fore in 1970 when Bortin published a report reviewing the outcome of 203 transplants between

1958-1968[22]. Out of 203 patients, 125 suffered from allograft failure, 49 developed GVHD and only 11 developed any kind of stable engraftment[22,23]. However, the most striking aspect of the report was that by the time it was published only 3 out of the 203 patients remained alive[23].

Barnes and Loutit: ‘Secondary Disease’

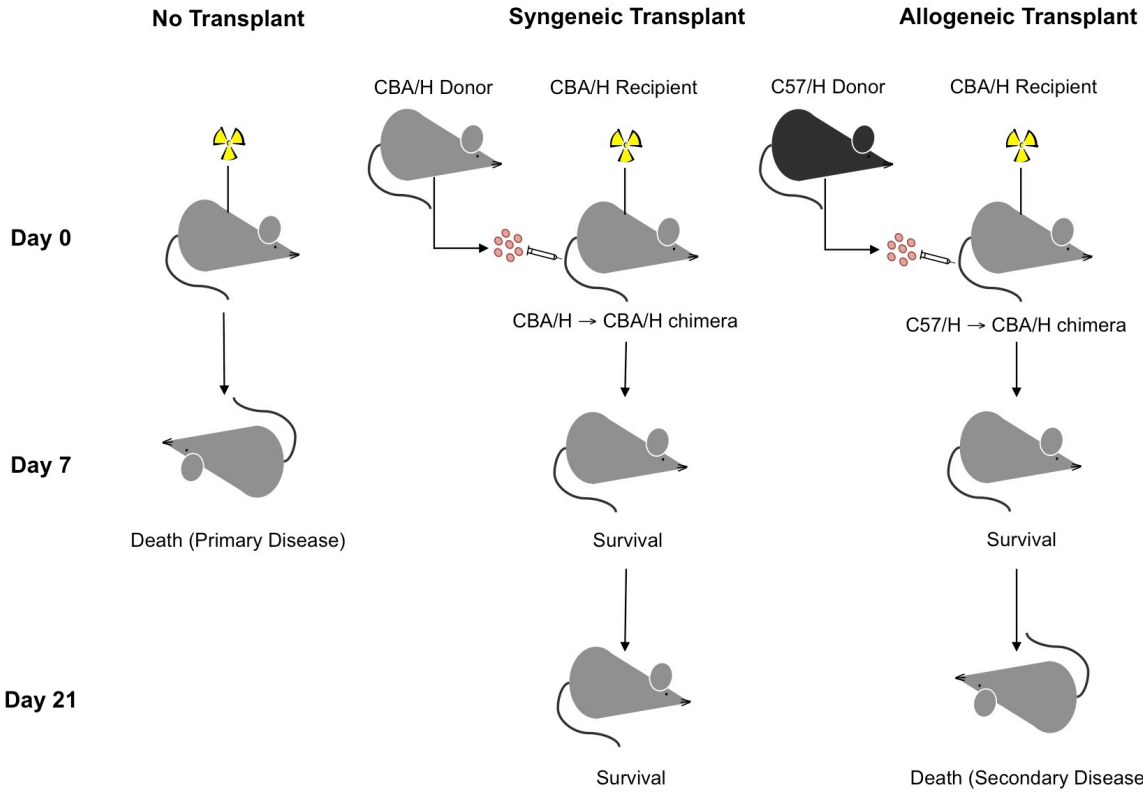

Figure 5: The infusion of bone marrow from an allogeneic donor after lethal irradiation causes a lethal and debilitating ‘secondary disease’. CBA/H mice were lethally irradiated with 10 Gy and reconstituted with bone marrow from the femora of either CBA/H (syngeneic) or C57/H (allogeneic) mice on the same day. As a control, a cohort of irradiated mice received no bone marrow. After 7 days, all mice that received no bone marrow died from bone marrow aplasia (primary disease). All mice that received bone marrow from either CBA/H or C57/H donors survived. Between 2-3 weeks after transplant, recipients that received bone marrow from C57/H donors began to develop a ‘secondary disease’ of wasting and diarrhoea. By day 21, all recipients of C57/H bone marrow had died. No evidence of ‘secondary disease’ was detected in recipients that received CBA/H bone marrow.

1.1.4 Progress in the lab and the second phase of clinical transplantation

Parallel to the problems faced in the clinic, progress continued to be made in the lab with donor selection, the development of high-dose conditioning regimes and the control of GVHD through immunosuppression becoming areas of intense research[23,24].

One of key reasons that the findings in the lab initially failed to translate into the clinic was the complete lack of understanding at the time of the immunological mechanisms underpinning graft rejection and GVHD. Much of the research to date had focused on transplantation models using highly inbred mice, which did not require histocompatibility matching[23]. This combined with the observation that graft-versus-host responses were incomparably more severe in humans than rodents after transplant led to the growing appreciation of the role genetic factors played in transplantation[21].

The widespread availability of many different inbred strains of mice permitted the fundamental genetic basis of transplantation to be elucidated[14]. By the late 1950's, it became clear that the severity of GVHD in mice after transplantation was controlled by genetic factors and that these in turn were governed by immunological responses driven by T cells to differences in the major histocompatibility complex (MHC)[25,26]. Although research using mouse models had been critical in elucidating the fundamental principles of transplantation, a more suitable preclinical model with greater genetic diversity needed to be identified. Dogs in particular appeared to be especially suitable, owing to their outbred nature, wide genetic diversity, large litter size and short gestation period[27].

Adapted from the MHC system in mice, a method to type MHC antigens in dogs, known as dog leukocyte antigen (DLA), was developed[28]. This allowed studies of donor-recipient combinations that were matched or mismatched for DLA antigens to be investigated. Early studies in dogs quickly highlighted the critical importance of DLA-typing for successfully transplantation, when it was found that recipients receiving bone

marrow from DLA-matched donors survived significantly longer with less GVHD than their DLA-mismatched donor-recipient counterparts[29]. Furthermore, while GVHD had already been described across MHC-mismatched transplant models in mice and unrelated primates, studies in dogs showed for the first time that mismatches across minor histocompatibility (H) antigens was sufficient to induce GVHD. This emphasised the need to develop effective immunosuppressive drug regimes[23,29].

This led to the development and widespread use of the anti-metabolite methotrexate. Using methotrexate, which suppresses T cell replication, researchers were able to successfully suppress GVHD in both mice and dogs[30–32]. Furthermore, long-term immunity in the animal was not compromised as it was found that the immunosuppressive therapy could frequently be discontinued after 3-6 months with the establishment of graft/host tolerance[23,31].

Further work in pre-clinical models saw the development of high-dose conditioning regimes, incorporating the use of high dose TBI with chemotherapy agents such as the alkylating agent cyclophosphamide. This acted to not only kill cancerous cells but also to suppress the host's own immune system, decreasing the chances of graft rejection[20,33–35].

The advances in our understanding of the MHC system in dogs, development of immunosuppressant's to reduce GVHD and the refinement of high-dose conditioning regimes in preclinical animal models renewed optimism for the use of BMT in the clinic and brought about the second phase of human trials.

1.1.5 The second phase of clinical transplantation

By the 1970's, the second phase of human trails using allogeneic BMT from HLA-matched sibling donors was well underway in patients with immunodeficiency diseases such as severe combined immunodeficiency (SCID), aplastic anemia and advanced leukemia/lymphoma[20].

With the discovery and characterisation of the MHC complex in humans, human leukocyte antigen (HLA), allogeneic transplantation in the clinic became feasible[36]. To account for differences in human leukocyte antigen (HLA), mixed lymphocyte cultures (MLC) were used to select donors, with weak responses *in vitro* being a good predictor of donor suitability[24,37].

Rapid advancements were also made in our understanding of the clinical management of transplant patients. Improvements in blood and platelet transfusions, the use of novel antibiotics and antifungal medications reduced the complications associated with pancytopenia and the intense conditioning regime[6].

By 1977, it was clear that the second phase of transplantation was achieving far greater success in the clinic when E Donnal Thomas and colleagues published articles reviewing the outcome of patients undergoing transplantation with advanced leukemia and aplastic anemia in which conventional treatment had failed. Despite a high transplant-related-mortality (TRM), long-term disease free survival was for the first time being achieved in the clinic[20,38,39]. Importantly, Thomas also noted in these studies that patients in good general condition at the time of transplant had significantly better outcomes than those in poorer conditions and that patients with advanced leukemia tended to have higher relapse rates (75%) regardless of the conditioning regime[20,39].

The 1980's saw a rapid increase in the use of BMT (Figure 6), which can be attributed to two independent but closely linked developments[6]. The first and perhaps the most important of these moves was the use of BMT at a much earlier stage in the treatment

plan based on Thomas's observations. When BMT began to be used to treat patients with acute leukemia in the first complete remission, survival rates dramatically increased[40,41]. Similar increases in survival were also seen when BMT was used to treat patients with chronic myeloid leukemia (CML) in the first chronic stage[42]. BMT was no longer a treatment of last resort but a curative therapy, capable of treating malignancies like CML that were once thought incurable.

The second was the development and use of the T cell activation inhibitor cyclosporine along with methotrexate. Although acute GVHD was managed well by the use of methotrexate, the development of chronic GVHD remained a problem, occurring in over 50% of patients receiving HLA-matched grafts and methotrexate[23,38]. The adoption of cyclosporine and tacrolimus into the treatment regime saw a reduction in GVHD and rapid improvement to patient survival rates[23,43,44].

An unexpected observation during clinical GVHD was the realisation that cells from the donor graft could also have potent anti-tumour properties. The potential of a graft-versus-leukemia (GVL) effect from cells in the donor graft was first noted by Barnes and Loutit in 1957, when mice transplanted with allogeneic bone marrow were found to eradicate leukaemia cells (Figure 7)[18]. However, it's potential in the clinic was first appreciated in 1979 when it was noted that onset of GVHD greatly reduced the chance that a patient's leukemia would relapse[45]. Conversely, when patients were transplanted with allogeneic grafts depleted of T cells or grafts from identical twin siblings, the development of GVHD was markedly reduced but the risk of relapse and graft failure was greatly increased (Figure 8)[46,47]. Despite the clinical complications associated with GVHD, the GVL effect is now seen as one the primary therapeutic modalities of allogeneic BMT.

Over the last two decades the field has continued to rapidly advance, enhancing both the range of indications that BMT is used to treat and the overall success of the

procedure. The establishment of detailed bone marrow registries, with over 23 million typed volunteers as of 2014 (www.bmdw.org), has enhanced a patient's chance of finding a haploidentical match outside of their family. The use of peripheral blood mononuclear cells (PBMC) and cord blood as stem cell sources reduced the risks and invasiveness of the procedure for donors. The introduction of DNA-based typing for HLA enhanced the quality of recipient-donor matching[48]. The development of non-myeloablative conditioning regimes has extended the use of allogeneic BMT, and as a result the therapeutic benefits of GVL, to elderly patients and patients with co-morbidities, cohorts that were previously unable to undergo transplantation previously due to the high toxicity associated with conventional high-dose conditioning regimes. These advances, among others, have seen the number of transplants rapidly rise over the years and there are over 60,000 worldwide each year today. However, significant challenges remain as BMT continues to be associated with a high rate of morbidity and mortality in the clinic. For his work in the field of transplantation, E Donnal Thomas went on to receive the Nobel Prize for physiology and medicine in 1990. For a more comprehensive overview of the history of BMT, the following sources provide an excellent review[6,23,24,49,50].

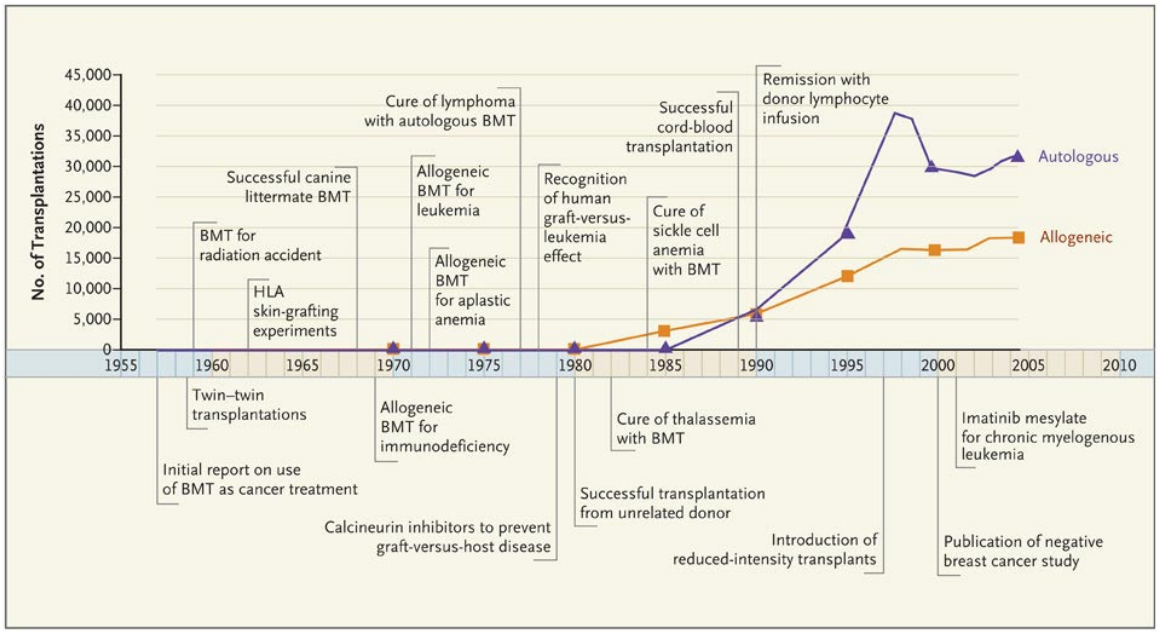

Figure 6: Timeline outlining the number of transplants performed each year in parallel to milestones in the field. By the 1980's the number of transplants rose rapidly each year as the challenges posed by graft-versus-host-disease and pancytopenia were addressed. Reprinted with permission from the New England Journal of Medicine, Copyright Massachusetts Medical Society[51].

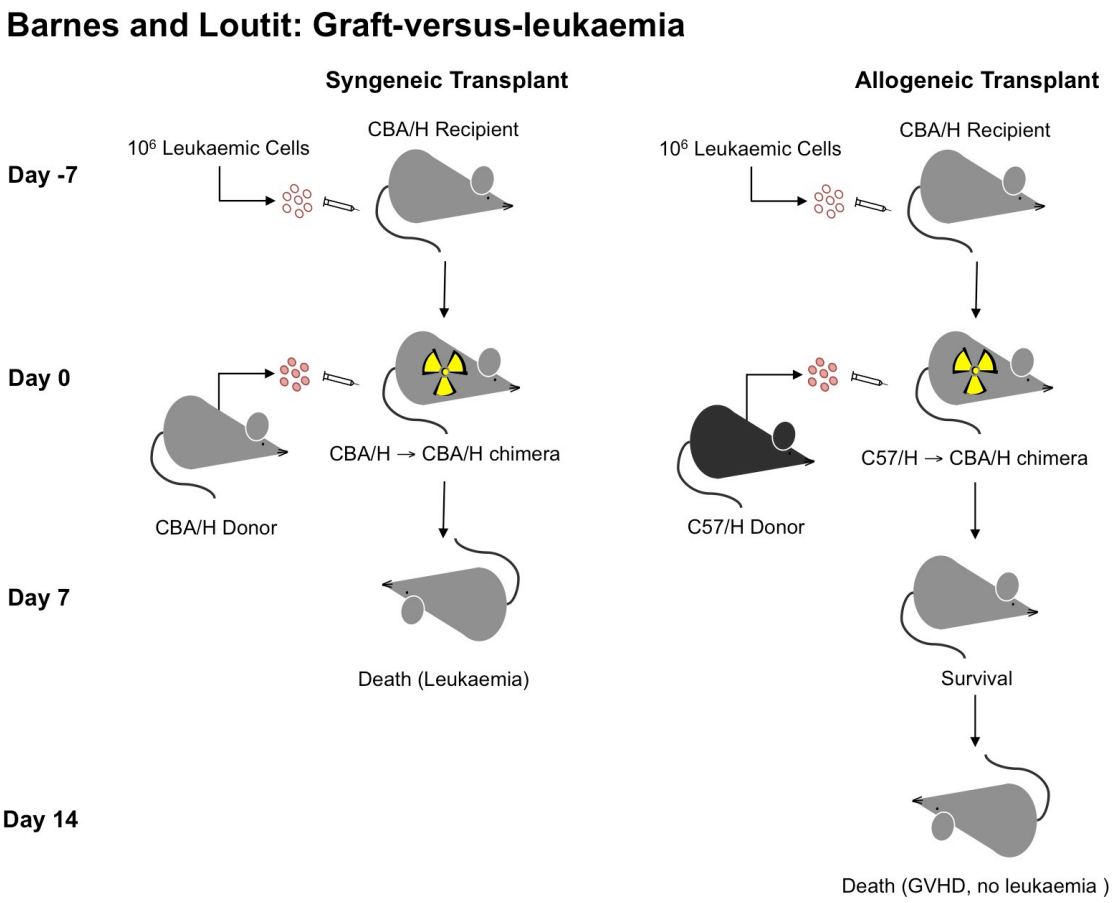

Figure 7: Leukaemic cells are eradicated in CBA/H recipient's that receive allogeneic, but not syngeneic, BMT. CBA/H mice were injected intraperitoneally with 10^6 leukaemic cells derived from a CBA/H mouse. 7 days later, recipients were lethally irradiated with 10 Gy and reconstituted with bone marrow from the femora of either CBA/H (syngeneic) or C57/H (allogeneic) mice on the same day. 7 days after transplant, mice that were transplanted with syngeneic bone marrow died from leukaemia. In mice that received bone marrow from a C57/H donor, a potent GVL effect was observed. All mice survived the initial tumour burden until they eventually succumbed to GVHD. This was the first observation of GVL *in vivo*, demonstrating the potent anti-leukaemic properties of cells from an allogeneic donor[18].

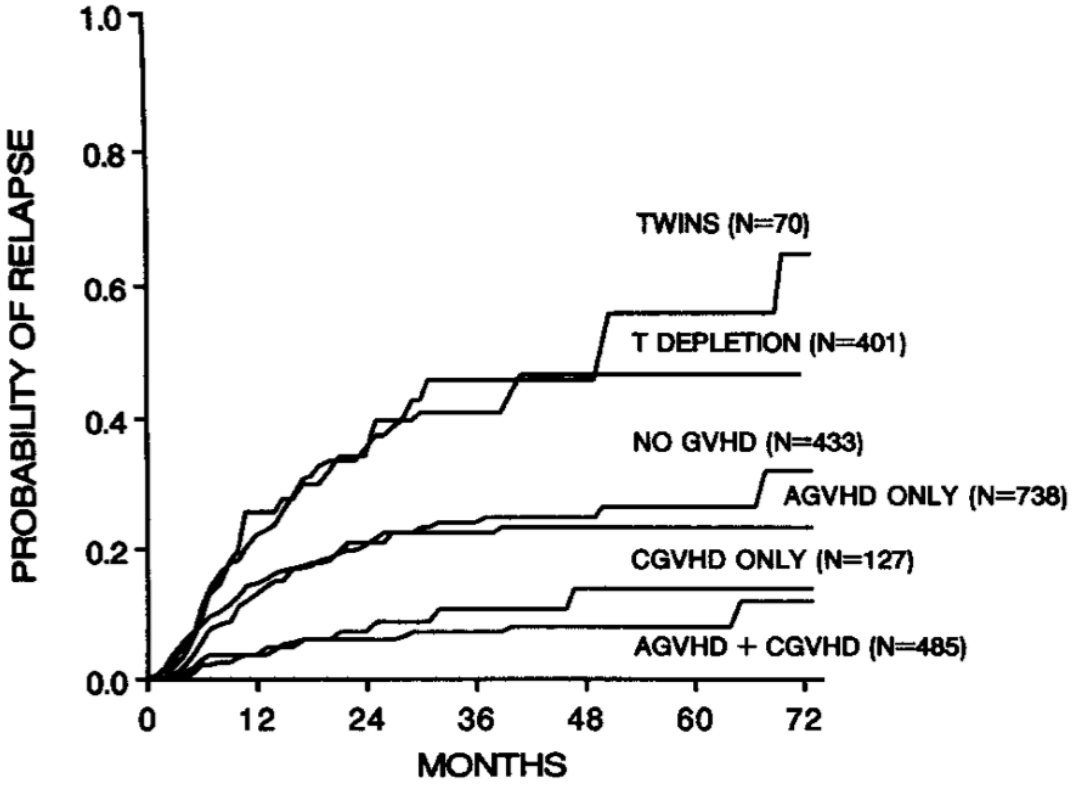

Figure 8: The probability of relapse after allogeneic or syngeneic transplantation according to the type of graft and level of GVHD. The onset of acute or chronic graft-versus-host-disease (GVHD) is associated with a decreased risk of relapse. Recipients that are transplanted with a graft from an identical twin (syngeneic) or receive an allogeneic depleted of T cells are at the greatest risk of relapse. Reprinted from Blood[46].

1.2 Graft-versus-host-disease

1.2.1 GVHD remains a major complication associated with allogeneic BMT

Despite over 50 years of intensive research, the development of GVHD continues to be a significant cause of morbidity and mortality in the clinic, limiting the overall success of allogeneic BMT (Figure 3). The vast majority of allogeneic transplants in the clinic are directed at patients with haematological malignancies such ALL and AML. Central to the therapeutic benefit of allogeneic BMT is the role of donor T cells, which have been shown to play a significant role maintaining remission after transplant. Paradoxically, it is this population of donor cells that is tightly associated with the development of GVHD, a disorder where alloreactive donor T cells recognise host tissues as 'non-self' and mediate acute and chronic tissue injury. There have been significant improvements in our understanding of the pathophysiology, predisposition and treatment of GVHD. However, despite these advancements, the development of GVHD remains widespread. In a recent study reviewing the outcome of patients undergoing allogeneic transplants between 1993 to 1997 and 2003 to 2007, it was reported that the incidence of acute GVHD had only decreased by 6% (77% to 71%)[52]. However, the overall incidence of severe GVHD (Grade III-IV) showed the greatest decrease, falling from 30% to 14%.

First reported by Barnes and Loutit in 1957, it was a number of years later before Billingham outlined his three requirements for GVHD that still hold true today[18,53]:

1. The graft must contain immunologically competent cells
2. The recipient must express alloantigens that are not present in the donor
3. The recipient must be incapable of mounting an immune response to eliminate the graft

50 years later, we now know that alloreactive donor T cells are the immunologically competent cells mediating GVHD in recipients, with the number of donor T cells closely

correlating with the severity of GVHD that develops[19,54]. The third requirement stipulates that the recipient must be incapable of mounting an immune response to eliminate the graft. For allogeneic BMT, this is a consequence of the conditioning regime (chemotherapy and/or radiotherapy), which acts to enhance stem cell engraftment by eliminating the recipient's haematopoietic system and treating the patient's malignancy (if present)[55].

Perhaps the most important predictor of GVHD is the degree of histocompatibility between the donor and the recipient. In humans, differences in the highly polymorphic Class I and Class II HLA glycoproteins, responsible for antigen presentation, are directly related to the frequency and severity of GVHD[56,57]. Class I HLA (A, B and C), responsible for the presentation of endogenous antigens, are expressed on almost all nucleated cells. Class II HLA (DR, DQ and DP), responsible for the presentation of exogenous antigen, are predominantly expressed on B cells and antigen presenting cells (APC) such as macrophages and dendritic cells (DC). In the clinic, donors are typically matched at HLA-A, HLA-B, HLA-C and HLA-DRB1 (referred to as 8/8 match) before they are considered suitable[56]. This kind of high resolution HLA-typing is necessary as even a single mismatch can significantly impact the clinical outcome for a patient. In a study published in 2007, high resolution DNA typing showed that a single mismatch at either HLA-A, HLA-B, HLA-C or HLA-DRB1 (7/8 match) was associated with higher mortality with patients having a 1-year survival rate of 43% compared with 52% for 8/8 matched pairs[58]. Certain HLA-mismatch combinations also carry a higher risk of developing GVHD than others, further complicating the process of finding a match[59].

Identifying a suitable donor begins in the family. The odds of finding a suitable HLA-match between siblings are 1:4 and this can be severely limiting. However, with the development of high resolution DNA typing techniques, the differences in the clinical outcomes of HLA-matched sibling donors (MSD) versus unrelated donors (UD) has

narrowed significantly; with a recent article examining the differences between MSD and UD (8/8 match) reporting that the difference in the 1-year survival for patients with leukaemia has moved from 21% in favour of MSD in 1988 to just 9% in 2008[5].

However, despite the majority of allogeneic transplants carried out coming from high resolution HLA-matched donor-recipient combinations, some level of GVHD requiring clinical intervention will develop in a large proportion of recipients. For recipients who receive grafts from HLA-matched sibling donors, around 40% of recipients will develop GVHD[56]. In this case, GVHD, and to an extent GVL, is driven by genetic differences between the donor and recipient in genes that are outside the HLA loci, encoding proteins that are referred to as minor H antigens[56].

Minor H antigens tend to be from highly polymorphic genes and can be derived from either autosomal chromosomes or the Y-chromosome. The disparities in minor H antigens between the donor and recipient can vary quite substantially. They can arise from polymorphisms that cause single or multiple changes in the amino acid sequence of a peptide. For example, the *Smcy* gene derived from the Y-chromosome differs from its homologue *Smcx* on the X-chromosome by more than 200 residues whereas the HA-1 and HA-2 allelic pairs differ by only a single amino acid residue[55]. These polymorphisms can have a profound effect on the immunogenicity of a peptide. They can alter the area where a T cell receptor (TCR) binds the peptide or interfere with the way the peptide is processed or post-translationally modified[60–62]. Minor H antigens can also arise from gene deletions, where the protein is expressed in the recipient but not the donor[63]. Thus, the immunodominance of minor H antigens can vary greatly.

Unlike Class I HLA, which is ubiquitously expressed by all nucleated cells, the distribution of minor H antigens is highly variable and can be either broadly expressed in most tissues or restricted to haematopoietic cells[56]. Minor H antigens derived from the Y-chromosome tend to have a broad expression pattern and are found in most

tissues, including those commonly targeted by GVHD such as the skin, gut and liver[64]. Other minor H antigens, such as autosomal HA-1, HA-2 and ACC-1 protein, have a restricted expression pattern and are restricted to haematopoietic cells, including leukaemic cells[64]. This can have a profound effect on their ability to induce both GVHD and GVL. It is well established that male recipients of HLA-matched female grafts are at a greater risk of developing GVHD than male recipients of HLA-matched male grafts[65]. However, these recipients are also at a lower risk of relapse[66]. On the other hand, restricting minor H mismatches to antigens restricted to haematopoietic cells could enhance GVL while diminishing GVHD, with one promising study showing a HA-1 specific CTL response inducing remission in patients with leukaemia after DLI[67,68]. The differential expression of minor H antigens between tissues and haematopoietic cells could also explain why GVL can occur without GVHD in some instances.

Importantly, the presentation of minor H antigens is also MHC restricted. To elicit an immune response, they need to be processed and presented via Class I or Class II MHC the same as any other antigen. This changes the pathophysiology of GVHD in comparison to MHC-mismatch models, as alloreactive donor T cells can recognise peptides from minor H antigens coupled with MHC from both donor and recipient antigen presenting cells (APC)[69]. The pool of precursor T cells specific for minor H antigens is also much lower (estimated to be between 1 in 10^5 to 1 in 10^6) than those specific for MHC-mismatches (estimated to be between 1-10% of all T cells), which also influences the severity of the response[69,70].

Historically, GVHD has been classified into two types depending on the time after transplant it first develops. GVHD arising within the first 100 days of transplant is defined as acute GVHD with GVHD occurring after the first 100 days defined as chronic GVHD[71]. The arbitrary nature of this definition has made the classification somewhat controversial as features of acute GVHD can present after 100 days and features of chronic GVHD before 100 days due to the evolving nature of transplant

regimes such as reduced intensity conditioning. However, for the remainder of this thesis I will focus on acute GVHD and the definition of acute and chronic GVHD is sufficient for the scope of this project.

1.2.2 Clinical features of acute GVHD

The incidence of acute GVHD after allogeneic BMT can vary significantly, from 10% to 80%, depending on a number of risk factors[72]. Risk factors increasing the likelihood a patient will develop acute GVHD include HLA-disparity, sex mismatch between the donor and recipient (F→M), increasing age of the recipient (>40), recipient CMV status, stem cell source (PBSC>Bone Marrow>Cord Blood) and the conditioning regime (High intensity>Reduced intensity)[73,74].

Acute GVHD usually manifests within the first 100 days of transplant and predominantly affects the skin, liver and gastrointestinal (GI) tract. The skin is the most commonly affected tissue (81%), followed by the GI tract (54%) and the liver (50%)[75]. Epithelial cells are the main target in acute GVHD and the onset of the disease typically begins with the development of a diffuse maculopapular rash in the skin that is often painful and pruritic[76]. This can begin anywhere but usually develops around the hands, feet and ears before progressing around the rest of the body although the scalp is usually spared[56]. In severe cases, the skin can blister and ulcerate with the formation of bullae and show signs of desquamation in the epidermal layers (Grade IV)[77]. Histopathological features include dyskeratosis of epidermal keratinocytes, lymphocyte infiltration and apoptosis at the base of epidermal rete pegs[56].

In the GI tract, acute GVHD typically manifests with profuse secretory diarrhoea[78]. A combination of nausea, vomiting, anorexia, weight loss and abdominal pain can develop as the disease progresses[78]. The diarrhoea may become bloody due to mucosal ulceration and ileus may develop, which is indicative of a poor prognosis[79]. Histopathological features of the GI tract include patchy ulcerations, flattening of the surface epithelium, crypt ulceration and apoptotic bodies at crypt bases[56,80].

In the liver, the development of acute GVHD is characterised by jaundice as a result of hyperbilirubinemia[81]. The bile canaliculi are damaged leading to a cholestatic pattern of

liver damage with elevated levels of conjugated bilirubin, alkaline phosphatase and gamma-glutamyl-transpeptidase[82]. Histopathological features include lymphocyte infiltration of the portal areas, endothelialitis, bile duct apoptosis and pericholangitis[80,82].

Originally developed in 1974, an updated version of the Glucksberg classification is typically used to determine the severity of GVHD[83]. To grade GVHD, each organ commonly affected by acute GVHD is independently assessed and assigned a stage. The skin is assessed by the percentage surface area involved, the liver by the elevation of bilirubin and the GI tract by the amount of diarrhoea[83]. These stages are then used to divide patients with acute GVHD into one of four grades (I-mild, II-moderate, III-severe, IV-very severe)[83]. The grade of GVHD has been shown to correlate with the overall survival and the development of severe GVHD (Grade III-IV) is associated with significant mortality, with only 25% of patients that develop Grade III GVHD and 5% of patients that develop Grade IV GVHD surviving longer than 5 years[84].

For patients that develop Grade I GVHD, treatment is usually not necessary although topical steroids may be used to treat localised symptoms in the skin[82]. Calcineurin inhibitors, such as cyclosporine, are commonly used as a means of prophylaxis for GVHD. This inhibits the activation of interleukin 2 (IL-2), which leads to a reduction in the activity of T cells. Changing the dosage administered can increase the therapeutic benefit once symptoms begin to manifest. However, this can significantly impact the therapeutic benefits of GVL with one study showing a 50% reduction in the rate of relapse when the dose of cyclosporine A was reduced[5]. For patients that develop Grade II-IV GVHD, the use of anti-inflammatory steroids, such as corticosteroids, remains the benchmark for treating acute GVHD (Figure 9). This results in complete remission in less than half of patients, although their effectiveness is reduced as the severity of GVHD increases[56,85]. However, the continued use of steroids renders

immunosuppressed patients susceptible to developing serious infections, leading to a significant level of mortality in the clinic in itself with a TRM of 15%[1].

Stage	Skin	Liver (Bilirubin)	GI Tract (Diarrhoea)
1	Maculopapular rash <25% of body surface	2-3 mg/dl	>500 ml
2	Maculopapular rash 25-50% of body surface	3.1-6 mg/dl	>100 ml
3	Maculopapular rash >50% of body surface	6.1-15 mg/dl	>1500 ml
4	Generalised erythroderma with bullae formation and desquamation	>15 mg/dl	Severe abdominal pain with or without ileus

Table 1: Acute graft-versus-host-disease staging[83].

Grade	Skin	Liver	GI Tract
I	Stage 1-2	Stage 0	Stage 0
II	Stage 3 or	Stage 1 or	Stage 1
III	-	Stage 2-3 or	Stage 2-4
IV	Stage 4 or	Stage 4	-

Table 2: 1994 Consensus Conference classification of acute graft-verus-host-disease[83].

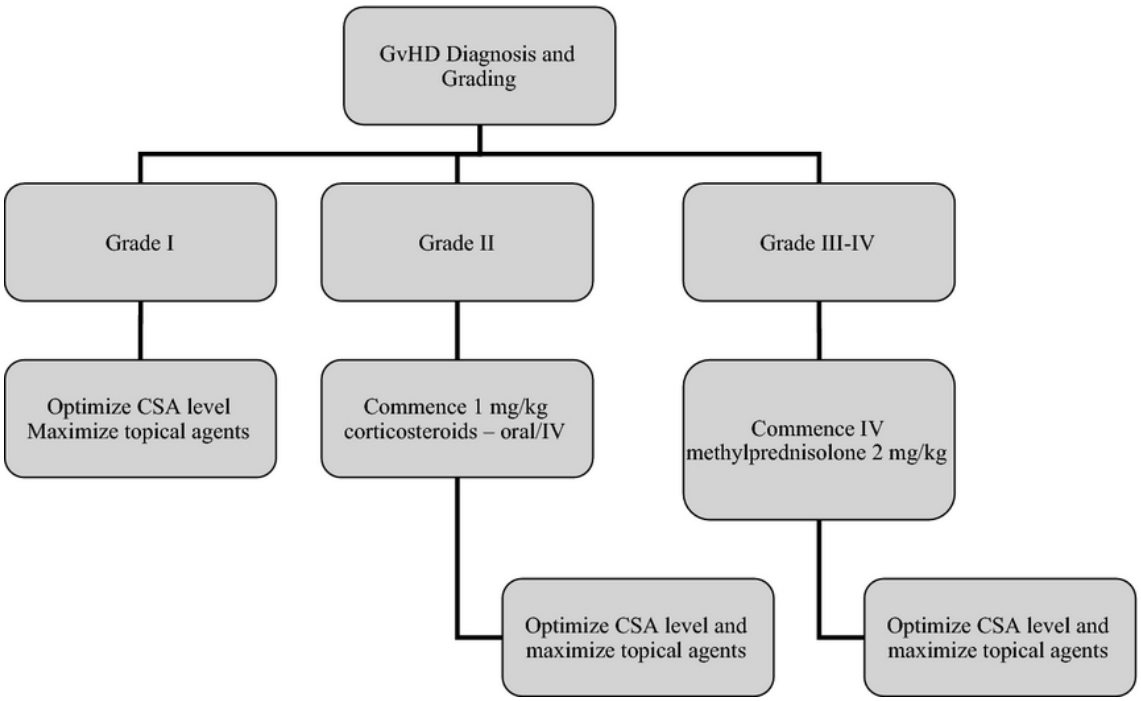

Figure 9: Summary of the strategy for the first line of treatment for acute graft-versus-host-disease. For Grade I-IV graft-versus-host-disease (GVHD), the levels of calcineurin inhibitors (Cyclosporine A) may be increased to therapeutic levels. The use of steroids remains the primary treatment for acute GVHD, ranging from IV>Oral>Topical administration depending on the severity of GVHD. Algorithm developed by a joint working group from the British Committee for Standards in Haematology and the British Society for Bone Marrow Transplantation. Reprinted with permission from the British Journal of Haematology[82].

1.2.3 Pathogenesis of acute graft-versus-host-disease

The precise pathophysiology of acute GVHD, which involves a complex cascade of humoral and cellular interactions between donor and host cells, remains incompletely understood[86]. However, to begin to understand some of the pathways involved, it is still useful to consider the development of GVHD as a three-step process in a model first proposed by Ferrara and Reddy (Figure 10)[87].

- Step 1: Tissue damage associated with conditioning activates recipient APC
- Step 2: The activation, differentiation and migration of alloreactive donor T cells
- Step 3: Development of clinical GVHD via target tissue apoptosis

The first step in this process involves the activation of host APC by the release of pro-inflammatory cytokines (TNF-α, IL-1) and damage-associated molecular patterns (DAMPs) such as adenosine-5'-triphosphate (ATP) as a result of tissue damage associated with the conditioning regime[4]. In secondary lymphoid tissues, activated host APC then present alloantigens and co-stimulatory signals to donor T cells infused as part of the graph promoting alloactivation and cytokine release[86]. Once primed, alloreactive T cells proliferate and differentiate into effector subsets before migrating to peripheral tissues such as the skin and GI tract where they drive acute GVHD via cellular (Cytotoxic T lymphocytes, NK cells) and inflammatory (TNF-α, IL-1) mediators[88]. The tissue damage associated with the effector phase is what underlies the clinical manifestations of acute GVHD.

It is important to consider acute GVHD as a highly dysregulated immune response, where the initial 'cytokine storm' generated by the conditioning regime and ubiquitous availability of alloantigen, leads to a self-perpetuating immune response where tissue damage mediated by effector cells promotes the recruitment of more effector cells. A more detailed overview of each step leading to the development of acute GVHD including the humoral and cellular factors involved will be expanded upon below.

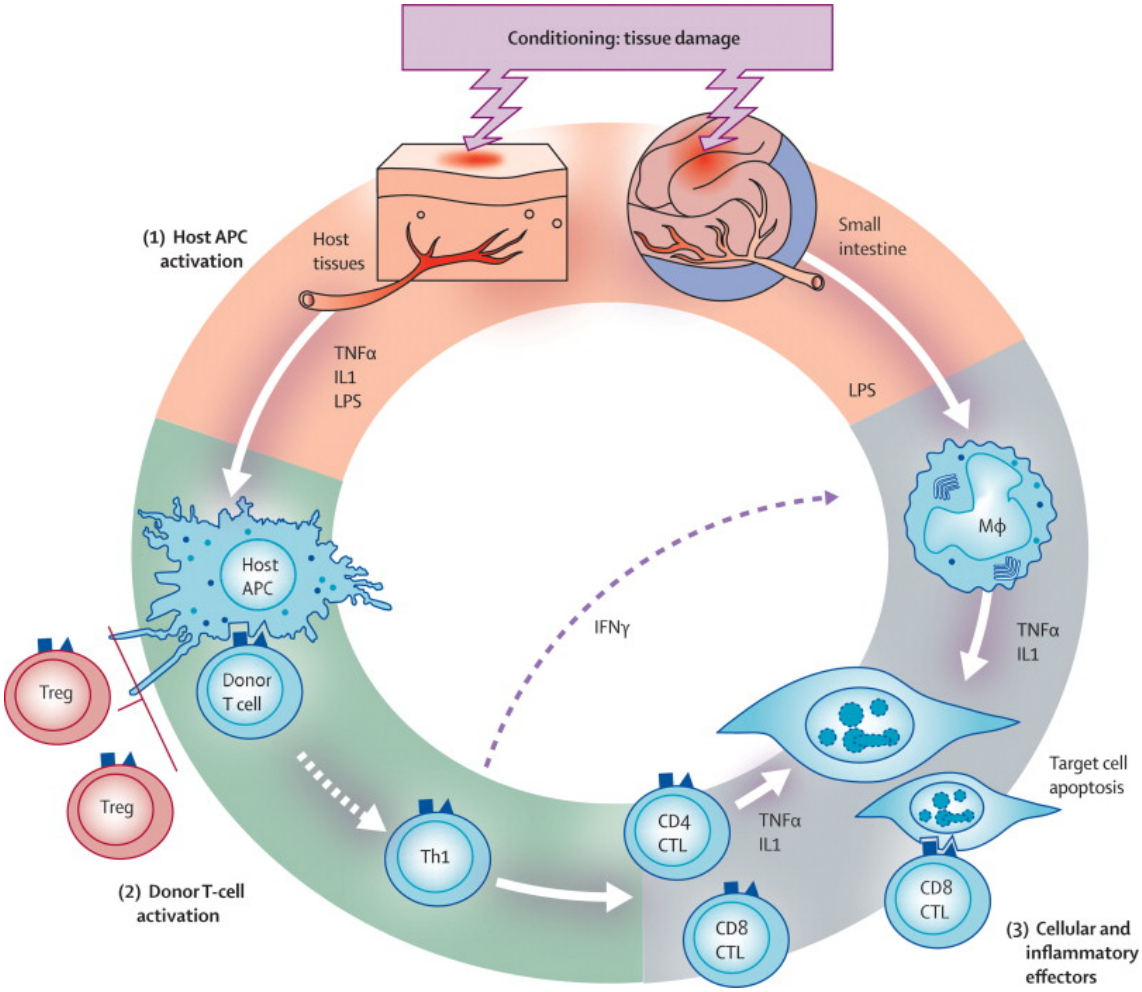

Figure 10: Pathogenesis of acute GVHD as proposed by Ferrara and Reddy. The development of acute GVHD is classically thought to occur in three sequential phases. 1. Tissue damage associated with the conditioning regime induces the release of danger/pattern-associated molecular patterns (DAMPs/PAMPs) and pro-inflammatory cytokines such as TNF-α, IL-1 and uric acid. This leads to the maturation of host APC and generates a pro-inflammatory environment for T cells in peripheral tissues. 2. Donor T cells are then primed by alloantigens in secondary lymphoid organs via donor and host APC and pro-inflammatory cytokines. T cells then differentiate and proliferate in response to pro-inflammatory molecules before migrating to peripheral tissues. 3. The combination of tissue damage associated with the conditioning regime and priming of T cells with alloantigens leads to a complex cascade where cellular (Cytotoxic T lymphocytes and NK cells) and inflammatory mediators (TNF-α and IL-1) are released which cause acute and chronic tissue injury in peripheral tissues such as the skin, GI tract and liver. Reprinted with permission from The Lancet[56].

1.2.3.1 Step 1: Tissue damage associated with conditioning activates recipient APC

To deplete the host haematopoietic system, promote stem cell engraftment and treat haematological malignancy, patients are myleosuppressed and immunosuppressed using chemotherapy and/or radiotherapy (γ–radiation). The cytotoxic effects of these treatments on both epithelial and endothelial cells in peripheral tissues leads to a significant degree of inflammation, which in turn supports the development of acute GVHD through the activation of APC[89]. This is widely known as the initiation phase.

The initiation phase begins when endogenous danger signals, known as damage-associated molecular patterns (DAMPs) and pathogen-associated molecular patterns (PAMPs) are released from damaged and dying cells following the conditioning regime. This leads to the secretion of pro-inflammatory cytokines like TNF-α, IL-1 and IL-6 in a process called the 'cytokine storm'. This mediates profound changes to the tissue microenvironment causing an increase in the expression of adhesion molecules, co-stimulatory molecules and antigens presented by MHC, as well as the development of chemokine gradients that promote the infiltration of immune effectors[90–92].

The release of DAMPs such as adenosine-5'-triphosphate (ATP), uric acid and high mobility group box 1 protein (HMGB1) activate the cellular components of the innate immune system through pattern recognition receptors (PRR) on the cell surface[89]. This converts professional APC from an immature phenotype, which specialise in the uptake of exogenous antigen and promote tolerance, to a mature phenotype, up-regulating MHC and co-stimulatory molecules on the cell surface, which in turn promote effector T cell responses[93].

ATP, a coenzyme responsible for energy transfer within cells, is an important example of a DAMP that has been shown to play a key role in the pathogenesis of GVHD[94]. Under physiological conditions, ATP is found at much lower concentrations in the extracellular space (10 nM) than the intracellular space (3-10 mM)[95]. However,

following tissue damage associated with the conditioning regime, the level of ATP is found to dramatically increase in the extracellular space of both humans and mice[94]. Once the extracellular concentration of ATP accumulates to levels indicative of cell stress, ATP binds the purinergic receptor $P2X_7$ leading to a calcium efflux which promotes the assembly and activation of the protein 3 (Nlrp3) or cryopirin inflammasome. Activation of the Nlrp3 inflammasome leads to the secretion of the potent inflammatory cytokine IL-1β inducing APC to upregulate co-stimulatory molecules and produce pro-inflammatory cytokines promoting T cell expansion[94,96,97]. The immunomodulatory effects of IL-1β is particularly evident in the skin, where secretion has been shown to upregulate co-stimulatory molecules CD80 and CD86 on Langerhans cells (LC) and induce keratinocytes to express pro-inflammatory cytokines[98,99].

The $P2X_7$ receptor ($P2X_7R$) is an important pathway to the development of acute GVHD. Pharmaceutical blockade of the $P2X_7R$ was found to significantly reduce the severity of GVHD in mice. A similar decrease in the severity of GVHD was also observed when ATP was metabolised using apyrase[94].

ATP has also been shown to significantly influence the migration of APC, attracting them to sites of increased apoptosis and imparting tissue resident DC with an increased capacity to migrate to peripheral lymph nodes[100,101].

Another important DAMP released from dying cells is uric acid. Uric acid promotes the Nlrp-3 inflammasome mediated production of IL-1β and the enzymatic digestion of uric acid in the GI tract of mice was found to significantly reduce the severity of GVHD[97]. Thus, the depletion of specific DAMPs and therapies directly targeting the Nlrp3-inflammasome remain attractive targets to reduce the severity of GVHD after transplantation.

In addition to the release of pro-inflammatory cytokines and DAMPs, the destruction of epithelial cells in tissues such as GI tract also leads to the loss of the epithelial barrier function. This enables both commensal and pathogenic bacteria that colonise the epithelial surface to translocate across the barrier, which further stimulates APC through the recognition of PAMPs. APC recognise these conserved structural moieties through PRR such as Toll-like receptors and the nucleotide binding oligomerisation domain (NOD)-like receptors (NLRs)[102]. Ligation of these receptors by PAMPs activates APC such as DC, increasing their expression of Class II MHC and promoting their subsequent migration back to secondary lymphoid tissues where they interact with T cells.

The contribution of gut microbiota to GVHD has long been recognised. In experiments conducted by Van Bekkum in the 1970's, decontamination of the GI tract using antibiotics was found to significantly reduce the severity of GVHD in the gut[103]. Similar observations were also made in humans that underwent gut decontamination[104].

The pathophysiology behind these observations became clearer when lipopolysaccharide (LPS) stimulation of TLR-4 was identified as a key driver of acute GVHD, generating a 'cytokine storm' that favours the development of GVHD[90]. In mice undergoing allogeneic BMT, treatment with either an LPS inhibitor or endotoxin neutralising antibodies was found to significantly reduce the severity of GVHD and increase the overall survival of mice[105–107]. Ferrara further clarified the importance of the LPS/TLR-4 pathway when mice transplanted with bone marrow from an LPS-resistant donor developed significantly less GVHD than mice transplanted with bone marrow from an LPS-sensitive donor[108].

To summarise, as the intensity of the conditioning regime increases, the degree of tissue injury and inflammation is greater which in turn generates a 'cytokine storm' that favours the development of GVHD. The generation of inflammation in peripheral

tissues has two main effects. It activates recipient APC enhancing their ability to prime T cells in secondary lymphoid tissues and subsequently provides alloreactive primed T cells with the chemokine gradient and co-stimulation they need to mediate their cytotoxic effects[109]. The intensity of the conditioning regime can also effect the expression of immunosuppressant molecules, with a recent study demonstrating that sialic acid–binding immunoglobulin-like lectin-G (Siglec-G) is downregulated in response to radiation induced tissue damage, rendering the host even more susceptible to the effects of DAMPs[110]. Thus, the intensity of the conditioning regime plays a significant role in the development of acute GVHD.

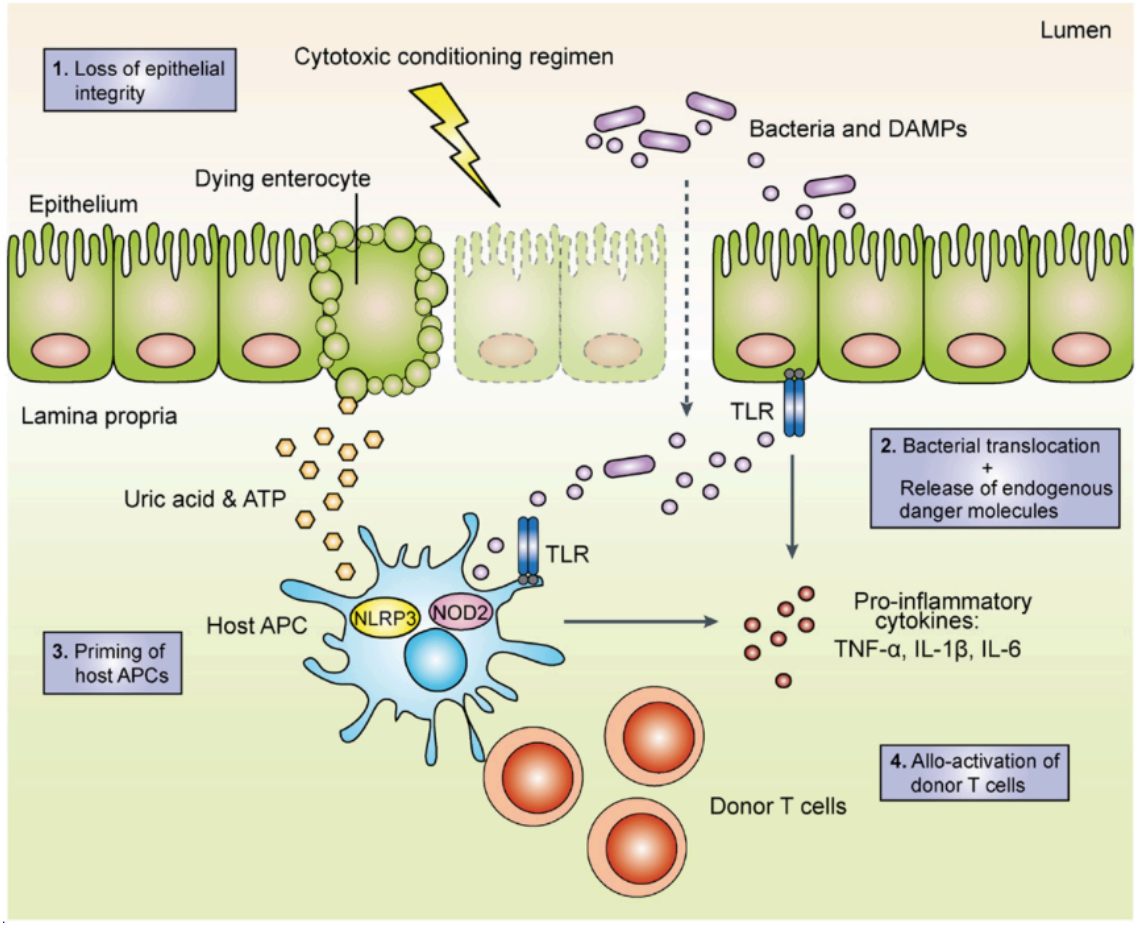

Figure 11: Tissue damage associated with the conditioning regime leads to the activation of recipient antigen-presenting cells in the gastrointestinal tract. During the conditioning regime, epithelial cells become damaged leading to the release of pro-inflammatory cytokines and damage-associated molecular patterns (DAMPs), which stimulate the maturation of antigen presenting cells (APC). In addition, bacteria can translocate the disrupted epithelial barrier and further stimulate pattern recognition receptors (PRR) on APC. These activated APC can then prime alloreactive donor T cells, which mediate acute and chronic tissue injury in peripheral tissues. Reprinted with permission from Frontiers in Immunology[89].

1.2.3.2 Step 2: Activation and differentiation of donor T cells

The second phase of GVHD involves the priming and subsequent differentiation of alloreactive donor T cells into effector cells capable of mounting an immune response. The site of this priming is predominantly, although not exclusively, in the spleen and secondary lymphoid tissues[111].

Central to this is the role of APC. Considered by many to be the 'sensors' of acute GVHD, APC are required to present alloantigen to donor T cells via the MHC molecule and provide critical co-stimulatory and cytokine signalling which strongly influence both the type and quality of the effector response[112].

There are several different types of APC capable of contributing to the development of GVHD. These include host haematopoietic APC that survive the conditioning regime, host non-haematopoietic APC and donor haematopoietic APC[86]. After transplantation, both host and donor haematopoietic APC are present in the secondary lymphoid organs[91]. However, MHC-disparity has significant influence on the role of host and donor APC in the development of acute GVHD[69].

In MHC-mismatched transplants, donor recognition of intact MHC molecules is the dominant mode of allorecognition and the MHC molecule itself contributes more to the TCR binding energy than the bound alloantigen[4,113]. In this setting, given that intact host MHC is the immunodominant antigen stimulating alloreactive T cells, antigen presentation is largely restricted to host APC, although donor APC may also contribute if they can acquire intact host MHC through a recently described phenomenon called cross-dressing[69,114].

Data supporting the importance of host APC (both haematopoietic and non-haematopoietic) in initiating acute GVHD across MHC-mismatches first came from experiments where the alloresponse was directly measured in the thoracic duct lymph of irradiated mice receiving MHC-mismatched BMT[115]. Isolating donor T cells from the

thoracic duct lymph of irradiated recipients, donor T cells appeared as activated blasts as little as 3-5 days after transplant and were capable of initiating GVHD upon transfer into a newly irradiated recipient[115]. The rapid appearance of these activated blasts indicated that host APC were driving this response, as it was too early for any meaningful contribution from donor derived APC[4]. Direct evidence supporting an important role for host APC in the initiation of acute GVHD came when alloreactive donor NK cells from MHC-mismatched donors, transplanted as part of the graft, were able to protect mice from GVHD[116]. NK cells amplified the eradication of haematopoietic cells, including APC that were unable to signal the cells via MHC Class I. This protection was still conferred even if the dose of donor T cells given was increased to 100-fold greater than the dose that would normally be lethal without NK cells[69]. This was further supported by observations in humans where the incidence of GVHD was reduced in HLA-matched recipients where NK cell alloreactivity was predicted based on the HLA-B and HLA-C haplotypes of donors and recipients[116].

Direct evidence that host haematopoietic APC alone are sufficient to induce acute GVHD has also been shown in an MHC-mismatched, minor H matched model[117]. Using H2bm12 and H2b1 mice that lack MHC Class $II^{-/-}$ and MHC Class $I^{-/-}$, respectively, Teshima et al. generated bone marrow chimeras using wild-type (WT) C57BL/6 (BL/6) as donors and H2bm12 and H2b1 mice as recipients. When these chimeras ([BL/6→H2bm12] and [BL/6→H2bm12]) were established, antigen presentation was restricted to the haematopoietic system as haematopoietic APC would now be derived from donor WT BL/6 stem cells whereas non-haematopoietic APC would still be derived from H2bm12 and H2b1 mice. Teshima et al. was then able to show that host haematopoietic APC were sufficient to induce both CD4- and CD8-mediated GVHD when alloantigen presentation and expression was restricted to the haematopoietic system[117].

In contrast to MHC-mismatched BMT, where the contribution of host APC which abundantly express MHC was not hard to predict, the contribution of both donor and host APC in MHC-matched, minor H mismatched is not as clear[69]. For many years, antigen presentation by host haematopoietic APC was considered essential for the induction of acute GVHD[55]. In the MHC-matched setting, peptide recognition of cognate antigen is the equivalent of pathogen peptide recognition and both host and donor APC are capable of presenting antigen[4]. Antigen can be directly presented, where antigen is derived from a protein synthesised in the cell, by host APC or it can be indirectly presented, where antigen is derived from an exogenous source, by both host and donor APC (Figure 12). In addition, antigen can also be cross-presented by both host and donor APC, a process where antigen derived from an exogenous source can be loaded in the MHC Class I processing pathway normally restricted to endogenous antigens (Figure 12). Another form of presentation has also been described in recent years, termed cross-dressing, where APC can acquire a peptide loaded MHC-molecule via 'trogocytosis'[118]. This could have a significant impact on the role of donor APC in transplantation, with a recent report observing very high levels of recipient haematopoietic cell derived MHC Class I and Class II transfer to donor cells after BMT[119].

In CD8-mediated GVHD, where alloreactive CD8 T cells are primed by alloantigen presented via MHC Class I, a requirement for host haematopoietic APC to induce acute GVHD has been demonstrated in several studies, with donor haematopoietic APC augmenting this response[120,121]. Using β_2-microglobulin (β_2m) deficient mice, which lack MHC Class $I^{-/-}$, Shlomchik generated bone marrow chimeras using BL/6 mice as recipients and β_2m mice as donors ([β_2m $\rightarrow$BL/6])[55]. In these chimeras, haematopoietic cells were deficient in MHC Class I and unable to present antigen to CD8 T cells. When the chimeras were subsequently retransplanted with C3H.SW BM supplemented with donor CD8 T cells, the chimeras were found to be highly resistant

to CD8-mediated GVHD[55]. Thus, demonstrating an important role for host haematopoietic APC in an MHC-matched, minor H mismatched model of GVHD.

To address whether the failure was due to inefficiency in cross-presentation or an issue with the kinetics of engraftment, the experiments were repeated using [C3H.SW→BL/6] bone marrow chimeras[4]. These were also found to be resistant to GVHD, indicating that cross-priming is inefficient in the induction of acute GVHD, although the addition of donor CD4 T cells was found to improve the priming of CD8-mediated GVHD via cross-presentation in another study[122]. Using the same MHC-matched, minor H mismatched model of BMT, Matte was able to demonstrate a role for donor haematopoietic APC in augmenting acute GVHD[121]. When BL/6 mice were transplanted with C3H.SW $\beta_2m^{-/-}$ along with donor CD8 T cells from a WT C3H.SW donor, GVHD was still induced but the severity was significantly reduced[121].

In MHC-matched, minor H mismatched GVHD mediated by donor CD4 T cells, both host and donor haematopoietic APC have been show to be sufficient to induce GVHD[69,123]. To further delineate the role of both donor and host APC, Anderson et al. performed transplants using CD80/CD86$^{-/-}$ B6.C (H-2^d) as donors and CD80/CD86$^{-/-}$ BALB/c (H-2^d) as recipients[124]. Both strains of mice were deficient in the co-stimulatory molecules CD80 and CD86 and when transplanted (CD80/CD86$^{-/-}$ B6.C → CD80/CD86$^{-/-}$ BALB/c), acute GVHD failed to develop highlighting the absolute importance of co-stimulation for CD4-mediated GVHD. However, when either WT B6.C mice were used as donors (B6.C → CD80/CD86$^{-/-}$ BALB/c) or WT BALB/c mice as recipients (CD80/CD86$^{-/-}$ B6.C → BALB/c), GVHD still developed in the absence of the co-stimulatory molecules CD80/CD86 in either donor or host derived APC, indicating a non-redundant role[124]. Although it is worth noting that there was less skin GVHD when host APC were deficient of co-stimulatory molecules and less gut GVHD when donor APC were deficient, indicating non-overlapping roles.

The importance of host haematopoietic APC in priming acute GVHD make them attractive targets for immunotherapy. However, a number of recent studies have challenged this concept, as depletion of host DC, LC and B cells all failed to prevent the development of GVHD in mice[125–127]. The depletion of host macrophages was even seen to increase the severity of GVHD[128]. Therefore, it remains unclear whether any particular APC subset has a non-redundant role in the development of acute GVHD with a recent study suggesting that non-haematopoietic APCs, which are capable of expressing MHC Class II and stimulatory molecules, are the most potent inducers of GVHD by 100- to 1000- fold compared to host and donor haematopoietic APC[129]. Another study was able to demonstrate CD8-mediated GVHD in a MHC-matched, minor H mismatched model of GVHD when antigen presentation by host and donor haematopoietic APC were unable to present antigen[130]. However, the severity of GVHD was significantly less than that observed when both host and donor haematopoietic APC were capable of presenting antigen.

The ligation of a TCR with its corresponding alloantigen presented by an APC alone is also insufficient to induce T cell activation[131]. T cells must also receive a 'second signal' mediated by co-stimulatory molecules on APC in order to proliferate, secrete cytokines and acquire effector functions[91]. This has been an area of intense research over the last two decades and co-stimulatory pathways from two main families are now known to deliver both positive and negative signals that are critical in the context of GVHD; the B7 family and the TNF receptor family[56,132]. The *in vivo* blockade of various positive co-stimulatory molecules such as CD28, ICOS, CD40 and CD30 has been shown to mitigate GVHD in pre-clinical models while the blockade of inhibitory signals such as PD-1 and CTLA-4 exacerbated GVHD[133–136].

In MHC-matched, minor H antigen mismatched models of BMT, both CD4 and CD8 T cells can contribute to the development of acute GVHD in response to minor H antigens[137]. Once primed, alloreactive donor T cells rapidly proliferate and differentiate

into T-helper 1 (Th1), T-helper 2 (Th2), T-helper 17 (Th17) and CTL effector subsets[56]. The mechanisms behind the polarisation of T cell subsets in acute GVHD is not well understood, but it is believed to be largely dependent on the dominant cytokines produced at the time of activation in secondary lymphoid tissues[136]. For example, the development of Th1 type cells has been linked to IL-12 provided by APC whereas the development of Th2 type cells has been linked to IL-4[138,139]. However, the proliferation of donor T cell subsets is strongly linked to IL-2 secretion and many of the prophylactic inhibitors of GVHD, such as anti-calcineurin inhibitors, target this pathway[109]. Donor Th1 type cytokines (TNF-α, IFN-γ) are also strongly linked to the pathology associated with acute GVHD[90]. Interestingly, several studies in pre-clinical models have also shown that the development of acute GVHD is predominantly dependent on the priming of naïve ($CD44^{low}$ $CD62L^{high}$) rather than effector memory ($CD44^{high}$ $CD62L^{low}$) T cell subsets raising the possibility that depletion of naïve T cell subsets may mitigate GVHD without compromising immunity[140,141].

After undergoing a period of clonal expansion and differentiation, alloreactive donor T cells exit the secondary lymphoid tissues and traffic to peripheral organs through a combination of chemokine-receptor, selectin- and integrin-ligand interactions[88,142]. For example, activated CD8 T cells lose their expression of both CD62L and CCR7, which prevent them from entering lymph nodes, and upregulate their expression of P- and E-selectin ligands such as P-selectin glycoprotein ligand-1 (PSGL1) and CD44, enabling them to efficiently roll on inflamed endothelium expressing their counter-receptors P- and E-selectin[143]. The secondary lymphoid environment can also 'imprint' T cells, fine-tuning their homing potential to a particular tissue[143]. CD8 T cells in the mesenteric lymph nodes preferentially migrate to the gut, upregulating their expression of $\alpha_4\beta_7$ and CCR9, while CD8 T cells in the peripheral lymph nodes preferentially migrate to the skin, upregulating their expression of CCR10 and E-selectin ligand[144,145].

In response to damage associated with the conditioning regime, chemokine gradients are established in peripheral tissues which mediate the arrest and subsequent migration of activated T cells into the tissue. In the skin, the IFN-γ inducible CXCL9 and CXCL10 are expressed in high levels in mice within the first week of transplant. The importance of this chemokine gradient for CD8 T cell infiltration into the skin has recently been described. In a model of cutaneous GVHD, CD8 T cells from CXCR3 knockout (KO) mice were found to migrate in significantly fewer numbers to the skin than CD8 T cells from WT controls in response to CXCL9 and CXCL10 signalling, despite CD8 T cells from CXCR3KO mice retaining full activation and effector functions[146].

At the end of the activation phase, alloreactive donor T cells are primed, have undergone clonal expansion and have begun to infiltrate peripheral tissues such as the skin to begin the effector phase. For years, host APC were an attractive target for novel therapies due to their central role in the initiation of GVHD. However, their overall contribution has been called into question in recent years by a number of studies. Much of the research to date has focused on the role of APC in priming the T cell response. However, one area that is less clear is the role of infiltrating and tissue resident APC in the development of GVHD pathology. Such organ specific interactions with alloreactive donor T cells would make attractive targets for immunosuppression, as it may not interfere with the therapeutic benefits of GVL[69].

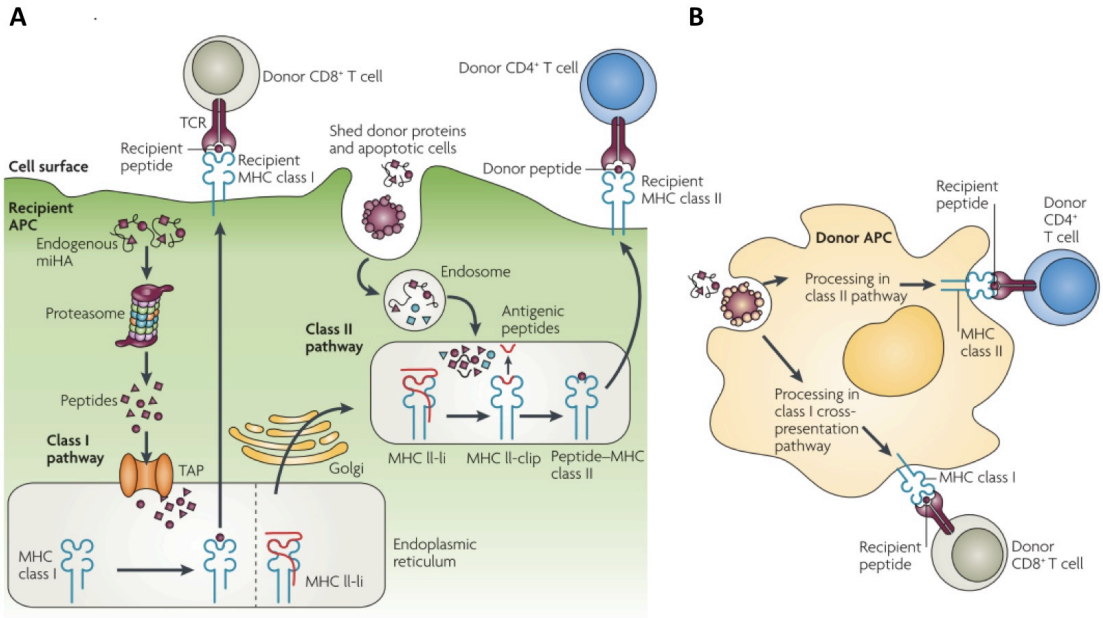

Figure 12: Antigen presentation by professional antigen-presenting cells in MHC-matched, minor H mismatched GVHD. A. Endogenous proteins can be directly presented to donor CD8 T cells via MHC Class I after being degraded by the proteasome in recipient antigen-presenting cells (APC). The allopeptides are loaded onto MHC Class I molecules after being pumped into the endoplasmic reticulum by the transporter associated with antigen processing (TAP). The MHC Class I molecule coupled with allopeptide is then exported to the cell surface where they present antigen to donor CD8 T cells (Direct Presentation). Exogenous proteins are typically degraded by lysosomal proteolysis in endosomes before being loaded onto MHC Class II molecules. The MHC Class II coupled with peptide is loaded on to the surface ready for presentation to donor CD4 T cells (Indirect Presentation). Allopeptides derived from endogenous proteins may also be loaded onto MHC Class II molecules and presented to donor CD4 T cells (Direct Presentation). Recipient APC can also cross-present exogenously acquired antigens on MHC Class I molecules by retrotranslocation from phagosomes. **B**. After the initiation phase, donor APCs can present exogenous alloantigens via MHC Class II (Indirect Presentation). Donor APC can also activate donor CD8 T cells by cross-presenting exogenous antigen (uptake of apoptotic recipient cells or shed proteins) via MHC Class I (Indirect Presentation). Reprinted with permission from Nature Reviews Immunology[4].

1.2.3.3 Step 3: Development of acute GVHD via target tissue apoptosis

The effector phase of acute GVHD begins with the development of end-organ damage in the skin, gut and liver mediated by a complex cascade of cellular effectors (CTLs, NK cells) and inflammatory cytokines (TNF-, IL-1, IL-6) that work synergistically to amplify the effects of one another[56]. Inflammatory cytokines can induce target tissue apoptosis without any cognate interaction, while cellular effectors require a cognate interaction (TCR:MHC Class I) to mediate killing[4]. Once fully initiated, acute GVHD is difficult to control as damage to host tissues perpetuates the disease, leading to further inflammation and the recruitment of even more effector cells that further augment the disease[112].

CTL are the main cellular effectors in acute GVHD, although NK cells can also contribute to the pathogenesis[147]. They require cognate interactions and mediate target cell apoptosis primarily via the perforin/granzyme and Fas/Fas Ligand (FasL) pathways (Figure 13)[91,147–149]. TNFR-like death receptors (DF), such as TNF-related apoptosis inducing ligand (TRAIL) and TNF-like weak inducers of apoptosis (TWEAK), can also play a role[91].

Using the granzyme/perforin pathway, CTLs secrete cytotoxic granules containing perforin and granzyme upon the cognate recognition of allopeptide bound to MHC Class I on a target cell. The secretion of perforin forms ‘pores’ on the membrane that facilitates the entry of granzyme into the cell, which mediates target cell apoptosis through the activation of a caspase signalling cascade[147,150].

The slower acting Fas/FasL pathway, involves the transmembrane protein FasL on CTLs binding the cell death surface receptor Fas on target cells. Upon binding FasL, the Fas receptor trimerises, leading to the formation of the death-inducing signalling-complex (DISC), which mediates target cell apoptosis again through the activation of a caspase signalling cascade[151,152]. The expression of Fas is upregulated in GVHD target

organs by inflammatory cytokines such as IFN-γ and TNF-α and the Fas/FasL pathway is an important effector pathway in GVHD[91,153].

The involvement of each of these pathways has been studied extensively in pre-clinical models of GVHD using genetically modified donor CD8 T cells deficient in each pathway. CD8 CTLs preferentially use the fast-acting perforin/granzyme pathway although the Fas/FasL pathway is important for the development of GVHD in the liver where Fas is expressed in high levels by hepatocytes[56,154,155]. CD4 CTLs preferentially use the Fas/FasL pathway[154]. However, the development of acute GVHD is not dependant on any particular pathway. In both MHC-mismatched and MHC-matched, minor H mismatched models of GVHD, transfer of perforin deficient T cells following transplant induced lethal GVHD albeit with delayed kinetics[156,157]. Similarly, when FasL deficient T cells were transferred across MHC-matched, minor H antigen mismatched models, lethal GVHD was induced although the severity was reduced in both the skin and liver[158].

In synergy with the cytolytic effects of CTLs are inflammatory effectors such as TNF-α, IL-1, IL-6, IL-12 and nitric oxide (NO), which amplify the levels of target tissue destruction and do not require cell-to-cell contact to mediate killing[91]. The expression of TNF-α and IL-1 in particular, which can be expressed by an abundance of cells involved in both innate and adaptive immunity, are strongly linked with the development of the 'cytokine storm' and subsequent tissue injury associated with acute GVHD[87].

The involvement of TNF-α was first recognised almost 30 years ago when damaged tissue in the skin, gut and liver of mice receiving allogeneic BMT was found to express high levels of TNF-α mRNA[159]. Pharmaceutical blockade of the TNF-α pathway further highlighted the importance of this pathway in acute GVHD, when mice receiving either anti-TNF-α monoclonal antibodies (Ab) or soluble TNF-α receptor developed significantly less pathology[91,160,161]. In the clinic, genetic polymorphisms associated with

an increase in the production of TNF-α by donor cells or heightened response by recipient cells to TNF-α were also found to increase the risk of GVHD developing[162,163].

The release of TNF-α by Th1 T cells and activated monocytes/macrophages promotes the development of acute GVHD in a number of different ways. It promotes the maturation of APC such as tissue resident DC, enhancing antigen presentation and co-stimulation of donor T cells[164]. It also promotes the expression of pro-inflammatory chemokines enhancing the recruitment of effector cells to the site of inflammation[90]. Finally, it can directly cause tissue damage by the induction of apoptosis and necrosis[165].

However, the precise effect of individual cytokines is difficult to predict as the timing, concentration and site of expression can either attenuate or amplify acute GVHD, as is the case with IFN-γ which appears to have a complex, dichotomous role in allogeneic BMT[155,166,167]. IFN-γ can be secreted by a wide variety of cells (Th1, CD8 CTLs, NK cells) and mediates a multitude of pro-inflammatory responses during the development of acute GHVD. However, the impact of IFN-γ appears to rely strongly on the timing of its production[166]. IFN-γ can have immunosuppressive effects immediately after transplant, but can also contribute to the pathogenesis of acute GVHD via its inflammatory properties at later stages[112]. In pre-clinical mouse models, the administration of high-dose IFN-γ or IL-12 (which stimulates the production of IFN-γ) immediately after BMT mediates a protective effect against acute GVHD[168,169]. However, the timing of this is critical as the administration of exogenous IFN-γ 3 days after transplant resulted in a substantial increase in GVHD-related mortality. Interestingly, transplanting lethally irradiated mice with T cells deficient in IFN-γ increased the severity of GVHD that developed, highlighting the complex role of cytokines in regulating acute GVHD[170,171].

Other immune cells that have an involvement in the effector phase of acute GVHD include neutrophils, NK cells, macrophages and B cells. Macrophages, which are primed in response to IFN-γ signalling by Th1 and CTLs, co-localise with T cells and can contribute to acute GVHD by secreting NO, which can impair the repair of damaged epithelial tissues by inhibiting stem cell proliferation[172]. Macrophages can also secrete the pro-inflammatory cytokines TNF-α and IL-1 in response to a secondary stimulus such as LPS following the translocation of bacteria through the disrupted epithelial barrier in the gut lumen[173,174]. Neutrophils can also enhance the severity of GVHD and are rapidly recruited to peripheral tissues such as the gut where they promote inflammation and T cell activation in response to TLR-signalling by microbial flora[86]. In humans, the severity of GVHD in the intestine strongly correlated with the level of neutrophils in lesions[175]. The physical or genetic deletion of neutrophils was found to significantly reduce the GVHD-related mortality that developed in pre-clinical models[175].

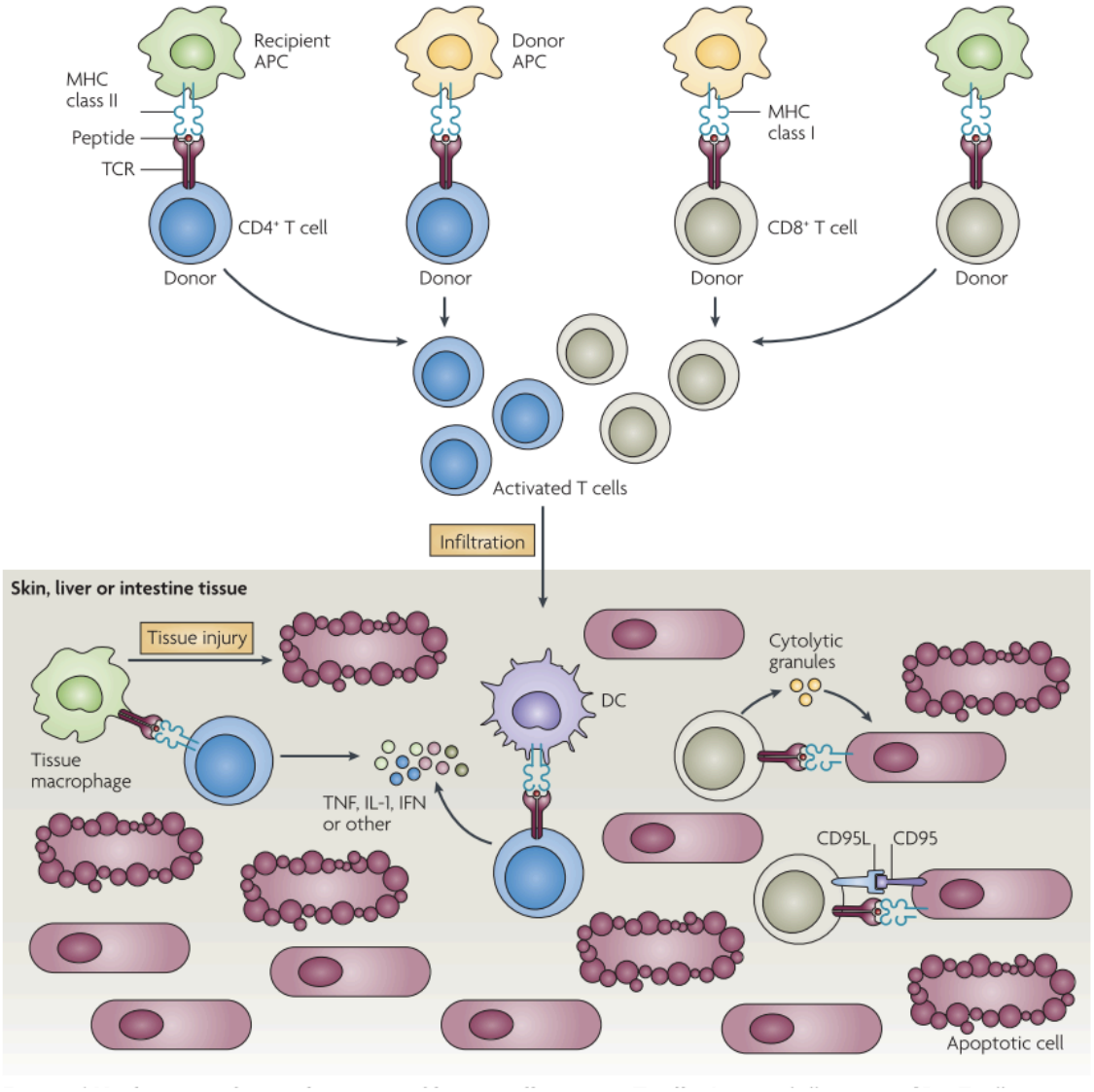

Figure 13: Mechanisms of tissue injury by alloreactive donor T cells in peripheral tissues. Activated alloreactive donor CD8 cytotoxic T lymphocytes (CTLs) require direct cognate interactions with MHC-Class I on non-haematopoietic cells in tissues such as skin, gut and liver to mediate damage. CTLs primarily kill target cells through one of two pathways. The Fas/Fas Ligand (CD95/CD95L) pathway involves the transmembrane protein FasL (CD95L) on CTLs binding the cell death surface receptor Fas (CD95) leading to the formation of the death-inducing signalling complex and apoptosis. In the perforin/granzyme pathway, CTLs secrete cytotoxic granules containing perforin and granzyme, which leads to the activation of a caspase-signalling cascade inducing apoptosis in target cells. In contrast, graft-versus-host-disease (GVHD) mediated by infiltrating CD4 T cells (Th1, Th2, Th17) does not require any cognate interaction with MHC-Class II on non-haematopoietic cells to induce target tissue apoptosis. The secretion of pro-inflammatory cytokines such as TNF-α, IL-1 and IFN-γ by Th1 cells can amplify the inflammatory response and lead to the recruitment of more effector cells augmenting the GVHD. Reprinted with permission from Nature Reviews Immunology[4].

1.2.4 Pre-clinical models of graft-versus-host-disease

1.2.4.1 Advantages and disadvantages of the mouse as a pre-clinical model of GVHD

Historically, the mouse has been an invaluable tool that has allowed many of the fundamental mechanisms of the human immune system to be elucidated. This is particularly true for BMT, where studies using mice led to the identification of the haematopoietic stem cell and the major histocompatibility complex, discoveries that underpin the biology behind transplants used in the clinic today[7,8,176]. GVHD was also demonstrated in mice first and the seminal studies by Korngold and Sprent were the first to confirm the dependence of GVHD on T cells[18,177–179].

The mouse remains the primary pre-clinical model used in the lab today to dissect the molecular mechanisms of GVHD, although the use of dogs has provided investigators with significant insights into the prevention and therapy of GVHD[109,112,180,181]. However, the mouse model has a number of advantages over other pre-clinical models[109,112]:

1. Highly controlled background: Mice are highly inbred. The genetic background and degree of MHC-disparity, which drives the pathogenesis of GVHD, can be strictly controlled. The environmental conditions such as the conditioning regime and microflora in the gut can also be controlled enhancing the scientific rigor of experiments.
2. High number of replicates: Mice have a short gestation period and large litters that can be housed in a relatively small amount of space. This allows researchers to conduct experiments using a high number of replicates, reducing the variance between observations.
3. Genetically modified strains: There is a large number of genetically modified strains available which allows researchers to test the role of key immune molecules or specific cell subsets in various models of GVHD. For example, the role of dendritic cells such as LC can be tested using conditional depletion

models such as the Langerin-DTR mice. The short gestation period and large litter of mice also makes it easier to generate new transgenic lines than other pre-clinical models.

4. Abundance of reagents and techniques: The extensive use of mice in the lab over the last 70 years has lead to a plethora of commercially available reagents. This can be extremely limiting in other pre-clinical models. For example, a quick search for anti-MHC Ab in the eBioscience catalogue (www.ebioscience.com) returns 64 anti-mouse Ab compared to just 2 anti-dog Ab. The immune response can also be imaged in real time using techniques such as intravital microscopy.
5. Relatively low cost: Compared to the cost of other pre-clinical models such as primates and dogs, mice are relatively cheap.

The main limitation of mouse models is their lack of genetic diversity[109,180]. Humans are genetically diverse and at the time of transplant vary in their age, disease state and range of immunomodulatory therapies they have received so far. This can have a fundamental impact on the type of GVHD that develops. Humans are also immunosuppressed after transplant using methotrexate and anti-calcineurin inhibitors[182]. These are rarely used in mouse models and the pathways involved in the pathogenesis of acute GVHD in mice may not be relevant in the clinical setting[109]. The development of mouse models of chronic GVHD that recapitulates all of the diverse characteristics associated with the disease has also proven difficult[112].

The majority of transplant models in the mouse also use TBI as the sole conditioning regime due to the difficultly in obtaining myeloablative chemotherapy drugs[109,129]. This contrasts the clinic where patients are predominantly treated with chemotherapy, with many transplant centres moving away from the use of TBI altogether[109].

In addition, although mice and humans are similar on a genetic level (>95%), slight differences have emerged in their immune systems over 65 million years of evolution[183]. For example, endothelial cells in both mice and humans express MHC Class I. However, endothelial cells in humans also express MHC Class II whereas endothelial cells in mice do not[184]. Differences like these can confound findings that are translated from pre-clinical models into humans and the literature is littered with examples of promising drugs that showed therapeutic effects in animals but failed to show any in humans. It is worth considering these differences when translating any discovery from a pre-clinical model in the lab to the clinic.

Nonetheless, the primary limitation of mouse models is also one of their strengths and as a reductionist model, the mouse remains an invaluable tool with many of the fundamental mechanisms in immunology largely conserved between the two species[183]. However, dogs remain an important pre-clinical model to validate the therapeutic efficacy of findings made in mice[109].

Mouse models of GVHD can be broadly subdivided into two categories based on the antigen driving the response; MHC-mismatched or MHC-matched, minor H antigen mismatched models of GVHD[91].

1.2.4.2 MHC-mismatched and MHC-matched, minor H mismatched models of GVHD

The majority of acute GVHD models in mice involve the transfer of T cell depleted (TCD) bone marrow from allogeneic donors supplemented with a defined number of donor T cells into lethally irradiated mice[181]. The bone marrow provides the stem cells required to reconstitute haematopoiesis after irradiation, preventing the mice from dying of bone marrow aplasia. T cells are normally depleted from the bone marrow graft in order to control the number and phenotype of donor T cells that are transferred. This can have a profound effect on the severity of acute GVHD, as the higher the number of donor T cells transferred, the greater the severity of GVHD that develops[19,179].

Mouse models of GVHD can be broadly subdivided into two categories based on the antigen driving the response; MHC-mismatched (Class I, Class II or both) or MHC-matched, minor H antigen mismatched models of GVHD[91]. Disparity in MHC (referred to as H-2 in mice) molecules is a key determinant of the severity of the GVHD that develops[181].

In models that are fully MHC-mismatched, the GVHD that develops is primarily CD4 T cell dependant and characterised by cytokine dysregulation and Th1 differentiation, although CD8 T cells do contribute to the pathology of the disease[91,117]. One of the most commonly used models of acute GVHD is the BL/6 (H-2b) → BALB/c (H-2d) strain combination, where BL/6 mice act as the donor and BALB/c mice as the recipient. BALB/c mice are transplanted with a combination of TCD BM and 0.5-2.0 $x10^6$ splenocytes derived from a BL/6 donor[185]. This is sufficient to induce system and lethal GVHD between 10 and 21 days after transplant depending on the number of splenocytes transplanted[181]. Incorporating transgenic strains such as B6.C-$H2^{bm1}$ (MHC Class $I^{-/-}$) and B6.C-$H2^{Bm12}$ (MHC Class $II^{-/-}$) into these models of acute GVHD has proven to be incredibly useful, enabling investigators to dissect the fundamental immunological mechanisms that underpin the pathogenesis of acute GVHD *in vivo*[186].

In MHC-matched, minor H mismatched models of GVHD, either donor CD8 T cells, CD4 T cells or both can be involved depending on the strain combination involved[91]. Since the majority of transplants in the clinic are HLA-matched, these models more closely reflect what occurs in the clinic and are associated with less morbidity than MHC-mismatched models[180,181].

One of the limitations of MHC-matched, minor H antigen mismatched models of GVHD is that it is difficult to know which alloantigen donor T cells are responding to. To address this, many models now use transgenic T cells that have a TCR with a defined specificity, usually to a single peptide epitope. This reduces the effect of bystander T cell activation as a result of the conditioning regime and allows the response to specific antigen to be closely tracked *in vivo*[181]. Using TCR transgenic T cells, the role of antigen affinity during acute GVHD was characterised using 2C TCR Tg T cells and more recently the role of host haematopoietic APC during H-Y mismatched GVHD using CD8 MataHari Tg T cells, which recognise a Y-chromosome derived peptide from the *Uty* gene[130,187–189]. These models have also been used to induce organ specific GVHD, where OT-1 CD8 T cells, which bear a TCR specific for ovalbumin peptide, transferred into K14-mOVA transgenic mouse, where keratinocytes constitutively express ovalbumin (OVA) peptide, induces skin specific GVHD[190].

The severity of acute GVHD that develops in mice is also dependant on a number of other factors[91,181]:

1. Radiation dose: The majority of models use TBI for conditioning. Several studies have now shown that the higher the dose of irradiation used the greater the degree of tissue damage that develops[191,192]. This results in a more intense ‘cytokine storm’ which is directly related to the severity of acute GVHD that develops. As a general rule, models that receive a myeloablative dose greater than 11 Gy require a split dose in order to reduce the gut toxicity associated

with the conditioning regime[181]. Different strains are also more sensitive to radiation than others and the maximally tolerated TBI or the dose that is myeloablative differs between strains (BALB/c>C57BL/6)[91]. In addition, F1 progeny are more resistant than parental strains (C57BL/6>F1)[91].

2. Dose and phenotype of donor T cells: The dose of donor T cells transferred into mice is directly proportional to the severity of GVHD that develops. In mice that receive TCD bone marrow alone, no acute GVHD will develop even across MHC-mismatches. The phenotype of T cells transferred into recipient mice is also important. In general, supplementing the bone marrow graft with alloreactive donor CD4 T cells will result in a higher GVHD-related mortality than that caused by the transfer of the equivalent number of alloreactive donor CD8 T cells[130,186,193]. The transfer of $CD44^{high}$ memory T cells or regulatory T cells (T_{Reg}) versus $CD44^{low}$ naïve T cells will also result in significantly less GVHD[140,194,195].
3. Environmental factors: The composition of the gut microflora can have a significant impact on the severity of GVHD. Mice kept under 'germ-free' conditions tend to be relatively resistant to acute GVHD, and gut decontamination using antibiotics can also reduce the severity of GVHD[108,196]. The difference in environmental pathogens between labs and suppliers can also introduce variance into acute GVHD models[181,197].

1.3 The relationship between antigen presenting cells and T cells

1.3.1 APC and T cell priming

To initiate acute GVHD, alloreactive T cells need to be primed. This is no easy task, given that the estimated precursor frequency for donor T cells specific for minor H antigens is between 1 in 10^5 and 1 in 10^6 and a single T cell occupies only one hundred-trillionth of the volume of the human body[70,198]. Yet, these T cells are still sufficient to drive acute GVHD in around 70% of patients undergoing allogeneic BMT[52]. Central to the development of acute GVHD are APC, which stimulate T cells to proliferate and differentiate into the effector cell subsets responsible for the tissue damage associated with acute GVHD.

APCs can be divided into two categories, haematopoietic and non-haematopoietic APC. Haematopoietic APC broadly include DC, macrophages, B cells and basophils[69]. Many of these cells are considered 'professional APC', cells that specialise in the uptake and presentation of exogenous antigen to lymphocytes via MHC Class I or Class II[199]. Non-haematopoietic APC include stromal cells in the lymphoid tissue and mesenchymal cells such as fibroblasts, myofibroblasts and pericytes found in the gut[200]. In response to inflammatory stimuli such as IFN-γ or TBI, these cells can upregulate their expression of MHC Class II and co-stimulatory molecules such as CD40, CD80 and CD86 and are capable of priming potent T cell responses to exogenous antigens[129,200–202].

Both haematopoietic and non-haematopoietic APC are capable of initiating acute GVHD. However, whether any specific population of APC has a non-redundant role in initiating GVHD remains controversial as depletion of DC, LC and B cells failed to prevent GVHD in pre-clinical models[125–127]. Non-haematopoietic APC can also replace the role of haematopoietic APC when antigen presentation is restricted in CD4-mediated GVHD[129].

To frame a discussion around the role of APC in GVHD, it is useful to consider their interactions with T cells from the perspective of a pathogen response. Among all APC subsets, DC are the most efficacious at priming naïve T cell responses *in vivo*[164]. Consistent with this and in the context of GVHD, in an MHC-mismatched transplant model where recipient mice were MHC Class II$^{-/-}$, the infusion of WT splenic DC was sufficient to induce GVHD when other APC subsets were incapable of presenting antigen[123].

DC are a heterogeneous population of bone marrow derived cells involved in the induction and regulation of adaptive immune responses[93]. First described in 1868, the contribution of DC to immunity was not fully appreciated until 1973 when Steinman and Cohn demonstrated that splenic DC in mice are key activators of adaptive immunity[203]. The importance of DC to T cell responses has been further highlighted using mouse models where conventional DC (cDC) are constitutively absent or conditionally depleted. In the absence of cDC, mice show diminished anti-viral, anti-bacterial and anti-tumour immune responses[204–206].

Although there are many different subsets, all DC are efficient antigen presenting cells and there are three specialised features that drive their capacity to promote immune responses[93]. Firstly, DC are widely disseminated throughout the body with many tissues such as the lung, gut and skin seeded with distinct subsets of DC that can migrate to local lymphoid organs[207–209]. This elegant sampling system exposes the adaptive arm of the immune system (T and B cells) to a diverse array of antigen increasing the chances of a rare T-cell clone encountering its target antigen.

Secondly, DC are equipped with a highly efficient endocytic system dedicated to the efficient capture, processing and presentation of antigen to lymphocytes[210,211]. In the steady state, “immature” DC in peripheral tissues specialise in the uptake of antigen via phagocytosis, macropinocytosis or adsorptive pinocytosis[93]. These antigens, usually in

the form of proteins, are enzymatically digested into immunogenic peptides and subsequently bound to MHC class I or class II molecules. Endogenous peptides are loaded onto MHC Class I promoting $CD8^+$ T cell responses whereas exogenous peptides are loaded on to MHC Class II promoting $CD4^+$ T cell responses (Figure 12)[212]. Certain subsets of DC can also "cross-present" antigen, a process first described by Bevan, whereby antigen synthesised in one cell can be captured exogenously and processed via the MHC class I pathway[213]. The cross-presentation pathway involves transfer of exogenously acquired antigens from the endosome to the cytosol, where they are subsequently trimmed by the proteasome, transported into the endoplasmic reticulum through the TAP complex and loaded onto MHC Class I molecules, similar to endogenous antigens[214]. This is an essential pathway for inducing CTL responses to viruses and intracellular bacteria that do not normally infect APC[215]. However, this also appears to be a restricted process, with DC by far the most efficient APC subset in terms of cross-presentation capabilities. For instance, $CD8^+$ DC appear to be especially efficient at the cross-presentation of antigen relative to $CD8^-$ DC, and are equipped with specialised machinery to control endosomal maturation and acidification that make them efficient at transporting antigens into the cytosol[216–218].

Thirdly, DC are equipped with a variety of pattern recognition receptors, including Toll-like receptors (TLRs) and lectins, conferring DC with enormous functional plasticity[219]. DC differentiate and mature in response to a variety of stimuli to generate an appropriate and targeted immune response[164]. This is an important step as DC exist in two functionally and phenotypically distinct states *in vivo*. Immature DC, which specialise in the uptake of antigen, are unable to stimulate T cells *in vitro* and induce peripheral tolerance *in vivo*[220]. Upon stimulation, a number of significant functional changes promoting migration and lymphocyte activation occur within a DC (Figure 14). The pH within endocytic vacuoles is lowered, activating proteolysis and the number of peptide-MHC complexes on the cell surface increases[210]. Co-stimulatory molecules

from the B7, TNF and Notch families begin to be expressed on the cell surface and immunostimulatory cytokines such as IL-12 and type 1 interferons are synthesised[164,221]. These 'secondary signals' are critical to the generation of a robust T cell response. In the steady state, DC laden with self-peptide migrate at low rates back to the draining lymph where they induce the deletion of autoreactive T cells and expand Treg populations due to the lack of co-stimulatory molecules and pro-inflammatory cytokine production[93,222].

Upon maturation, tissue-resident DC also become more motile, acquiring a phenotype that encourages their egress from the site of antigen uptake to secondary lymphoid tissues where they can interact with T cells[223]. In the skin, LC downregulate their expression of E-cadherin, a molecule that mediates their adhesion to keratinocytes, and upregulate their expression of the chemokine receptor CCR7 that allows their active and passive translocation from the skin to the T cell zone of skin draining lymph nodes (LN)[223–225]. In essence, DC maturation links innate and adaptive immune responses together.

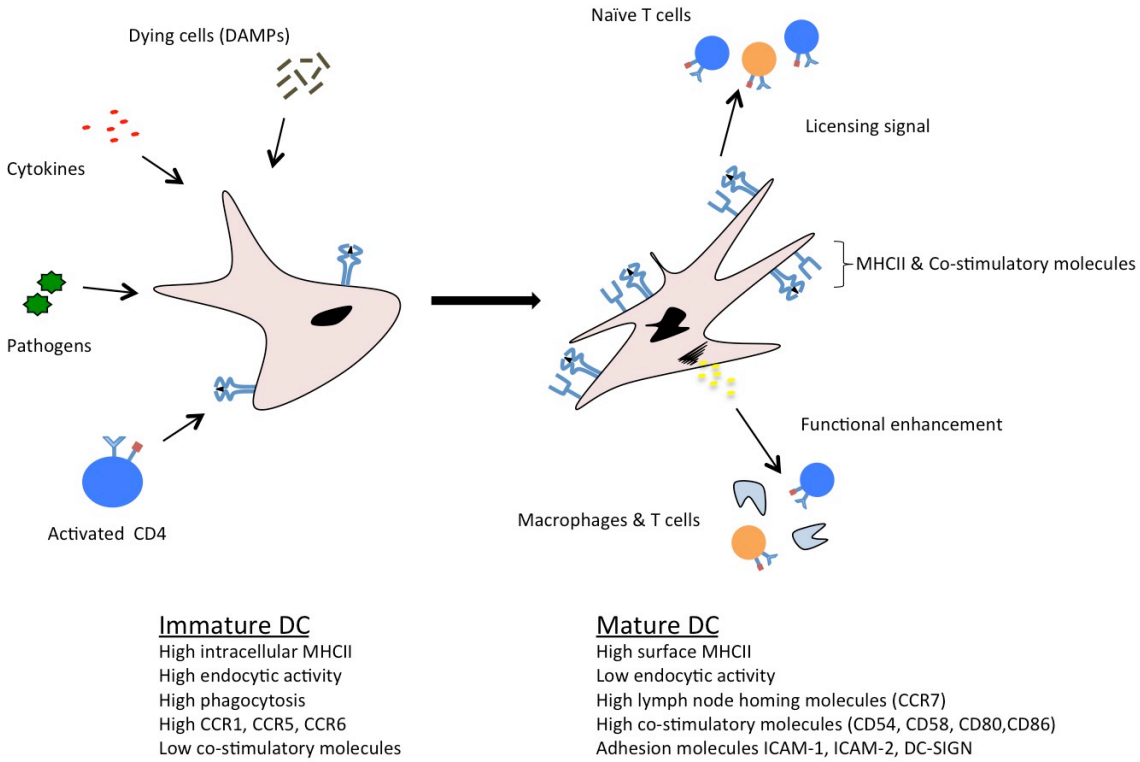

Figure 14: Overview of the dendritic cell maturation process. DC can be activated by a variety of stimuli via their pathogen-associated molecular pattern and danger-associated molecular pattern receptors. Following activation, DC undergo a maturation and differentiation process that switches their cellular machinery from antigen uptake to antigen presentation, promoting a phenotype that induces their active and passive migration to secondary lymphoid organs. Figure adapted from concepts proposed by Professor Steinman[93,164].

1.3.2 The role of tissue-resident APC in the peripheral regulation of T cells *in situ*

It is well established that T cells are essential for immunity against a wide array of pathogens and that DC are key activators of this response. To date, the role of DC in immunity has primarily been focused on the priming stage of the response. The paradigm follows that DC egress from the site of infection or inflammation following activation through their PRR and migrate to peripheral lymph nodes (pLN) in order to elicit an adaptive immune response[164]. DC then deliver antigen to the TCR of naïve T cells and provide them with the necessary co-stimulation and cytokines to prime them. Following activation, these T cells then undergo a programmed response of expansion and differentiation, upregulating effector molecules (perforin/granzyme) and cytokines before migrating to peripheral tissues where they aid in the clearance of a pathogen[226].

After this initial encounter in the draining LN (dLN), it is widely believed that T cells require no further interactions with DC to mediate their effector functions. However, several studies have now challenged this notion, advancing the idea that DC within peripheral tissues can significantly modulate the effector T cell (Teff) response *in situ*, shifting the balance away from regulation towards immunity[226,227].

Although maturation is typically associated with the migration of DC out of peripheral tissues, significant numbers do remain in infected and inflamed tissues[228]. In a mouse model of influenza A (IA), tissue-resident rDC were found to become refractory to migration signals after a period of transient migration to the lung dLN, leaving a significant population of respiratory DC (rDC) in the lungs[228]. This phenomenon is not isolated to the lungs with a significant population of LC remaining in the inflamed epidermis in a model of acute GVHD[229]. In addition, DC precursors are rapidly recruited to inflamed tissues where they rapidly replenish DC that have migrated to dLN. In models of herpes simplex virus (HSV) infection in the skin or IA infection in the lungs of mice, the number of DC present in the skin or lung after infection can far exceed that found in the steady state[230,231].

The development of murine models where DC can be conditionally depleted has enabled investigators to examine their role *in vivo* more closely and there is increasing evidence that tissue-resident and infiltrating DC populations can directly mediate changes in the activation, effector function, localisation and memory response of infiltrating Teff cells *in situ* at the site of infection or inflammation[226,227].

Depleting a specific cell type such as LC *in vivo* is a useful way of ascribing a function-based definition to a cell type, when its precise contribution to an immune response is unknown. There are two approaches commonly used to deplete cells *in vivo*, constitutive and conditional approaches. Given the multifaceted nature of DC and possible importance during development, inducible systems, such as the Diphtheria toxin receptor-Diphtheria toxin (DTR-DT) system, of conditional cell ablation have become a popular tool used to dissect the function of cells *in vivo*. Diphtheria toxin (DT) is a protein produced by *Corynebacterium diphtheria*, which once internalised inhibits protein synthesis via ADP-ribosylation causing cell death[232]. Taking advantage of rodent cells insensitivity to DT, the engineered expression of a human or simian DT receptor (DTR) by a particular cell type will render that cell susceptible to depletion by DT. However, other unmanipulated cell types will be unaffected upon exposure to DT[233]. This system is capable of depleting both non-dividing and terminally differentiated cells and has the added advantage of inducing cell death via apoptosis.

A critical role for DC *in situ* has been particularly well described in a model of IA infection in the lungs of mice. During infection, naïve CD8 T cells are primed in the dLN and subsequently traffic to the lung to clear the infection. Interestingly, these activated CD8 T cells rapidly proliferate upon entry into the lung in a way that directly correlates with the increased migration of DC to the lung[234]. Tissue-resident rDC were also found to promote rapid memory CD8 T cell responses *in situ* following reinfection[235]. Importantly, these tissue-resident memory CD8 T cells were maintained and activated by rDC even in the absence of secondary lymphoid organs[236].

However, the most interesting observations came from depletion models. Depleting respiratory DC (rDC) that remain in the lung 48 hr after infection with IA, by administering clodronate liposomes intranasally (i.n.), was also found to profoundly impair the CD8 T cell response *in situ*, resulting in increased mortality and viral titers[237]. In the absence of rDC, pathogen specific CD8 T cells did not proliferate or survive *in situ* in the lung and died via apoptosis[237]. Interestingly, this phenotype could be rescued by reconstituting infected lungs with pulmonary DC i.n. in a direct, MHC Class I dependent manner that was antigen specific and required co-stimulatory molecules (IL-15 and CD28)[237–239]. Thus, after their initial activation in the dLN, activated CD8 T cells require an antigen specific signal for a second time, provided here by rDC, for full effector function in the lung.

This observation and the proposed "two-hit" hypothesis where Teff cells require a second signal at the site of infection or inflammation has many implications. This phenomenon is also not isolated to CD8 T cells or the lung[226,227]. A similar observation has also been made in the mucosal tract of the vagina infected with HSV-2, where infiltrating $CD11b^+$ $CD11c^+$ inflammatory DC were required to elicit IFN-γ production by infiltrating CD4 T cells to mediate viral clearance[240]. In a model of atherosclerosis, DC localised in lesions express CCL17 which limited the expansion of Treg cells, enhancing disease[241].

In the liver, infiltrating $CD11b^+$ $CD11c^+$ inflammatory DC were observed to co-localise with CD8 T cells and are directly responsible for their proliferation *in situ* following lymphocytic choriomeningitis virus (LCMV) or hepatitis B virus (HBV) infection[242]. In these models of infection, DC:T cell interactions also required co-stimulation as pharmacological blockade of CD80, CD86 and OX40L on the surface of inflammatory DC prevented CD8 T cell proliferation[242]. In an experimental model of autoimmunity, CD4 T cells were shown to interact with kidney DC *in situ* in the liver to produce cytokines and recruit autoreactive CD8 T cells[243].

Similarly, in the skin, the depletion of CD11b^{high} dermal DC (dDC) impaired CD4 Teff responses in the skin[244]. CD11b^{high} dDC were required to present antigen to CD4 Teff directly in the skin for full effector function, promoting IFN-γ secretion by Th1 type cells that impaired the expansion of Tregs[244].

It is clear from the number of recent studies that the role of DC in mediating T cell responses extends far beyond the initial priming event in the dLN. Tissue-resident DC can modulate both CD4 and CD8 Teff responses in a wide variety of tissues, and contribute to the activation, survival and memory response of these T cells[226,245]. In the context of acute GVHD, the role of tissue-resident and infiltrating APC, such as DC, outside of the initial priming response remains an area less well investigated.

1.4 Langerhans cells and T cell-mediated immunopathology in the skin

1.4.1 Immunopathology in the skin

The skin is the largest organ in the body by surface area and is the primary interface between the body and the environment. Acting as a barrier to a variety of chemical, microbial and physical challenges, the skin has evolved a highly sophisticated system of immune surveillance and defense that maintains a finely tuned equilibrium[209,246]. One such feature is the rich and complex network of DC found in both the epidermis and dermis.

DC play a key role maintaining immune homeostasis in the skin, where they facilitate a rapid and protective immune response to infections when required. However, the regulation of these responses is also critical as inappropriate or misdirected activity can lead to a variety of inflammatory skin disorders such as atopic and contact dermatitis and psoriasis[247–249]. Therapies to disease have also led to the development of new autoimmune disorders of the skin, with cutaneous GVHD after allogeneic BMT a detrimental side effect of an otherwise life-saving therapy[247].

The contribution of dysfunctional DC responses to the pathogenesis of autoimmune disorders in the skin has long been recognised[250]. DC can directly prime autoreactive T cells, secrete cytokines to enhance innate and adaptive immune responses and more recently, have been recognised to interact with autoreactive T cells *in situ* to maintain this response. In psoriatic lesions in the skin, high numbers of infiltrating $CD11c^+$ DC expressing the inflammatory mediators TNF-α and inducible nitric oxide synthase (iNOS) directly damage tissue[251]. The pathogenesis of this expression profile to psoriasis is highlighted by the effectiveness of TNF-α blockers in ameliorating disease[252]. Delineating the regulatory and functional mechanisms of DC *in situ* in the skin may bring about an important therapeutic step to the treatment of acute and

chronic autoimmune disorders or to the enhancement of pathogen and tumour clearance.

1.4.2 Immunosurveillance in the skin: Langerhans cells

LC are a population of DC found in the skin that form a dense interlacing network within the epidermis[253]. The only DC population found within the epidermis, they are characterised by their expression of the C-type lectin, Langerin, and presence of Birbeck granules in the cytoplasm[253]. Originally thought to be similar to most other non-lymphoid cDC, LC are well equipped to efficiently capture, process and present antigen via MHC and migrate to the skin dLN upon maturation[254]. However, LC are now known to have a number of unique features that distinguishes them from other cDC found in the skin (dermis).

Unlike dermal DC (dDC), which arise from pre-DC precursors from the bone marrow and are dependent on fms-like tyrosine kinase 3 ligand (Flt3L), LC are derived from yolk sac derived precursors and fetal liver monocytes that seed the skin before birth and differentiate in response to IL-34 secreted by keratinocytes[255–257]. LC also have the unique ability to maintain themselves in the epidermis throughout life by proliferating *in situ*, without any further input from bone marrow derived precursors[258]. Furthermore, LC were also found to be radioresistant and remain of host origin in the epidermis after lethally irradiated mice are reconstituted with congenic bone marrow, unlike radiosensitive DC in the dermis[258]. Taken together, it is hypothesized that this mode of replenishment by LC may constitute a unique adaption to the epidermis, which lacks a vascular system of its own and is separated from dermal blood vessels by the basement membrane, making their environment quite distinct from other DC found in the dermis[259].

Despite extensive research, the precise role of LC *in vivo* remains elusive with evidence supporting a role for LC in a number of functions that are both immunogenic and tolerogenic[259]. The development of new mouse models has stimulated LC research somewhat and yielded a number of new insights. Adapting the inducible DTR-DT system of conditional depletion to the field of LC, a simian DTR and enhanced green

fluorescent protein (EGFP) cassette was integrated into the Langerin gene to create the Langerin-DTR mouse[260]. This new model enabled LC to be conditionally depleted at any time with a single injection of DT without any apparent side effects enabling investigators to specifically test the role of LC *in vivo*[260].

Accounting for around 3-5% of all nucleated cells in the epidermis of both humans and mice, LC are tightly associated with keratinocytes via E-cadherin and are the first APC to encounter antigen in the skin[254,259]. This lead to the widespread belief by many investigators that LC were immunogenic and pivotal to the development of cutaneous immunity ("The LC Paradigm"). Initial *in vitro* studies supported this hypothesis, as matured LCs from both humans and mice were found to be intrinsically potent inducers of naïve T cells[261,262]. However, with the development of cell depletion models, doubts surrounding the immunodominance of LC in initiating cutaneous immunity *in vivo* began to emerge.

The first study questioning their role came from a mouse model of HSV infection, when LC failed to prime virus-specific CTL in the skin dLN[263]. Similar observations were also made in a model of murine Leishmaniasis, where LC again failed to prime an immune response to a pathogen invading the skin[264].

Several recent studies have now demonstrated that LC can have immunosuppressive functions, suggesting a role for LC as negative regulators of cutaneous immunity that can inhibit T cell responses elicited by other DC in the skin. In a murine model of contact hypersensitivity (CHS), the acute ablation of LC was found to increase CHS in response to the topical application of low doses of haptens[265]. Revisiting the murine model of Leishmaniasis, the selective depletion of LC attenuated the disease, with a reduction in Treg infiltration and an enhanced Th1 response[266]. In an experimental model of allergic contact dermatitis in mice, LC conferred protection from the

development of CHS, dampening the pathogenic allergen-specific CD8 T cell response and promoting the expansion of Treg[267].

However, the roles ascribed to LC *in vivo* have not been entirely tolerogenic. Using a Candida albicans infection model, direct presentation of antigen by LC was required to generate antigen-specific Th17 cells[268]. Similarly, LC that sampled antigen through keratinocyte tight junctions by extending their dendrites were able to elicit humoral immunity to staphylococcal antigens that had not yet penetrated the skin[269]. Thus, the role of LC in the skin can no longer be thought of as purely immunogenic and substantial controversy remains as to their precise function *in vivo*.

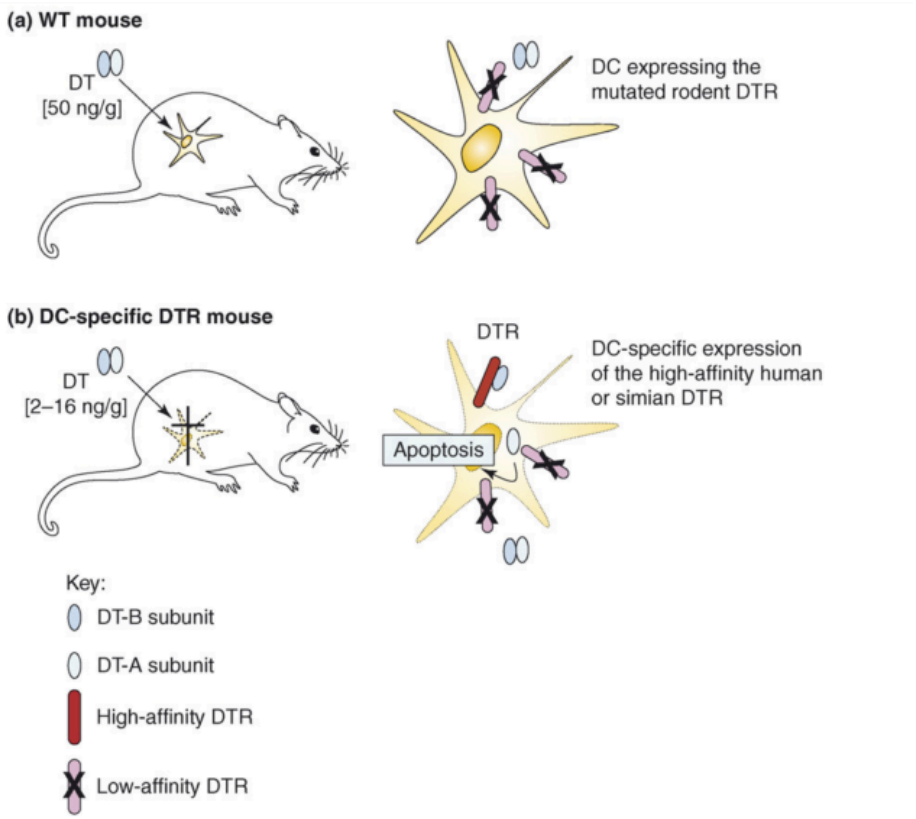

Figure 15: Depletion of Langerhans cells via the DTR-DT system in mice. A. Mouse cells are 10^3 to 10^5 times more resistant to DT mediated apoptosis than human or simian cells, due to a mutation in the receptor that binds the DT-B subunit. The injection of DT i.p. into a WT BL/6 mouse has no effect on LC or Langerin$^+$ dermal DC *in vivo*. **B.** A high affinity simian DTR was knocked into the Langerin gene that is expressed in LC and Langerin$^+$ dDC cells rendering both populations sensitive to DT-mediated apoptosis. This was found to have no effect on the natural development of LC or Langerin$^+$ dermal DC *in vivo*. After a single injection of 400 ng of DT i.p., both LC and Langerin$^+$ dDC are efficiently depleted within 24 hr. The DT-B subunit binds the high affinity simian receptor and facilitates the entry of the DT-A subunit into the cell that inhibits protein synthesis by ADP-ribosylation, inducing apoptosis. Reprinted with permission from Trends in Immunology[270].

1.4.3 Immunosurveillance in the skin: Langerin$^+$ dermal dendritic cells

The remarkable heterogeneity and functional plasticity of DC has long been recognised and the skin is no different[271]. Finding a role for LC *in vivo* became even more complex with the discovery of a novel Langerin expressing DC population in the dermis of mice, the aptly named Langerin$^+$ dDC[272–274]. An unexpected finding, Langerin$^+$ were first identified when a Langerin$^+$ population was seen to rapidly repopulate the dermis (<7 days) shortly after LC depletion in the Langerin-DTR mouse[275]. This was an unusual observation as LC were not normally found in the skin less than 6 weeks after depletion. Once thought to be migrating LC, Langerin$^+$ dDC are now known to be distinct subset of DC in mice. In contrast to LC, they develop independently of TGFβ1, exhibit differential expression of both EpCAM and CD11b, express CD103 and have dissimilar repopulation and migratory kinetics[275,276].

In terms of function, Langerin$^+$ dDC appear to be highly immunogenic[253,259]. Refining the HSV-1 skin infection model, Langerin$^+$ CD103$^+$ dDC were the only migratory subset of DC from the skin to efficiently present HSV-1 antigens to naïve CD8 T cells, although all subsets presented HSV-1 antigens to CD4 T cells[277]. In the same study, Langerin$^+$ CD103$^+$ dDC were also shown to efficiently cross-present skin derived self-antigens[277]. Similarly, using K5.mOVA mice that express OVA peptide in the epidermis, Langerin$^+$ dDC excelled in the cross-presentation of antigen to OT-I T cells, irrespective of the presence or absence of LC[276]. Using a Candida albicans model, Langerin$^+$ CD103$^+$ dDC were also required for the generation of a Th1 type response and inhibited the ability of LC and other DC to promote Th17 type responses[268].

Langerin$^+$ CD103$^+$ dDC are now purported to be the main cross-presenting APC in the skin in terms of CD8 T cell immunity[276,278]. The potency of Langerin$^+$ dDC in these responses is remarkable as they account for less than 5% of DC in the dermis[254]. A homologue to the Langerin$^+$ dDC has now been found in the skin of humans and similar Langerin$^+$ dDC like subsets of DC have now been found in the liver, lung and

kidney, yet their precise function remains poorly studied *in vivo*[272,279,280]. However, in the lung, a Langerin$^+$ DC has been shown to be essential in the clearance of influenza in mice[231].

1.5 Project Rationale

1.5.1 A role for Langerhans cells in regulating cutaneous GVHD?

LC are radioresistant in both humans and mice and have been found to persist in skin allografts years after transplant through continuous *in situ* proliferation[258]. In the context of allogeneic BMT, a recent study observed a significant delay in the engraftment of donor LC in patients that receive non-myeloablative conditioning compared to patients that receive myeloablative conditioning and full donor LC chimerism was only reached 84 days after transplant[281]. Recipient LC were able to proliferate *in situ*, indicating they remained viable and capable of maturation for a significant period of time after non-myeloablative transplant.

This feature along with the immunogenic nature of host APC in the initiation of acute GVHD make LC of interest to transplant clinicians. Elegant bone marrow chimera experiments, exploiting LC radioresistance, have already shown that LC are capable of initiating GVHD-like lesions in the skin under circumstances where all other DC subsets in the skin are incapable of antigen presentation[282]. This suggested that host LC directly interacted with alloreactive donor T cells in the skin, dLN or both. However, in the presence of other DC subsets in the skin, LC were found to be redundant with systemic CD8- and CD4-mediated GVHD developing in a pre-clinical mouse model in the presence or absence of both donor and host LC[126].

An area less well investigated is the role of tissue-resident APC populations in GVHD target organs after alloreactive donor T cells are primed. Previous work in our lab showed that an inflammatory checkpoint operates in the skin that is critical to the recruitment and function of effector cells[283]. In this model, topical application of the TLR 7-8 agonist Imiquimod to the skin of established MHC-mismatched mixed chimeras (where donor and host haematopoietic cells co-exist) at the time of allogeneic donor T

cell transfer, induces the recruitment of alloreactive CD8 T cells to the epidermis and development of localised cutaneous GVHD.

To assess whether host LC have a role regulating this checkpoint when other DC populations are present, we adapted the model of localised cutaneous inflammation described above to Langerin-DTR mice, enabling us to specifically deplete host LC upon a single injection of DT[229]. Interestingly, in the absence of host LC, mice developed significantly less GVHD in the skin as evidenced by histopathological scoring[229]. The absence of host LC had no effect on the priming or number of alloreactive T cells found in skin draining lymph nodes, nor was the homing ability of CD8 T cells to the epidermis impaired. However, the capacity of CD8 T cells, recruited to the epidermis, to induce localised GVHD was impaired. When infiltrating T cells were purified from the epidermis, the expression of a number of key effector molecules such as IFN-γ, TNF-α and TRAIL were significantly reduced in the absence of host LC.

This study described a new regulatory role for LC in the skin, where primed infiltrating CD8 T cells required a "second-hit" for full effector function[229]. Whether this interaction *in situ* has a role in the development of cutaneous GVHD in a model of acute GVHD remains to be determined. Haematopoietic APC subsets appear to be dispensable in the context of priming GVHD. However, given the number of recent reports expanding the role of DC beyond T cell priming in the dLN, it is worth investigating the role of tissue-resident APC in the development of organ specific pathology in pre-clinical models of acute GVHD. The identification of cell subsets that are critical for this response could lead to the development of novel targets for organ specific immunosuppression that may not interfere with the beneficial effects of systemic GVL.

Hypothesis: Host Langerin$^+$ DC are required for the development of cutaneous GVHD.

1.5.2 Aims & Objectives

The primary aim of my project was to investigate the nature of DC:T cell interactions in the skin, using GVHD as a model of immune pathology. Dissecting the nature of these interactions could lead to the identification of novel skin-specific targets for immunosuppression without compromising the therapeutic benefits of GVL. To date, the role of LC in GVHD remains controversial and the contribution of other DC populations in the skin, such as Langerin$^+$ dDC, remains unclear. To address these questions, I developed three objectives:

1. The first objective of the project was to investigate the role of LC and Langerin$^+$ dDC in an established MHC-mismatched model of BMT. Our lab has already identified a role for host LC in this model[229], therefore I investigated whether host Langerin$^+$ dDC were required for cutaneous GVHD in this model.
2. The second objective of the project was to investigate the role of LC and Langerin$^+$ dDC in a MHC-matched, minor H antigen mismatch model of GVHD. This type of model more accurately reflects what happens in the clinic as the majority of allogeneic transplants are HLA-matched. However, minor H antigens are still capable of inducing GVHD and recipients of sex-mismatched grafts are known to have a poorer outcome than those that receive grafts that are sex-matched[284]. To accomplish this, I developed a minor H antigen-mismatched transplant model in the lab, using sex mismatched transplants (F→M) and transgenic (Tg) T cells specific for H-Y peptide to induce GVHD.
3. The third objective of the project was to further explore the nature of LC and T cell interactions in the skin. To this end, I developed a model whereby LC could be locally depleted *in situ* to investigate whether LC were required directly in the skin for GVHD. I also sorted LC and T cells from the epidermis and dermis of transplanted mice (F→M) to investigate differences in gene expression in the presence or absence of host LC.

2 Materials and Methods

2.1 Antibodies

Anti-CD103 (M290), anti-CD11c (HL3), anti-CD45.2 (104) anti-CD8α (53-6.7), anti-H2Dd (34-2-12), anti-H2Kb (AFC-88.5), anti-Vβ8.3 (1B3.3) and anti-IFNγ (XMG1.2) were purchased from BD Bioscience (USA). Anti-CD11b (M1/70), anti-CD24 (M1/69), anti-CD4 (GK1.5), anti-CD44 (IM7), andti-CD45.1 (A20) anti-CD62L (MEL-14), anti-CD8β (H35-17.2), anti-EpCAM (G8.8), anti-MHCII (M5114.15.2), anti-Thy1.1 (HIS51) and anti-γδ (eBioGL3) were purchased from eBioscience (USA). Anti-CD86 (RMMP-1) was purchased from Immunotech (Beckman Coulter, USA). Detection of biotinylated antibodies was performed using APC, FITC, PE and PerCp-Cy.5.5 conjugated to streptavidin (BD Bioscience, Germany). More recently, eFluor450 conjugated to streptavidin was used (eBioscience, USA). Intracellular staining of Langerin (CD207) was performed using BD's Cytofix/CytopermTM fixation/permeabilisation solution kit (BD Bioscience, Germany) in conjunction with an anti-CD207 PE (eBioL31) antibody purchased from eBioscience.

2.2 Animals

C57BL/6 and BALB/c mice were purchased from Charles River Laboratories (Margate, UK) and bred in house by UCL Biological Services (Royal Free Hospital, UK). BALB/c.PL-ThyaCy (Thy1.1) mice were purchased from The Jackson Laboratory (Bay Harbour, USA) and bred in house. Langerin.DTREGFP (Langerin-DTR) mice were kindly provided by Bernard Malissen and Adrien Kissenpfennig (Université de la Mediterrannée, France) and bred in house. H-Y TCR transgenic MataHari mice were kindly provided by Jian Chai (Imperial College London, UK) and bred in house. Mice used as recipients for BMT were between 10 and 20 weeks old. Mice used as donors were between 8 and 20 weeks old. All procedures were conducted in accordance with the United Kingdom Home Office Animals (Scientific Procedure) Act of 1986. The present experiments were reviewed and approved by the Ethics and Welfare Committee of the Comparative Biology Unit, Royal Free and University College London Medical School, London.

2.3 Assessment of GVHD

To evaluate the severity of GVHD both clinical and histological parameters were used to access mice. Clinical signs of GVHD were assessed using a six parameter scoring system. Mice were scored for ruffled fur, hunching, loss in activity, diarrhoea and eye opening (Table 3). Recipient mice were also weighed on the day of BMT and at least three times weekly thereafter to track weight loss relative to Day 0. Mice were culled for humane reasons if their cumulative score was ≥4. Upon death, specimens of GVHD target organs were collected, fixed in 4% formaldehyde, embedded in paraffin, cut into sections and stained with haematoxylin and eosin for examination.

These histopathological sections were then scored single blinded using a severity scale, as reported previously[283]. The severity scale ranged from 0-4: 0, normal; 0.5, focal and rare; 1, focal and mild; 2, diffuse and mild; 3, diffuse and moderate; 4, diffuse and severe. Changes in the colon (crypt regeneration, crypt epithelial cell apoptosis, crypt loss, surface colonocyte attenuation, lamina propria inflammatory cell infiltrate, mucosal ulceration and thickness of the mucosa), liver (portal tract inflammatory cell infiltrate, lymphocytic infiltrate of bile ducts, bile duct epithelial cell apoptosis, vascular endothelialitis, parenchymal apoptosis, parenchymal microabcesses and parenchymal mitotic figures), lung (perivascular cell infiltrate, peribronchiolar cell infiltrate and alveolar/interstitial infiltrate) and skin (epidermal/dermal lymphocytic infiltrate, dyskeratotic epidermal keratinocytes and epidermal thickening) could then be assessed for signs of GVHD.

Score	Fur (Angle, °)	Hunching	Activity	Diarrhoea	Eyes (% Closed)	Weight Loss (%)
0	Normal	No hunching	Normal	Absent	Normal	≤10
0.25	-	-	-	-	>0 - ≤25	-
0.5	>0 - ≤45	Slight, lost on movement	Mild reduction, resists handling	-	>25 - ≤50	-
1	>45 - ≤90	Significant, reduced on movement	Severe reduction, no resistance	Present	>50 - ≤75	≥10
1.5	-	-	-	-	>75 - ≤100	-
2	>90	Severe, present on movement	No spontaneous movement	-	Closed	-

Table 3: Overview of the clinical scoring system used to assess GVHD in mice.

2.4 Bone Marrow Transplantation

BMT was performed as described before with modifications[285,286]. The fluoroquinolone Baytril (0.15 mg/ml; Bayer, Germany) was added to the drinking water of all transplant recipients a week before transplant. In MHC-matched, minor H mismatch of model of GVHD, male BL/6 (or Langerin-DTR) recipients were lethally irradiated (11 GY, 0.55 GY/min separated into 2 cycles over 48 hr) and reconstituted with mixture of 5 $x10^6$ bone marrow cells and 2 $x10^6$ CD4 T cells derived from female WT BL/6 mice and 1 $x10^6$ Mh CD8 T cells derived from female H-Y TCR transgenic MataHari mice injected intravenously (i.v.) in the tail vein 4 h later. The bone marrow was harvested by flushing the tibia and fibula with bone marrow medium (RPMI-1640, 10 mM HEPES, 10 μg Gentamycin). $CD8^+$ and $CD4^+$ T cells were isolated from the spleens of female MataHari and WT BL/6 mice respectively, by positive selection using anti-CD8α (Ly-2; Miltenyi, Germany) and anti-CD4 (L3T4; Miltenyi, Germany) magnetic-activated cell sorting (MACS) beads and LS columns (Miltenyi, Germany). Briefly, spleens were mashed, passed through a 40 μm cell strainer (BD, USA) and ACK lysed (Lonza, Switzerland), as per manufacturers instructions. The splenocytes were then washed in ice cold MACS buffer (PBS, 2% BSA, 2mM EDTA) and resuspended in 90 µL buffer per 1 $x10^7$ cells. 10 µL anti-CD8α- or anti-CD4 microbeads were added per 1 $x10^7$ cells and the suspension was incubated for 15 min at 4°C. Cell were washed by adding 1 ml of MACS buffer per 1 $x10^7$, resuspended in minimum of 500 µL per $1x10^8$ cells and transferred to a rinsed LS column attached to a MidiMACS separator. The column was washed with 3 x 3ml of MACS buffer before being removed from the separator. The purified $CD8^+$ and $CD4^+$ T cells were then flushed from the LS column with 5 mL of MACS buffer using the plunger provided. Purity was confirmed by flow cytometry before Mh CD8 T cells, polyclonal CD4 T cells and BM were resuspended in PBS and stored on ice before infusion.

To generate [Langerin-DTR+BALB/c→BL/6] mixed chimeras (MC), recipient BL/6 mice were lethally irradiated (11 GY, 0.55 GY/min separated into 2 cycles over 48 hr) and reconstituted with 20 $x10^6$ TCD BM derived from the tibia and fibula of Langerin-DTR and BALB/c mice mixed at a 1:1 ratio injected i.v. in the tail vein 4 h later. The bone marrow was by TCD by negative selection using anti-CD3ε-biotin, anti-biotin microbeads and an LD column (Miltenyi, Germany), as per manufacturers instructions. T cell depletion was confirmed by flow cytometry before the BM mix was resuspended in PBS and infused into recipients. Mixed chimeras were allowed to recover for 8 weeks before their chimerism was analysed. All mice are female unless otherwise stated. In GVHD experiments, DLI was administered to chimeras no less than 8 weeks after transplant. An allogeneic SC suspension of 30 $x10^6$ cells injected i.v. was used for DLI as described previously[229]. 4 mg Imiquimod (3M Pharmaceuticals, USA) was then applied to a shaved area of skin at the base of the tail on days 0, 5 and 10 after donor SC to induce cutaneous GVHD.

To generate [Langerin-DTR→BL/6] chimeras, recipient male BL/6 mice were lethally irradiated (11 GY, 0.55 GY/min separated into 2 cycles over 48 hr) and reconstituted with 5 $x10^6$ TCD BM derived from the tibia and fibula of male Langerin-DTR mice injected i.v. in the tail vein 4 h later. TCD was carried out as described before.

2.5 Depletion of Langerin$^+$ DC

To systemically deplete Langerin$^+$ DC, Langerin-DTR mice were injected i.p. with 400 ng of DT in 200 μl sterile PBS. All experiments involving DT were controlled with the i.p. injection of 200 μl sterile PBS into littermates in parallel.

To locally deplete Langerhans cells. Langerin-DTR mice were placed under general anaesthesia using an isoflurane machine. Briefly, mice were moved to an induction chamber and placed under general anaesthesia using 3-4% isoflurane with an oxygen flow rate of 1 l/min. Once asleep, anaesthesia was maintained using a nose cone while Langerin-DTR mice were injected with 25 ng of DT in 20 μl i.d. into the dorsal and ventral side of the left ear. Mice were placed under a heat source and observed until fully recovered.

2.6 Flow cytometry

Homogenous single cell suspensions were incubated with 2.4 G2 antibody for 10 min at 4°C to block Fc receptors. Cells were washed using FACS buffer (PBS, 2% FBS, 2mM EDTA) and subsequently incubated with flurochrome-conjugated primary antibodies in 75 μl at saturating concentrations for 15 min at 4°C. The samples were washed using FACS buffer and the cells were incubated with a secondary antibody if necessary. For intracellular staining, samples were incubated with BD Cytofix solution for 10 min at 4°C. Samples were washed with X1 BD Perm buffer. The fixed samples were incubated with intracellular antibody (IFN-γ or CD207) in X1 BD Perm buffer for at least 1 hr at 4°C and subsequently washed with X1 BD Perm buffer. All stained samples were re- suspended in FACS buffer before flow cytometry.

Multiparamter flow cytometry was performed using BD LSRII, LSRFortessa and FACSCalibur systems (BD Bioscience, Germany). All samples were filtered using a 40 μm cell strainer before acquisition. Propidium iodide (PI) was added to samples derived from the liver, lung and LP+PP at least 10 min before acquisition. Analysis was carried out using Tree Stars Flowjo software (v8.7). For each experiment appropriate single stain controls were used to compensate each channel.

2.7 Isolation of epidermal and dermal cells

Skin tissue from the ears and/or body skin was excised and stored in HBSS on ice. The skin was processed in accordance with a published protocol with slight modifications[276]. The ears were split into dorsal and ventral sections. Samples were then incubated at 4°C overnight or for 45 min at 36°C in a solution of HBSS containing 2.5 mg/ml Dispase II (Roche, Germany) and 2% FBS (Biosera Ltd, UK). The epidermis and dermis was carefully separated using a fine forceps. Epidermal sheets were transferred into a bijou containing PBS and 5% FBS. Bijou is vortexed repeatedly before the sample was passed through a 40 μm cell strainer (BD Bioscience, USA) into a 50 ml falcon tube washing with FACS buffer (PBS, 2% FBS, 2mM EDTA) to create a homogenous cell suspension. Dermal sheets were cut into small pieces and digested for 1 hour at 37°C in HBSS containing 2750 U/ml collagenase type IV (Worthington Biochemical Corporation, USA) and 5% FBS. 1mM EDTA was added and the samples incubated for 5 minutes at room temperature. The samples were then agitated and passed through a 40 μm nylon cell strainer into a 50 ml falcon tube washing with PBS to create a homogenous single cell suspension.

2.8 Isolation of lymphocytes from lymphoid and peripheral tissues

To isolate SC, a cell strainer was placed in a mini petri dish in 1 ml of ACK lysis buffer. The spleen was added to the cell strainer and mechanically disassociated using the plunger from a syringe. The sample was swirled for 1 min before 9 ml of PBS was added. The sample was subsequently washed in FACS buffer.

To isolate skin draining lymph nodes (axial, brachial, inguinal and cervical), samples were mechanically disassociated using the barrel of a 2ml syringe and passed through a 40 μm cell strainer before being washed and resuspended in FACS buffer.

Lymphoid cells were counted using a haemocytometer under a light microscope. Cell viability was assessed using 0.1% trypan blue (Sigma, USA) in PBS.

To isolate lymphocytes from the blood, 100 μl of blood was collected from the tail vein into an eppendorf containing 10 μl heparin. RBC were lysed using water shock treatment where 100 μl of blood was added to 9 ml of distilled H_2O for 10 sec before 1 ml of X10 PBS was added. Samples were subsequently washed in FACS buffer.

To isolate lymphocytes from the lung, a needle was carefully inserted into the trachea post mortem and the lungs flushed with PBS. The lungs were excised, cut into small pieces and digested for 1 hour at 37°C in HBSS containing 2750 U/ml collagenase type IV and 5% FBS. Using the plunger from a 2 ml syringe the sample was mechanically disassociated passing it through a 40 μm cell strainer into a falcon tube, washing with FACS buffer. RBC were lysed using ACK lysis buffer and the cells were washed with FACS buffer.

To isolate lymphocytes from the liver, a needle was carefully inserted into the portal tract vein post mortem and the liver perfused with PBS. The liver was excised, cut into small pieces and digested for 1 hour at 37°C in HBSS containing 2750 U/ml collagenase type IV and 5% FBS. Using the plunger from a 2 ml syringe the sample

was mechanically disassociated passing it through a 40 μm cell strainer into a falcon tube, washing with FACS buffer. RBC were lysed using ACK lysis buffer and the cells were washed with FACS buffer.

To isolate lymphocytes from the lamina propria and peyer's patches (LP+PP), two 5 cm of the small intestine were excised and flushed with PBS using a syringe and a forceps to remove faecal matter. LP+PP samples were cut longitudinally to increase surface area and incubated with HBSS containing 10 mM EDTA and 2% FBS in a bijou at 36°C with shaking (200 rpm) for 10 min. LP+PP samples were washed with HBSS and the process repeated twice more. LP+PP samples were cut into small pieces and digested for 1 hour at 37°C in HBSS containing 2750 U/ml collagenase type IV and 5% FBS. Using the plunger from a 2 ml syringe the sample was mechanically disassociated passing it through a 40 μm cell strainer into a falcon tube, washing with FACS buffer.

2.9 Isolation of primed MataHari T cells for secondary transfer

Adapting a previously published protocol with slight modification, primed Mh T cells were isolated from the skin draining lymph nodes using nylon wool[287]. 0.5 g of nylon wool (G Kisker, Germany) was loaded into a 10 ml syringe up to the 5 ml mark. This was then autoclaved. The column was washed with 20 ml sterile CML-V medium (RPMI-1640, 2nM L-Glutamine, 100 μM β-mercaptoethanol, 100 units/ml Penicillin, 100 μg/ml Streptomycin, 5% FCS, 10 mM HEPES), the syringe end capped and 2 ml of CML-V added. This is then incubated for 30 min at 37°C. The syringe was kept sterile, storing it in a 50 ml falcon tube.

The skin draining lymph nodes are harvested from the transplanted recipient. Using the plunger from a 2 ml syringe the sample was mechanically disassociated passing it through a 40 μm cell strainer into a falcon tube, washing with warmed CML-V medium. The sample was resuspended in 2 ml warmed CML-V medium.

The 2 ml of medium used to rinse the nylon wool was drained and the syringe end capped again. 2 ml of the lymph node suspension was added drip wise and more 2 ml of CML-V medium added on top. The sample was incubated for 45 min at 37°C and the suspension subsequently eluted using 10 ml of medium. The sample was washed three times with PBS and counted using a haemocytometer.

2.10 Langerin-DTR genotyping

To genotype Langerin-DTR mice, a small excision of skin was taken from tail. To isolate genomic DNA, the tissue was placed in a 1.5 ml eppendorf with 75 μl of Buffer A (25 mM NaOH, 0.2 mM EDTA, pH12) and incubated for 15 min at 95°C. Sample was allowed to cool before 75 μl of Buffer B (40 mM Tris-HCL, pH 5.5) was added to neutralise the reaction[288]. 1 μl of the mix was then used for PCR.

For PCR, 1 μl of genomic DNA was added to a master mix containing, 1 μl of each primer in Table 4, 5 μl 2X Phusion PCR Master Mix (New England BioLabs, USA) and 1 μl H_2O. Samples were run on a DNAEngine (BioRad, USA) thermal cycler according to the cycle specified in Table 4. All samples were run with positive and negative controls.

Genomic DNA (10 μl) was then combined with 2 μl of X6 blue gel loading dye (NEB, USA) and loaded on to a 1.5% agarose gel containing SYBR safe (Life Technologies, USA) in X1 TAE buffer (Thermo Scientific, USA) and run at 100 V for 35 min. using Gel Doc XR system (BioRad, USA). Langerin-DTR band was 700 bp. WT BL/6 was 300 bp.

Primer	**Oligonucleotide Sequence (5' – 3')**	
WT Forward	GAA TGA CAG ATC TGG CCT GAG CTC G	
DT Forward	TTC CAG CAG CTA GCC CTC TCC GAA	
Common	GTA GCT TTT ATA TGG TCA GCC AAG G	
Step	**Temp (°C)**	**Time (min)**
1	94	5
2	94	1
3	60	1
4	72	2
5	Repeat steps 2-4 35 times	
6	72	3
7	10	Hold

Table 4: Langerin.DTREGFP primers and cycling protocol.

2.11 MataHari *in vitro* restimulation assay

Spleens were harvested from transplanted recipients and female WT BL/6 donors and mashed through a 40 μm cell strainer (BD, USA) using sterile PBS (Lonza, USA) into a 50 ml falcon tube. SC were centrifuged for 5 min at 1500 RPM using an Eppendorf 5804 centrifuge (Eppendorf, Germany). SC were resuspended in ACK lysis buffer and allowed to stand for 1 min before 9 ml of sterile PBS was added. SC were washed twice by suspending the samples in PBS and centrifuging for 5 min at 1500 RPM. SC were counted using a haemocytometer and resuspended in CML-V medium (RPMI-1640, 2nM L-Glutamine, 100 μM β-mercaptoethanol, 100 units/ml Penicillin, 100 μg/ml Streptomycin, 5% FCS, 10 mM HEPES) at a concentration of 1 x10^7 cells/ml. 100 μl of SC from transplanted recipients and female WT BL/6 donors were plated together in a 96 well, round bottomed plate (Corning, USA). 5 μM of relevant (WMHHNMDLI) was added to SC and 5 μM of irrelevant (SIINFEKL) peptide added to another as a control. SC were incubated for 4 h before 10 μg/ml of Brefeldin A was added to each well. SC were incubated for another 4 h before SC were transferred to 96 well, v bottomed cell culture plate, resuspended in FACS buffer and stained using antibodies conjugated with fluorochromes as described before.

2.12 Statistical analysis

Comparisons of absolute numbers, frequencies and histopathological scores for significance were made using a Mann-Whitney U test in GraphPads Prism (v6.0). A p-value ≤0.05 was considered significant.

For the gene level differential expression analysis, an absolute linear fold change (LFC) ±2 and an Analysis of Variance (ANOVA) p-value ≤0.05 was considered significant. For the gene set enrichment analysis (GSEA), a false discovery rate (FDR) ≤0.25 was chosen as the cut off.

2.13 Transcriptional profiling

In collaboration with Professor Frederic Geissman and Dr Elisa Gomez Perdiguero, Mh T cells were flow sorted from the skin draining lymph nodes, dermis and epidermis directly into RLT lysis buffer containing 1μM β-mercaptoethanol using a BD FACSAria II. Mh T cells were identified in the skin based on their expression of CD45.2, CD45.1 Thy1.1, Vβ8.3 and CD8. In parallel, host LC were flow sorted from the epidermis. In Langerin-DTR mice, LC were identified based on their expression of CD45.2, CD11b, GFP. In BL/6 mice, LC were identified based on their expression of CD45.2, CD11b, CD11c and CD24. A minimum of 5 $x10^3$ cells were collected per replicate with purity ≥95%.

Methods used for quantitative PCR (qPCR) have been described previously[289,290]. The samples were kindly amplified by Dr Terry Means at Massachusetts University Hospital using the primers listed in Table 5. mRNA quantification for each transcript was relative to expression of β_2M.

For the microarray study, RNA was purified using an RNeasy Micro Kit (Qiagen, Holland) as per the manufacturers protocol. Dr Simone Sharma subsequently processed RNA samples at a core facility in the Wolfson Institute for Biomedical Research, UCL. RNA purity was assessed using an RNA 6000 Pico Kit with an Agilent Bioanalsyer 2100 (Agilent, USA). cDNA was synthesised and labelled using the Oviation Pico WTA System V2 and Encore Biotin Module (NuGEN, USA). The amplified cDNA probes were then hybridised onto an Affymetrix GeneChip Mouse Gene 2.0 ST Array and scanned using a GeneChip Scanner 3000 7G (Affymetrix, USA).

The microarray data was kindly analysed and annotated by Dr Pedro Ascensao Santos E Sousa in our lab using Affymetrix Expression Console Software (v1.3.1.187), applying the robust multi-array average (RMA) algorithm for probe-level normalisation

and background correction. GenePattern software was used to perform a Principal Variance Component Analysis (PVCA) and unsupervised agglomerative cluster analysis on the dataset[291]. Affymetrix Transcriptome Analysis Console Software was used for a gene level differential expression analysis. A gene set enrichment analysis (GSEA) was performed using GSEA software and the Molecular Signatures Database Collection 2[292].

Gene	Forward Primer (5' – 3')	Reverse Primer (5' – 3')
β_2M	CCGAACATACTGAACTGCTACGTAA	CCCGTTCTTCAGCATTTGGA
IFN-γ	AACGCTACACACTGCATCTTGG	GCCGTGGCAGTAACAGCC
TNF-α	CCCTCACACTCAGATCATCTTCT	GCTACGACGTGGGCTACAG
IL-10	TTTGAATTCCCTGGGTGAGAA	GGAGAAATCGATGACAGCGC
Perforin	AACTCCCTAATGAGAGACGCC	CCACACGCCAGTCGTTATTGA
TRAIL	ATGGTGATTTGCATAGTGCTCC	GCAAGCAGGGTCTGTTCAAGA
RANTES	CAAGTGCTCCAATCTTGCAGTC	TTCTCTGGGTTGGCACACAC
Granzyme B	CCCACAACATCAAAGAACAGGA	CTCTTCAGCTTTAGCAGCATGA
CCR2	ATCCACGGCATACTATCAACATC	CAAGGCTCACCATCATCGTAG
CCR4	TCCTGACGGACGTGTACCT	CAGACCTAGTCCAAAAACCCAC
CCR5	TGGATTTTCAAGGGTCAGTTCC	GAGCCGCAATTTGTTTCACA
CCR10	TCAATCCGGTGCTTTATGCC	AGCAGCCTCCGCAGGTC
CX3CR1	ACCGGTACCTTGCCATCGT	ACACCGTGCTGCACTGTCC
Ki67	AACTCAGCGCCTTGTTCCAG	GGCCAGAGCAAGTCTGTTCG
BCL-xL	GACAAGGAGATGCAGGTATTGG	TCCCGTAGAGATCCACAAAAGT
FasL	TCCGTGAGTTCACCAACCAAA	GGGGGTTCCCTGTTAAATGGG

Table 5: Primers used for qPCR study.

3 Langerin$^+$ dermal DC are not required for cutaneous GVHD

The first objective of my project was to investigate the role of Langerin$^+$ dDC in an established MHC-mismatched model of localised cutaneous GVHD, where we have already shown a role for host LC.

This required new protocols to identify DC populations in the skin to be developed in the lab, as Langerin$^+$ dDC in the dermis are present in relatively low frequencies. Once established, I investigated the chimerism of LC and Langerin$^+$ dDC in the skin of established MC, where LC were expected to be of host origin and Langerin$^+$ dDC were expected to be donor derived. This was important as I needed to confirm that host Langerin$^+$ dDC were radiosensitive in order to deplete them in our MHC-mismatched model of localised cutaneous GVHD.

In the last part of this chapter, I investigated the role of Langerin$^+$ dDC in the development of acute GVHD. Langerin$^+$ dDC are potent stimulators of CD8 T cell immunity, yet their role in GVHD remains uncharacterised. Adapting the transgenic Langerin-DTR mouse to our established model of localised cutaneous GVHD, I was able to generate MC where host Langerin$^+$ dDC but not LC could be depleted. Thus, enabling me to investigate the role of host Langerin$^+$ dDC in a model of localised cutaneous GVHD when other host APC populations were capable of presenting antigen.

3.1 Characterising dendritic cells in the skin

3.1.1 Characterising cutaneous DC in the steady state

To investigate the function of specific DC populations in the skin, protocols to consistently identify DC by flow cytometry were developed. Staining protocols were adapted from two recently published papers to identify DC in both the epidermis and dermis[275,276]. Firstly, the epidermis and dermis were separated by treating ears and/or whole body skin in trypsin, a serine protease, for 45 min at 37°C. The dermis was subsequently digested using a mixture containing collagenase IV. Varying the concentration and incubation time of collagenase IV with the dermis was found to have no effect on the viability of the sample (Figure 16, A). Therefore, the lowest concentration and incubation time (2750 U/ml for 1 hr) was used in future experiments. Fetal bovine serum (FBS) was subsequently added to the collagenase digestion in order to improve dermal cell viability (Figure 16, B)[293].

This protocol proved ineffective, with inconsistent staining of the dermis a common problem. An alternative protocol using dispase II, a protease that cleaves leucine-phenyalanine bonds, instead of trypsin was subsequently used. Skin samples were incubated with a mixture of dispase II (2.5 mg/ml) and FBS overnight at 4°C or for 45 min at 37°C. Dispase has low cytotoxicity and remains active in the presence of serum[294]. The dermis was subsequently digested using a mixture containing collagenase IV and FBS as described before. This protocol yielded a much more consistent staining pattern within the dermal compartment and was used to stain for DC and T cells in the skin moving forward.

To identify cutaneous DC by flow cytometry, a staining panel of 5-6 antibodies, usually CD45, MHCII, CD207 (Langerin), CD11b, EpCAM and CD24 was used based on phenotypes described in previously published studies (Table 6)[275,276,295]. After an initial gate excluding low FSC cells, which tend to be apoptotic[296], and low SSC cells which

tend to be γδ T cells, MHCII$^+$ cells were gated and analysed for the expression of CD207, EpCAM and CD11b.

DC Subset	MHCII	CD11c	CD11b	CD24	CD207	EpCAM	CD103
LC	+	+	inter/high	+	+	+	-
Langerin$^+$ dDC	+	+	-/low	+	+	-	-/+
CD11b$^+$ dDC	+	+	+	-	-	-	-
CD11b$^-$ dDC	+	+	-/low	-	-	-	-

Table 6: Phenotype of DC subsets found in the skin of mice.

In Figure 17, the gating strategies employed to identify DC in the epidermis and dermis is illustrated. Analysing MHCII$^+$ cells in the epidermis for the expression of CD207 and EpCAM, the majority of DC found are LC in accordance with the literature[276]. In contrast, using the same strategy in the dermis, three distinct populations of DC can be clearly identified; migrating LC, Langerin$^+$ dDC and conventional dDC. Conventional dDC can be further subdivided into two subpopulations based on their expression of CD11b.

Overall, the relative frequencies of DC observed in the skin showed good concordance with previously published observations (Table 7)[276].

Tissue	DC Subset	Frequency
Epidermis	LC	89.9 ± 2.7
Dermis	Migrating LC	6.8 ± 3.7
	Langerin$^+$ dDC	4.8 ± 2.2
	CD11b$^+$ dDC	55.5 ± 11.8
	CD11b$^-$ dDC	29.2 ± 10

Table 7: Frequency ± SD of DC subsets in the epidermis and dermis among MHC$^+$ cells. Data is representative of 12 samples from 7 independent experiments.

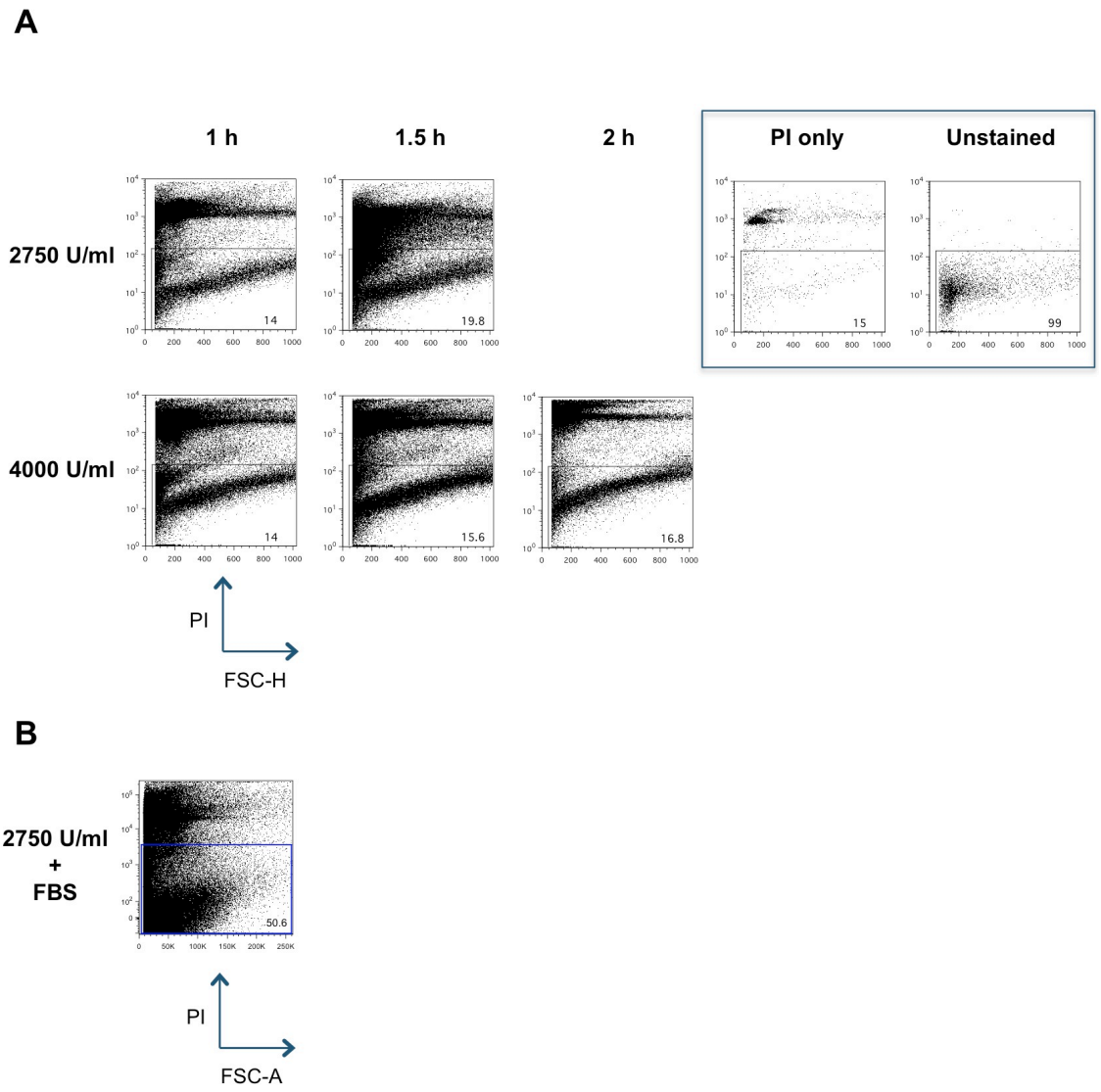

Figure 16: The addition of FBS improved the viability of collagenase treated dermal samples. A *Left*- A suspension of dermal cells taken from the skin of a BL/6 mouse and incubated with either 2750 or 4000 U/ml of Collagenase IV for 1, 1.5 or 2 h. Varying the concentration and incubation time had no effect on the viability of dermal cells. No difference in the frequency of PI^- was observed between samples. *Right*- Single stain controls. Dermal samples incubated with 2750 U/ml of Collagenase IV for 1 h stained with either PI or FACS buffer. **B** Dermal suspension incubated with 2750 U/ml of Collagenase IV for 1 h and 2.5% FBS stained with PI. The frequency of PI^- cells increased with the addition of FBS compared to dermal samples incubated with Collagenase IV alone.

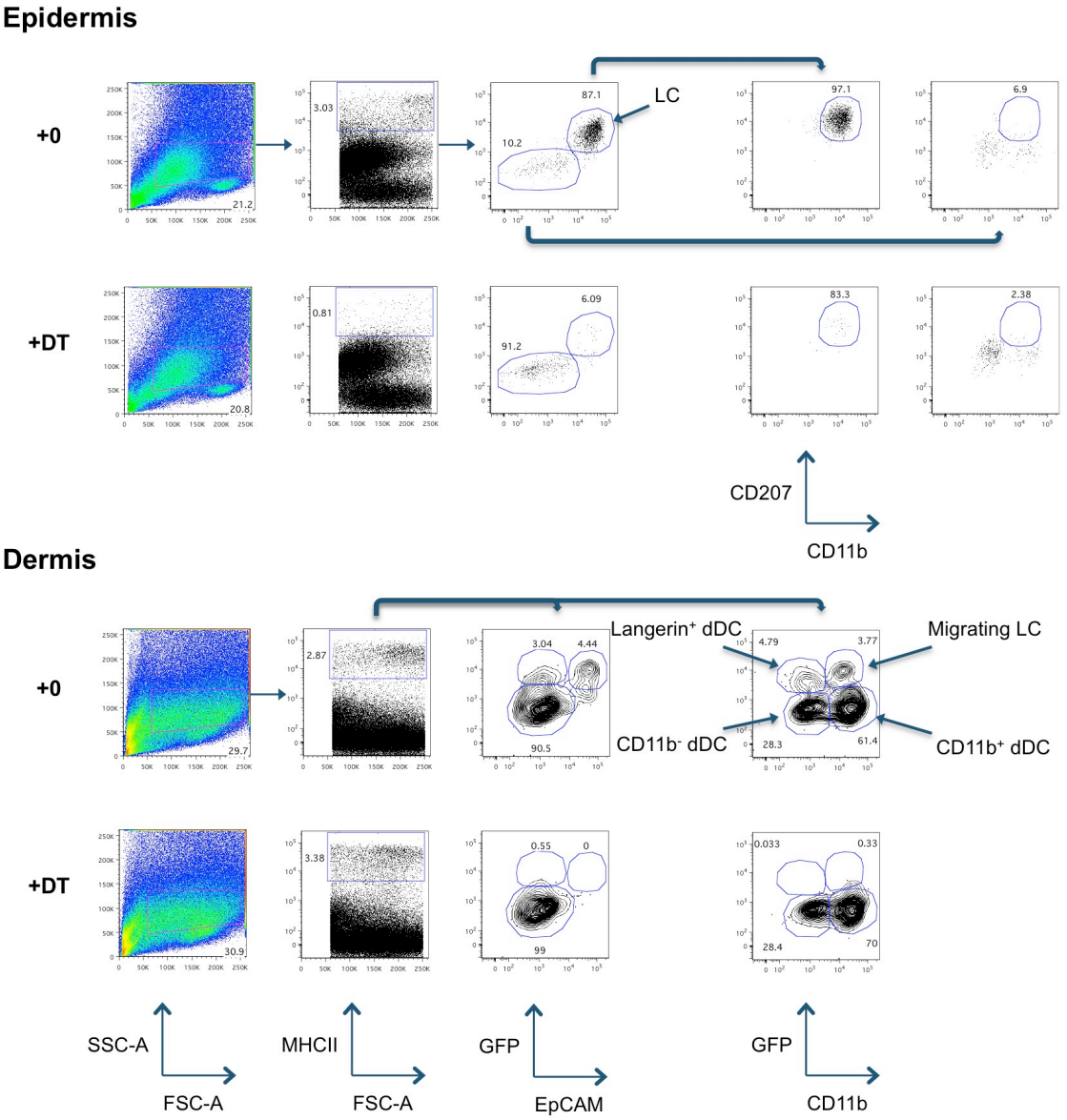

Figure 17: Overview of cutaneous dendritic cells and the depletion of Langerin$^+$ DC in Langerin-DTR mice. Representative dot and contour plots of the epidermis and dermis taken from Langerin-DTR mice injected with either 400 ng of DT or PBS i.p. 24 h earlier. In the epidermis, following a broad DC gate, the majority of MHCII$^+$ cells were found to be LC (GFP$^+$, EpCAM$^+$, CD207$^+$ and CD11b$^+$). In the dermis, four populations of DC could be identified from MHCII$^+$ cells. In addition to migrating LC, Langerin$^+$ dDC (GFP$^+$, CD11b$^-$ and EpCAM$^-$) could be identified as an addition DC subset expressing Langerin in the skin. Following exposure to DT, both LC and Langerin$^+$ dDC are depleted within 24 h as evidenced in the dot and contour plots above.

3.1.2 LC and Langerin$^+$ dDC are depleted in Langerin-DTR mice

To investigate the role of Langerin$^+$ DC in cutaneous GVHD, the knock-in Langerin-DTR mouse was used. Upon a single injection of 400 ng of DT i.p., both LC and Langerin$^+$ dDC in the epidermis and dermis were efficiently depleted within 24 h compared to PBS controls (Figure 17). Langerin$^+$ dDC repopulate the skin much more rapidly than LC upon depletion[275,276]. This was confirmed when DT treated Langerin-DTR mouse were culled 20 days post DT treatment where Langerin$^+$ dDC were found to have fully repopulated the dermis while LC remained depleted in the epidermis and dermis (Figure 18). The LC compartment was fully reconstituted when the epidermis of Langerin-DTR mice was examined 22 weeks after DT treatment (Figure 18).

The effect of the pro-inflammatory TLR 7-8 agonist Imiquimod (Imiq) on Langerin-DTR mice was then investigated[297]. This was of interest as depletion of DC in the skin of CD11c-DTR mice, where cells expressing the integrin CD11c are conditionally depleted in the presence of DT, was found to be inefficient when Imiquimod is painted on to the skin. CD11c$^+$ DC in the epidermis of Imiquimod treated mice failed to deplete when mice were injected with DT 24 h later in contrast to untreated controls (Figure 19).

In Langerin-DTR mice, CD11b$^+$ cells in the epidermis, the majority of which are LC, were found to increase their expression of MHCII and the co-stimulatory molecule CD86 in the presence of Imiquimod (Figure 20), indicating LC maturation[93,298]. However, the inflammation generated by Imiquimod had no significant effect on the depletion of both LC and Langerin$^+$ dDC in Langerin-DTR mice treated with DT 24 h after Imiquimod application (Figure 21 and Figure 22).

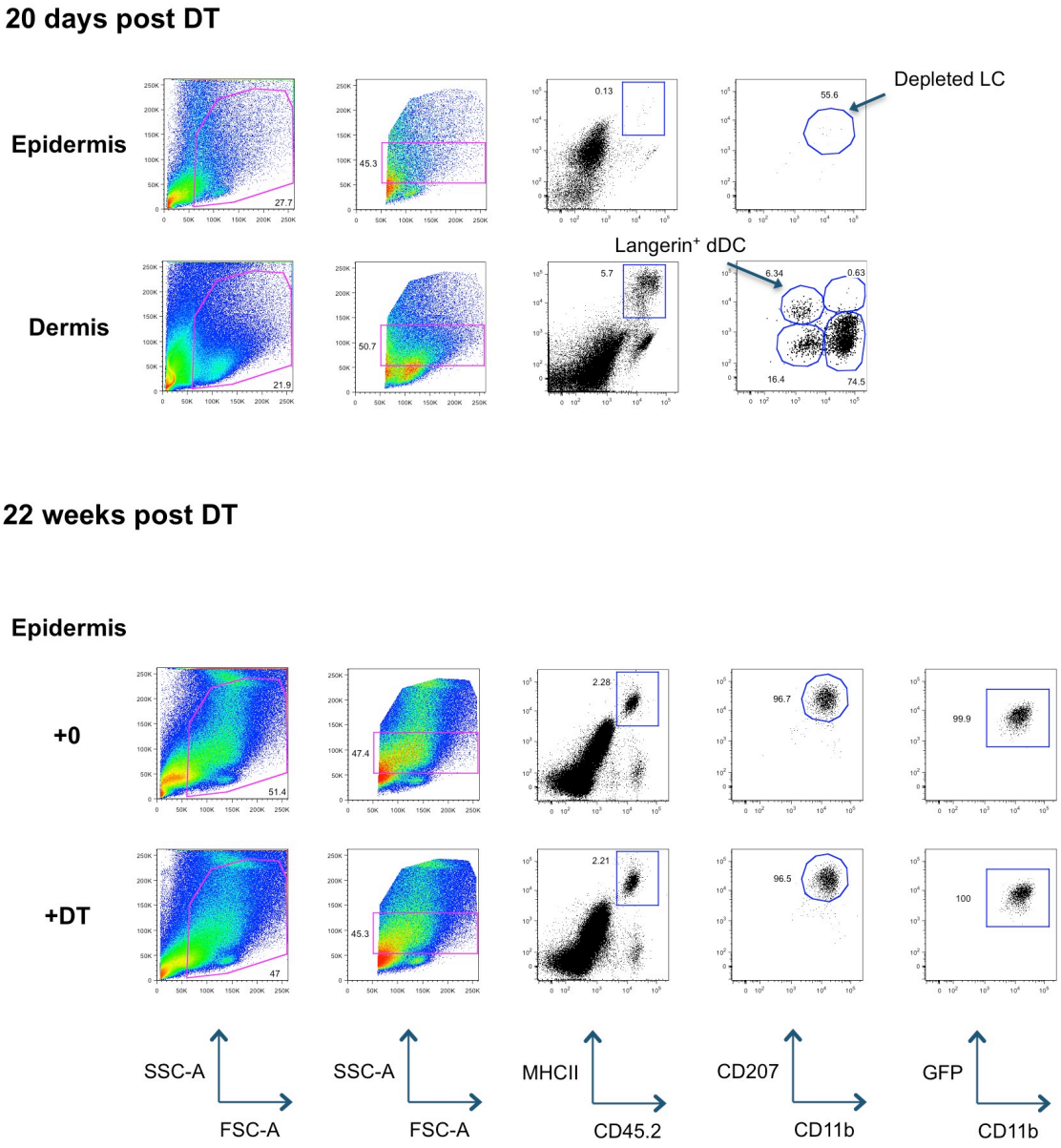

Figure 18: Langerin$^+$ dDC repopulate the skin more rapidly than Langerhans cells upon depletion with DT. Representative dot plots of the epidermis and dermis taken from Langerin-DTR mice injected with either 400 ng of DT or PBS i.p., culled either 20 days or 22 weeks post DT/PBS treatment. 20 days post DT, LC remain depleted in both the epidermis and dermis. However, the Langerin$^+$ dDC have repopulated the dermis. 22 weeks post DT, LC have fully repopulated the epidermis of DT treated Langerin-DTR mice and are similar to PBS controls.

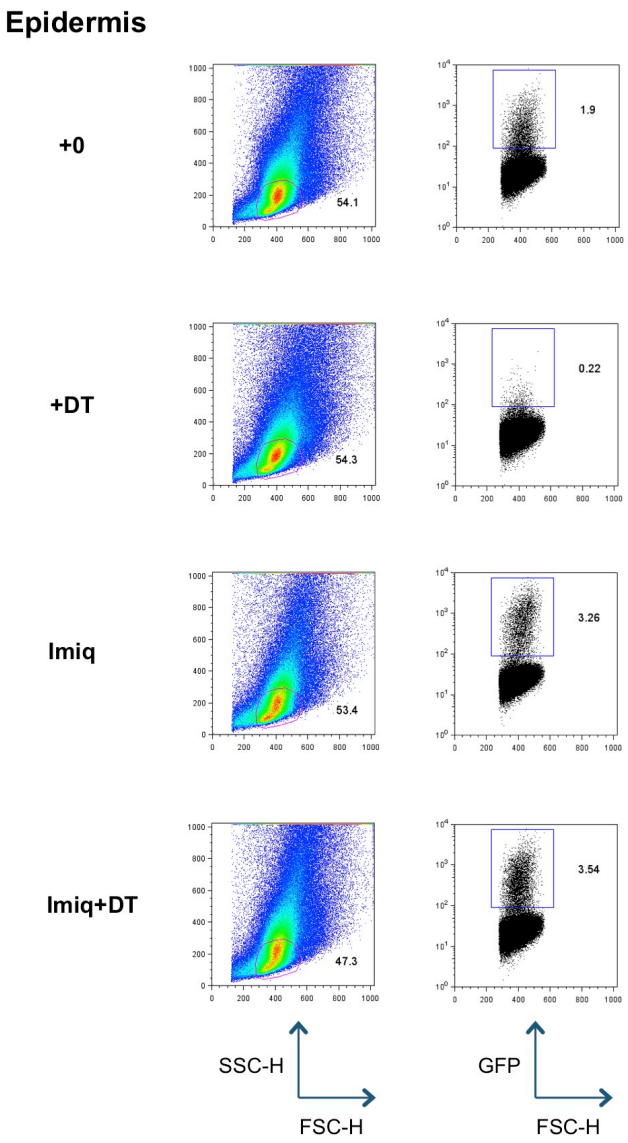

Figure 19: CD11c$^+$ cells in the epidermis are inefficiently depleted in CD11c-DTR mice in the presence of Imiquimod. Dot plots of the epidermis taken from the ears of CD11c-DTR mice injected with 100 ng of DT or PBS i.p. and painted with or without 4 mg of Imiquimod 24 h earlier. DC were identified by the expression of GFP (CD11c). In the absence of Imiquimod, GFP$^+$ cells were depleted upon injection of DT. In the presence of Imiquimod, GFP$^+$ DC were inefficiently depleted upon injection of DT.

Epidermis

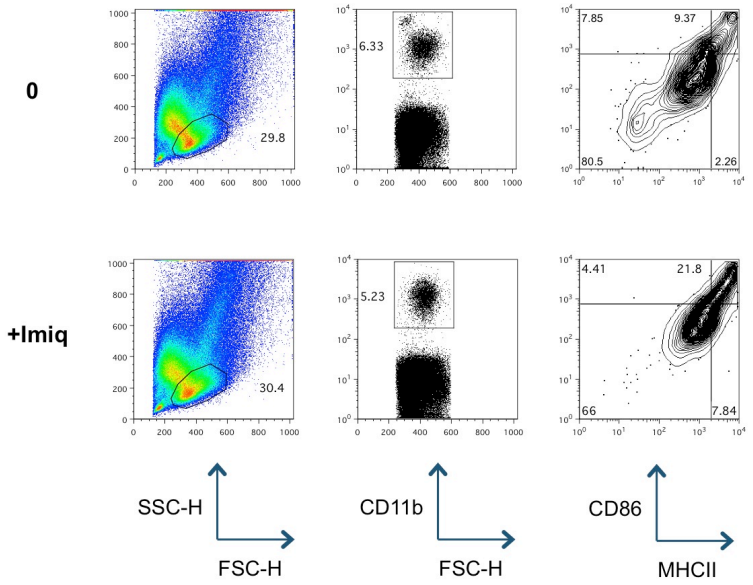

Figure 20: Imiquimod activates dendritic cells in the skin. Dot and contour plots of the epidermis taken from mice painted with or without the TLR agonist Imiquimod 24 h earlier. Following exposure to Imiquimod, $CD11b^{+}$ cells in the epidermis exhibited an increase in both the expression of MHCII and CD86 compared to untreated ears.

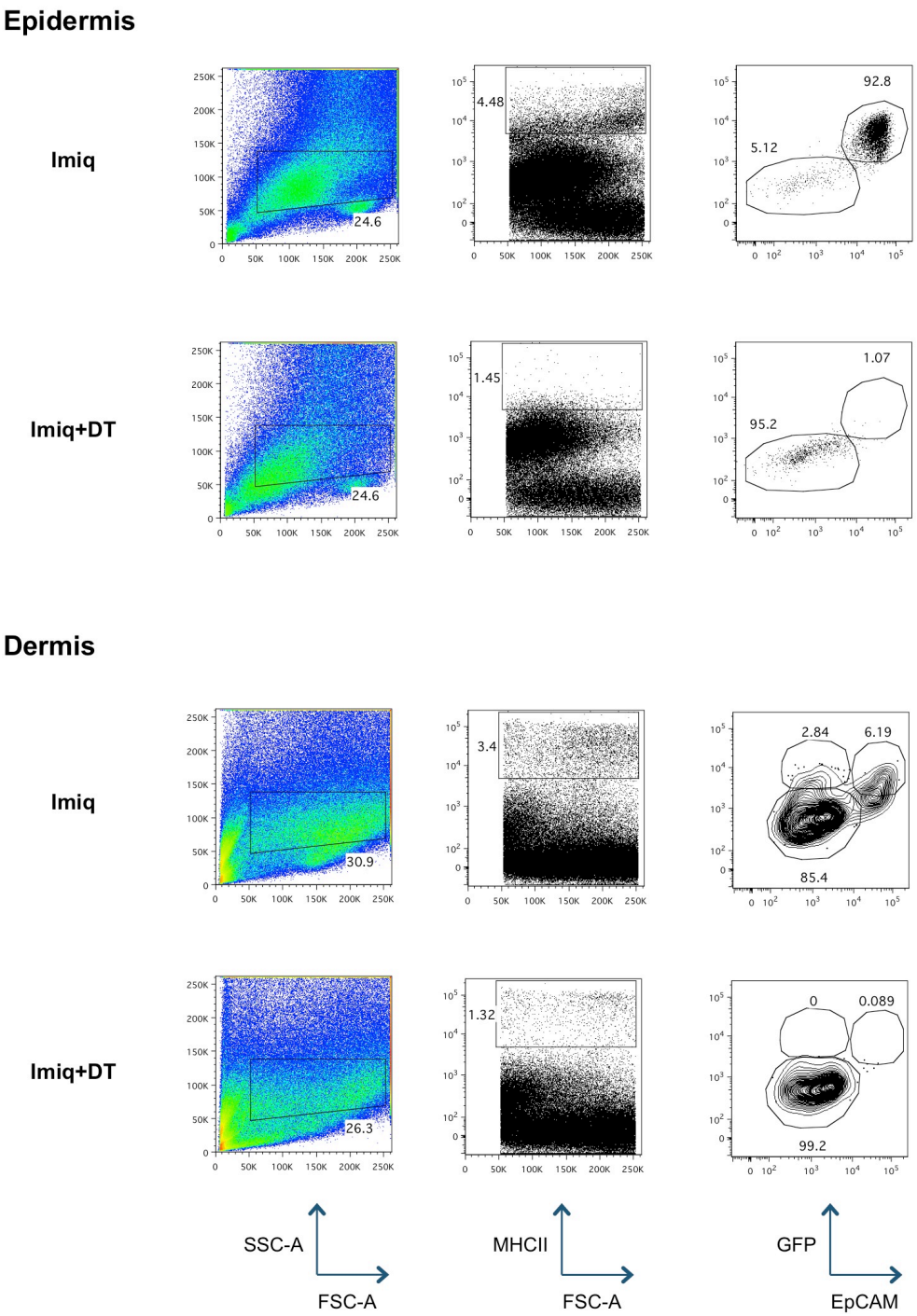

Figure 21: Langerhans cells and Langerin$^+$ dDC are depleted in the presence of Imiquimod in Langerin-DTR mice. Representative dot and contour plots of the epidermis and dermis from the ears of Langerin-DTR mice injected with 400 ng of DT or PBS i.p. and painted with or without 4 mg of Imiquimod 24 hr earlier. In the presence of Imiquimod, both LC and Langerin$^+$ dDC were efficiently depleted in the epidermis and dermis of mice.

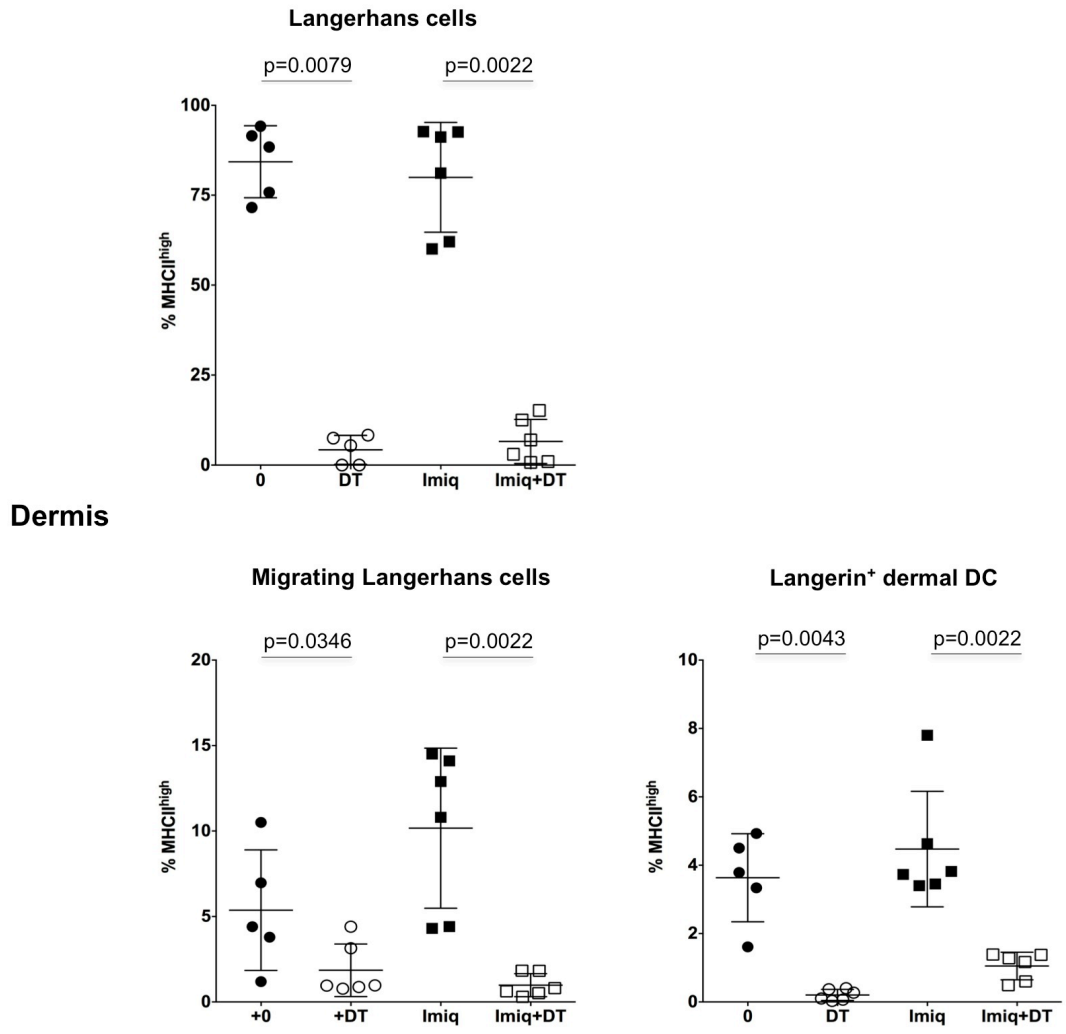

Figure 22: Langerin$^+$ DC are efficiently depleted in the presence or absence of Imiquimod in Langerin-DTR mice. Summary data showing the percentage of gated MHC^{high} cells that were either LC or Langerin$^+$ dDC (n=5-6 per group, data pooled from 3 independent experiments, analysed using a Mann-Whitney test. The mean ±SD is indicated by the horizontal bar.). *Top*- In the epidermis, there was a significant reduction in the frequency of LC in mice treated with DT and Imiq+DT compared to controls. *Bottom left*- In the dermis, there was a significant reduction in the frequency of migrating LC in mice treated with DT and Imiq+DT compared to controls. *Bottom right*- There was a significant reduction in the frequency of Langerin$^+$ dDC in mice treated with DT and Imiq+DT compared to controls.

3.2 Host Langerhans cells are radioresistant but donor Langerhans cells were observed in established mixed chimeras

3.2.1 LC derived from donor MHC-mismatched BM co-populate the epidermis of established MC with host LC

Previous studies have shown that LC are radioresistant and can self-renew and proliferate *in situ* in the steady state independently of precursor cells from the blood and bone marrow[258,299]. Exploiting theses unique characteristics, we adapted an established model of localised cutaneous GVHD using MC to the Langerin-DTR system (Figure 23, A)[229,283]. This enabled us to selectively deplete host LC and investigate the role of LC in the development of cutaneous GVHD (Figure 23, B).

Briefly, Langerin-DTR (H-2b) mice were lethally irradiated with a split dose of 11 Gy and reconstituted with 20 x10^6 TCD BM from MHC-matched BL/6 (H-2b) and MHC-mismatched BALB/c (H-2d) mice mixed at a 1:1 ratio (Figure 23**,** A). The mice were allowed to recover for at least 8 weeks and their chimerism was subsequently checked.

In the haematopoietic system, myeloid, T and B cells were mixed between donor BL/6 (H-2b) and BALB/c (H-2d) derived cells as expected[229]. The chimerism of LCs in the MC ([BL/6+BALB/c] → Langerin-DTR) was then examined to confirm host origin (Langerin-DTR). $MHCII^+$ and $CD11b^+$ in the epidermis were gated and analysed for the expression of H-2Kb (Langerin-DTR and BL/6) and H2-Dd (BALB/c). Two populations of LC were found (Figure 24): H-$2Kb^+$ $H2Dd^-$ and H-$2Kb^-$ $H2Dd^+$ LCs, contrary to what was expected from previously published data where all LC were derived from the host[258]. Both populations were then analysed for their expression of GFP (LC from Langerin-DTR mice are GFP^+). LCs that were H-$2Kb^+$ $H2Dd^-$ were entirely GFP^+ and therefore of host origin (Langerin-DTR, H-2b) whereas H-$2Kb^-$ $H2Dd^+$ LCs were GFP^- and derived from donor (BALB/c, H-2d) origin (Figure 24). Interestingly, within the H-

2Kb^{+} H-2Dd^{-} population of LC, virtually none were derived from donor BL/6 (MHC-matched, H-2b) BM despite a large proportion of LC in the epidermis being derived from infiltrating donor BALB/c (MHC-mismatched, H-2d) precursors (Figure 24).

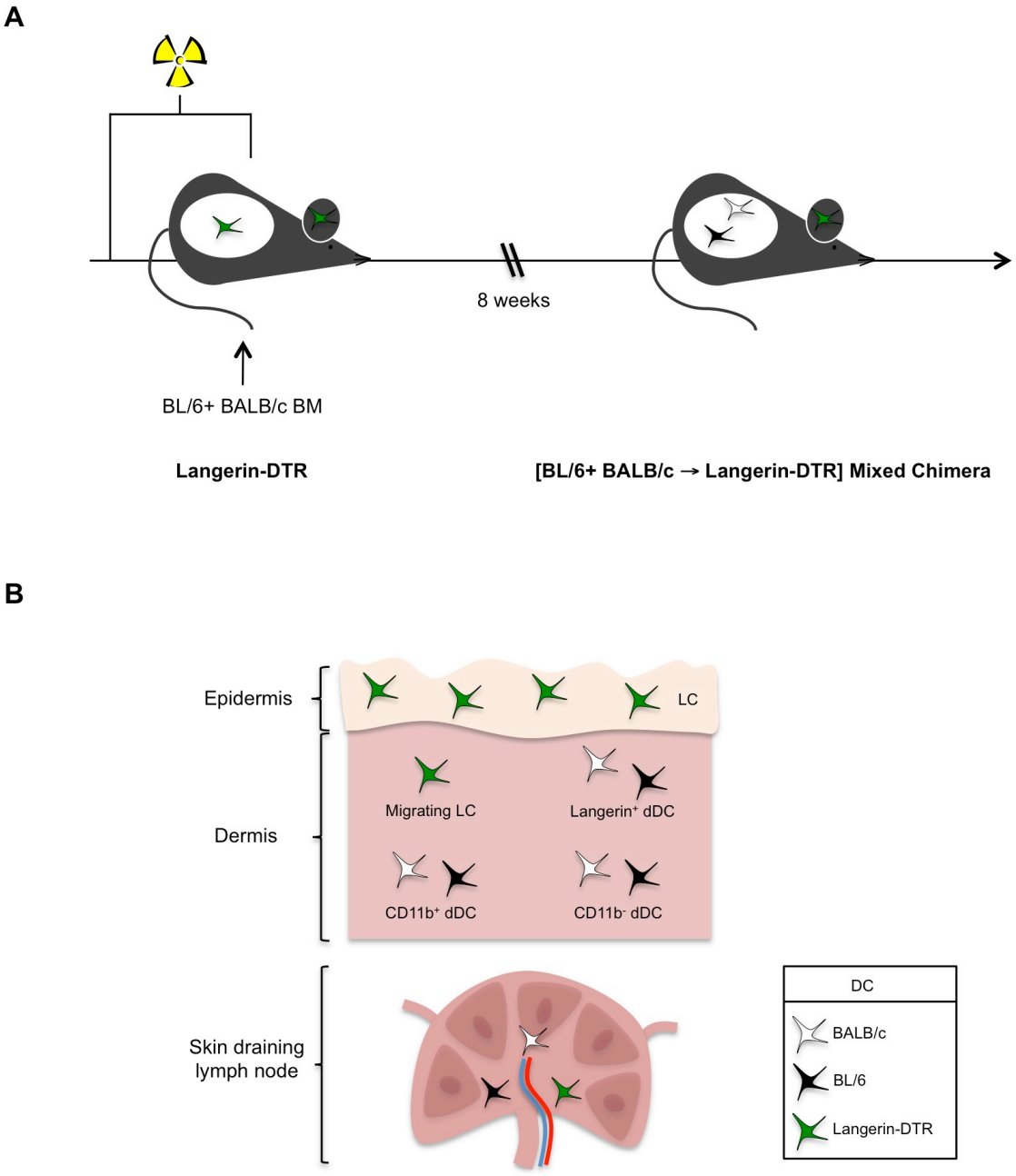

Figure 23: [BL/6 + BALB/c] → Langerin-DTR allogeneic mixed chimera model. A. Langerin-DTR (H-2b) mice are lethally irradiated with a split dose of 11 GY and reconstituted with a 1:1 mix of TCD MHC-matched BL/6 (H-2b) and MHC-mismatched BALB/c (H-2d) BM and allowed to recover for 8 weeks. **B.** Overview of the expected chimerism of DC in MC based on current literature. In the epidermis, LC are radioresistant and expected to be entirely of host (Langerin-DTR) origin. In the dermis, Langerin$^+$ dDC, CD11b$^+$ and CD11b$^-$ dDC are expected to be donor derived, a mix between BL/6 and BALB/c derived cells.

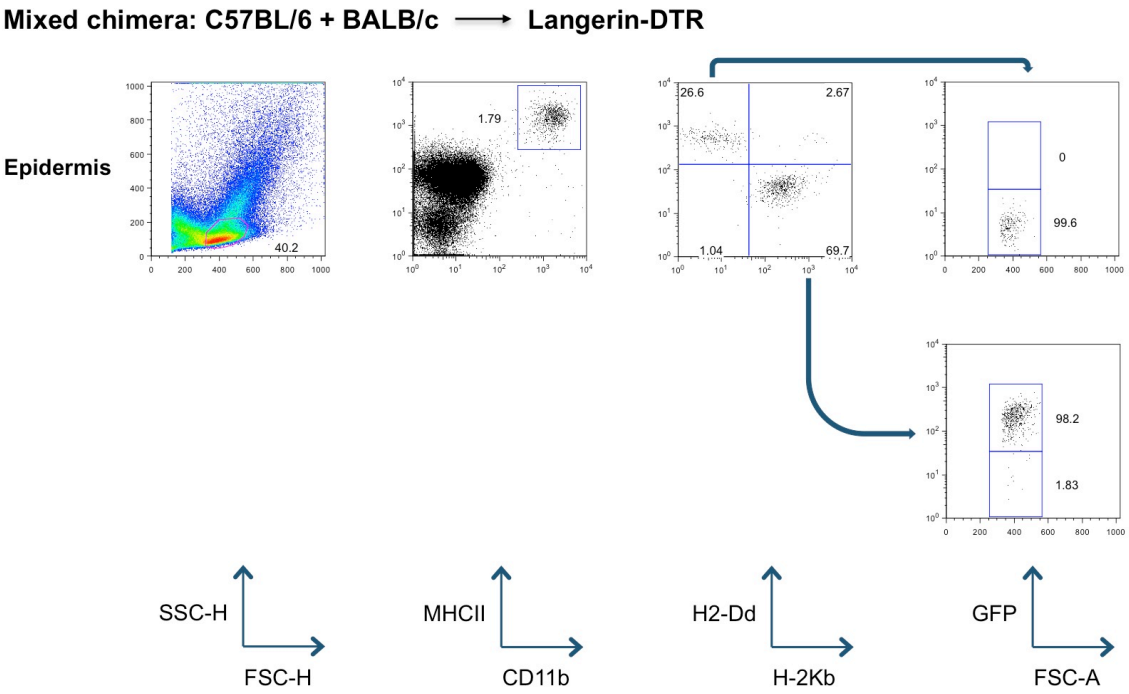

Figure 24: Langerhans cells in allogeneic mixed chimeras are both host and donor in origin. Dot plots from the epidermis of a [BL/6 + BALB/c] → Langerin-DTR MC that was culled 12 weeks after transplant. LC characterised here as MHCII$^+$ and CD11b$^+$ cells, were analysed for the expression of the MHCI molecules H2-Dd and H-2Kb. Interestingly, the population of LC in the epidermis was mixed between H2-Dd$^+$ and H-2Kb$^+$ LC. H2-Dd$^+$ LC were GFP$^-$ and derived from donor MHC-mismatched BALB/c (H-2d) BM. H-2Kb$^+$ LC were GFP$^+$ and entirely of host (Langerin-DTR, H-2b) origin with no LC derived from donor MHC-matched BL/6 (H-2b, GFP$^-$) BM detected.

3.2.2 LC derived from donor MHC-matched BM did not repopulate the epidermis when host LC were present but DC derived from MHC-matched BM did repopulate the dermis

In 5 independent experiments, the LC compartment was primarily derived from two cell subsets, with host (Langerin-DTR) cells comprising the majority of LC found in the epidermis (Figure 25, Left~). However, Langerin$^+$ dDC in the dermis, which are not radioresistant like LC, were found to be entirely of donor origin and mixed equally between BL/6 and BALB/c derived cells as expected (Figure 25, Right~).

To explore whether this finding would be reproducible in another strain background independent of the Langerin-DTR system, a 1:1 mix of MHC-matched BL/6 (CD45.2.CD45.1 heterozygotes, H-2b) and MHC-mismatched B62DF1 (CD45.2, H-2db) TCD BM was used to reconstitute lethally irradiated BL/6 mice (CD45.1, H-2b). In these MC, the chimerism of each cutaneous DC population could be easily tracked *in vivo* due to the differential expression of the congenic markers CD45.1 and CD45.2 between host and donor cells.

The majority of LC in the epidermis were again derived from host (BL/6, CD45.1, H-2b) and donor cells from MHC-mismatched B62DF1 (CD45.2, H-2db) BM, consistent with what was observed using Langerin-DTR mice (Figure 26, A). Virtually, no LC were derived from donor cells from MHC-matched BL/6 (CD45.2.CD45.1, H-2b) BM.

In the dermis, migrating LC were again split between host (BL/6, CD45.1, H-2b) and donor cells derived from MHC-mismatched B62DF1 (CD45.2, H-2db) BM but Langerin$^+$, CD11b$^+$ and CD11b$^-$ dDC were entirely derived from donor cells and mixed equally between DC derived from MHC-matched BL/6 (CD45.2.CD45.1, H-2b) and MHC-mismatched B62DF1 (CD45.2, H-2db) BM (Figure 26, A).

The chimerism of epidermal γδ T cells in [BL/6(CD45.2.CD45.1)+B62DF1(CD45.2)] → BL/6(CD45.1) MC was also examined. Cells that were γδ TCR$^+$ were gated and

analysed for the expression of CD45.1 and CD45.2. Interestingly, in contrast to LC, the majority of γδ T cells were derived from host (BL/6, CD45.1, H-2b) and donor cells derived from MHC-matched BL/6 (CD45.2.CD45.1, H-2b) BM (Figure 26, B). This was consistent across the three mice analysed from 1 independent experiment.

To investigate whether the infiltration of donor LC into the epidermis could be skewed towards syngeneic precursors, the ratio of donor MHC-matched (BL/6, H-2b) to MHC-mismatched (BALB/c, H-2d) BM transplanted into irradiated Langerin-DTR (H-2b) recipients was altered from 1:1 to 3:1 and the subsequent chimerism of cutaneous DC investigated.

In the epidermis, LC were again split between host (Langerin-DTR, H-2b) and donor cells derived from MHC-mismatched BALB/c (H-2d) BM (Figure 27). Increasing the ratio of MHC-matched BL/6 (H-2b) to MHC-mismatched BALB/c (H-2d) BM had no effect on the chimerism of LC (Figure 27). In the dermis, dDC were again entirely derived from donor cells derived from MHC-matched BL/6 (H-2b) and MHC-mismatched BALB/c (H-2d) BM.

However, increasing the ratio of MHC-matched BL/6 (H-2b) to MHC-mismatched BALB/c (H-2d) BM did have a noticeable effect on the chimerism of DC in the dermis, with an increase in the frequency of donor dDC derived from MHC-matched BM observed for all dDC populations in the dermis compared to controls (Figure 27).

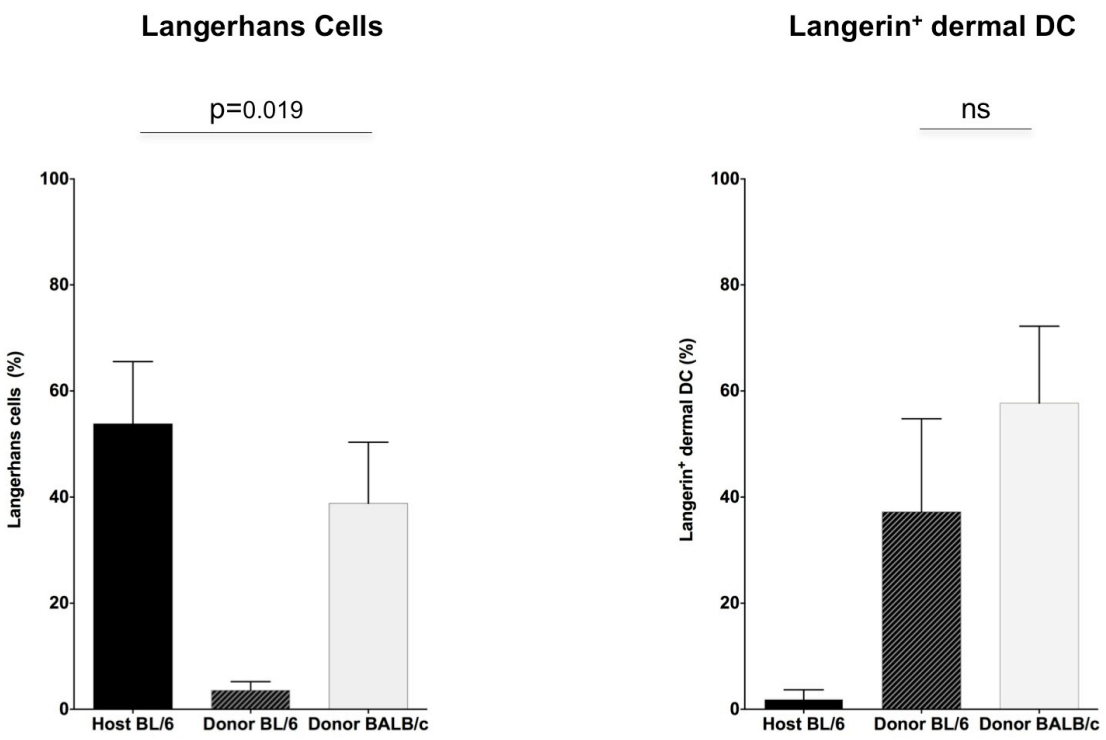

Figure 25: Langerhans cells are mixed between donor and host whereas Langerin$^+$ dDC are entirely donor in origin. *Left*- Summary data showing the percentage of LC in the epidermis that were either host BL/6 (H-2b), donor BL/6 (MHC-matched, H-2b) or donor BALB/c (MHC-mismatched, H-2d) in origin. Host BL/6 (H-2b) derived LC comprised the majority of LC in MC, followed by donor BALB/c (MHC-mismatched, H-2d) derived LC. Virtually no donor BL/6 (MHC-matched, H-2b) derived LC were detected (n=9 per group, data pooled from 5 independent experiments >12 weeks after transplant, analysed using a Mann-Whitney test. The mean ±SD is indicated by the horizontal bar.). *Right*- Summary data showing the percentage of Langerin$^+$ dDC that were either host BL/6 (H-2b), donor BL/6 (MHC-matched, H-2b) or donor BALB/c (MHC-mismatched, H-2d) in origin. Langerin$^+$ dDC were entirely of donor origin and there was no significant difference between the proportion of BL/6 and BALB/c derived cells (n=6 per group, data pooled from 3 independent experiments >12 weeks after transplant, analysed using a Mann-Whitney test. The mean ±SD is indicated by the horizontal bar.).

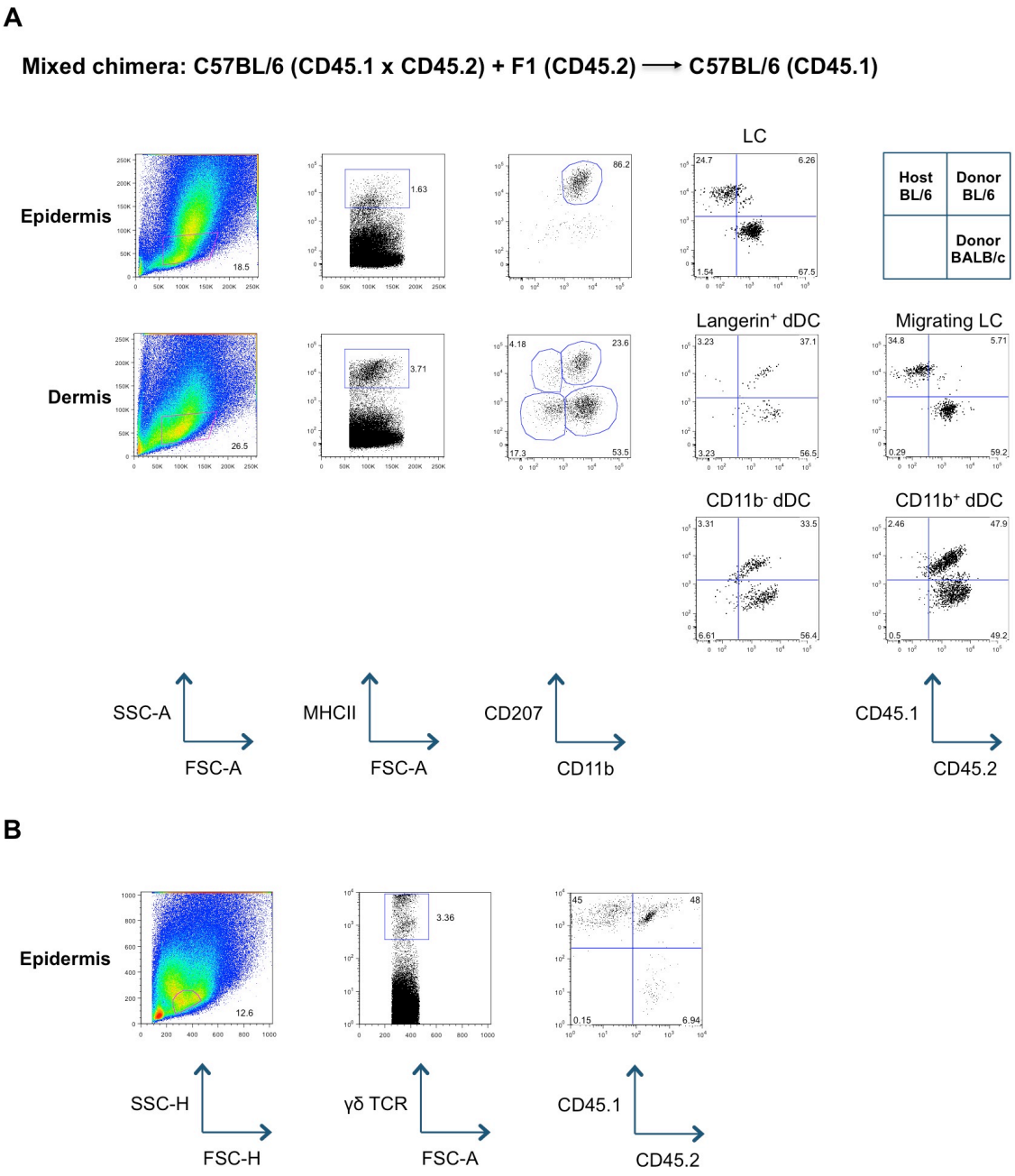

Figure 26: Dermal dendritic cells are derived from donor cells while epidermal γδ T cells are mixed between host and donor cells. A. Representative dot plots of the epidermis and dermis from [BL/6 (CD45.1.CD45.2) + B62DF1 (CD45.2)] → BL/6 (CD45.1) MC culled 22 weeks after transplant. In the epidermis, LC were derived from host (BL/6, CD45.1, H-2b) and donor cells derived from MHC-mismatched B62DF1 (CD45.2, H-2db) BM. In the dermis, Langerin^{+}, CD11b^{+} and CD11b^{-} dDC were derived entirely from a mixture of donor cells (BL/6 (CD45.1.CD45.2, H-2b) and B62DF1 (CD45.2, H-2db)). **B.** γδ T cells were dervied from both host (BL/6 (CD45.1) and donor (BL/6 (CD45.1.CD45.2, H-2b) + B62DF1 (CD45.2, H-2db)) cells. In contrast to LC, the majority of donor derived γδ T cells were from MHC-matched donor BL/6 (CD45.1 x CD45.2, H-2b) BM.

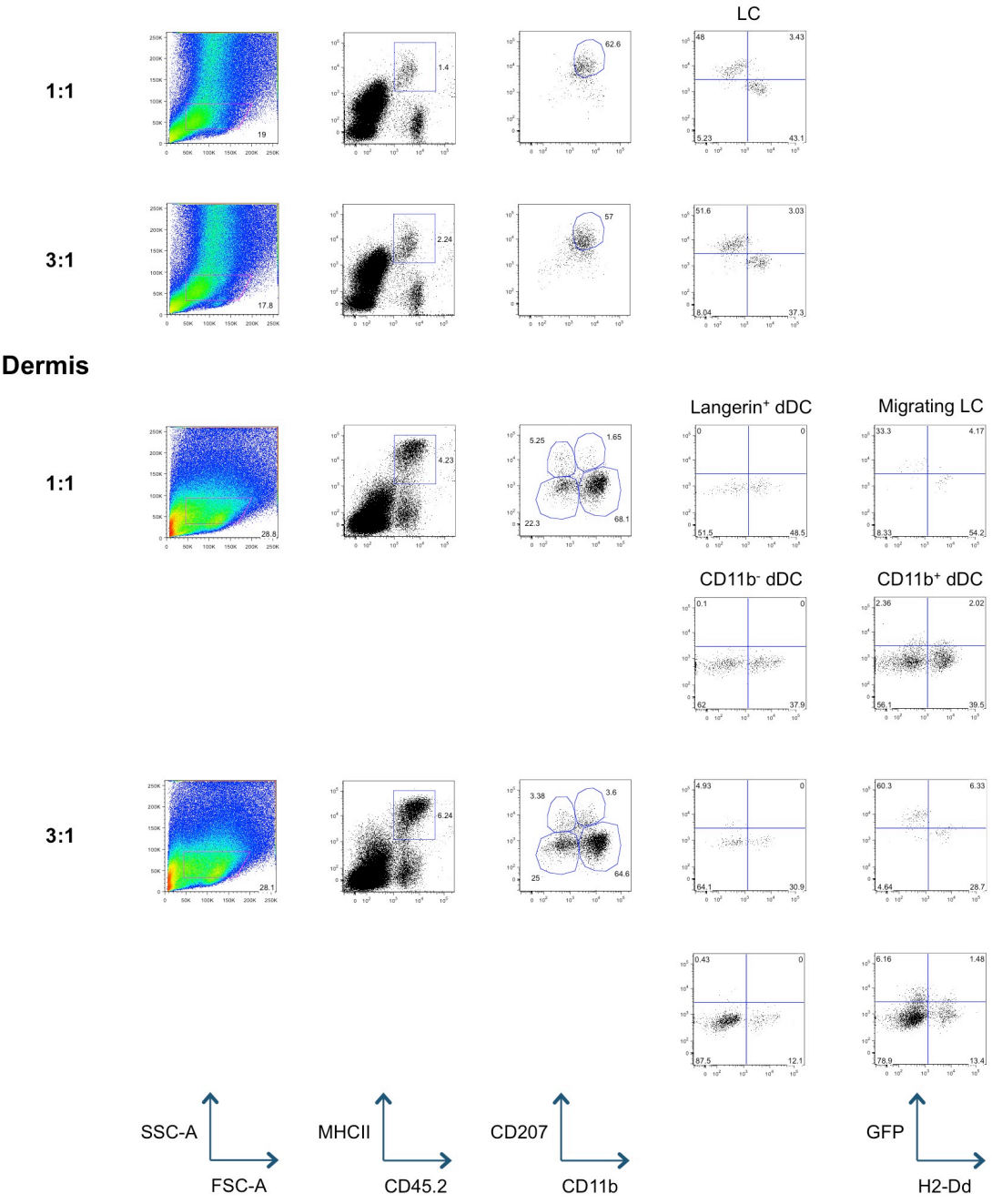

Figure 27: Increasing the ratio of donor BL/6(H-2b):BALB/c(H-2d) BM transplanted had no effect on the chimerism of Langerhans cells in mixed chimeras. Representative dot plots of the epidermis and dermis from [BL/6 + BALB/c] → Langerin-DTR MC culled 14 weeks after transplant. In the epidermis, LC were derived from host (Langerin-DTR, H-2b) and donor cells derived from MHC-mismatched BALB/c (H-2d) BM. Increasing the ratio of donor MHC-matched BL/6 (H-2b) to MHC-mismatched BALB/c (H-2d) BM from 1:1 to 3:1 had no effect on the chimerism of LC in the epidermis of lethally irradiated Langerin-DTR (H-2b) recipients. In the dermis, Langerin$^+$ dDC, CD11b$^+$ and CD11b$^-$ dDC were derived from a mixture of donor cells (BL/6 and BALB/c). Increasing the ratio of donor MHC-matched BL/6 (H-2b) to MHC-mismatched BALB/c (H-2d) BM led to a minor increase in the proportion dDC dervied from donor MHC-matched BL/6 BM.

3.3 Host Langerin$^+$ dDC are not required for cutaneous GVHD

3.3.1 Generating [BALB/c+Langerin-DTR] → BL/6 MC and the induction of GVHD

By modifying our MC model of localised cutaneous GVHD described previously[229,283], I established a model where host Langerin$^+$ dDC but not host LC could be conditionally depleted (Figure 28, A). This allowed a role for host Langerin$^+$ dDC in the development of localised cutaneous GVHD to be investigated. Briefly, BL/6 (H-2b) mice were lethally irradiated and reconstituted with TCD BM from MHC-matched Langerin-DTR (H-2b) and MHC-mismatched BALB/c (H-2d) mice mixed at a 1:1 ratio. TCD was confirmed by flow cytometry before each transplant (Figure 29, A). In these MC, Langerin$^+$ dDC are mixed between donor Langerin-DTR (MHC-matched, H2-b) and BALB/c (MHC-mismatched, H2-d) derived cells. Injecting these MCs with DT will only deplete Langerin$^+$ dDC derived from Langerin-DTR mice (Figure 28, B). LC in these MC will be mixed between host (BL/6, H-2b) and donor cells derived from MHC-mismatched (BALB/c, H-2d) BM and are not depleted, unlike the [BL/6+BALB/c] → Langerin-DTR MC discussed in the previous section.

After transplant, the MC were allowed to recover for at least 8 weeks and their chimerism was subsequently checked (Figure 30, A). Gating for lymphocytes, both CD8$^+$ and B220$^+$ cells were examined for their expression of H2-Dd. Both populations were mixed and derived equally from both Langerin-DTR and BALB/c donor cells. However, when granulocytes were gated based on their higher SSC properties[300], and CD11b$^+$ granulocytes examined for the expression of H2-Dd (BALB/c), there was a significant skewing towards BALB/c derived cells (Figure 30, B). This phenomenon had been noted in [BL/6+BALB/c] → Langerin-DTR MCs and had no effect on the chimerism of Langerin$^+$ dDC (Figure 26, A).

To induce localised cutaneous GVHD, I transferred 30 x10^6 Thy1.1$^+$ BALB/c splenocytes as DLI into established [BALB/c+Langerin-DTR] → B6 MC that received

either DT or PBS 2 days previously (Figure 29, B). A shaved area at the base of the tail was then painted with the TLR 7-8 agonist Imiquimod or PBS 0, 5 and 10 days after DLI, as described elsewhere, to induce inflammation. MC were subsequently injected with DT or PBS 1, 4, 7, 10, and 13 days post-transplant to ensure continual depletion of host-type (Langerin-DTR, H-2b) Langerin^{+} dDC.

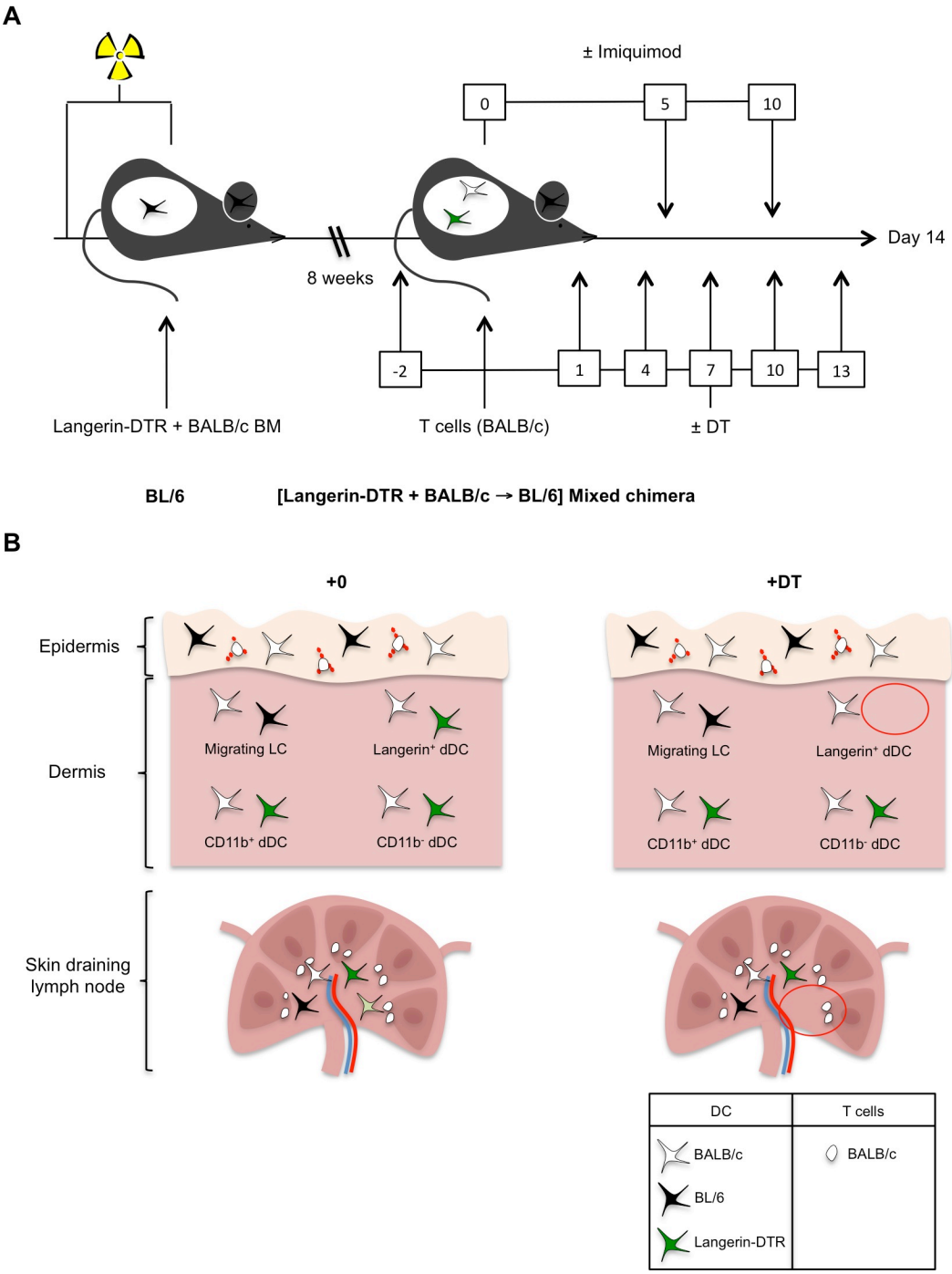

Figure 28: [Langerin-DTR + BALB/c] → BL/6 allogeneic mixed chimera model. A. BL/6 (H-2b) mice were lethally irradiated with a split dose of 11 GY and reconstituted with a 1:1 mix of the TCD MHC-matched Langerin-DTR (H-2b) and BALB/c (H-2d) BM and allowed to recover for 8 weeks. The MC were injected with 400 ng of DT or PBS i.p. on days -2, +1, +4, +7, +10, +13 following the infusion of 3 x10^7 BALB/c (H-2d) SC. MC were treated topically with or without Imiquimod on days 0, 5 and 10 following donor SC infusion. **B.** Overview of the chimerism of cutaneous DC in [Langerin-DTR + BALB/c] → BL/6 allogeneic MC. LC are mixed between host (BL/6, H-2b) and donor cells derived from MHC-mismatched BALB/c (H-2d) BM. Dermal DC are mixed between both types donor (Langerin-DTR and BALB/c) cells. When 400 ng of DT is injected i.p. only donor Langerin$^+$ dDC derived from Langerin-DTR (H-2b) BM will be depleted.

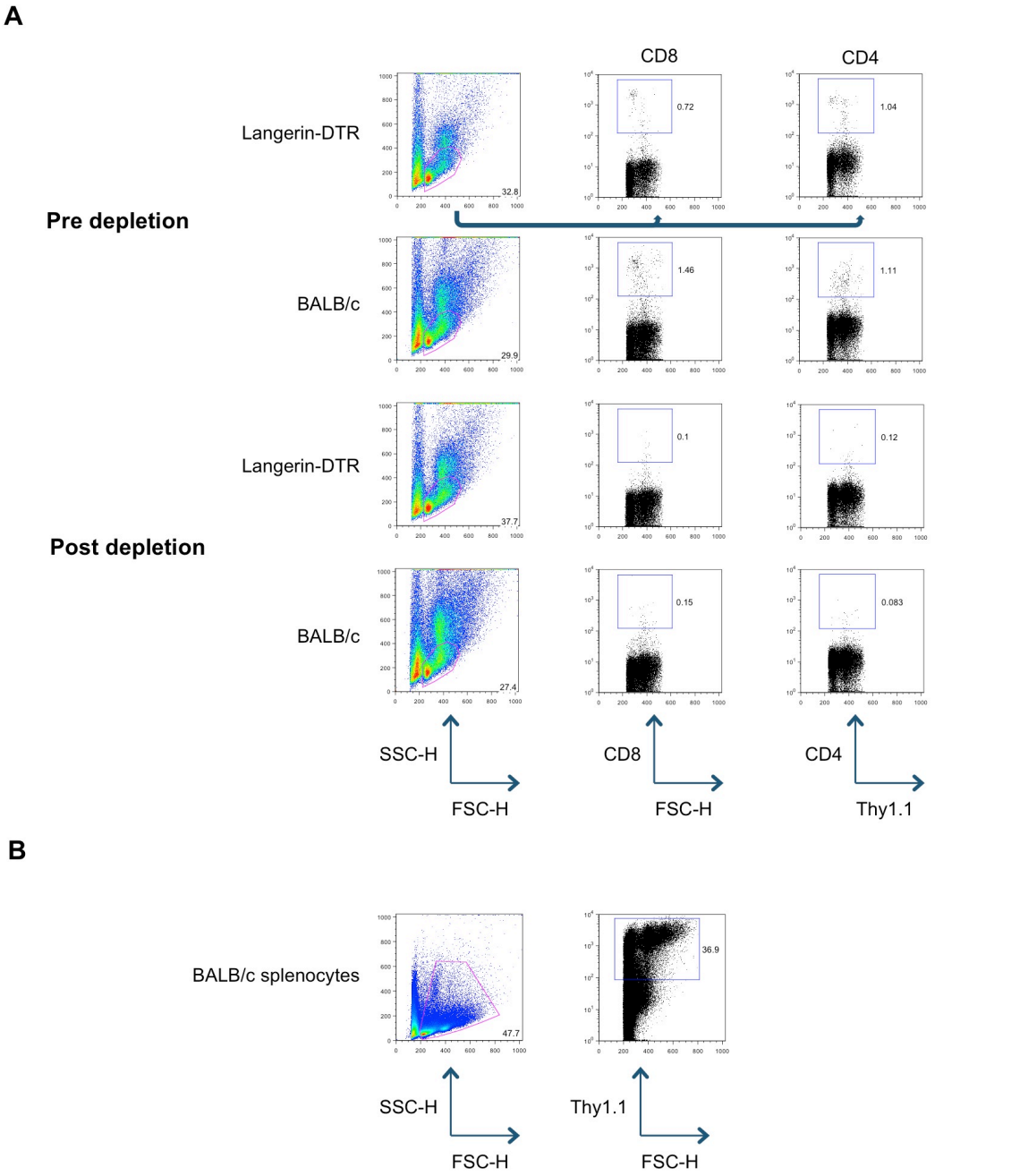

Figure 29: T cells were efficiently depleted from the bone marrow before transplant. A. Representative dot plots of bone marrows cell pre- and post-T cell depletion. Bone marrow harvested from Langerin-DTR and BALB/c mice was processed and depleted of T cells using anti- CD4 and CD8 microbeads (Miltenyi, Germany). T cell depletion was confirmed through FACS and depleted BM used for transplant. **B.** Representative dot plots of splenocytes harvested from a Thy1.1 BALB/c donor. Splenocytes were confirmed to be Thy1.1^{+} before being used for DLI.

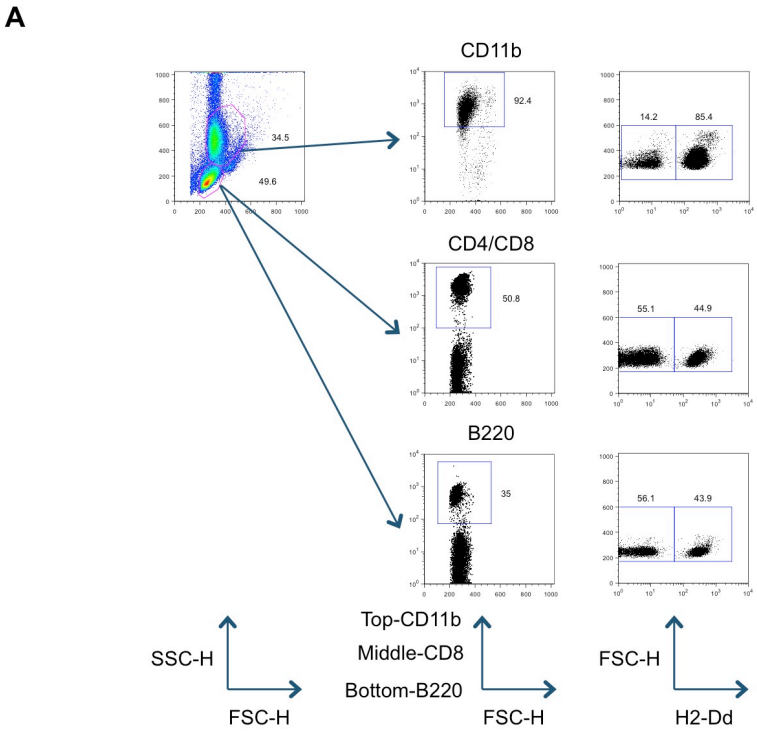

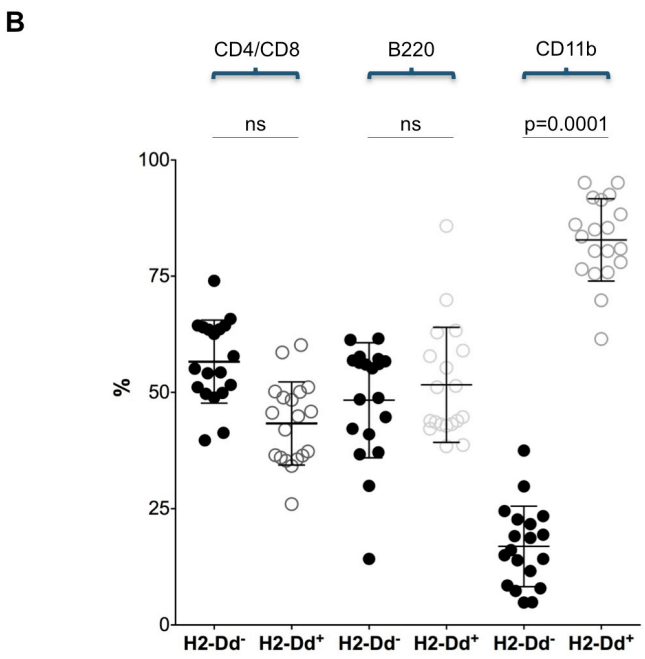

Figure 30: The haematopoietic system of mixed chimeras is mixed between donor Langerin-DTR and BALB/c cells. A. Representative dot plots of RBC lysed blood samples taken from a MC >8 weeks after being transplanted with 1:1 mix of Langerin-DTR and BALB/c BM. Granulocytes were gated and $CD11b^+$ cells examined for their expression of H2-Dd. Lymphocytes were gated and $CD8^+$ or $B220^+$ cells were examined for their expression of H2-Dd. **B.** Percentage of gated CD4/CD8 T cells, B cells and granulocytes in blood samples from MC that were either $H2\text{-}Dd^-$ (Langerin-DTR) or $H2\text{-}Dd^+$ (BALB/c). There was no difference in the frequency of Langerin-DTR and BALB/c derivied CD4/CD8 T and B cell populations. The $CD11b^+$ granulocyte population was skewed towards BALB/c derived cells (n=19, data pooled from 2 independent experiments, analysed using a Mann-Whitney test, the mean ±SD is indicated by the horizontal bars.).

3.3.2 Host Langerin$^+$ dDC are not required for the accumulation and activation of alloreactive T cells

The MCs were tracked for changes in weight and clinical observation scores, key indicators of GVHD, and culled 14 days after receiving DLI (Figure 31, A). In the spleen, after a broad gate excluding low FSC cells, the congenic T cell marker Thy1.1 was used to track allogeneic donor T lymphocytes *in vivo* (Figure 31, B). As shown in Figure 31 C, the depletion of host-type Langerin$^+$ dDC (H-2b) had no effect on the absolute number of either Thy1.1$^+$ CD8 or CD4 donor T cells in the spleens of MCs treated with Imiquimod.

In the skin draining lymph nodes, Thy1.1$^+$ CD8 donor T cells were gated and analysed for their expression of the T cell effector/memory markers CD44 and CD62L (Figure 31, A). There was no significant difference in either the effector phenotype or absolute number of either Thy1.1$^+$ CD8 donor T cells in Imiquimod treated mice in the presence or absence of host Langerin$^+$ dDC (Figure 32, B+C). There also appeared to be no difference in the frequency of donor Thy1.1$^+$ CD8$^+$ T cells expressing E-selectin ligand, indicating similar skin homing potential in both populations (Figure 32, D).

Taken together, these data shows that host-type Langerin$^+$ dDC are not required during the initial clonal expansion and priming phase of the allogeneic response.

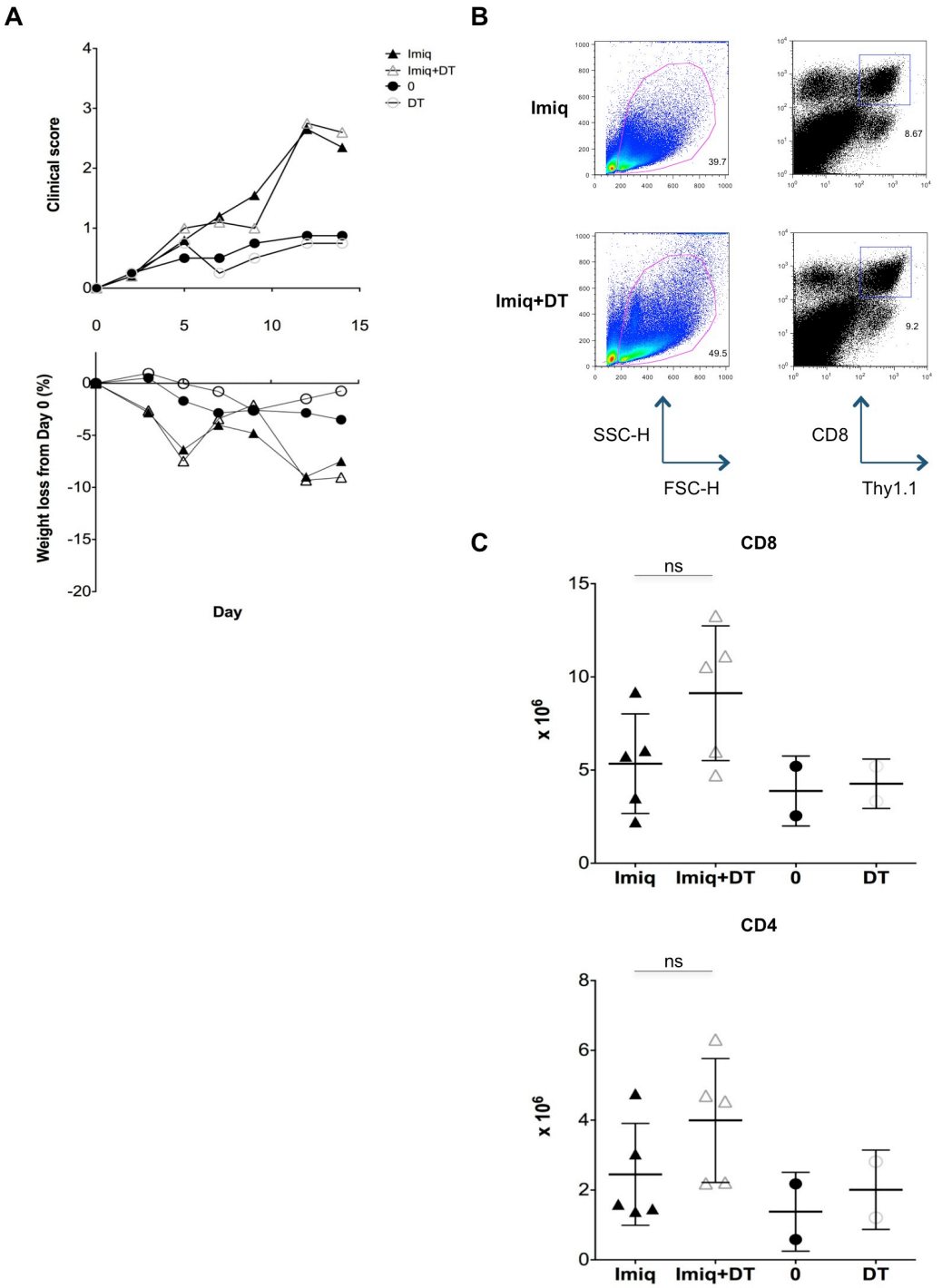

Figure 31: The depletion of host Langerin$^+$ dDC had no effect on the systemic expansion of alloreactive donor T cells. A. Clincal score and weight loss plots (n=2-5, data pooled from 3 independent experiments.). There was no diferrence in the level of systemic GVHD that developed in Imiquimod treated mice with or without host Langerin$^+$ dDC. **B.** Representative dot plots of the spleen of Imiq+PBS and Imiq+DT treated MC on day +14 post donor SC infusion. **C.** Absolute numbers of Thy1.1$^+$ CD8 and CD4 T cells in the spleen of MC on day +14 (n=2-5, data pooled from 3 independent experiments, analysed using a Mann-Whitney test, the mean ±SD is indicated by the horizontal bars.). There was no significant difference in the absolute number of either CD4 or CD8 donor T cells in MC with or without host Langerin$^+$ dDC.

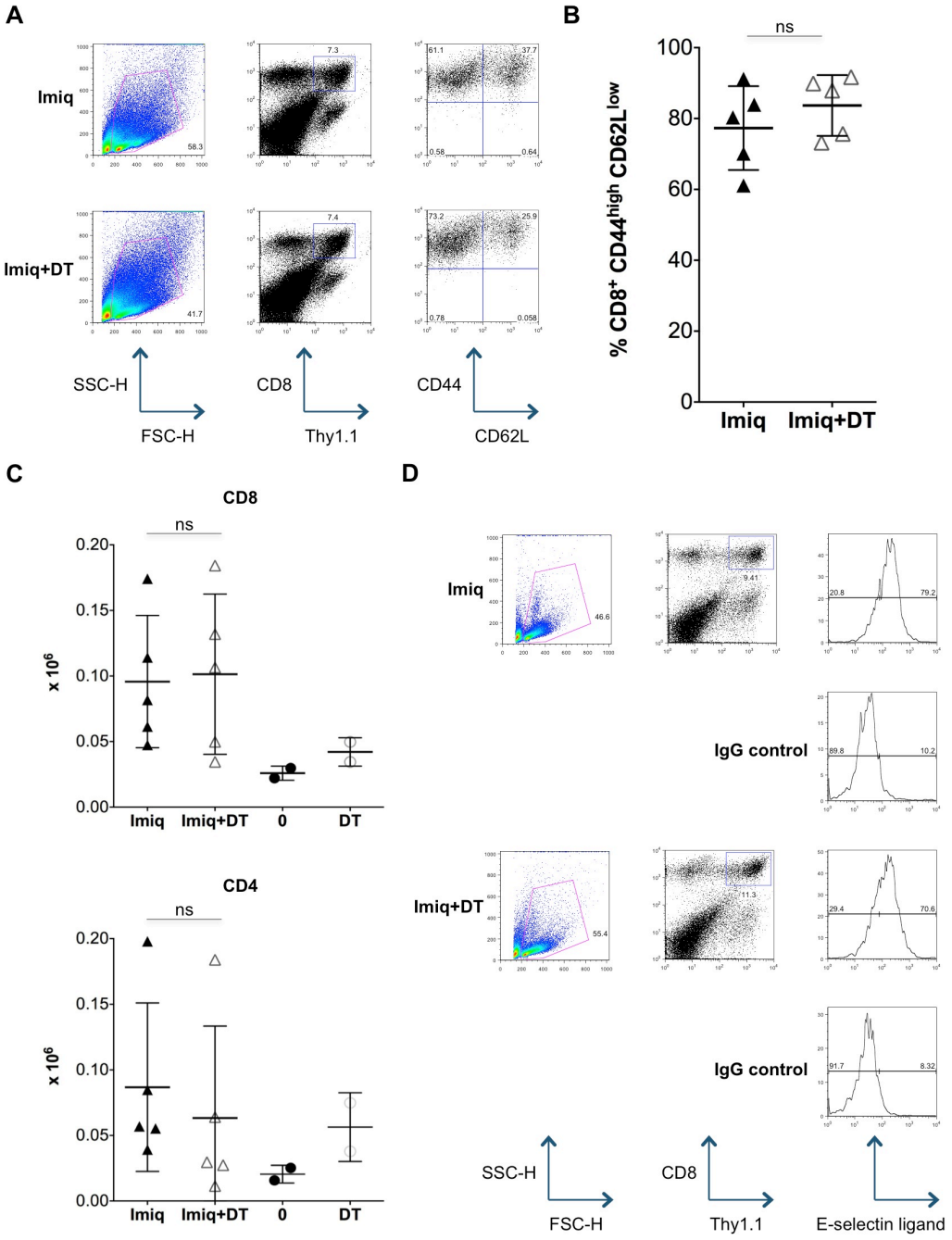

Figure 32: Depletion of host Langerin$^+$ dDC had no effect on the activation and expansion of donor T cells in the skin draining lymph nodes. A. Representative dot plots of the skin draining LN of Imiq+PBS and Imiq+DT treated MC on day +14 post donor SC infusion. **B.** Percentage of gated Thy1.1$^+$ CD8$^+$ T cells that were CD44^{high} CD62L^{low} (n=5, data pooled from 3 independent experiments, analysed using a Mann-Whitney test, the mean ±SD is indicated by the horizontal bars.). There was no difference in the frequency of CD8 T effector memory cells in the presence or absence of host Langerin$^+$ dDC. **C.** Absolute numbers of Thy1.1$^+$ CD8 and CD4 T cells in the skin draining LN of MC on day +14 (n=2-5, data pooled from 3 independent experiments, analysed using a Mann-Whitney test, the mean ±SD is indicated by the horizontal bars.). There was no significant difference in the absolute number of either CD4 or CD8 donor T cells in MC with or without host Langerin$^+$ dDC. **D.** Dot plots of the skin draining LN of Imiq+PBS and Imiq+DT treated MC on day +14 post donor SC infusion. There appeared to be no difference in the frequency of donor Thy1.1$^+$ CD8$^+$ expressing E-selectin ligand.

3.3.3 Host Langerin$^+$ dDC are not required for the development of cutaneous GVHD

In accordance with previous findings[229,283], topical application of Imiquimod initiated the recruitment of effector CTLs into the epidermis inducing localised cutaneous GVHD. After an initial lymphocyte gate, GFP$^-$ were gated to exclude any autofluorescence and examined for their expression of Thy1.1 (Figure 33, A). The depletion of host-type Langerin$^+$ dDC had no significant effect on the frequency of Thy1.1$^+$ donor T cells recruited to the epidermis compared to Imiquimod treated controls (Figure 33, B).

Sections of skin were also H&E stained and examined for histopathological signs of cutaneous GVHD, which includes epidermal thickening, dyskeratosis and inflammatory cell infiltrate. In MCs treated with Imiquimod, evidence of skin pathology was observed indicating that these MCs had developed cutaneous GVHD (Figure 34, A). In the absence of inflammation, no signs of cutaneous GVHD were present (Figure 34, A+B). The depletion of host Langerin$^+$ dDC was found to have no effect on the severity of GVHD observed (Figure 34, B).

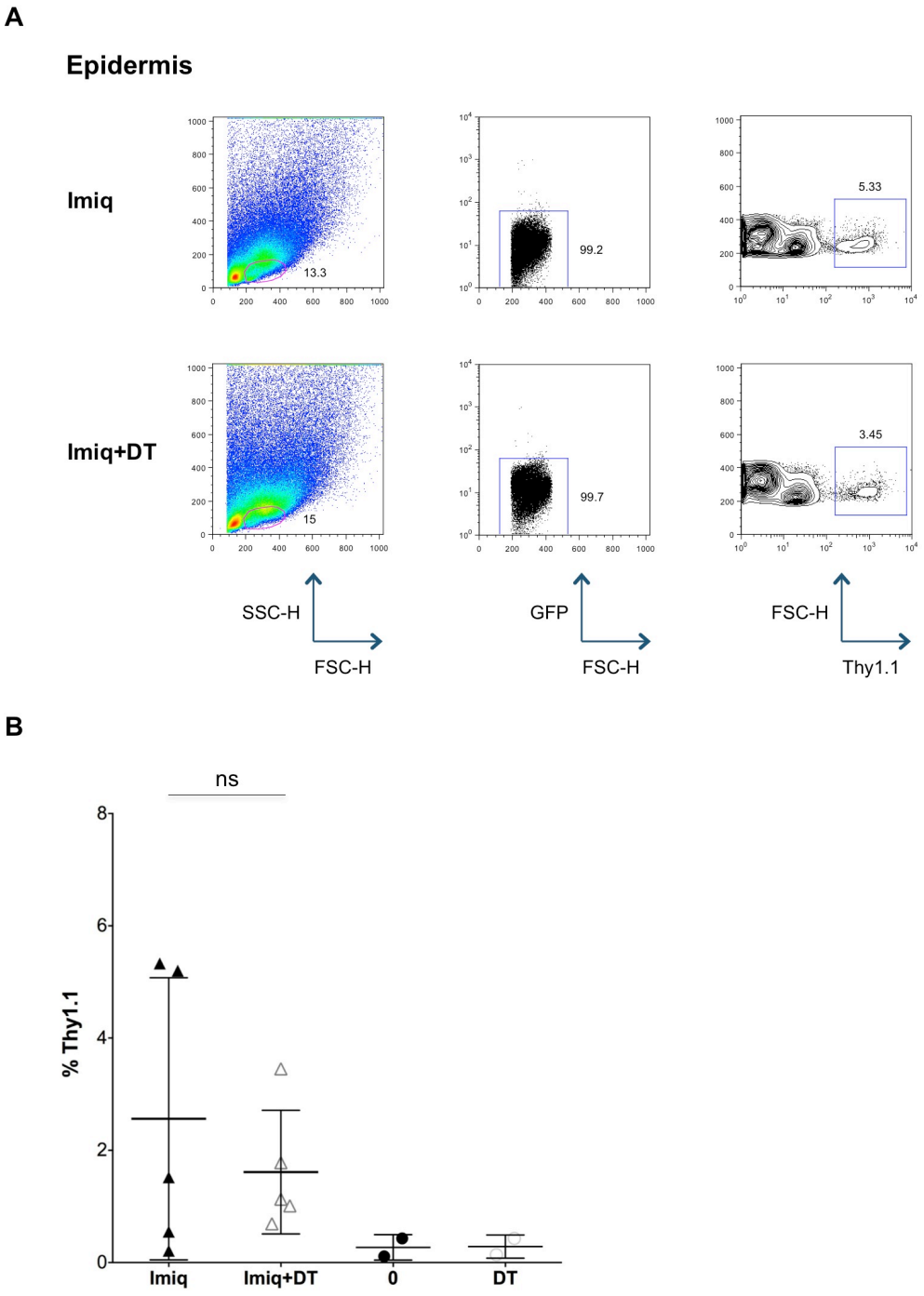

Figure 33: Depletion of host Langerin$^+$ dDC has no effect on the infiltration of donor T cells into the epidermis. A. Representative dot plots of the epidermis of Imiquimod+PBS and Imiquimod+DT treated MC on day +14 post donor SC infusion. After an initial lymphocyte gate, autofluorescent cells were gated out and the sample analysed for the frequency of donor Thy1.1$^+$ T cells. **B.** Summary data showing the accumulation of donor Thy1.1$^+$ T cells as a percentage of the initial FSC-H, SSC-H lymphocyte gate (n=2-5, data pooled from 3 independent experiments, analysed using a Mann-Whitney test, the mean ±SD is indicated by the horizontal bars.). There was no difference in the accumulation of donor Thy1.1$^+$ T cells when host Langerin$^+$ dDC were depleted.

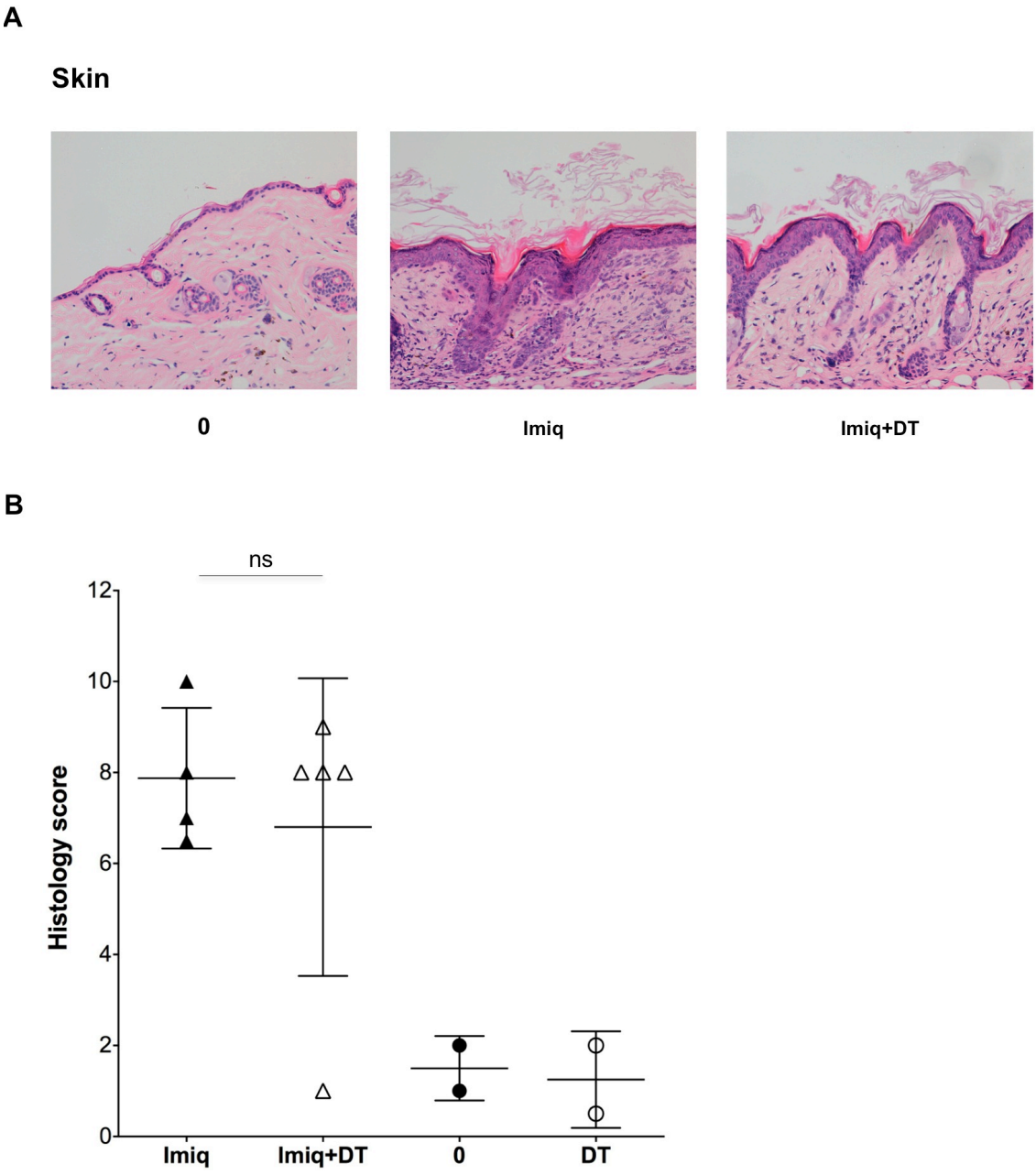

Figure 34: The depletion of host Langerin$^+$ dDC had no effect on the severity of cutaneous GVHD. **A.** Histological sections of back skin on day +14 post donor SC infusion. Images captured at X20 magnification using a Leica DMD108 light microscope. **B.** Summary data of histological GVHD score as evaluated single blind (n=2-5, data pooled from 3 independent experiments, analysed using a Mann-Whitney test, the mean ±SD is indicated by the horizontal bars.). There was no difference in the severity between MC that received Imiquimod and Imiquimod+DT. Mice that received no Imiquimod showed no histological signs of cutaneous GVHD.

3.4 Discussion

3.4.1 Flow cytometry staining of the skin and the Langerin-DTR model

In the first part of this project, I adapted and developed new protocols in the laboratory to consistently identify DC in the skin of mice using flow cytometry. This was important as future experiments relied on my ability to confirm depletion of Langerin$^+$ DC in the skin. Initially, samples exhibited poor viability, as evidenced by the PI staining in Figure 16, and inconsistent staining patterns. Switching to Dispase II, the addition of EDTA to FACS buffer and FBS to the dispase and collagenase steps yielded much more consistent staining patterns in line with published observations[276].

To investigate the role of Langerin$^+$ DC in cutaneous GVHD, we have adopted the inducible Langerin-DTR mouse in our models of GVHD. Incorporating a high-affinity simian DTR and EGFP cassette downstream of the internal stop codon of the Langerin gene, LC and Langerin$^+$ dDC can be selectively depleted via apoptosis upon exposure to DT. LC and Langerin$^+$ dDC develop normally and there are no known side effects associated with the construct. Using the newly established flow cytometry staining protocols in the lab I determined that a single injection of 400 ng was sufficient to deplete both LC and Langerin$^+$ dDC within 24 h. The injection of PBS i.p. as a control had no discernable effects. In line with literature, Langerin$^+$ dDC were found to repopulate the skin more rapidly than host LC. Langerin$^+$ dDC repopulate the dermis by 7 days whereas LC take 6 weeks plus to fully repopulate the epidermis upon depletion[275].

The effect of Imiquimod on the depletion of Langerin$^+$ DC in Langerin-DTR was then examined. In the CD11c-DTR mouse, a transgenic line where the expression of integrin, alpha x (CD11c) is linked to a high affinity diphtheria toxin receptor[204], we noticed that the topical application of Imiquimod reduced the efficiency of DC depletion in the skin. To ensure inflammation induced by Imiquimod did not interfere with the

depletion of Langerin^{+} DC in my models I administered 4 mg of Imiquimod to a cohort of mice 24 h before DT/PBS. This was found to have no effect on the depletion of LC or Langerin^{+} dDC. When using Tg lines of mice it is important to investigate any potential anomalies in the system as meaningful biological observations may be misconstrued.

3.4.2 Investigating the role of host LC in cutaneous GVHD using MCs

The development of GVHD remains a significant clinical burden associated with allogeneic transplantation. The skin is the most commonly affected organ, with cutaneous GVHD developing in 81% of patients with acute GVHD[75]. In MHC-mismatched models of GVHD, recipient APCs that survive the conditioning are essential in the development of GVHD[55]. The skin contains a number of phenotypically distinct dendritic cell populations, including LC and Langerin$^+$ dermal DC. Host LC are of potential interest due to their radioresistance, ability to persist post transplant and immunogenicity of host APC.

Exploiting theses unique characteristics, elegant BM chimera experiments have shown that LC are capable of inducing GVHD-like lesions in the skin when presentation of relevant antigen in the skin is restricted to LC[282,301]. We decided to investigate whether LC were required in the presence of other host-type (BL/6 derived) cutaneous DCs that are capable of presenting relevant antigen. In [BL/6+BALB/c] → Langerin-DTR MCs, it was hypothesised based on the literature that the LC compartment would remain of host (Langerin-DTR) origin (Figure 23, B). LC could therefore be depleted using DT allowing us to investigate the role of host LC in cutaneous GVHD.

However, when the chimerism of LC in established [BL/6+BALB/c] → Langerin-DTR MCs was examined, two populations of LC derived from host and donor cells derived from MHC-mismatched BM were observed. Although the majority of LC in the epidermis were host derived (Langerin-DTR) LC, BALB/c derived LC constituted around ~38% of the total population.

This was an unexpected observation based on the literature and is the first time donor infiltration of LC into the epidermis in mice that have received TCD BM has been reported. Research conducted by Merad et al. has shown that LC in BL/6 mice which expressed the CD45.2 allele were lethally irradiated and reconstituted with CD45.1

congenic donor BM, were found to be of host origin up to 18 months after transplant[258]. In addition, when lethally irradiated BALB/c (H-2d) mice were reconstituted with MHC-mismatched allogeneic TCD BM from a BL/6 (H-2b) donor, LC again remained of host origin for at least 12 months after transplantation[282]. However, when BALB/c recipients were reconstituted with whole BM which contained around ~2% T cells, host LC were largely replaced with donor derived LC, suggesting alloreactive T cells are required for donor conversion[282]. In the [BL/6+BALB/c] → Langerin-DTR MC, the depletion of T cells in donor BM was confirmed before transplant.

Interestingly, despite the presence of donor BALB/c (H-2d) derived LC, virtually no donor BL/6 (H-2b) derived LCs were observed. However, Langerin$^+$ dDC in the dermis were mixed and derived equally from donor BL/6 (H-2b) and BALB/c (H-2d) bone marrow. This indicated that BM precursors from donor BL/6 mice were able to access the skin. The ratio of BL/6:BALB/c BM was then changed from 1:1 to 3:1. Increasing the number of donor BL/6 BM precursors had no effect on the chimerism of LC in the epidermis. In the dermis, the chimerism of dermal DC was altered and skewed towards donor BL/6 derived cells. Taken together, these data suggests there is an active mechanism preventing donor BL/6 precursors establishing LCs in the epidermis.

To account for any inherent strain variation, [BL/6(CD45.2.CD45.1)+B6D2F1(CD45.2)] → BL/6(CD45.1) MCs were generated. In these MC, dermal DC were donor derived and again equally mixed between BL/6 (H-2b) and B62DF1 (H-2db) cells. In the epidermis, no donor BL/6 (H-2b) derived LC were observed. However, when the chimerism of epidermal γδ T cells was examined, the population was split between donor and host BL/6 derived cells with very few donor B62DF1 derived cells detected. This was the converse of what was observed in LC and indicated that BM precursors were in fact able to access the epidermis as well as the dermis. γδ T cells colocalise with LC in the epidermis and have also shown reactivity to self-MHC independent of the antigen[302,303]. Using Tcrd^{tm1Mom} knockout mice (H-2b), in which epidermal γδ T cells

are constitutively absent, one possible experiment to test the role of γδ T cells in the repopulation of host-type LC would be to generate [$\gamma\delta^{-/-}$+BALB/c→ $\gamma\delta^{-/-}$] mixed chimeras. In this model, host-type γδ T cells would be constitutively depleted and therefore unable to influence the repopulation of host-type LC. However, due to time constraints, dissecting the precise mechanism behind this observation was outside the scope of this project.

This is an important observation as MCs are commonly used in the field to dissect the function of cells and genes alike. It appears there is an active, yet to be described mechanism, which prevents LC precursors derived from host-type BL/6 precursors from seeding the epidermis in the presence of host LC. Increasing the number of BL/6 precursors had no effect on LC chimerism despite increasing the frequency of BL/6 derived DC in the dermis. This mechanism also appears to be dependant on the MHC haplotype of donor cells rather than the genetic background of mice. Similar populations of donor derived LC were observed using both BALB/c (H2-d) and B62DF1 (H2-db) as allogeneic donors.

Despite the presence of donor BALB/c derived LC, the depletion of host LC was found to significantly decrease the severity of cutaneous GVHD in MC[229]. This would indicate that a direct interaction of host LC with T cells or another immunomodulatory cell type is important. Inflammation mediated by the TLR 7-8 agonist Imiquimod would have the same effect on donor and host derived LC in the epidermis. The cytokines and/or chemokines released by LC in specific response to Imiquimod could be compensated for by BALB/c derived LC when host LC have been depleted using DT.

3.4.3 Host Langerin$^+$ dDC are not required for cutaneous GVHD

Finding a precise role for LC *in vivo* became even more complex with the discovery of Langerin$^+$ dDC. Modifying the MC model we used to deplete host LC, I was able to generate MCs where host-type (H2-b) Langerin$^+$ dDC but not host LC could be depleted. This was important, as many of the immunological functions ascribed to LC in the past have now been attributed to the newly discovered Langerin$^+$ dDC[263,304].

To date, a role for Langerin$^+$ dDC in cutaneous GVHD has never been investigated. In our MC model of localised cutaneous GVHD, host Langerin$^+$ dDC in contrast to host LC had no effect on the severity of GVHD that developed in the skin[229]. Other host-type DC subsets present in the skin such as LC and conventional dDC likely compensated for the depletion of host Langerin$^+$ dDC. However, as Langerin$^+$ dDC are efficient at cross-presenting self-antigens, BALB/c-derived Langerin$^+$ dDC, which will not be depleted by DT, may be able to compensate for the depletion of host Langerin$^+$ dDC. To definitively rule out a non-redundant role for Langerin$^+$ dDC in the development of cutaneous GVHD, a model where all other DC are present except Langerin$^+$ dDC would need to be developed.

The MC model is a reductionist system and the use of the TLR 7-8 agonist Imiquimod stimulates a potent response in the skin of the MC. Any contribution of host Langerin$^+$ dDC may also be masked by the potent inflammatory response mediated by Imiquimod. Another technical difficulty using the MC model was identifying host Langerin$^+$ dDC during the allogeneic response. To analyse the cells in this series of experiments, I used the FACSCalibur (BD) flow cytometry system, which permitted a maximum staining panel of 4 separate flurophores. Langerin$^+$ dDC account for around ~4.8% of DC found in the dermis (Table 7), further separating this population into Langerin-DTR and BALB/c derived cells using 4 flurophores proved challenging. In future experiments, the LSRFortessa (BD) and a minimum staining panel of 5 antibodies was used to characterise DC.

4 The depletion of host Langerhans cells significantly reduced the severity of cutaneous GVHD

In the previous chapter, I developed protocols to consistently identify DC in the skin and investigated the role of host Langerin$^+$ dDC in a model of localised cutaneous GVHD. Previous work in our lab using this model has already established a role for host LC in the skin during inflammation. However, the role of host haematopoietic APC such as DC in the development of acute GVHD remains controversial, with a number of studies reporting that host non-haematopoietic APC are sufficient to induce both CD4- and CD8-mediated GVHD[129,130].

To investigate whether host LC had a role in the development of GVHD in a more clinically relevant pre-clinical model of acute systemic GVHD, a MHC-matched, minor H antigen mismatched model of GVHD was developed. This model represents transplants in the clinic more closely than MHC-mismatched models, as MHC-mismatched transplants are not commonly performed in humans. This model was then adapted to the Langerin-DTR mouse to investigate whether the conditional depletion of host LC and/or Langerin$^+$ dDC had any influence on the development of either systemic or cutaneous GVHD.

4.1 MataHari minor H mismatch model of acute GVHD

4.1.1 1 x10^6 MataHari CD8 T cells and 2 x10^6 polyclonal CD4 T cells is sufficient to induce GVHD

In the clinic, male recipients of female MHC-matched BMT (F→M) are at greater risk of developing GVHD than other sex combinations and show strong alloresponses to H-Y derived minor histocompatibility antigens (H)[66,305,306]. Using MataHari (Mh) Tg CD8 T cells to initiate GVHD, a F→M, MHC-matched, minor H mismatch model of acute GVHD was developed.

Mh CD8 T cells are monoclonal and bear a TCR specific for the ubiquitous male antigen (H-Y) derived peptide WMHHNMDLI (from the *Uty* gene), combined with the MHC class I molecule H-2D^{b}[189]. To investigate whether Mh T cells were capable of initiating systemic GVHD, male BL/6 mice were lethally irradiated with a split dose of 11 Gy and transplanted with a mixture of 1 x10^6 Mh T cells and 5 x10^6 BM, derived from a female BL/6 donor. In some models of CD8 T cell mediated GVHD, CD4 “help” can enhance the severity of GVHD[188,307]. Therefore, an additional cohort of recipients was injected with 2 x10^6 polyclonal CD4 T cells, derived from a female BL/6 donor, along with the BM and Mh T cell mixture. An exact outline of model is illustrated in Figure 35A.

Male BL/6 recipients were tracked for changes in weight and clinical observation score, key indicators of clinical GVHD, and culled 7 and 14 days after transplant. All recipients survived until the day of takedown but recipients that received 1x10^6 Mh T cells developed clinical GVHD as indicated by observation scores and weight loss compared to BM controls (Figure 35, B). However, the clinical score and weight loss observed was higher in recipients that received Mh+CD4 T cells than Mh T cells alone (Figure 35, B).

In the spleen, Vβ8.3$^+$ CD8$^+$ Mh T cells were gated and analysed for their expression of CD44 and CD62L. A dose of 1 x10^6 Mh T cells was sufficient for Mh T cells to engraft and expand *in vivo* in the presence or absence of 2 x10^6 polyclonal CD4 T cells (Figure 36, A). However, there was an increase in the absolute number of Mh T cells in the spleen by day 7 when Mh T cells were transplanted with polyclonal CD4 T cells (Figure 36, B). There was no difference in the absolute number of Mh T cells by day 14. In controls, which received BM alone, a small frequency of Vβ8.3$^+$ and CD8$^+$ was identified. These represent endogenous donor CD8 T cells derived from the donor BM. To definitively track and characterise Mh T cells in future experiments a specific congenic marker, such as Thy1.1, was used.

A dose 1 x10^6 cells was also sufficient for Mh T cells to infiltrate and accumulate in the skin 7 days after transplant (Figure 37, A). After an initial live cell gate, followed by a lymphocyte gate, Mh T cells were gated based on their expression of VB8.3$^+$ CD45.2$^+$ and CD8$^+$. Mh T cells in the skin were both Vβ8.3$^+$ CD45.2$^+$. However, the expression of CD8 was inconsistent, with a large frequency of cells CD8$^-$ (Figure 37, A). This indicated that either Mh T cells down-regulate their expression of CD8 or an enzymatic step during processing was interfering with staining. Similar to the spleen, there was an increase in the frequency of Mh T cells in recipients that received Mh+CD4 T cells versus Mh T cells alone by day 7. However, there was no difference in the frequency of Mh T cells by day 14.

Due to the increase of clinical GVHD and higher numbers/frequency of Mh T cells in both the spleen and epidermis 7 days after transplant, future experiments using the Mh minor H mismatch model will use 1 x10^6 Mh T cells and 2 x10^6 female polyclonal CD4 T cells to induce GVHD. This dose was sufficient to induce acute GVHD in lethally irradiated male recipients, with GVHD like-pathology developing in GVHD target organs such as the skin and gut as evidenced by histological sections (Figure 38).

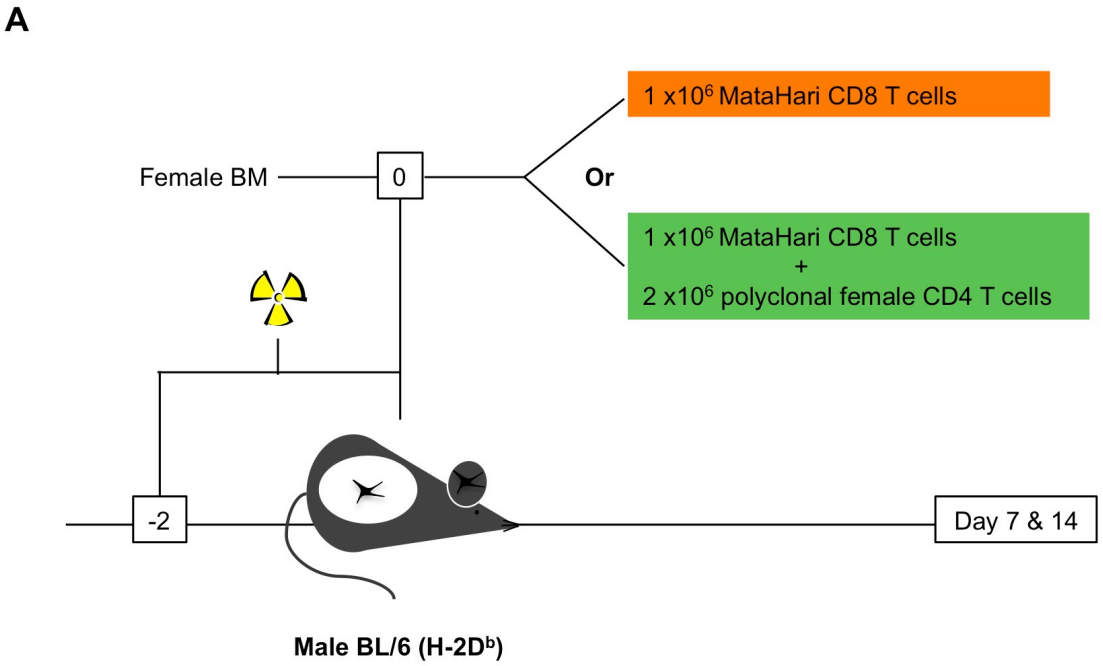

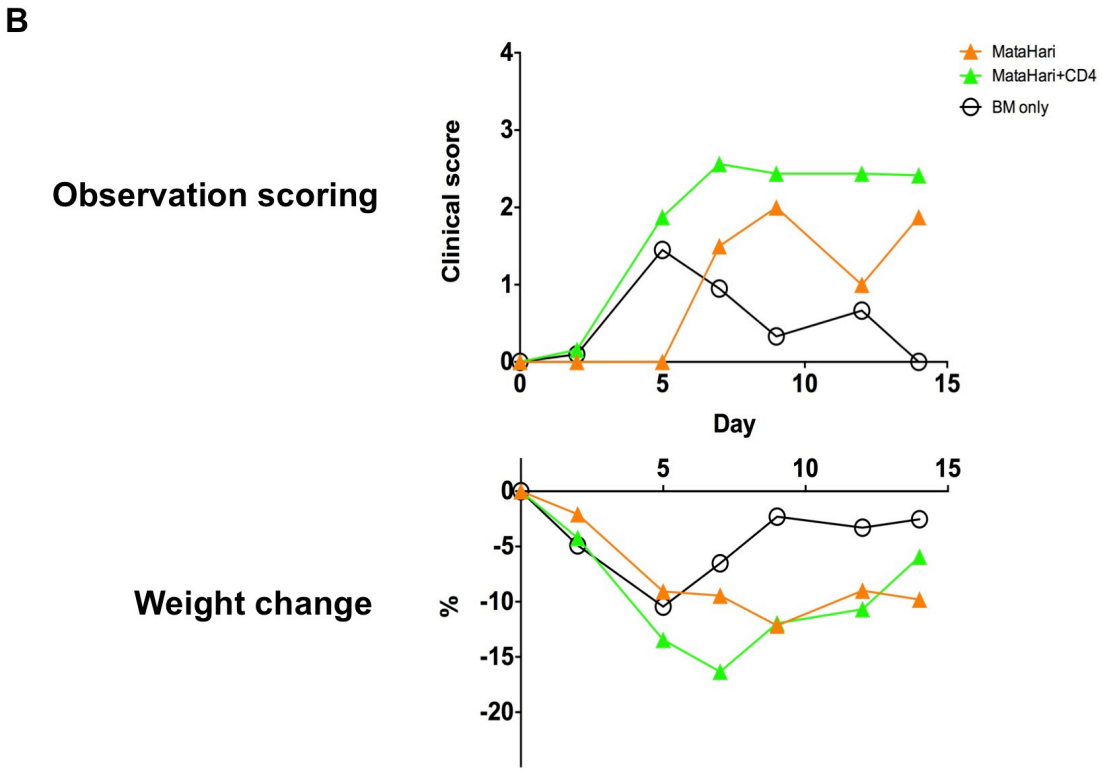

Figure 35: MataHari minor H mismatch model of GVHD. A. Male BL/6 mice (H-2b) were lethally irradiated with a split dose of 11 Gy and transplanted with a mixture of 1x10^6 Mh CD8 T cells and 5 x10^6 BM, derived from a female BL/6 donor. Another cohort of recipients received 2 x10^6 polyclonal CD4 T cells, derived from a female BL/6 donor, along with BM and Mh T cells. The mice were culled 7 and 14 days post transplant. **B.** Clinical score and weight loss plots (n=4-8, data pooled from 2 independent experiments, each data points represents the mean). Male BL/6 recipients that received Mh+CD4 T cells developed higher levels of clinical GVHD than recipients that received Mh T cells alone.

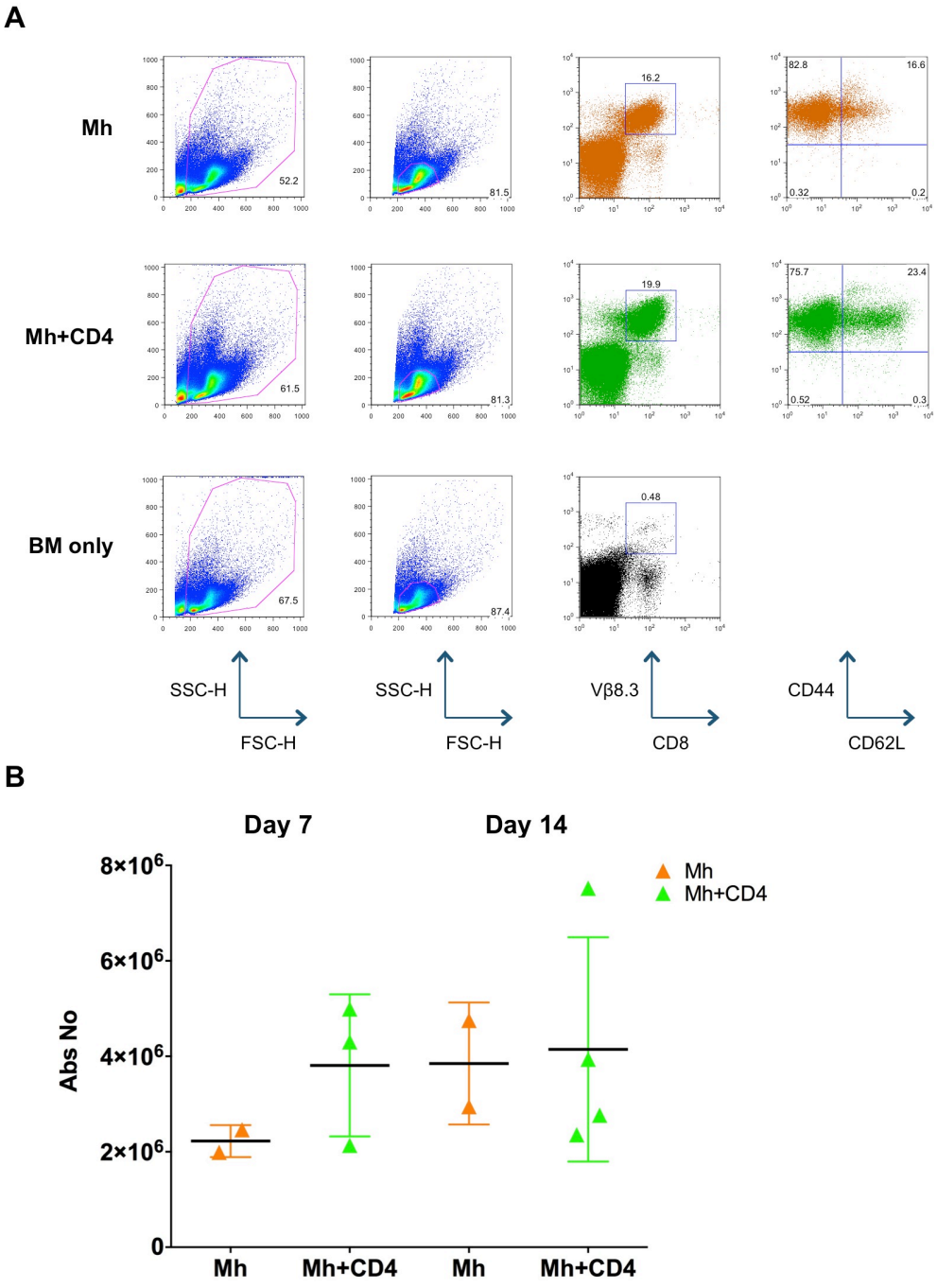

Figure 36: A dose of 1 x10^6 cell is sufficient for MataHari T cells to engraft and expand *in vivo.* A. Representative dot plots of SC taken from male BL/6 recipients 7 days after transplant. After an initial live gate, followed by a lymphocyte gate, Mh T cells were identified based on their expression of Vβ8.3 and CD8. The activation profile of Mh T cells was also analysed using CD44 and CD62L. In the spleen of recipients that were transplanted with Mh and Mh+CD4 T cells, 1 x10^6 Mh T cells was sufficient for Mh T cells to engraft and expand *in vivo*. **B.** Absolute numbers of Vβ8.3$^+$ CD8$^+$ Mh T cells in the spleen of male BL/6 recipients 7 and 14 days after transplant (n=2-4, data pooled from 2 independent experiments, horizontal bars indicate the mean±SD). There was a small increase in the number of Mh T cells in the spleen of recipients that received Mh+CD4 T cells compared to Mh T cells alone by day +7 after transplant. There was difference in the number of Mh T cells in the spleen by day +14 after transplant.

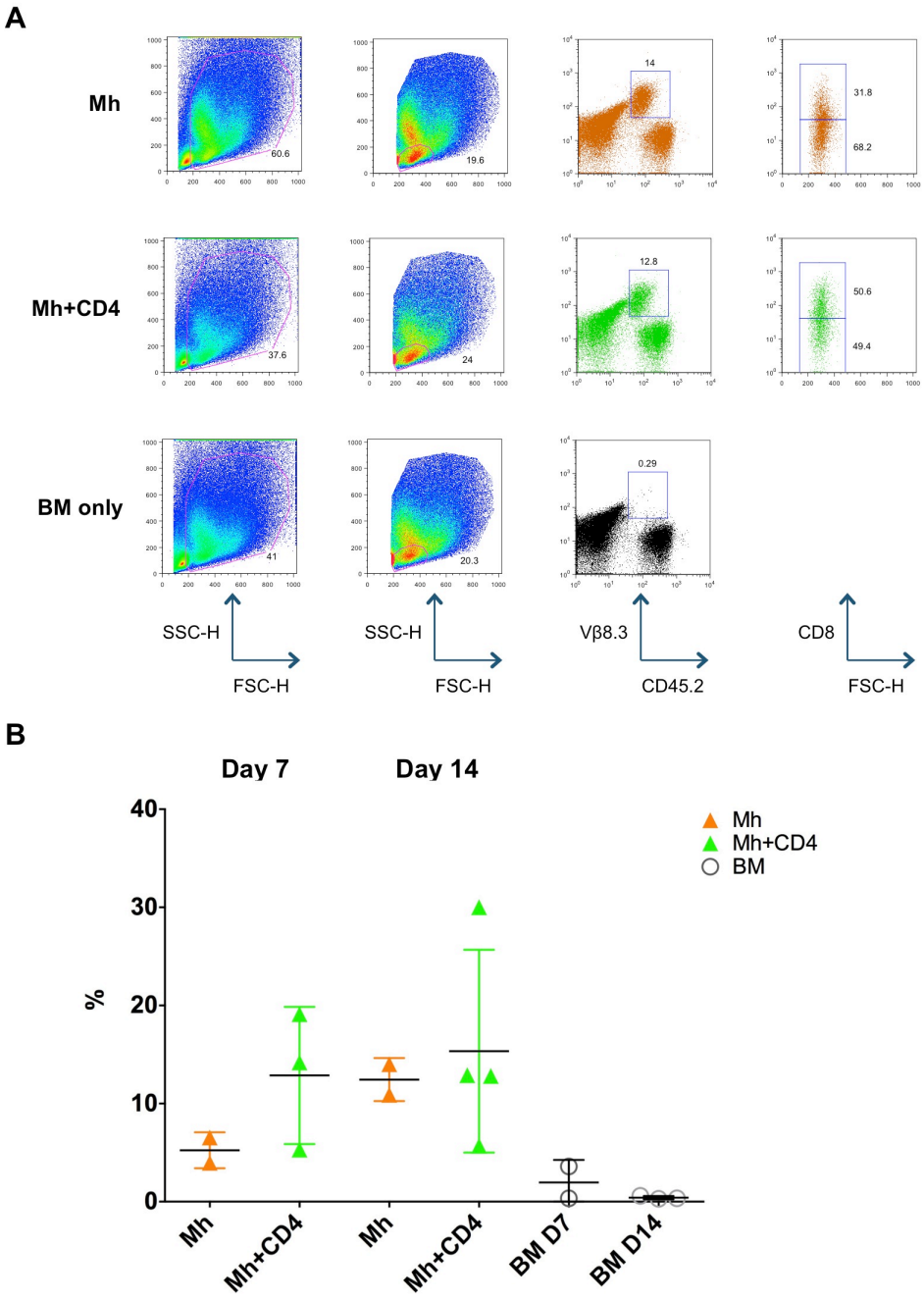

Figure 37: A dose of 1 x10^6 cells is sufficient for MataHari T cells to accumulate in the skin 7 days after transplant. A. Representative dot plots of the epidermis taken from male BL/6 recipients 14 days after transplant. After an initial live cell gate, followed by a lymphocyte gate, Mh T cells were identified based on their expression of Vβ8.3, CD45.2 and CD8β. In the epidermis of recipients that were transplanted with Mh and Mh+CD4 T cells, 1 x10^6 Mh T cells was sufficient for Mh T cells to accumulate in the skin. However, the expression of CD8β on Mh T cells was inconsistent. **B.** Summary data showing the accumulation of Vβ8.3$^+$ CD45.2$^+$ Mh T cells in the epidermis of male BL/6 recipients 7 and 14 days after transplant as a percentage of the initial FSC-H, SSC-H lymphocyte gate (n=2-4, data pooled from 2 independent experiments, horizontal bars indicate the mean±SD). There was a small increase in the number of Mh T cells in the epidermis of recipients that received Mh+CD4 T cells compared to Mh T cells alone by day 7. There was no difference by day 14. In controls that received BM alone, no Mh T cell accumulated in the skin.

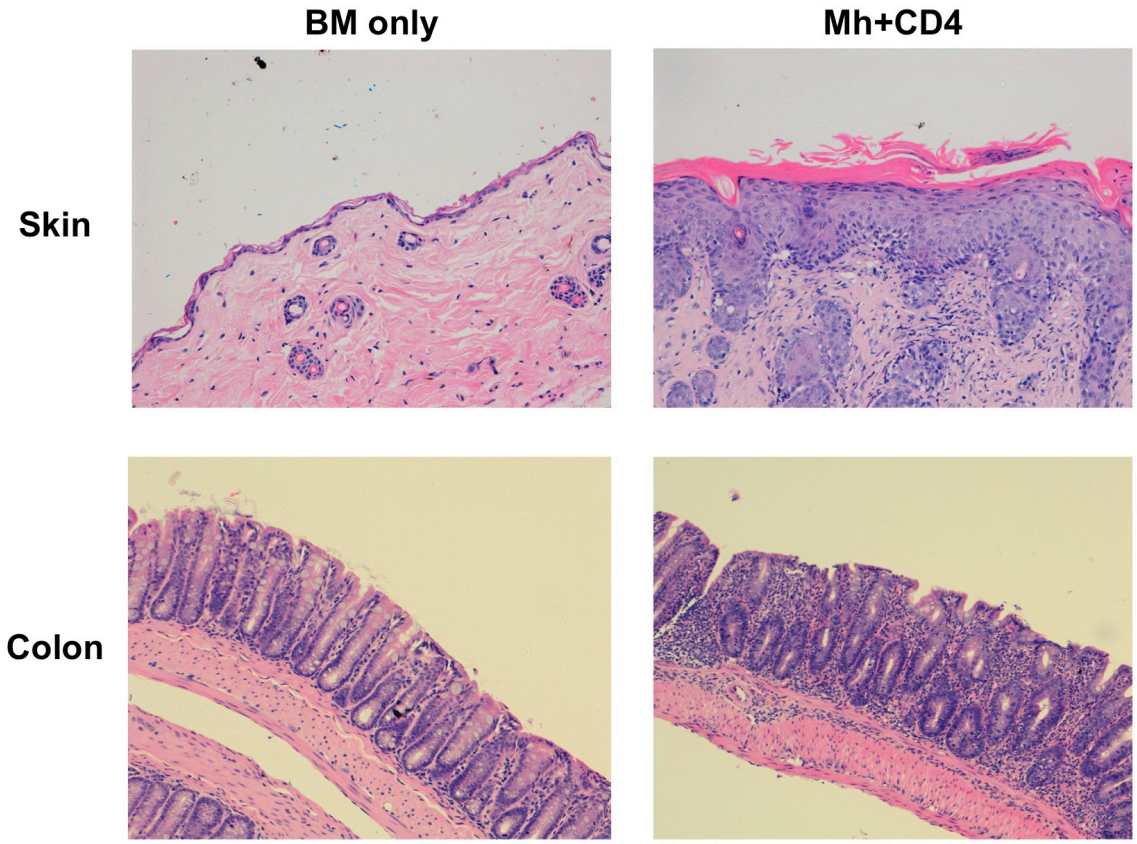

Figure 38: 1 x10^6 MataHari T cells is sufficient to induce GVHD 7 days after transplant. Histological sections of back skin and the colon of male recipients 7 days post transplant. Images captured at x10 magnification using a Leica DMD108 light microscope. Evidence of histological GVHD can be observed in both the skin and colon of recipients that received Mh+CD4 T cells. In the skin, significant levels of epidermal thickening, dyskeratosis and lymphocyte infiltration was present in recipients that received Mh+CD4 T cells compared to BM controls. In the colon, significant levels of lamina propria inflammatory cell infiltrate, crypt epithelial cell apoptosis and crypt loss was present in recipients that received Mh+CD4 T cells compared to BM controls.

4.1.2 Incubating SC with Dispase II impedes the staining of Mh T cells with CD8

The expression of CD8β on Mh T cells in the skin was inconsistent. It has previously been shown that Dispase II can interfere with the expression of CD8 on lymphocytes[308]. To investigate whether Dispase II interfered with the staining of Mh T cells with anti-CD8 antibodies, SC were harvested from BL/6 recipients 7 days after transplant with Thy1.1^{+} Mh T cells, 2 x10^{6} CD4 T cells and 5 x10^{6} BM. SC were incubated at 36 °C and 2.5 mg/ml Dispase II added for 0, 30, 60 and 90 min. The samples were then stained for Mh T cells and the expression of CD8 examined.

After 30 min with Dispase II, the expression of CD8α on Mh T cells was undetectable (Figure 39). Mh T cells remained CD8β^{+} until SC samples were incubated with Dispase II for 90 min (Figure 39). However, the expression of CD8β was reduced compared to controls the longer samples were incubated with Dispase II. In controls, which were incubated for 90 min without Dispase II, Mh T cells expressed both CD8α and CD8β (Figure 39). Therefore, the use of anti-CD8α or anit-CD8β as an antibody to identify Mh T cells in Dispase II treated samples was discontinued.

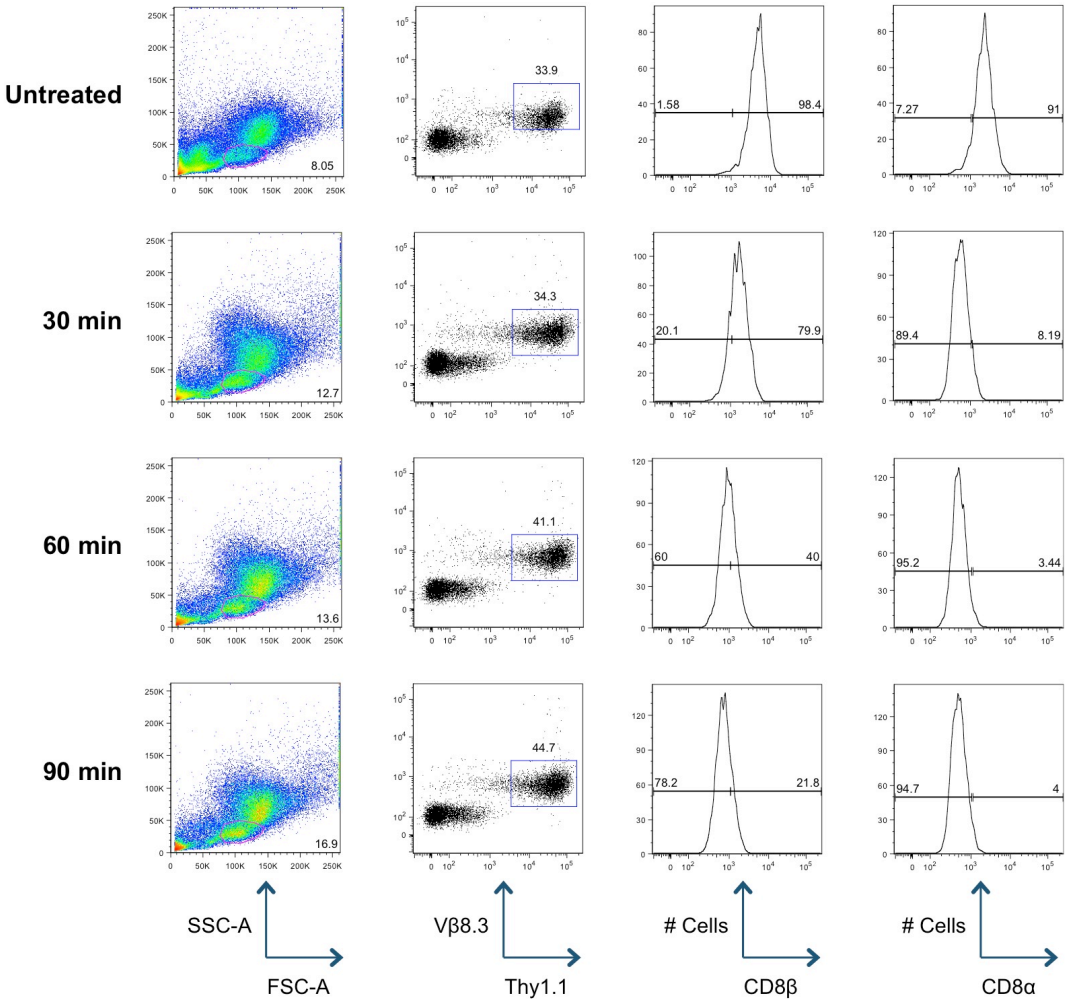

Figure 39: Incubating splenocytes with Dispase II restricts the identification of T cells using CD8. Representative dot plots of SC samples treated with or without 2.5 mg/ml Dispase II taken from a BL/6 mouse 7 days after BMT with 1x10^6 Mh T cells, 2 x10^6 CD4 T cells and 5 x10^6 BM. After a lymphocyte gate based on FSC-A, SSC-A, donor Mh T cells were identified based on their expression of Vβ8.3 and Thy1.1. Mh T cells were CD8α^+ and CD8β^+ in untreated controls. In SC samples incubated with Dispase II for 30, 60, 90 min, the expression of CD8α on Mh T cells was undetectable. The expression of CD8β was detectable until samples were incubated with Dispase II for 90 min. However, the expression was reduced compared to controls in all samples treated with Dispase II.

4.2 The depletion of host Langerhans Cells reduced the severity of cutaneous GVHD

4.2.1 Depletion of host Langerin$^+$ DC has no effect on systemic GVHD

The MataHari minor H mismatch model was then adapted to Langerin-DTR mice, enabling us to investigate the role of host Langerin$^+$ DC in a more clinically relevant model of GVHD.

Male Langerin-DTR mice were lethally irradiated and reconstituted with a mixture of 1 x10^6 Thy1.1$^+$ Mh T cells along with 5 x10^6 BM and 2 x10^6 CD4 T cells, derived from a female WT BL/6 donor. To deplete host Langerin$^+$ DC, Langerin-DTR mice were injected on day -2, 1, 4 and 7 days post transplant with 400 ng of DT. This was sufficient to deplete both host LC and Langerin$^+$ dDC during the development of acute GVHD mediated by Mh T cells. As a control, another cohort of Langerin-DTR recipients were treated with PBS (Figure 40, A).

Langerin-DTR recipients were tracked for changes in weight and clinical observation scores blinded, 3 times a week for 7 weeks (Figure 40, B). Langerin-DTR recipients that received Mh T cells developed clinical GVHD, with a number of recipients sacrificed for humane reasons when either the percentage weight loss exceeded 20% from original weight recorded at day 0 or clinical observations score exceeded 4. This contrasted recipients that were transplanted with BM alone, which had a 100% survival rate. However, there was no significant difference in the severity of acute GVHD that developed in Langerin-DTR recipients in the presence or absence of host Langerin$^+$ DC as evidenced by weight loss and survival, two key indicators of clinical GVHD (Figure 40, B).

The depletion of Langerin$^+$ DC had no effect on the expansion and activation of circulating Mh T cells in the blood 14 days after transplant. After an initial lymphocyte gate, Vβ8.3$^+$ and CD8$^+$ Mh T cells were analysed for their expression of CD44 and

CD62L (Figure 41, A). There was no significant difference in either the frequency of Mh T cells or frequency of $CD44^{high}$ $CD62L^{low}$ effector Mh T cells circulating in the blood in the presence or absence of host $Langerin^+$ DC (Figure 41, B).

Focusing on weight loss and survival of Langerin-DTR recipients, clinical GVHD appeared to peak 26 days after transplant (Figure 40, B). Langerin-DTR recipients were then culled either 7 days, during the initial cytokine storm phase, or 26 days after transplant to investigate whether $Langerin^+$ DC have a role in the development of GVHD. In the spleen, the depletion of $Langerin^+$ DC had no effect on the expansion, activation or function of donor T cells 7 and 26 days after transplant. After a lymphocyte gate, $V\beta8.3^+$ $Thy1.1^+$ $CD8^+$ Mh T cells and $CD4^+$ T cells were analysed for their expression of CD44 and CD62L (Figure 42, A). There was no significant difference in either the absolute number of Mh and CD4 T cells or frequency of $CD44^{high}$ $CD62L^{low}$ effector Mh and CD4 T cells in the presence or absence of host $Langerin^+$ DC at both time points (Figure 42, B). In BM controls, no evidence of Mh T cells was detected.

Mh T cells were then taken from the spleen of Langerin-DTR recipients 7 days after transplant and restimulated for 8 h with 5 μm of relevant (WMH) or irrelevant (SIINFEKL) peptide *in vitro*. After a lymphocyte gate, $V\beta8.3^+$ $Thy1.1^+$ Mh T cells were analysed for their expression of the type II interferon, IFN-γ, a potent cytokine which shows a strong correlation with GVHD (Figure 43, A)[309]. After 8 h, Mh T cells stimulated with relevant peptide expressed IFN-γ. However, there was no significant difference in the expression of IFN-γ by Mh T cells from recipients with or without host $Langerin^+$ DC (Figure 43, B). IFN-γ expression was also antigen specific, as Mh T cell in controls stimulated with irrelevant peptide did not express IFN-γ after restimulation.

In the skin draining LN, defined in this study as the axial, brachial, cervical and inguinal LN, the depletion of $Langerin^+$ DC again had no effect on either the expansion or activation of Mh T cells 7 and 26 days after transplant. After a lymphocyte gate, Mh T

Vβ8.3^{+} Thy1.1^{+} and CD8^{+} Mh T cells and CD4^{+} T cells were analysed for their expression of CD44 and CD62L (Figure 44). There was no significant difference in either the absolute number of Mh T cells or frequency of CD44^{high} CD62L^{low} effector Mh T cells in the presence or absence of host Langerin^{+} DC 7 and 26 days after transplant (Figure 45). There was also no significant difference in either the absolute number of CD4 T cells or frequency of CD44^{high} CD62L^{low} effector CD4 T cells in the presence or absence of host Langerin^{+} DC 26 days after transplant. No data for CD4 T cells was recorded 7 days after transplant.

Taken together, these data shows that the depletion of host Langerin^{+} DC has no effect on the severity of GVHD that develops in this model.

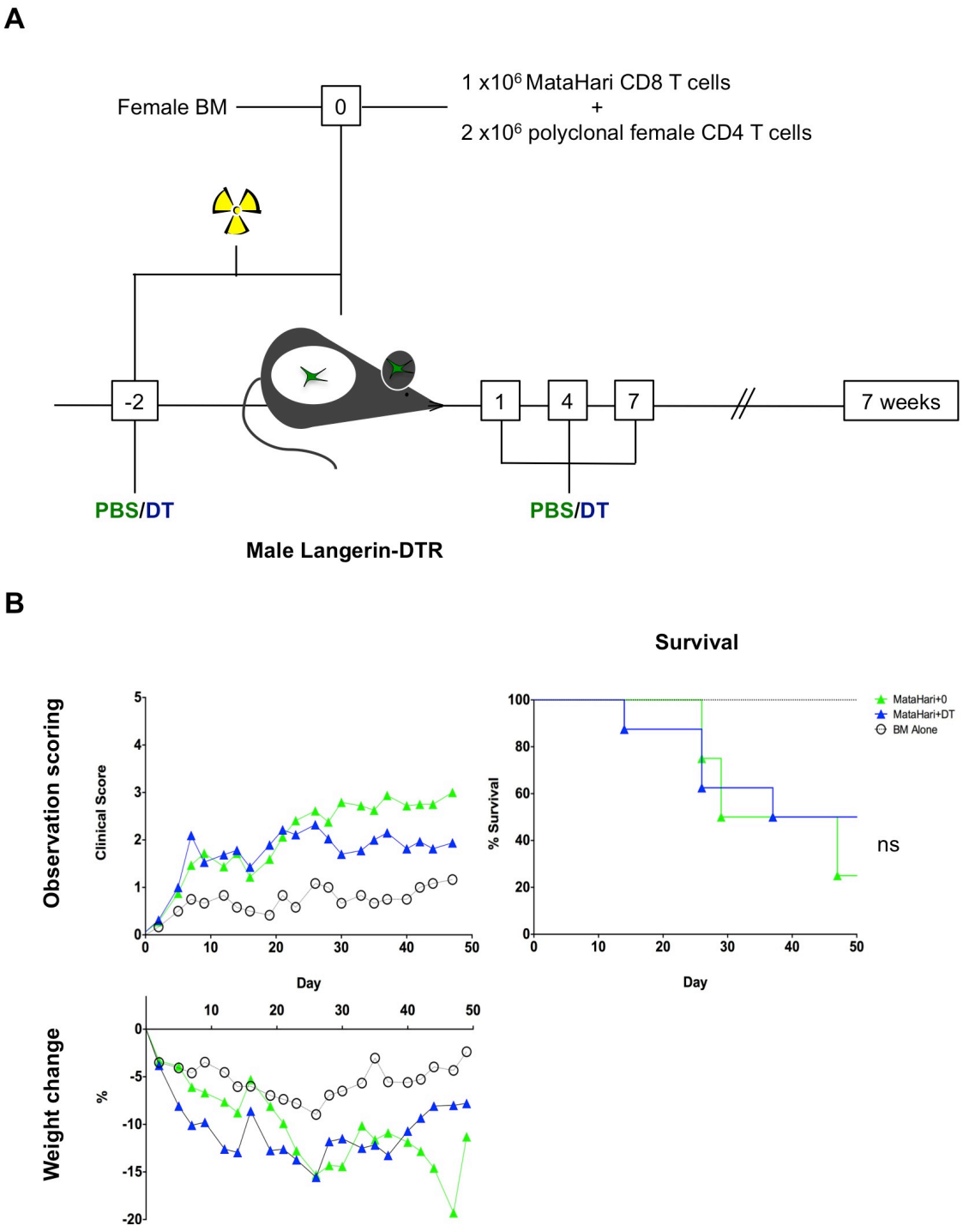

Figure 40: The depletion of host Langerin$^+$ DC had no effect on the development of acute GVHD. A. Male Langerin-DTR mice were lethally irradiated with a split dose of 11 Gy and reconstituted with a mixture of 1 x10^6 Thy1.1$^+$ Mh T cells, 2 x10^6 CD4 T cells and 5 x 10^6 BM. To deplete host Langerin$^+$ DC, Langerin-DTR recipients were injected i.p. with 400 ng of DT on day -2, 1, 4 and 7 post transplant. Controls were treated with PBS. Langerin-DTR recipients were tracked for changes in weight and clinical score and culled 7 weeks later. **B.** Clinical score, weight loss and survival plots (n=3-8, data pooled from 2 independent experiments, each data point represents the mean, survival curve analysed using a log-rank (Mantel-Cox) test). The depletion of Langerin$^+$ DC had no effect on the severity of GVHD that developed.

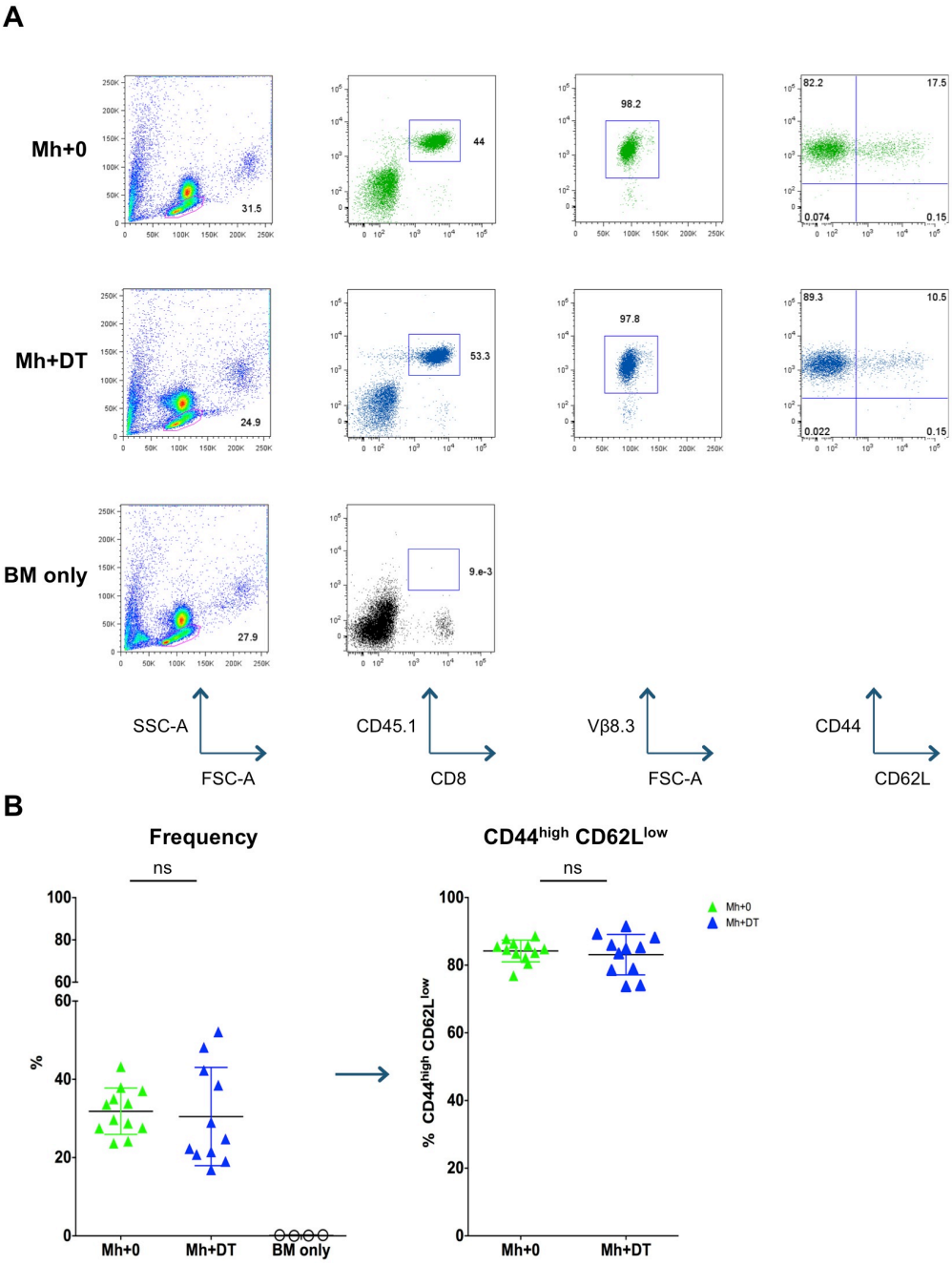

Figure 41: The depletion of host Langerin$^+$ DC had no effect on the frequency of Mh T cells in the blood. A. Representative dot plots of blood taken from Langerin-DTR recipients 14 days after transplant. After a lymphocyte gate based on FSC-A, SSC-A, Mh T cells were identified based on their expression of Vβ8.3, CD45.1 and CD8. The activation profile of Mh T cells was also analysed using CD44 and CD62L. Mh T cells were circulating in the blood in the presence or absence of host Langerin$^+$ DC. In BM controls, no Mh T cells were detected. **B.** *Left-* Summary data showing the frequency of Mh T cells as a percentage of the initial lymphocyte gate 14 days after transplant (n=11-12, data pooled from 3 independent experiments, horizontal lines represent the mean±SD, data analysed using a Mann-Whitney test). *Right-* Summary data showing the frequency of CD44^{high} CD62L^{low} effector Mh T cells as a percentage of Mh cells gated 14 days after transplant (n=11-12, data pooled from 3 independent experiments, horizontal lines represent the mean±SD, data analysed using a Mann-Whitney test). The depletion of host Langerin$^+$ DC had no effect on the expansion or activation of circulating Mh T cells.

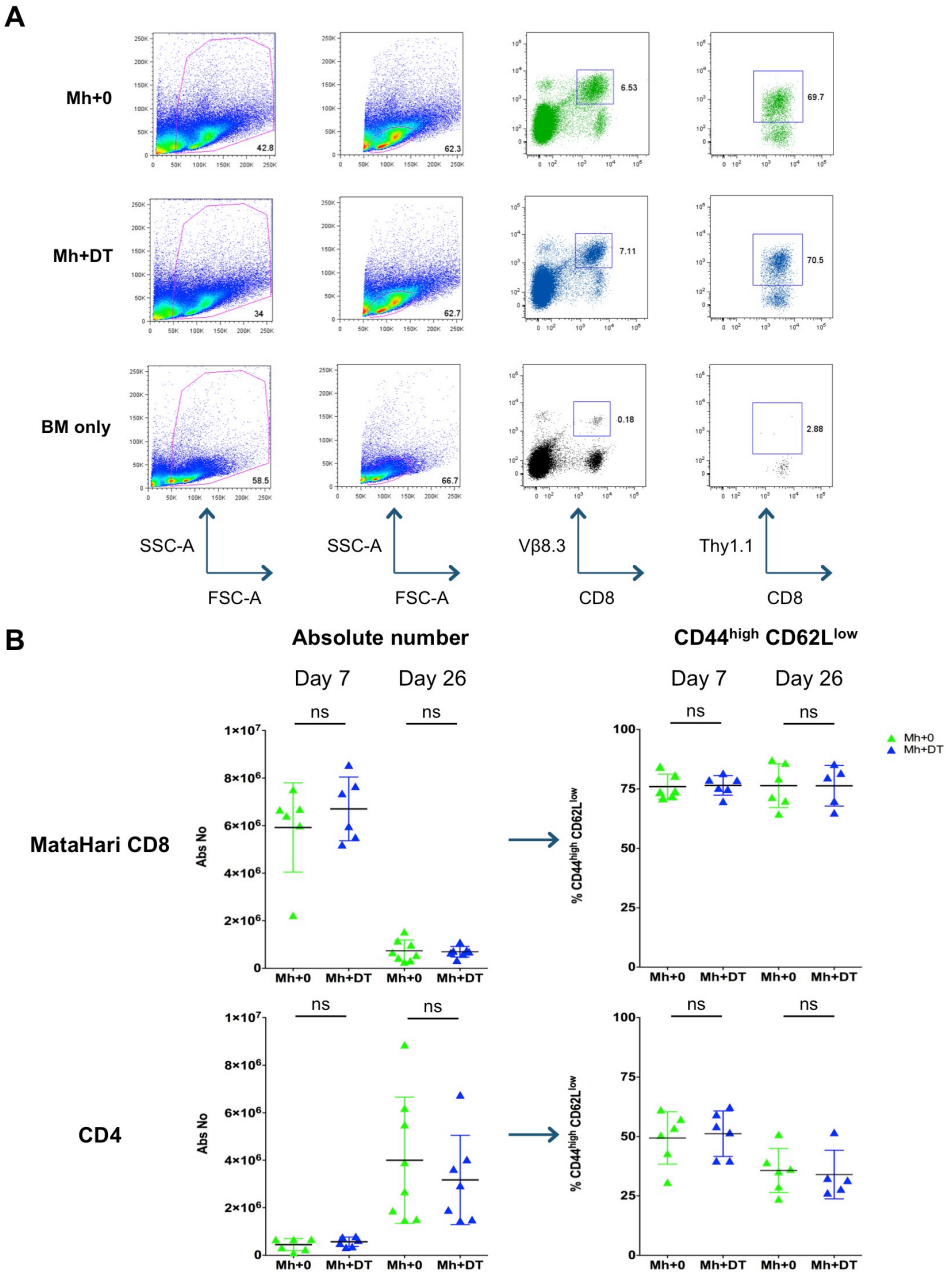

Figure 42: The depletion of host Langerin$^+$ DC had no effect on the expansion and activation of donor T cells in the spleen. A. Representative dot plots of SC taken from Langerin-DTR recipients 7 and 26 days after transplant. After an initial anti-apoptotic cell gate followed by a lymphocyte gate, Mh T cells were identified based on their expression of Vβ8.3, Thy1.1 and CD8. The activation profile of Mh T cells was also analysed using CD44 and CD62L. Mh T cells expanded in the spleen in the presence or absence of host Langerin$^+$ DC. In BM controls, no Mh T cells were detected. **B.** *Left*- Absolute number of Vβ8.3$^+$ Thy1.1$^+$ Mh and CD4$^+$ T cells in the spleen 7 and 26 days after transplant (n=6-8, data pooled from 3 independent experiments, horizontal lines represent the mean±SD, data analysed using a Mann-Whitney test). *Right*- Summary data showing the frequency of CD44^{high} CD62L^{low} effector Mh T cells as a percentage of Mh and CD4 T cells gated (n=6-8, data pooled from 3 independent experiments, horizontal lines represent the mean±SD, data analysed using a Mann-Whitney test). The depletion of host Langerin$^+$ DC had no effect on the expansion or activation of donor T cells in the spleen.

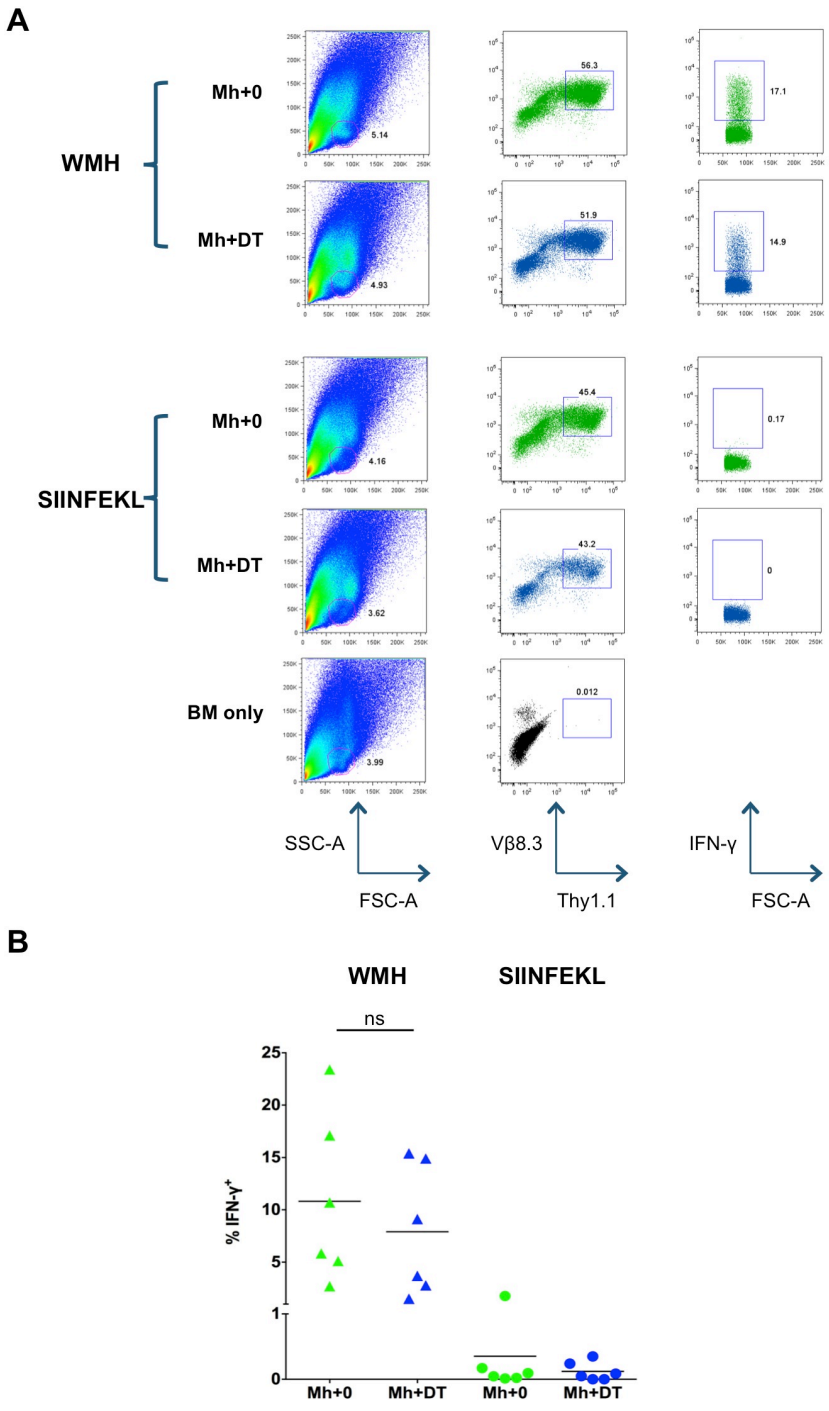

Figure 43: The depletion of Langerin$^+$ DC had no effect on the function of Mh T cells in the spleen. **A.** Representative dot plots of SC taken from Langerin-DTR recipients 7 days after transplant, restimulated with 5 μm of WMH or SIINFEKL peptide for 8 h. After an initial lymphocyte gate, Mh T cells were identified based on their expression of Vβ8.3, Thy1.1. The expression of IFN-γ by Mh T cells was then examined. Mh T cells from the spleen restimulated with relevant antigen expressed IFN-γ in the presence or absence of host Langerin$^+$ DC. In SIINFEKL controls, no IFN-γ expression was detected. **B.** Summary data showing the frequency of IFN-γ$^+$ Vβ8.3$^+$ Thy1.1$^+$ Mh T cells after 8 h restimulation with peptide as a percentage of Mh T cells gated (n=6, data pooled from 2 independent experiments, horizontal lines represent the mean±SD, data analysed using a Mann-Whitney test). The depletion of host Langerin$^+$ DC had no significant effect on the function of Mh T cells in the spleen.

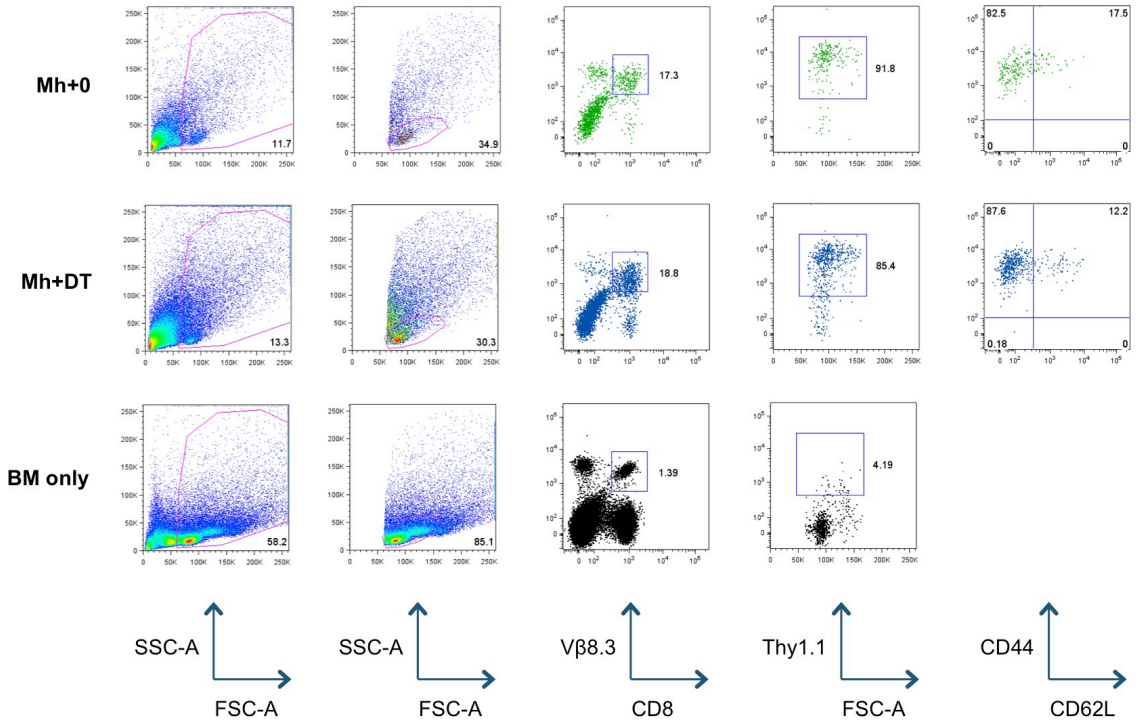

Figure 44: Gating strategy used to identify MataHari T cells in the skin draining lymph nodes. Representative dot plots from the skin draining LN taken from Langerin-DTR recipients 7 and 26 days after transplant. After an initial live cell gate followed by a lymphocyte gate, Mh T cells were identified based on their expression of Vβ8.3, Thy1.1 and CD8. The activation profile of Mh T cells was also analysed using CD44 and CD62L. Mh T cells expanded in the skin draining LN in the presence or absence of host Langerin^{+} DC. In BM controls, no Mh T cells were detected.

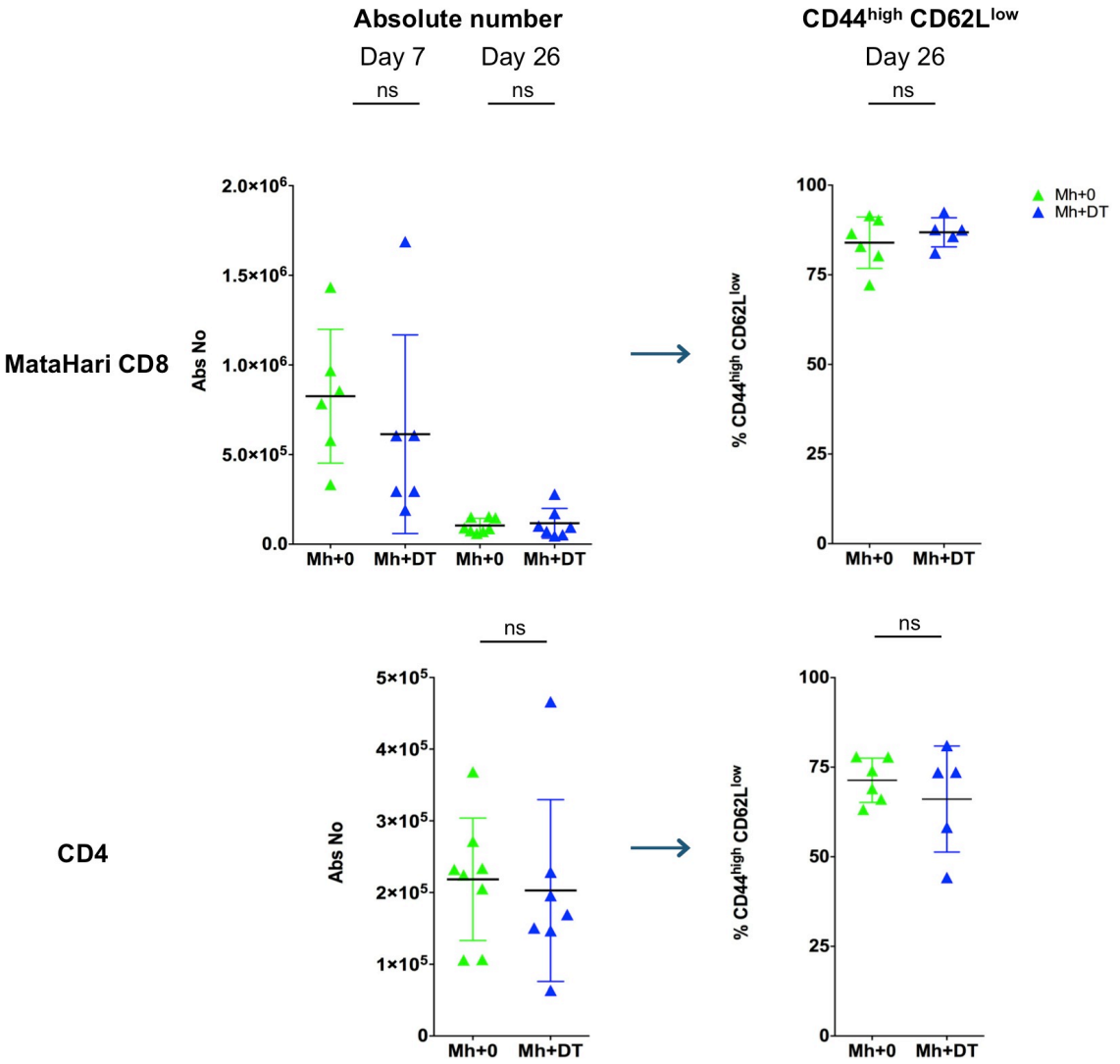

Figure 45: The depletion of host Langerin$^+$ DC had no effect on the expansion and activation of donor T cells in the skin draining LN. *Left*- Absolute number of Vβ8.3$^+$ Thy1.1$^+$ Mh and CD4$^+$ T cells in the spleen 7 and 26 days after transplant (n=5-8, data pooled from 3 independent experiments, horizontal lines represent the mean±SD, data analysed using a Mann-Whitney test). *Right*- Summary data showing the frequency of CD44^{high} CD62L^{low} effector T cells as a percentage of Mh and CD4 T cells gated (n=5-8, data pooled from 3 independent experiments, horizontal lines represent the mean±SD, data analysed using a Mann-Whitney test). The depletion of host Langerin$^+$ DC had no effect on the expansion or activation of donor T cells in the skin draining LN.

4.2.2 The majority of host Langerin$^+$ DC are depleted 26 days after transplant

Treating Langerin-DTR recipients with DT on days -2, 1, 4 and 7 post transplant was highly effective at depleting host Langerin$^+$ DC for the duration of the experiment. 7 days after transplant, no LC were detected in the skin of Langerin-DTR recipients treated with DT (Figure 46). In both PBS treated recipients of Mh T cells and BM controls, host LC (GFP$^+$) remained in the epidermis (Figure 48).

A different pattern emerged 26 days after transplant. In the presence of donor Mh T cells, the majority of host Langerin$^+$ DC were depleted. After an initial live cell gate followed by a DC gate, LC were identified based on their expression of MHCII, CD11b, CD24, CD45.2 and GFP (Figure 47). LC were now present in the epidermis of both PBS and DT treated Langerin-DTR recipients. However, the majority of LC in the skin of PBS treated mice were now GFP$^-$ CD45.2$^-$ donor derived LC (Figure 48). This contrasted the epidermis of BM controls, where the majority of LC remained host derived (Figure 48). Both donor and host LC populations could be distinguished from one another as CD45.2$^+$ Langerin-DTR recipients were transplanted with congenically marked CD45.1$^+$ BM from a female WT BL/6 donor (Figure 47).

Of note, there remained significantly more LC in the epidermis of PBS versus DT treated recipients 26 days after transplant, despite the majority of these cells being GFP$^-$ CD45.2$^-$ donor derived LC. There were also significantly more MHCII$^+$ CD11b$^+$ cells in PBS versus DT treated recipients 26 days after transplant with alloreactive donor T cells, the majority of which were not LC (Figure 49).

Taken together, DT efficiently depletes Langerin$^+$ DC. In contrast to BM controls, the majority of host derived Langerin$^+$, including radio-resistant LC, are depleted in PBS treated recipients 26 days after transplant with alloreactive Mh T cells. Interestingly, the frequency of MHCII$^+$ CD11b$^+$ cells in the epidermis is higher in PBS versus DT treated recipients by day 26 despite the majority of cells in both recipients being donor derived.

The presence of Langerin$^+$ DC at the time of transplant increases the frequency of MHCII$^+$ CD11b$^+$ cells that infiltrate the epidermis.

LC depletion

Epidermis – Day 7

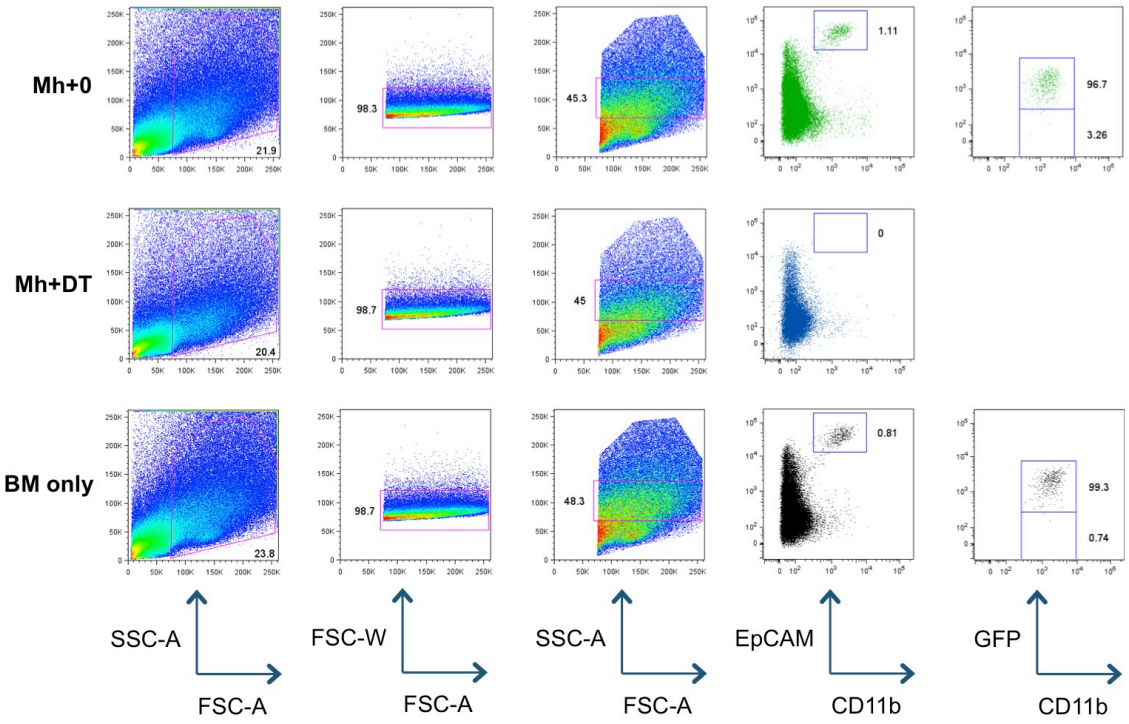

Figure 46: Host Langerhans cells are depleted in Langerin-DTR recipients 7 days after transplant. Representative dot plots of the epidermis from Langerin-DTR recipients 7 days after transplant. After an initial live cell gate, followed by FSC-W versus FSC-A gate to eliminate doublets and a broad DC gate based on FSC-A, SSC-A, LC were identified based on their expression of EpCAM, CD11b and GFP. Host LC were efficiently depleted in Langerin-DTR recipients treated with DT. Host LC persisted in both PBS treated recipients and BM controls 7 days after transplant.

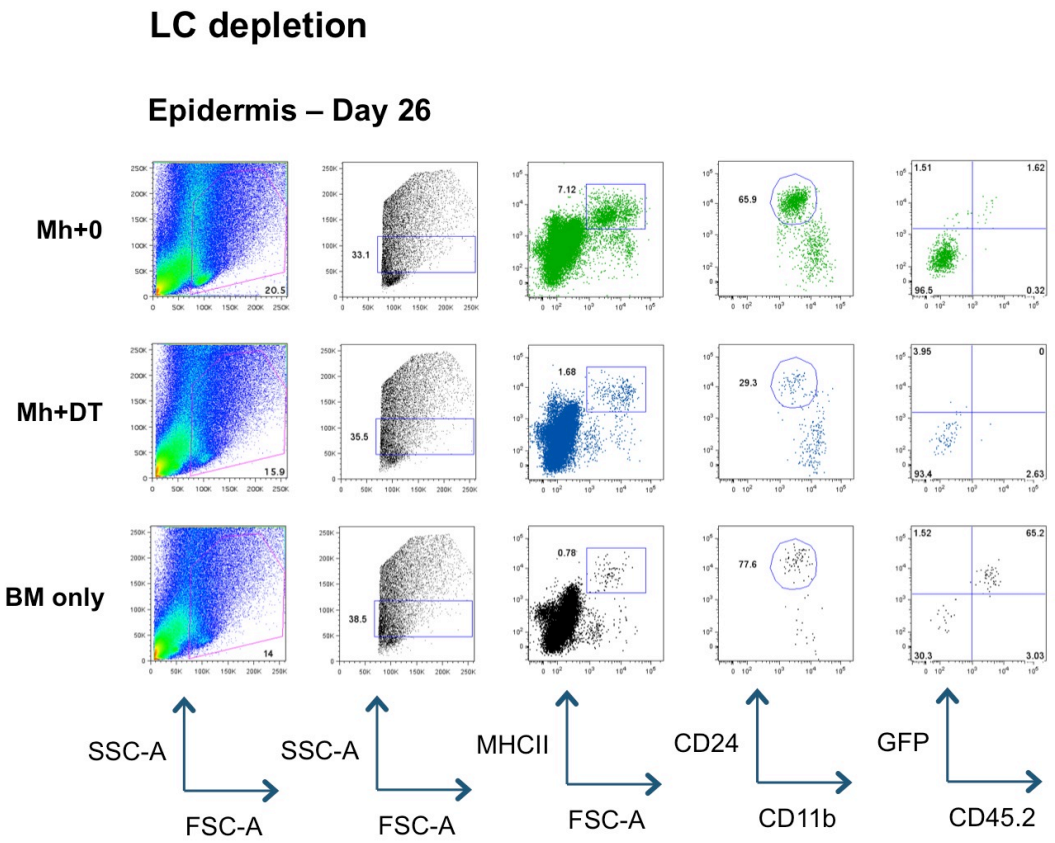

Figure 47: Langerhans cells remain depleted in DT treated Langerin-DTR recipients 26 days after transplant with Mh T cells are donor derived. A. Representative dot plots of the epidermis from Langerin-DTR recipients 26 days after transplant. After an initial live cell gate, followed by a DC gate, LC were identified based on their expression of MHCII, CD11b, CD24, CD45.2 and GFP. In Langerin-DTR recipients transplanted with Mh T cells the majority of LC were donor derived ($CD45.2^-$ GFP^-). In contrast, the majority of LC in BM controls were host derived. Donor derived LC were observed in DT treated recipients. However, the frequency of donor derived LC was higher in PBS versus DT treated recipients.

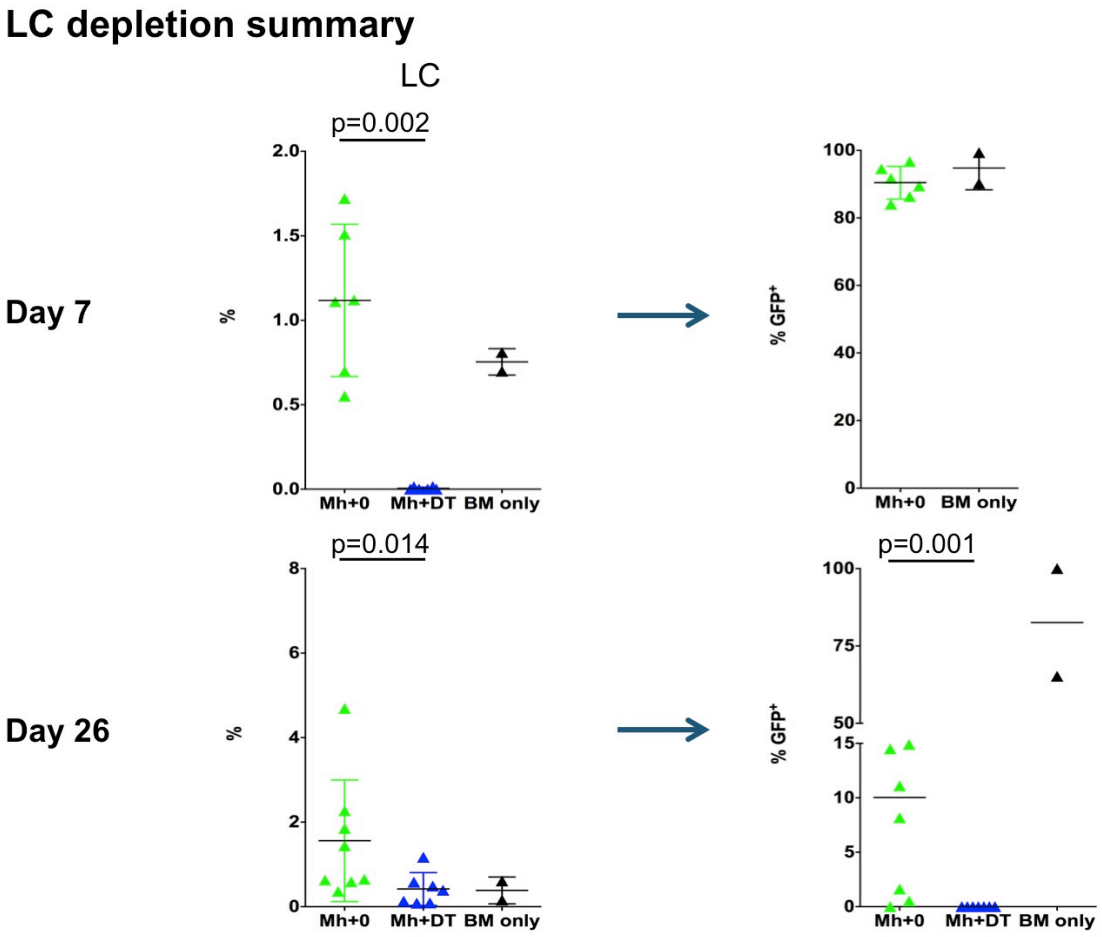

Figure 48: The majority of Langerhans cells in the epidermis 26 days after transplant with Mh T cells are donor derived. *Top left*- Summary data showing the frequency of EpCAM$^+$ CD11b$^+$ LC as a percentage of the initial DC gate 7 days after transplant (n=2-6, data pooled from 2 independent experiments, horizontal lines represent the mean±SD, data analysed using a Mann-Whitney test). LC were efficiently depleted in Langerin-DTR recipients treated with DT 7 days after transplant. *Top right*- Summary data showing the frequency of CD45.2$^+$ GFP$^+$ LC as a percentage of LC gated 7 days after transplant (n=2-6, data pooled from 2 independent experiments, horizontal lines represent the mean±SD). The majority of LC in Langerin-DTR recipients 7 days after transplant are CD45.2$^+$ GFP$^+$ host derived. *Bottom left*- Summary data showing the frequency of MHCII$^+$ CD11b$^+$ CD24$^+$ LC as a percentage of the initial DC gate 26 days after transplant (n=2-8, data pooled from 3 independent experiments, horizontal lines represent the mean±SD, data analysed using a Mann-Whitney test). LC were observed in both PBS and DT treated Langerin-DTR recipients of Mh T cells 26 days after transplant. However, there was significantly more LC in PBS versus DT treated recipients. *Bottom right*- Summary data showing the frequency of CD45.2$^+$ GFP$^+$ LC as a percentage of the LC gated 26 days after transplant (n=2-8, data pooled from 3 independent experiments, horizontal lines represent the mean±SD, data analysed using a Mann-Whitney test). The majority of LC in PBS treated Langerin-DTR recipients were donor derived LC (CD45.2$^-$ GFP$^-$) 26 days after transplant. In BM controls, the majority of LC remained of host origin (CD45.2$^+$ GFP$^+$).

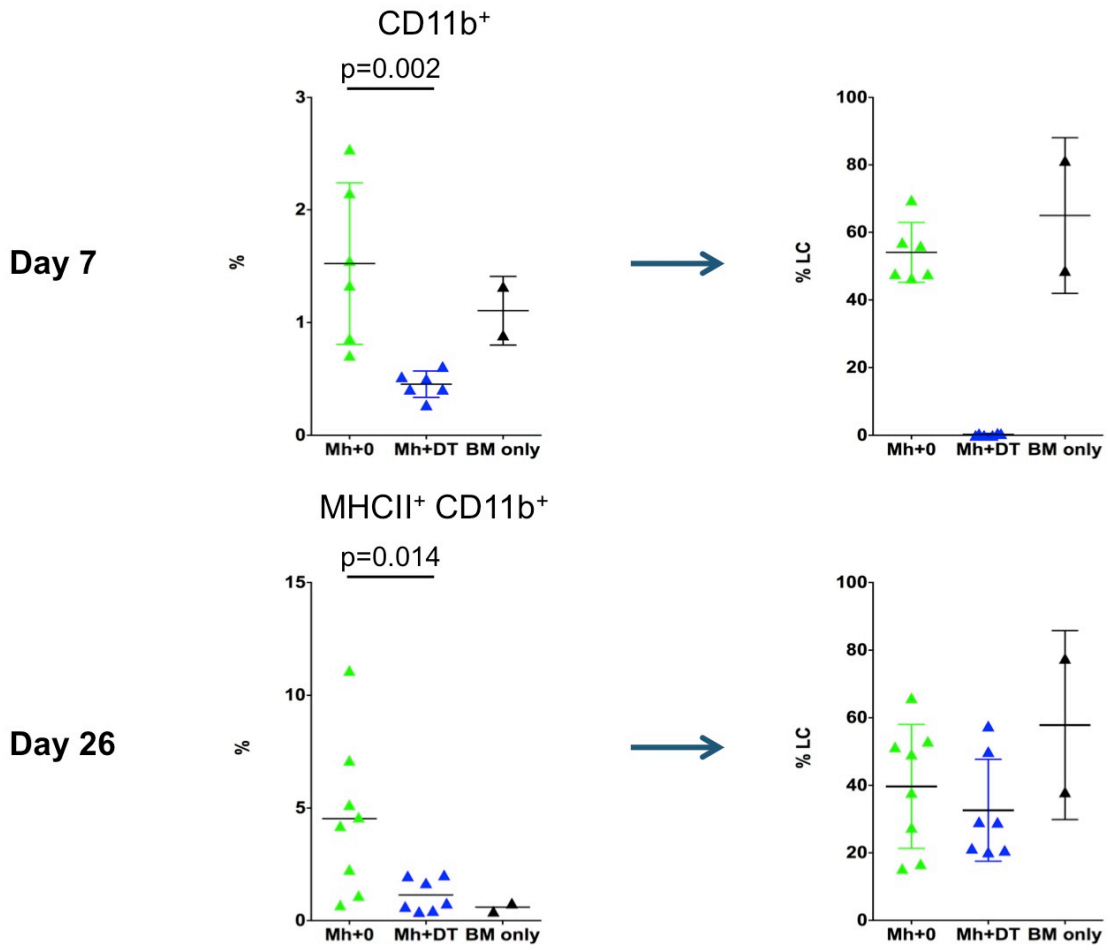

Figure 49: The depletion of host Langerin$^+$ DC influences the repopulation kinetics of donor dendritic cells in the skin. *Top left*- Summary data showing the frequency of CD11b$^+$ cells as a percentage of the initial DC gate 7 days after transplant (n=2-6, data pooled from 2 independent experiments, horizontal lines represent the mean±SD, data analysed using a Mann-Whitney test). There were significantly more CD11b$^+$ cells in the PBS versus DT recipients that were transplanted with Mh T cells. *Top right*- Summary data showing the frequency of EpCAM$^+$ GFP$^+$ LC as a percentage of CD11b cells gated 26 days after transplant (n=2-6, data pooled from 2 independent experiments, horizontal lines represent the mean±SD). The majority of CD11b$^+$ in Langerin-DTR recipients 7 days after are CD45.2$^+$ GFP$^+$ host derived LC, but there is a significant infiltration of other CD11b$^+$ cells. *Bottom left*- Summary data showing the frequency of MHCII$^+$ CD11b$^+$ DC as a percentage of the initial DC gate 26 days after transplant (n=2-8, data pooled from 3 independent experiments, horizontal lines represent the mean±SD, data analysed using a Mann-Whitney test). There were significantly more cells expressing a DC-like phenotype in PBS versus DT treated Langerin-DTR recipients of Mh T cells 26 days after transplant. The depletion of host Langerin$^+$ DC significantly reduced the infiltration of donor DC into the epidermis. *Bottom right*- Summary data showing the frequency of CD24$^+$ LC as a percentage of the MHCII$^+$ CD11b$^+$ cells gated (n=2-8, data pooled from 3 independent experiments, horizontal lines represent the mean±SD). The majority of DC gated were not LC 26 days after transplant.

4.2.3 Depletion of host Langerin$^+$ DC reduced the accumulation of MataHari CD8 T cells in the skin

To determine the role of Langerin$^+$ DC in the development of cutaneous GVHD, the infiltration and accumulation of donor T cells in the skin of Langerin-DTR recipients, treated with either PBS or DT, was assessed 7 and 26 days after transplant with Mh T cells.

After an initial live cell gate, followed by a lymphocyte gate, Mh T cells were identified based on their expression of Vβ8.3 and Thy1.1. The epidermis and dermis were separated using dispase II, therefore the use of anti-CD8 antibodies for staining was precluded. CD4 T cells were identified using CD4 and CD45.2 (Figure 50).

Both Mh and CD4 T cells could be easily identified in the epidermis and dermis of Langerin-DTR recipients transplanted with Mh T cells. Interestingly, the depletion of host Langerin$^+$ DC significantly reduced the accumulation of Mh T cells in the epidermis 7 and 26 days after transplant (Figure 51). In the dermis, there was a strong trend towards a lower frequency of Mh T cells in the absence of Langerin$^+$ DC but this was not significant ($p=0.0584$) 7 days after transplant. By day 26 post transplant, there was a highly significant reduction in the frequency of Mh T cells in the dermis (Figure 51).

The frequency of CD4 T cells in the epidermis was not affected by the depletion of Langerin$^+$ DC 7 days after transplant. However, by day 26, there was a strong trend towards there being less CD4 T cells in the epidermis of Langerin-DTR recipients treated with DT, but this was not significant ($p=0.0514$). The frequency of CD4 T cells in the dermis was unaffected by the depletion of host Langerin$^+$ DC depletion (Figure 51). Unlike the lymphoid tissues, the depletion of host Langerin$^+$ DC had a profound effect on the frequency of Mh T cells in the skin, indicating a possible reduction the degree of cutaneous GVHD that developed.

Skin – T cell infiltration

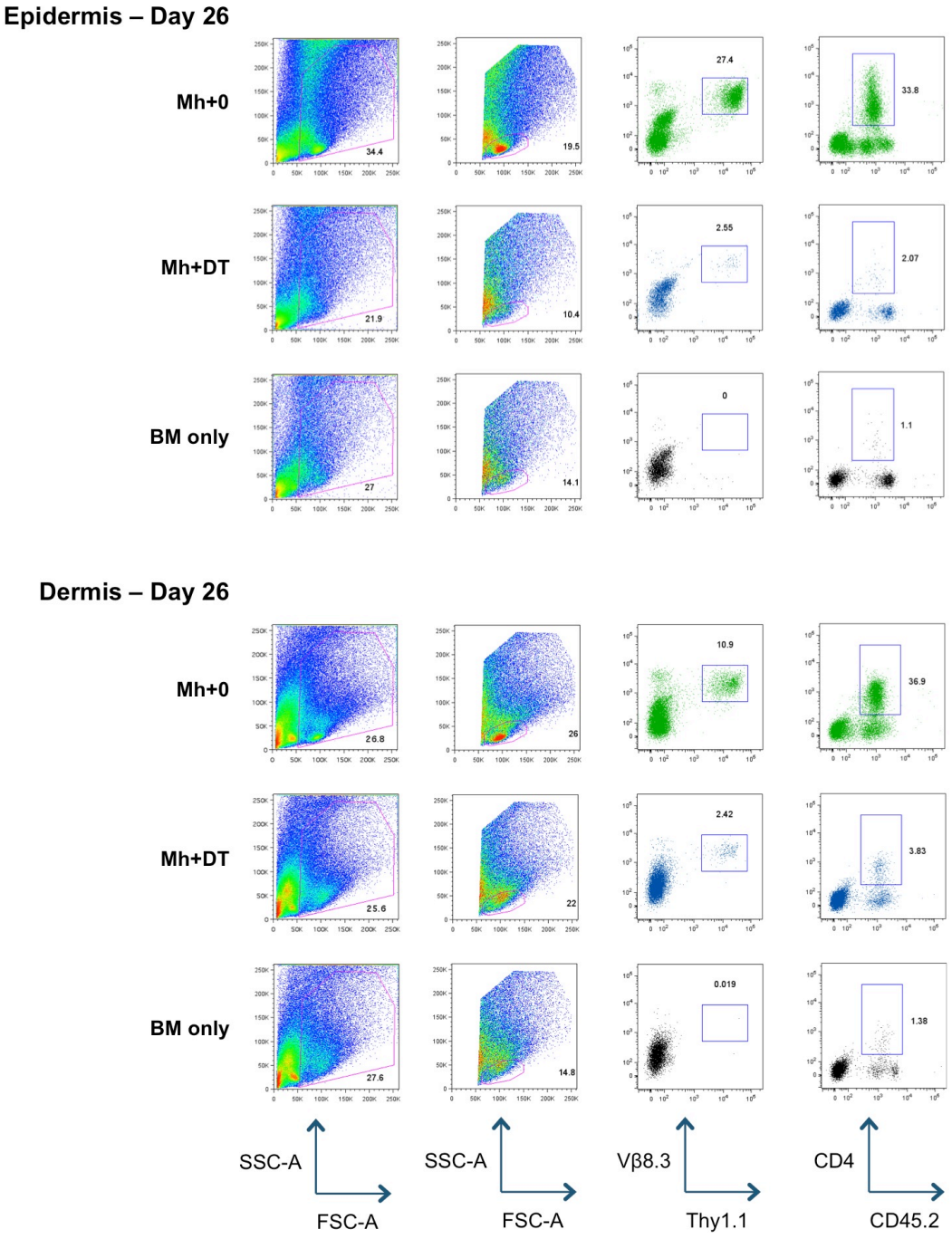

Figure 50: The depletion of host Langerin$^+$ DC reduces the accumulation of donor T cells in the skin 26 days after transplant. Representative dot plots of the epidermis and dermis from Langerin-DTR recipients 26 days after transplant. After an initial live cell gate followed by a lymphocyte gate, Mh T cells were identified based on their expression of Vβ8.3 and Thy1.1. CD4 T cells were identified based on their expression of CD4 and CD45.2. In both the epidermis and dermis, the frequency of both Mh and CD4 T cells was reduced in DT versus PBS treated Langerin-DTR recipients 26 days after transplant. In BM controls, a small frequency of CD4 T cells but no Mh T cells were detected.

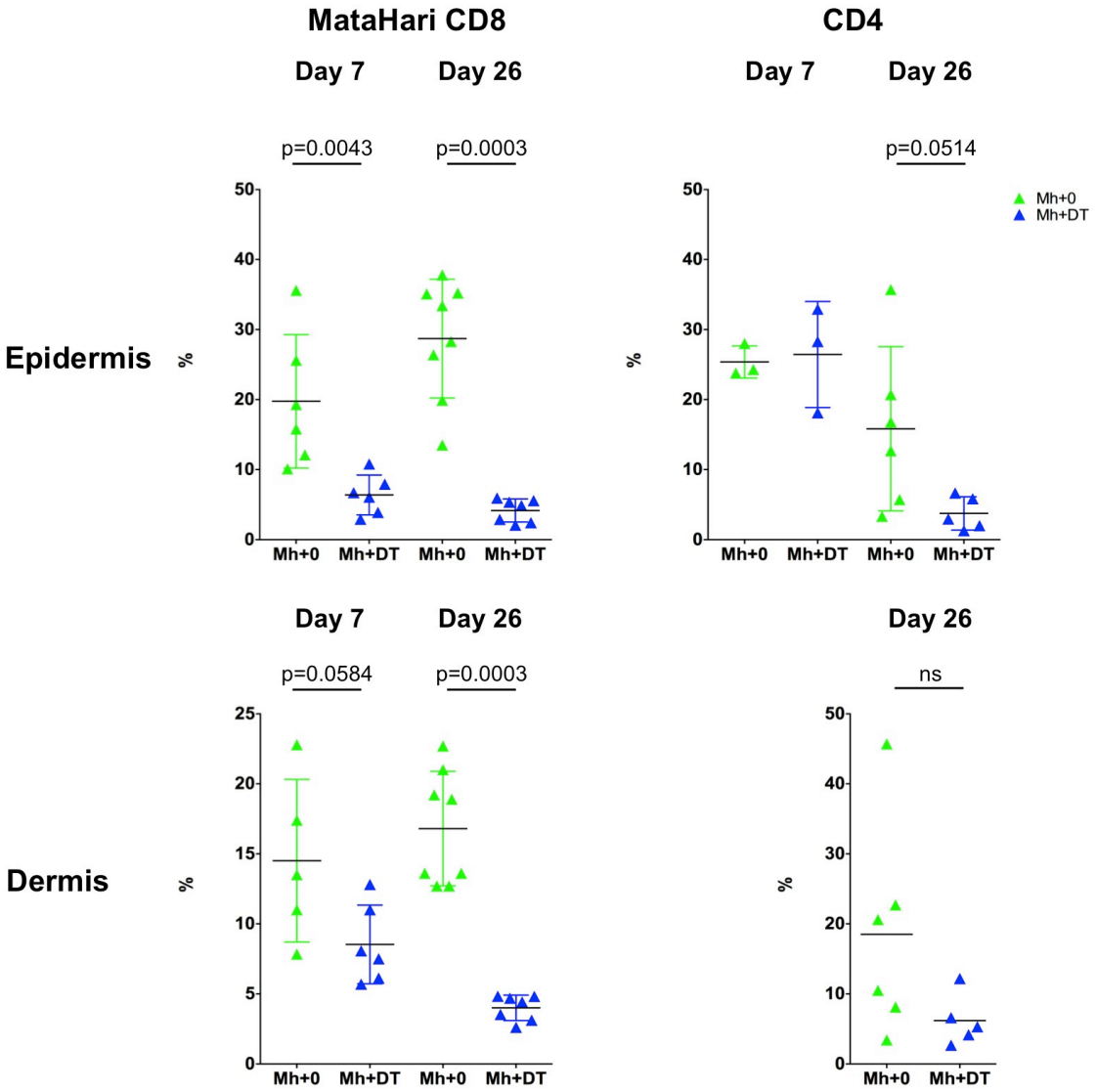

Figure 51: The depletion of host Langerin$^+$ DC significantly reduces the accumulation of MataHari T cells in the skin by day 7. *Top & Bottom Left*- Summary data showing the frequency of Vβ8.3$^+$ Thy1.1$^+$ Mh T cells in the epidermis and dermis as a percentage of lymphocytes gated 7 and 26 days after transplant (n=5-8, data pooled from 3 independent experiments, horizontal lines represent the mean±SD, data analysed using a Mann-Whitney test). The accumulation of Mh T cells was significantly reduced in the absence of host Langerin$^+$ DC in both the epidermis and dermis 7 and 26 days after transplant. *Top & Bottom Right*- Summary data showing the frequency of CD45.2$^+$ CD4$^+$ T cells in the epidermis and dermis as a percentage of lymphocytes gated 7 and 26 days after transplant (n=3-5, data pooled from 1-2 independent experiments, horizontal lines represent the mean±SD, data analysed using a Mann-Whitney test). There was no difference in the accumulation of CD4 T cells in the epidermis by day 7. However, there was a significant reduction in the absence of host Langerin$^+$ DC in the epidermis 26 days after transplant. There was no difference in the dermis, although there was a trend towards there being less CD4 T cells in the absence of host Langerin$^+$ DC.

4.2.4 The depletion of host LC, but not Langerin$^+$ dDC, reduced the severity of cutaneous GVHD

GVHD experiments using Langerin-DTR recipients have so far depleted both LC and Langerin$^+$ dDC. As both populations are migratory DC, each is capable of presenting host antigen to donor T cells. To determine whether the reduction in the frequency and of Mh T cells in the skin is dependent on the depletion of either host LC or Langerin$^+$ dDC, a series of experiments were designed taking advantage of the unique characteristics of each population. This enabled us to investigate whether a similar Mh T cell phenotype was observed in the skin when either host LC were depleted but not Langerin$^+$ dDC or vice versa.

Taking advantage of the repopulation kinetics of Langerin$^+$ dDC, which fully reconstitute its dermal niche 7 days after acute depletion, Langerin-DTR recipients were injected with DT 20 days before transplant to deplete host LC but not Langerin$^+$ dDC (Figure 52)[275]. At Day 0 (time of transplant), host LC but not Langerin$^+$ dDC would be depleted in the skin of DT treated Langerin-DTR recipients. This was confirmed through flow cytometry of epidermal and dermal samples of Langerin-DTR mice treated with DT 20 days earlier (Figure 53). After an initial live cell gate followed by a DC gate, LC and Langerin$^+$ dDC were identified based on their expression of MHCII, CD45.2, CD11b, CD207 and GFP. In the epidermis, LC were efficiently depleted. However, CD11b$^{-/low}$ GFP$^+$ Langerin$^+$ dDC had reconstituted the dermis as expected.

To deplete host Langerin$^+$ dDC but not LC, male WT BL/6 mice were lethally irradiated and reconstituted with 5 x10^6 TCD BM cells from male Langerin-DTR mice (Figure 54). The [Langerin-DTR → BL/6] chimeras were allowed to recover for 8 weeks before being subsequently transplanted with Mh T cells and female BM + CD4 T cells derived from a WT BL/6 donor. To deplete host Langerin$^+$ dDC but not LC, the [Langerin-DTR → BL/6] chimeras were treated on days -2, 1, 4 and 7 days post transplant with DT. LC are radioresistant and in [Langerin-DTR → BL/6] chimeras, LC are derived from WT

BL/6 and resistant to depletion via DT. This was confirmed by flow cytometry when LC were not depleted in the epidermis of DT treated chimeras 7 days after transplant (Figure 55). Langerin$^+$ dDC are not radioresistant and will be derived from Langerin-DTR BM and thus be susceptible to depletion via DT. This was highlighted in previous chapter where host LC in MC were derived from host and donor cells whereas Langerin$^+$ dDC were derived entirely of donor cells.

The accumulation of donor T cells in the skin when either host LC or Langerin$^+$ dDC were depleted was then investigated. The same gating strategy was applied to both data sets so the frequencies of T cells could be directly compared (Figure 56). Mh T cells were identified based on their expression of Vβ8.3 and Thy1.1. CD4 T cells on their expression of CD4 and CD45.2.

The depletion of host LC, but not Langerin$^+$ dDC, significantly reduced the accumulation of Mh T cells in the epidermis (Figure 57). The magnitude of this reduction was similar to that seen when Langerin$^+$ DC were depleted. There was no significant difference in the frequency of CD4 T cells in the epidermis. However, similar to when Langerin$^+$ DC were depleted, there was a trend towards there being less CD4 T cells when host LC were depleted. A similar pattern to the epidermis for both Mh and CD4 T cells was observed in the dermis (Figure 58).

In contrast, the depletion of host Langerin$^+$ dDC, but not LC, in chimeras 20 days after transplant had no effect on the accumulation of Mh T cells in the epidermis (Figure 57). The frequency of Mh T cells in the epidermis of both PBS and DT treated chimeras was similar to that of PBS treated Langerin-DTR recipients culled 26 days after transplant. There was also no difference in the frequency of CD4 T cells although the frequency in chimeras was lower than that of Langerin-DTR recipients (Figure 57). A similar pattern to the epidermis was again observed in the dermis (Figure 58). Combining these

results together, it is clear that host LC, but not Langerin$^+$ dDC, are responsible for the phenotype that has been described so far.

Histological sections of skin were also collected from the ears of Langerin-DTR recipients 26 days after transplant, where only host LC had or had not been depleted (Figure 59, A). Sections were evaluated single blind for evidence of histopathological GVHD (dyskeratosis, epidermal thickening and lymphocyte infiltration). In the absence of host LC, there was a highly significant reduction in the severity of pathology that developed in the skin (Figure 59, B). This reduction was consistent across all three independent experiments and no evidence of cutaneous GVHD was observed in a BM control. Thus, the depletion of host LC, but not Langerin$^+$ dDC, is responsible for a significant reduction both in the accumulation of alloreactive Mh T cells in the skin and the severity of cutaneous GVHD that develops.

A

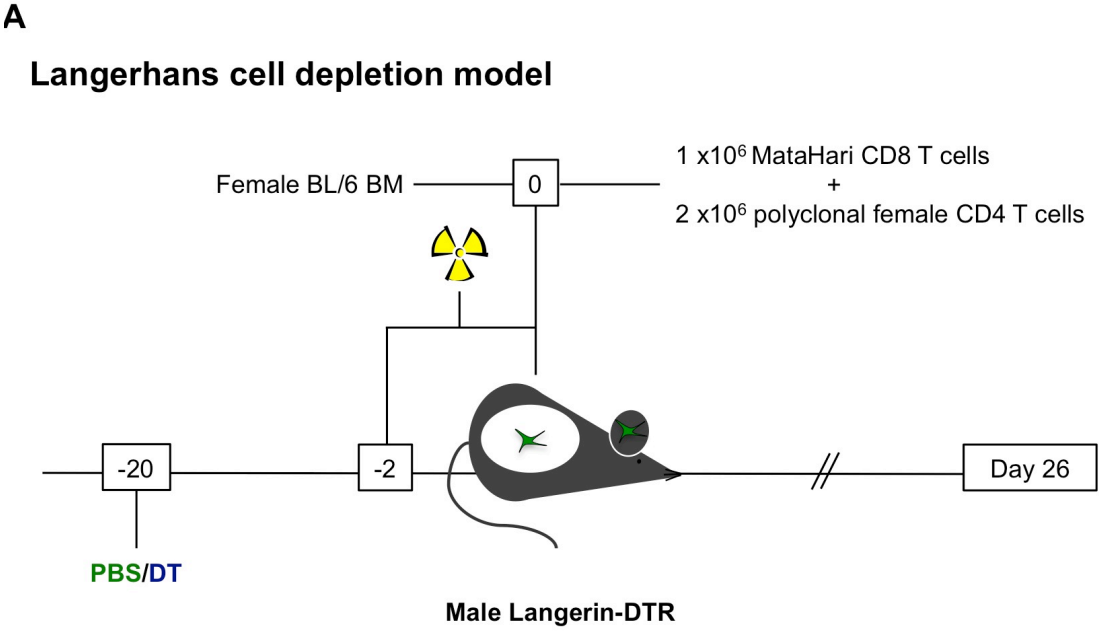

B

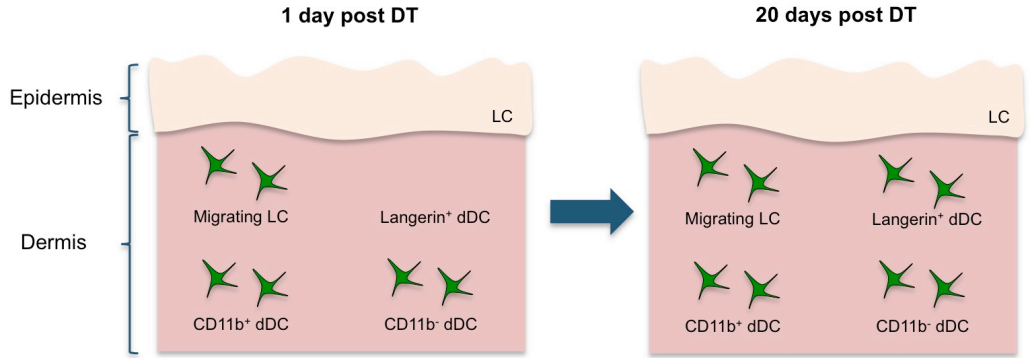

Figure 52: The depletion of host Langerhans cells but not Langerin$^+$ dDC in the MataHari minor H mismatch model. A. Male Langerin-DTR mice were lethally irradiated with a split dose of 11 Gy and reconstituted with a mixture of 1 x10^6 Thy1.1$^+$ Mh T cells, 2 x10^6 CD4 T cells and 5 x 10^6 BM. To deplete host LC but not Langerin$^+$ dDC, Langerin-DTR recipients were injected i.p. with 400 ng of DT on day -20 before transplant. Controls were injected PBS. **B.** Overview of the DC populations 1 and 20 days post DT based on data in the previous chapter. After 1 day, both host LC and Langerin$^+$ dDC are depleted. However, by day 20, host Langerin$^+$ dDC have repopulated the dermis while host LC remain depleted in the epidermis.

20 days post DT

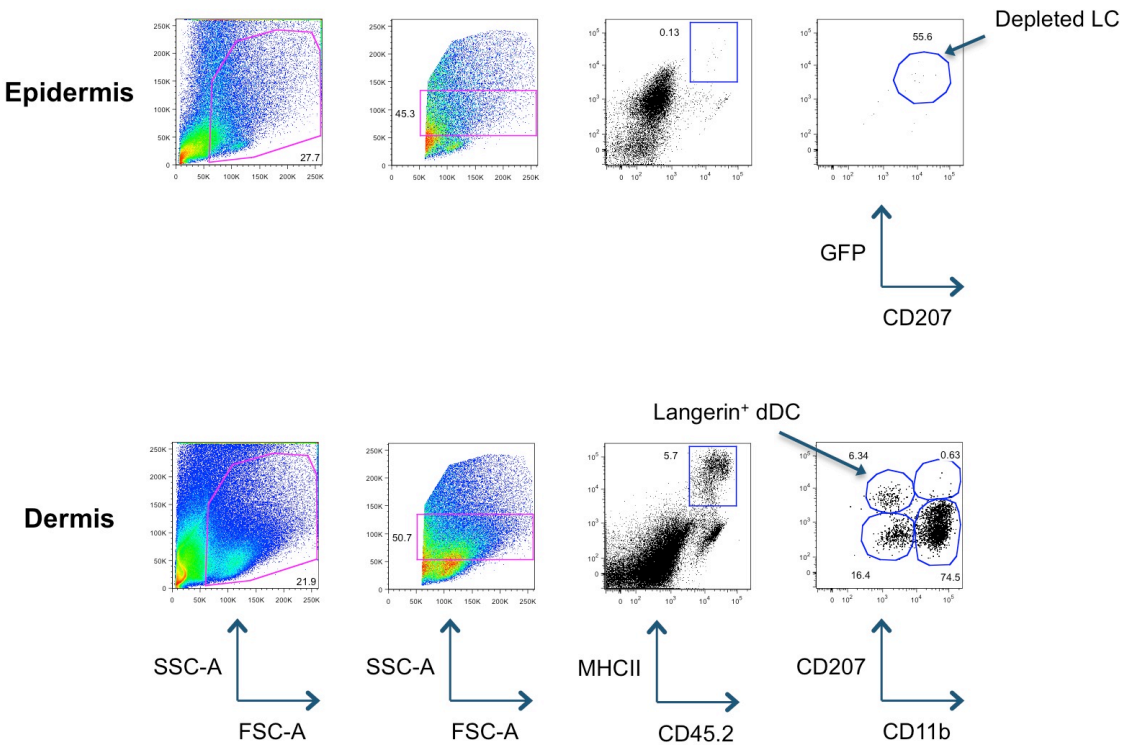

Figure 53: Langerin$^+$ dDC repopulate the dermis of Langerin-DTR mice 20 days after exposure to DT. Representative dot plots of the epidermis and dermis from Langerin-DTR mouse 20 days after treatment with 400 ng of DT. After an initial anti-apoptotic cell gate, followed by a DC gate, LC and Langerin$^+$ dDC were identified based on their expression of MHCII, CD45.2, CD207 and GFP. LC remained depleted 20 days after exposure to DT. However, Langerin$^+$ dDC had repopulated the dermis 20 days after DT treatment.

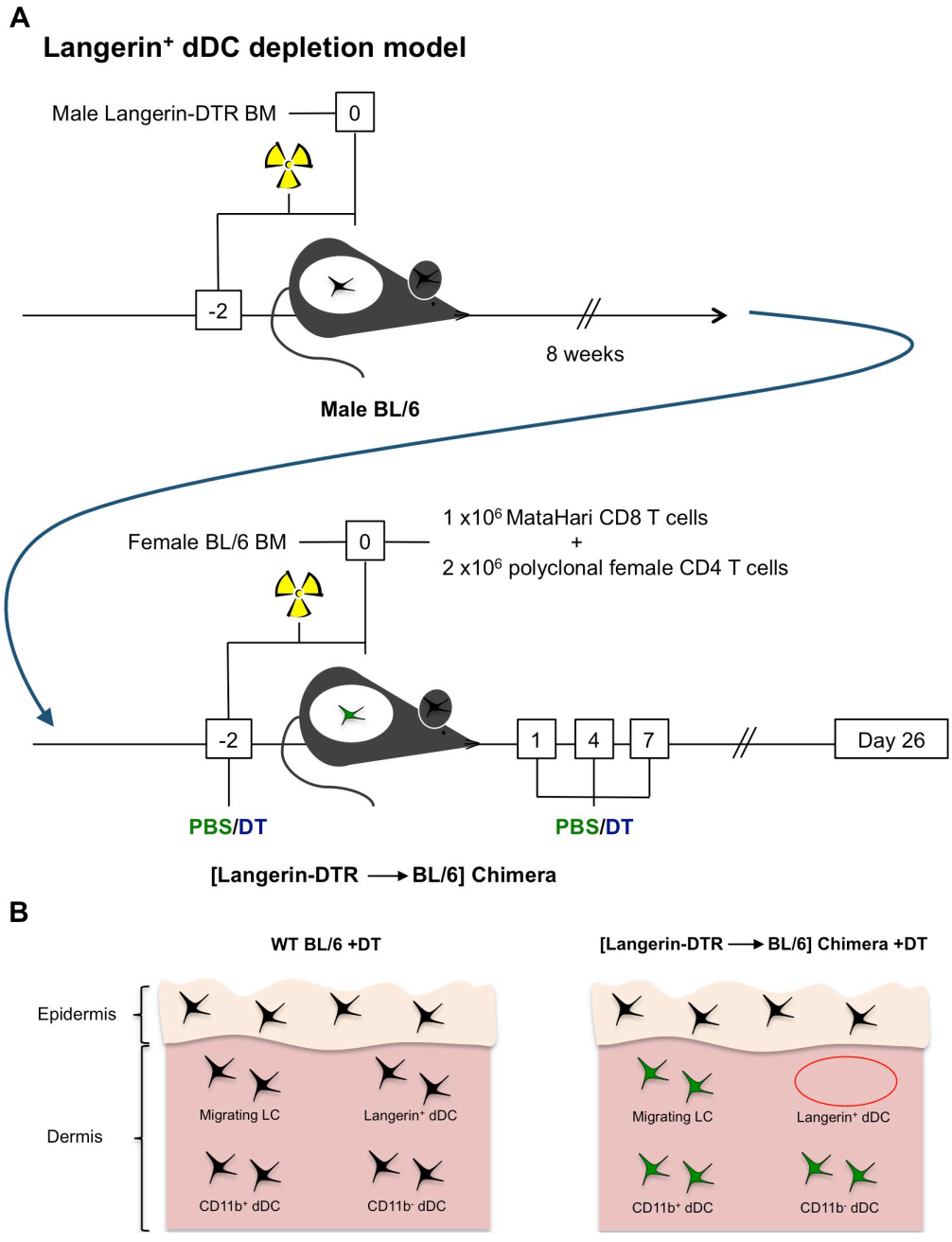

Figure 54: The depletion of host Langerin$^+$ dDC but not Langerhans cells in the MataHari minor H mismatch model. A. Male BL/6 mice were lethally irradiated with a split dose of 11 Gy and reconstituted with 5 x106 BM derived from male Langerin-DTR mice. After 8 weeks, [Langerin-DTR → BL/6] chimeras were lethally irradiated and transplanted with a mixture of 1 x10^6 Thy1.1$^+$ Mh T cells, 2 x10^6 CD4 T cells and 5 x 10^6 BM. To deplete host Langerin$^+$ dDC [Langerin-DTR → BL/6] recipients were injected i.p. with 400 ng of DT on days -2, 1, 4 and 7 before transplant. Controls were injected PBS. **B.** Overview of the DC populations in the skin of WT BL/6 mice and [Langerin-DTR → BL/6] chimeras based on data in Chapter 1 and the literature. In WT BL/6 mice, treatment with DT has no effect on DC populations in the skin. LC are radioresistant. In [Langerin-DTR → BL/6] chimeras, LC are derived from BL/6 mice and will not be depleted by DT. However, Langerin+ dDC will be entirely derived from Langerin-DTR BM and susceptible to depletion via DT. Therefore, treating [Langerin-DTR → BL/6] chimeras with DT will deplete host Langerin$^+$ dDC but not LC.

Langerin^{+} dDC depletion model

Epidermis - 7 days post transplant

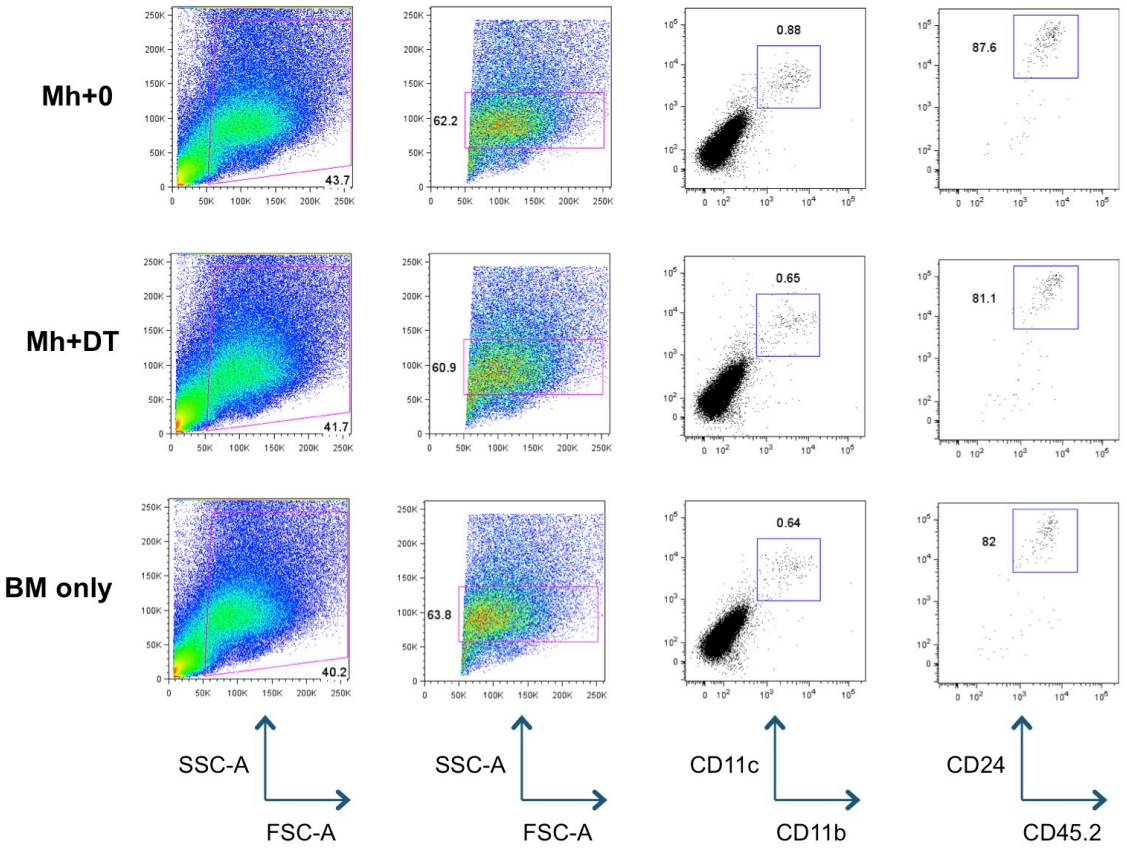

Figure 55: Host Langerhans cells are not depleted by DT in [Langerin-DTR → BL/6] chimeras. Representative dot plots of the epidermis from [Langerin-DTR → BL/6] chimeras 7 days after transplant. After an initial live cell gate, followed by a DC gate, LC were identified based on their expression of CD11c, CD11b, CD24 and CD45.2. In the epidermis, LC were not depleted by DT.

Epidermis – T cells

LC depletion

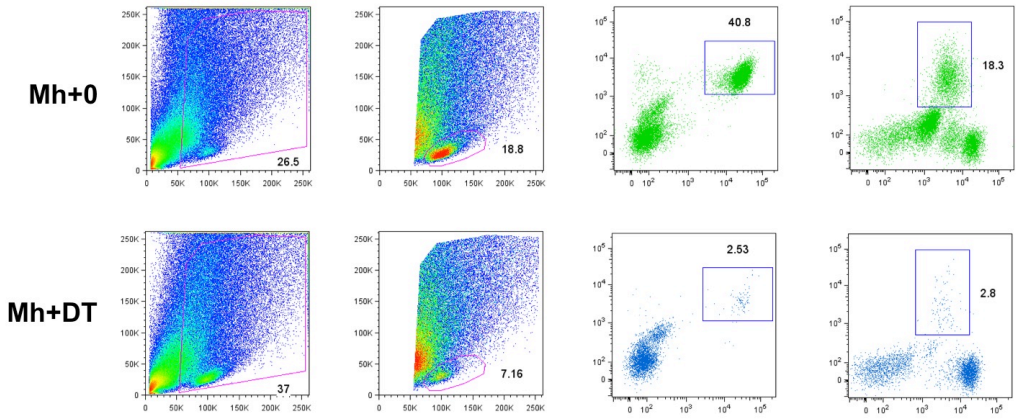

Langerin^{+} dDC depletion

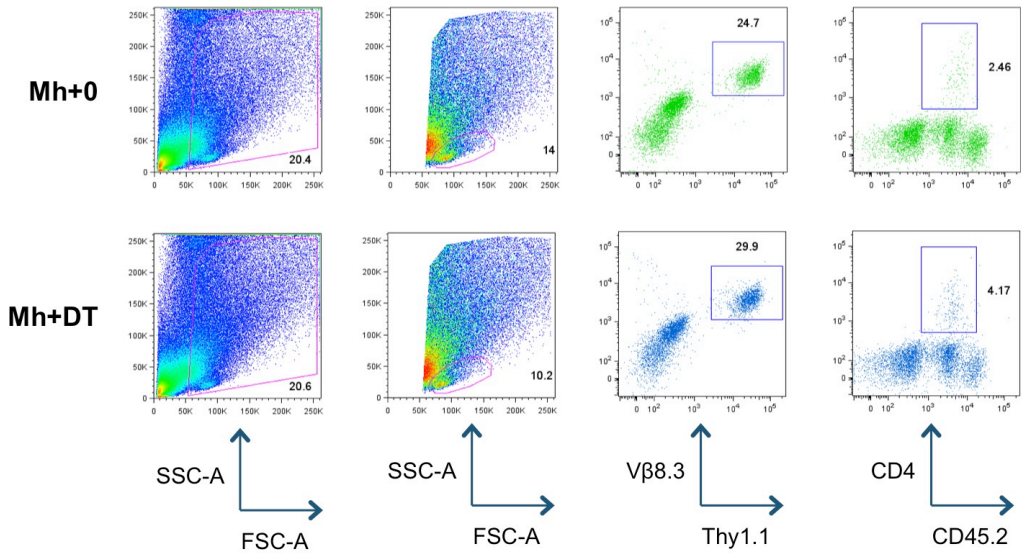

Figure 56: Gating strategy used to identify MataHari and CD4 T cells in the skin. Representative dot plots of the epidermis Langerin-DTR and [Langerin-DTR → BL/6] recipients 26 and 20 days after transplant respectively. After a live cell gate followed by a lymphocyte gate, Mh T cells were identified based on their expression of Vβ8.3 and Thy1.1. CD4 T cells were identified based on their expression of CD4 and CD45.2. The depletion of host LC reduced the accumulation of Mh T cells in the epidermis. However, the depletion of host Langerin^{+} dDC had no effect on the accumulation of Mh T cells in the epidermis.

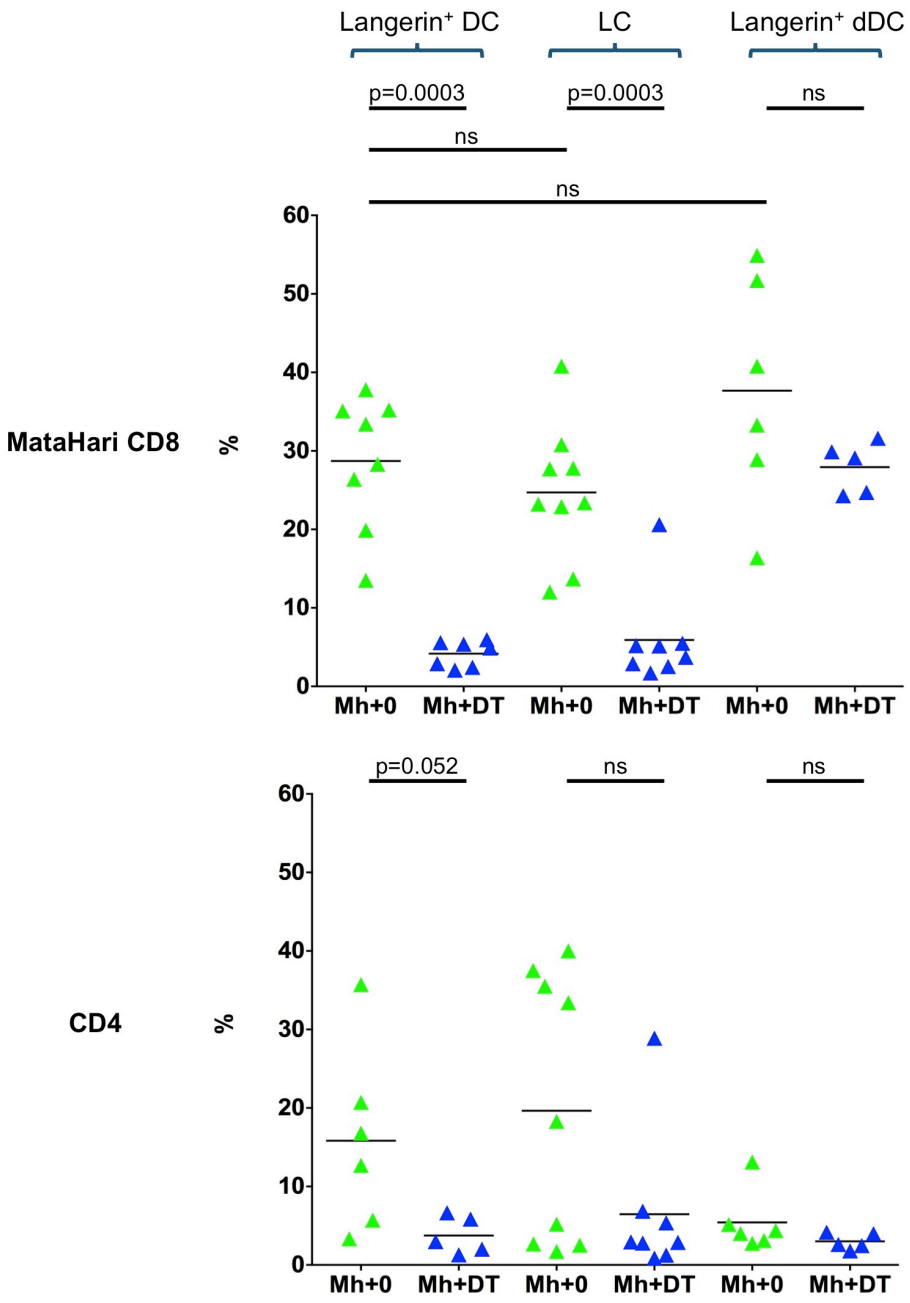

Figure 57: The depletion host Langerhans cells but not Langerin$^+$ dDC reduced the accumulation of MataHari T cells in the epidermis. Summary data showing the accumulation of Vβ8.3$^+$ Thy1.1$^+$ Mh and CD45.2$^+$ CD4$^+$ T cells in the epidermis as a percentage of the initial lymphocyte gate (n=5-9, data pooled from 2-3 independent experiments, analysed using a Mann-Whitney test, the mean ±SD is indicated by the horizontal bars). There was a significant reduction in the accumulation of Mh T cells 26 days after transplant when host LC were depleted. However, there was no reduction in the accumulation of Mh T cells 20 days after transplant when host Langerin$^+$ dDC were depleted. There was no significant difference in the accumulation of CD4 T cells. However there was a trends towards there being less in recipients depleted of host LC only. Thus, the depletion of host LC are responsible for the reduction in Mh T cells observed in the epidermis.

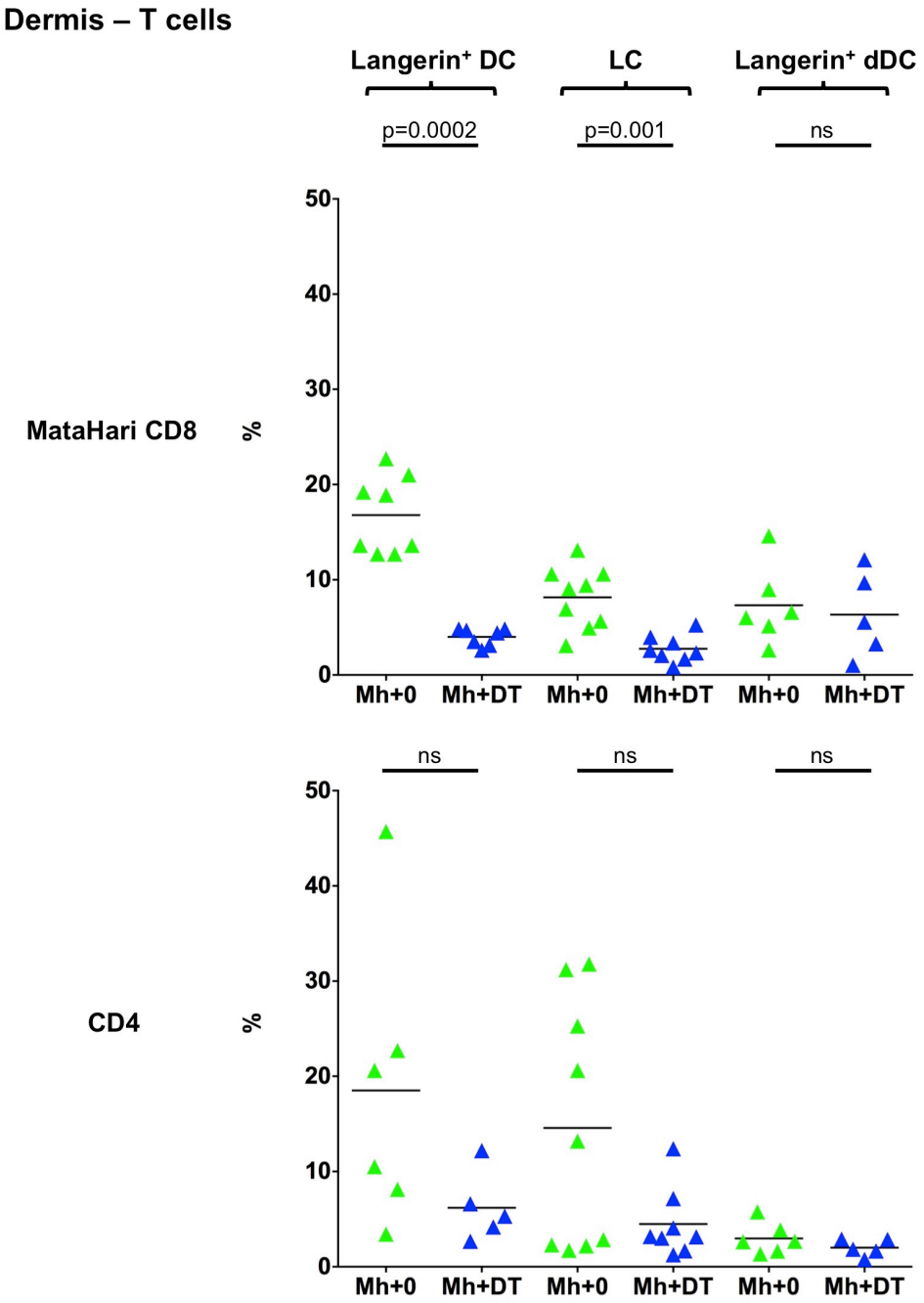

Figure 58: The depletion host Langerhans cells but not Langerin$^+$ dDC reduced the accumulation of MataHari T cells in the dermis. Summary data showing the accumulation of Vβ8.3$^+$ Thy1.1$^+$ Mh and CD45.2$^+$ CD4$^+$ T cells in the dermis as a percentage of the initial lymphocyte gate (n=5-9, data pooled from 2-3 independent experiments, analysed using a Mann-Whitney test, the mean ±SD is indicated by the horizontal bars). A similar pattern to the epidermis emerged. There was a significant reduction in the accumulation of Mh T cells 26 days after transplant when host LC were depleted. However, there was no reduction in the accumulation of Mh T cells 20 days after transplant when host Langerin$^+$ dDC were depleted. There was no difference in the accumulation of CD4 T cells. However there was a trends towards there being less in recipients depleted of host LC only. Thus, the depletion of host LC are responsible for the reduction in Mh T cells observed in the skin.

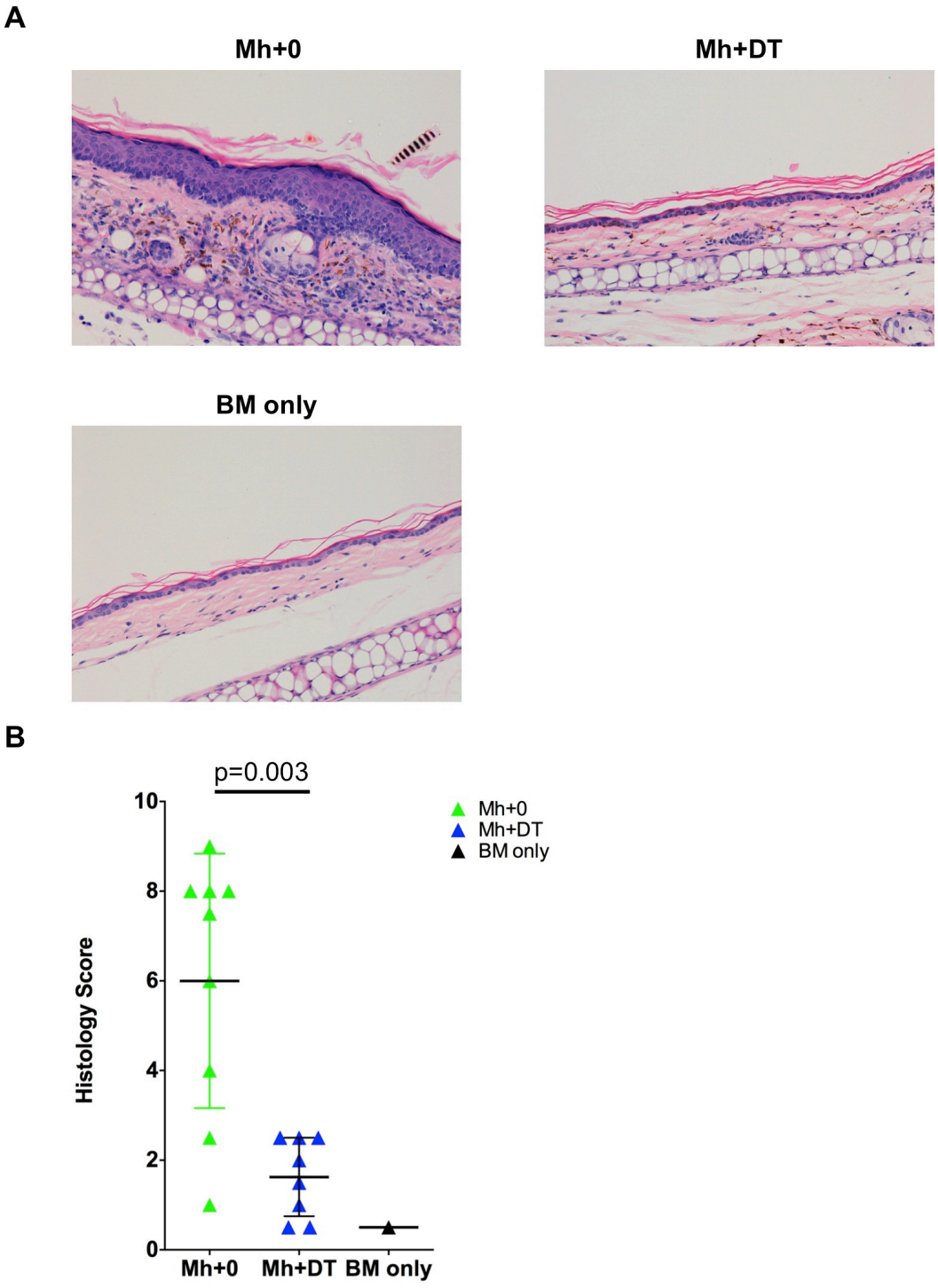

Figure 59: The severity of GVHD is significantly reduced in the absence of host Langerhans cells. **A.** Histological sections of ear skin taken from Langerin-DTR recipeints 26 days after transplant. Only host LC were depleted in DT samples. Images captured at X20 magnification using a Leica DMD108 light microscope. **B.** Summary data of histological GVHD score as evaluated single blind (n=1-9, data pooled from 1-3 independent experiments, analysed using a Mann-Whitney test, the mean ±SD is indicated by the horizontal bars.). There was a significant reduction in the severity of cutaneous GVHD between DT versus PBS treated recipients.

4.2.5 The depletion of host LC and Langerin$^+$ dDC had no effect on the severity of acute GVHD in the lung, liver or gut

The depletion of host LC but not Langerin$^+$ dDC resulted in a highly significant reduction of cutaneous GVHD. Whether the depletion of host LC or Langerin$^+$ dDC had any influence on the development of GVHD in other tissues commonly affected was also investigated.

In the previous section, the effect of host LC or Langerin$^+$ dDC on the accumulation of donor T cells in the skin was evaluated. In parallel, the liver, lamina propria + peyer's patches (LP+PP) and lung were also harvested from these recipients and the accumulation of donor T cells and pathology of GVHD analysed.

For the liver, cells were stained for propidium iodide (PI), an intercalating agent that binds nucleic acid, to eliminate dead cells and PI$^+$ were first gated out. After a live cell gate followed by a lymphocyte were gate, Mh T cells were identified based on their expression of Vβ8.3 and Thy1.1. CD4 T cells were identified based on their expression of CD4 and CD45.2 (Figure 60). A similar gating strategy was later used to analyse both the LP+PP and lung. Mh and CD4 T cells were easily identified in the liver. The depletion of either host LC or Langerin$^+$ dDC had no significant effect on the frequency of either Mh or CD4 T cells in the liver (Figure 60). The frequency of both Mh and CD4 T cells between the livers of Langerin-DTR recipients and [Langerin-DTR BL/6] chimeras was also similar. The depletion of host LC was also found to have no significant effect on the severity of GVHD that developed in the liver, as evidenced by histological sections evaluated single blind, although the degree of pathology that developed in this tissue was relatively mild overall (Figure 61).

In the LP+PP, a similar phenotype to the liver developed. The depletion of either host LC or Langerin$^+$ dDC had no effect on the frequency of both Mh and CD4 T cells in the LP+PP (Figure 62). The frequency of donor T cells infiltrating the LP+PP was again

similar between Langerin-DTR recipients and [Langerin-DTR BL/6] chimeras. Of note, the degree of pathology that developed in this tissue was markedly more severe than the liver, although the depletion of host LC had no effect on the level of GVHD that developed (Figure 63).

In the lung, there again was no difference in the frequency of either Mh or CD4 T cells when host LC or Langerin^{+} dDC were depleted and donor T cells again infiltrated both sets of recipients equally (Figure 64). However, there was a significant reduction in the severity of GVHD in the lung when host LC were depleted, although the magnitude of this reduction was much lower than that observed in the skin (Figure 65). Combining the data from the skin together with the tissues analysed here, the response of Mh T cells to the depletion of host LC is restricted mostly to the skin.

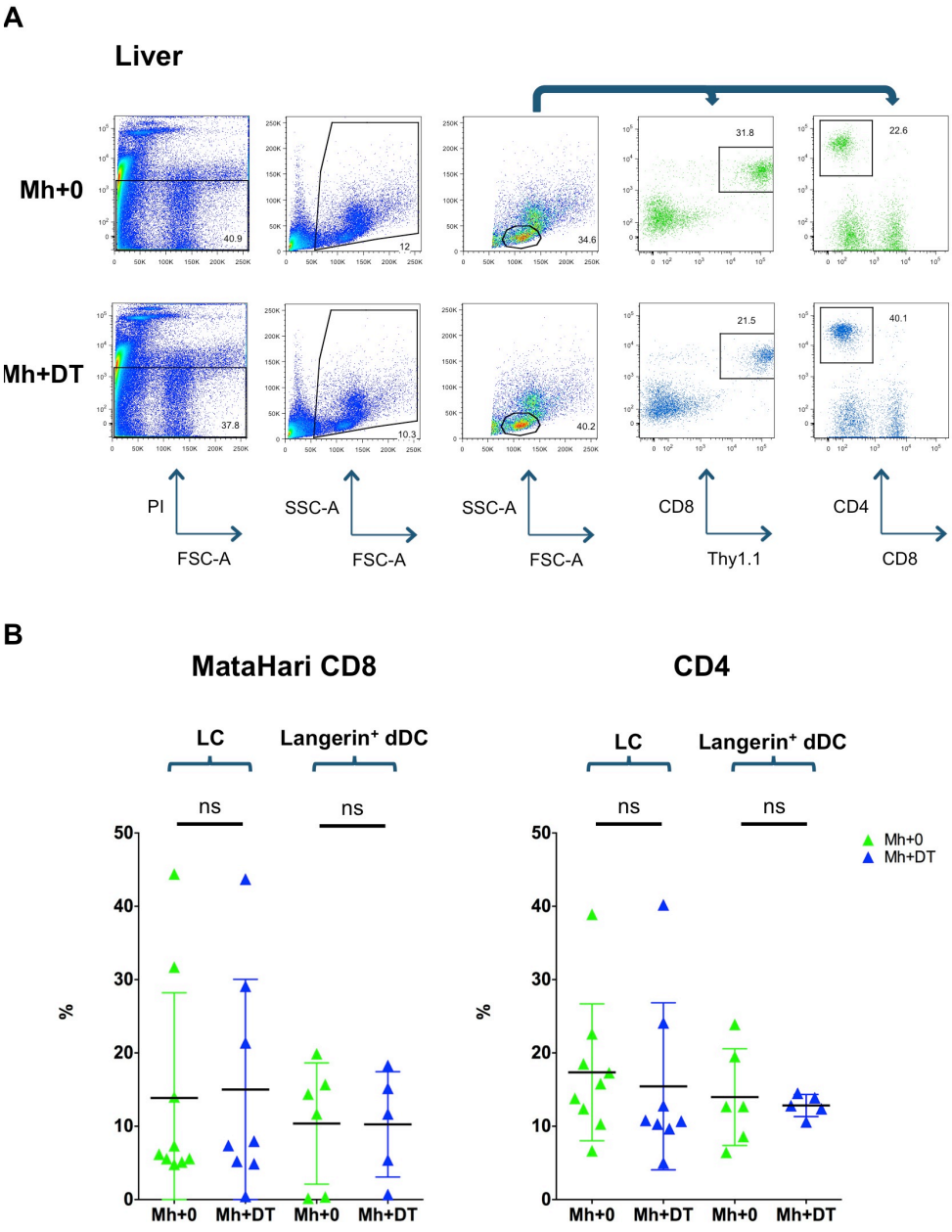

Figure 60: The depletion of host Langerin$^+$ DC had no effect on the accumulation of donor T cells in the liver. A. Representative dot plots of the liver taken from Langerin-DTR recipients 26 days after transplant. PI$^-$ cells were gated to eliminate dead cells. After a live cell gate followed by a lymphocyte gate, Mh T cells were identified based on their expression of Thy1.1 and CD8. CD4 T cells were identified based on their expression of CD4. This gating strategy was applied to all samples analysed. **B.** *Left*- Summary data showing the frequency of Mh T cells in the liver as a percentage of the initial lymphocyte gate 26 (LC depletion) and 20 (Langerin$^+$ dDC) days after transplant (n=5-9, data pooled from 2-3 independent experiments, horizontal lines represent the mean±SD, data analysed using a Mann-Whitney test). There was no difference in the accumulation of Mh T cells when either population of Langerin$^+$ DC was depleted. *Right*- Summary data showing the frequency of CD4 T cells as a percentage of the initial lymphocyte gate 26 (LC depletion) and 20 (Langerin$^+$ dDC) days after transplant (n=5-9, data pooled from 2-3 independent experiments, horizontal lines represent the mean±SD, data analysed using a Mann-Whitney test). There was no difference in the accumulation of CD4 T cells when either population of Langerin$^+$ DC was depleted.

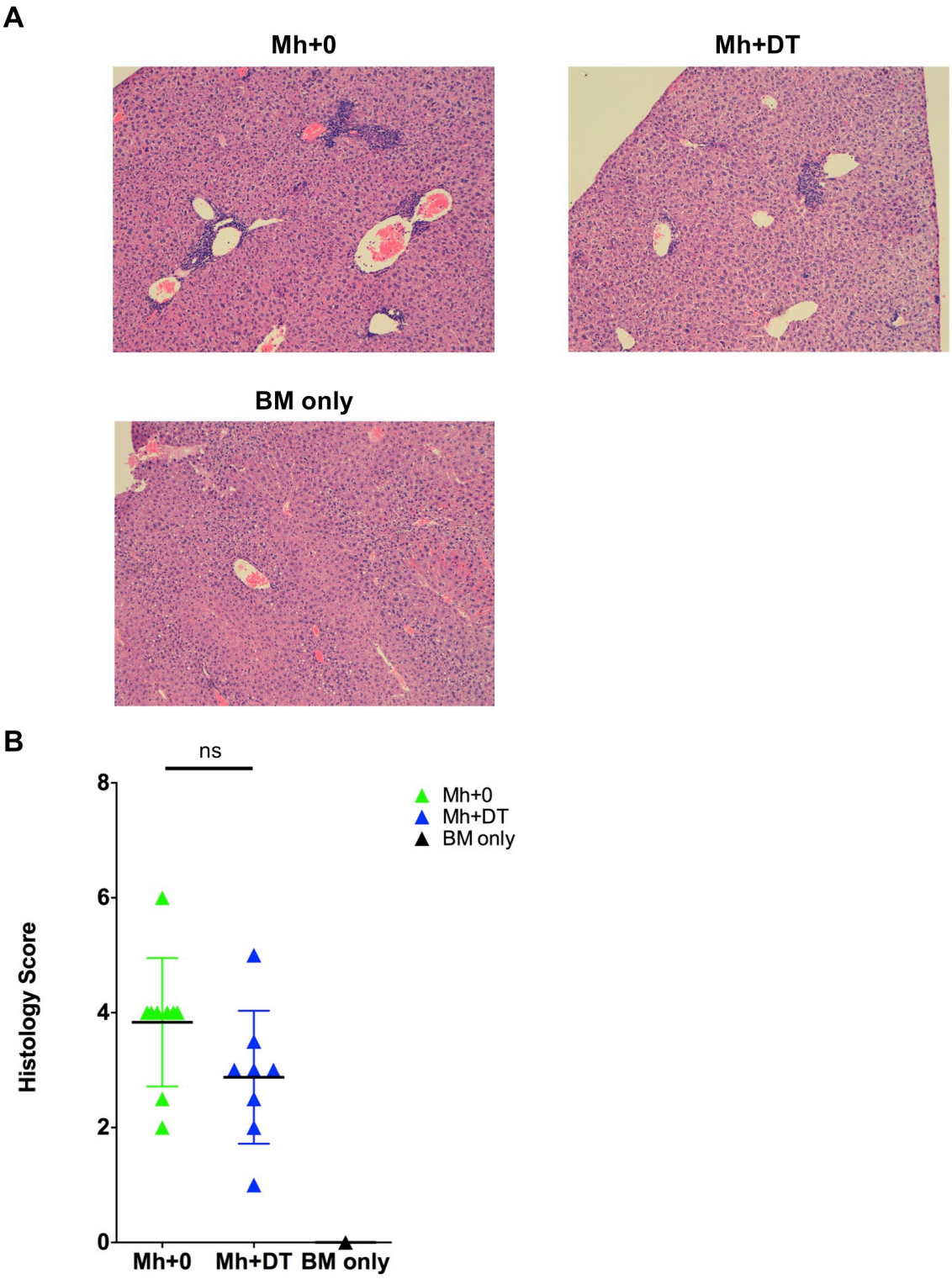

Figure 61: The depletion of host Langerhans cells had no effect on the severity of GVHD in the liver. A. Histological sections of liver taken from Langerin-DTR recipeints 26 days after transplant. Only host LC were depleted in DT treated samples. Images captured at X20 magnification using a Leica DMD108 light microscope. **B.** Summary data of histological GVHD score as evaluated single blind (n=1-9, data pooled from 3 independent experiments, analysed using a Mann-Whitney test, the mean ±SD is indicated by the horizontal bars.). The liver developed mild GVHD in this model and there was no significant reduction in the severity of GVHD in the liver when host LC were depleted.

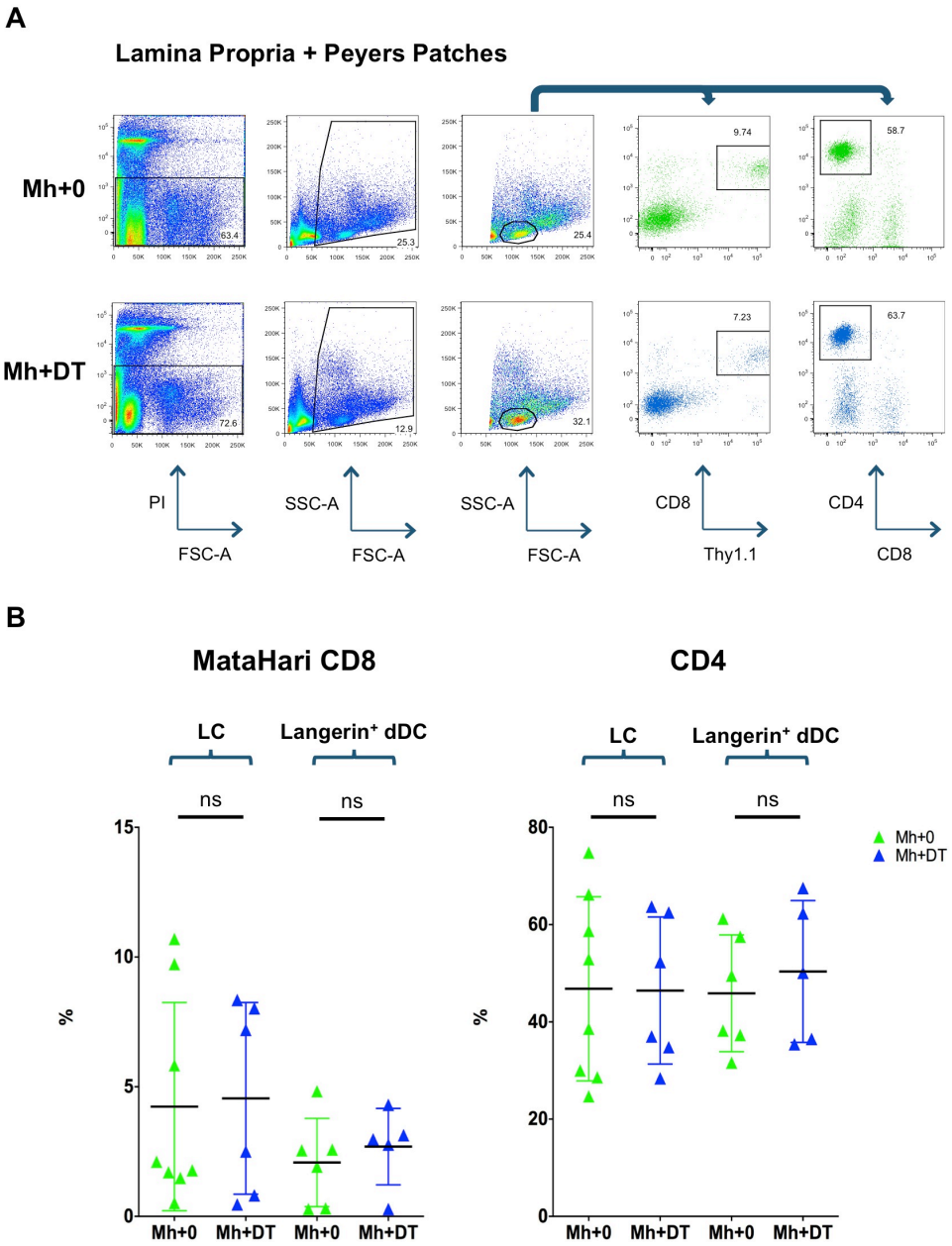

Figure 62: The depletion of host Langerin$^+$ DC had no effect on the accumulation of donor T cells in the LP+PP. A. Representative dot plots of the LP+PP taken from Langerin-DTR recipients 26 days after transplant. PI$^-$ cells were gated to eliminate dead cells. After a live cell gate followed by a lymphocyte gate, Mh T cells were identified based on their expression of Thy1.1 and CD8. CD4 T cells were identified based on their expression of CD4. This gating strategy was applied to all samples analysed. **B.** *Left*- Summary data showing the frequency of Mh T cells in the LP+PP as a percentage of the initial lymphocyte gate 26 (LC depletion) and 20 (Langerin$^+$ dDC) days after transplant (n=5-9, data pooled from 2-3 independent experiments, horizontal lines represent the mean±SD, data analysed using a Mann-Whitney test). There was no difference in the accumulation of Mh T cells when either population of Langerin$^+$ DC was depleted. *Right*- Summary data showing the frequency of CD4 T cells in the LP+PP as a percentage of the initial lymphocyte gate 26 (LC depletion) and 20 (Langerin$^+$ dDC) days after transplant (n=5-9, data pooled from 2-3 independent experiments, horizontal lines represent the mean±SD, data analysed using a Mann-Whitney test). There was no difference in the accumulation of CD4 T cells when either population of Langerin$^+$ DC were depleted.

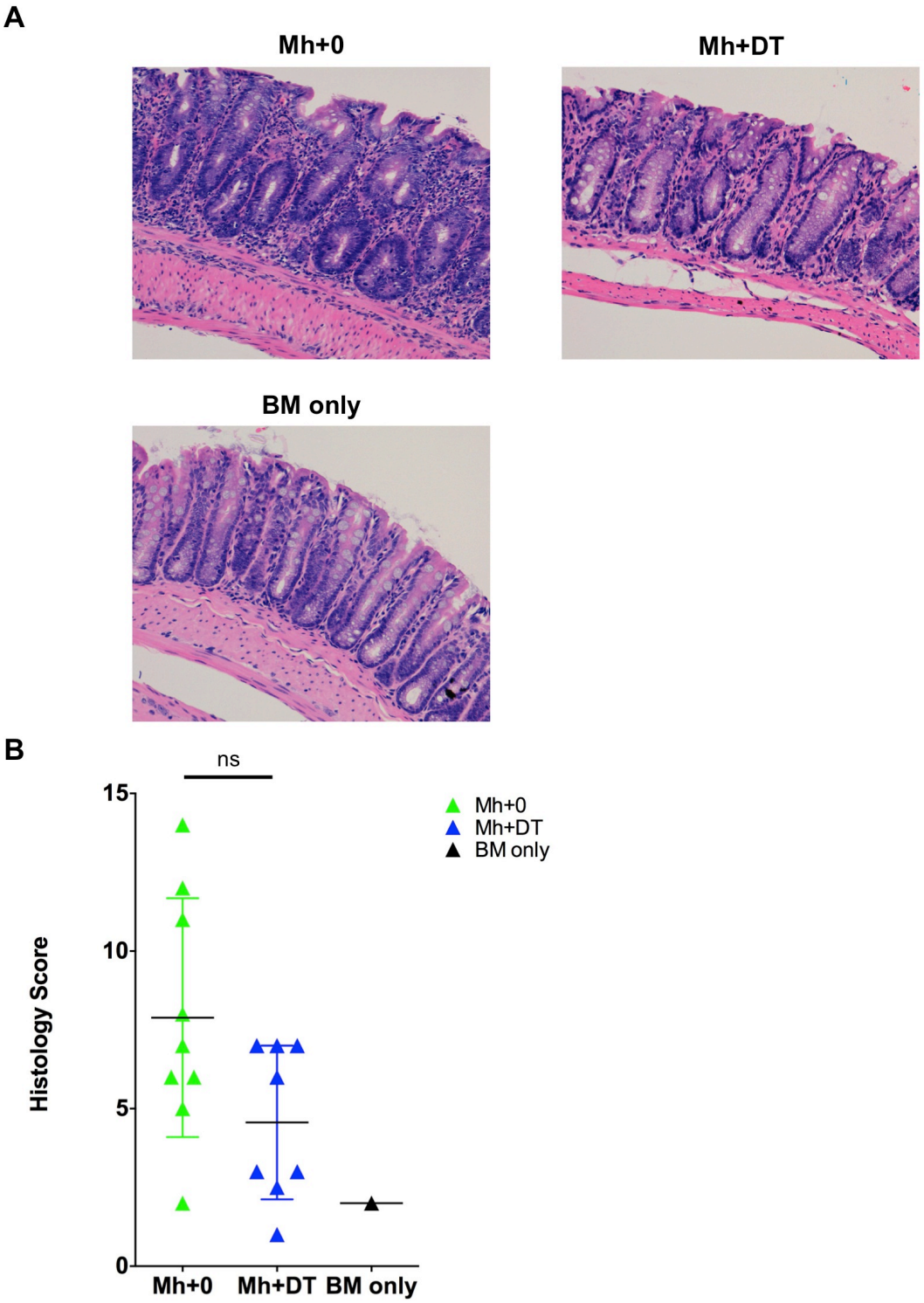

Figure 63: The depletion of host Langerhans cells had no effect on the severity of GVHD in the colon. A. Histological sections of the colon taken from Langerin-DTR recipeints 26 days after transplant. Only host LC were depleted in DT treated samples. Images captured at X20 magnification using a Leica DMD108 light microscope. **B.** Summary data of histological GVHD score as evaluated single blind (n=1-9, data pooled from 3 independent experiments, analysed using a Mann-Whitney test, the mean ±SD is indicated by the horizontal bars.). There was no significant reduction in the severity of GVHD in the colon when host LC were depleted.

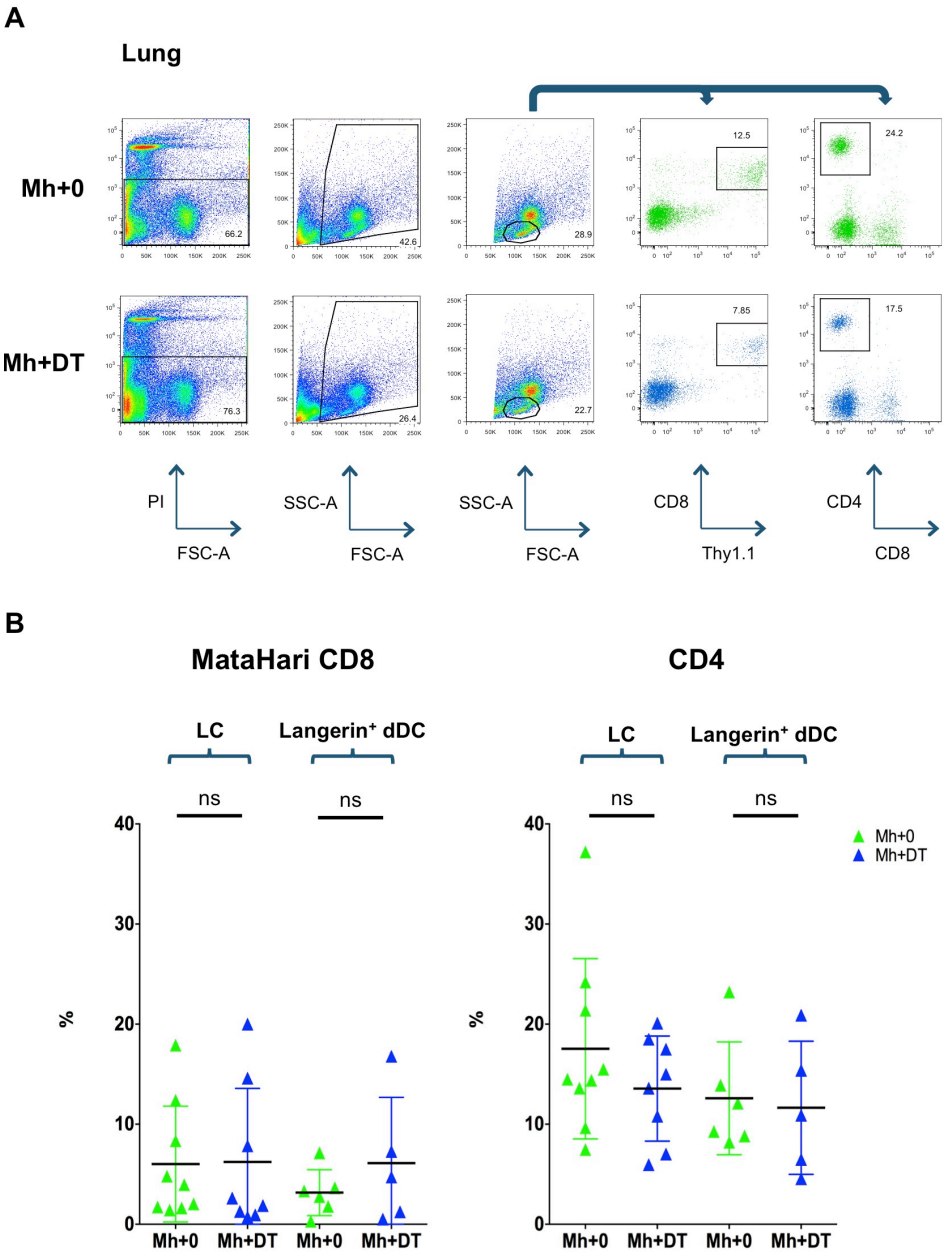

Figure 64: The depletion of host Langerin$^+$ DC had no effect on the accumulation of donor T cells in the lung. A. Representative dot plots of the lung taken from Langerin-DTR recipients 26 days after transplant. PI$^-$ cells were gated to eliminate dead cells. After a live cell gate followed by a lymphocyte gate, Mh T cells were identified based on their expression of Thy1.1 and CD8. CD4 T cells were identified based on their expression of CD4. This gating strategy was applied to all samples analysed in B. **B.** *Left-* Summary data showing the frequency of Mh T cells in the lung as a percentage of the initial lymphocyte gate 26 (LC depletion) and 20 (Langerin$^+$ dDC) days after transplant (n=5-9, data pooled from 2-3 independent experiments, horizontal lines represent the mean±SD, data analysed using a Mann-Whitney test). There was no difference in the accumulation of Mh T cells when either population of Langerin$^+$ DC was depleted. *Right-* Summary data showing the frequency of CD4 T cells in the lung as a percentage of the initial lymphocyte gate 26 (LC depletion) and 20 (Langerin$^+$ dDC) days after transplant (n=5-9, data pooled from 2-3 independent experiments, horizontal lines represent the mean±SD, data analysed using a Mann-Whitney test). There was no difference in the accumulation of CD4 T cells when either population of Langerin$^+$ DC were depleted.

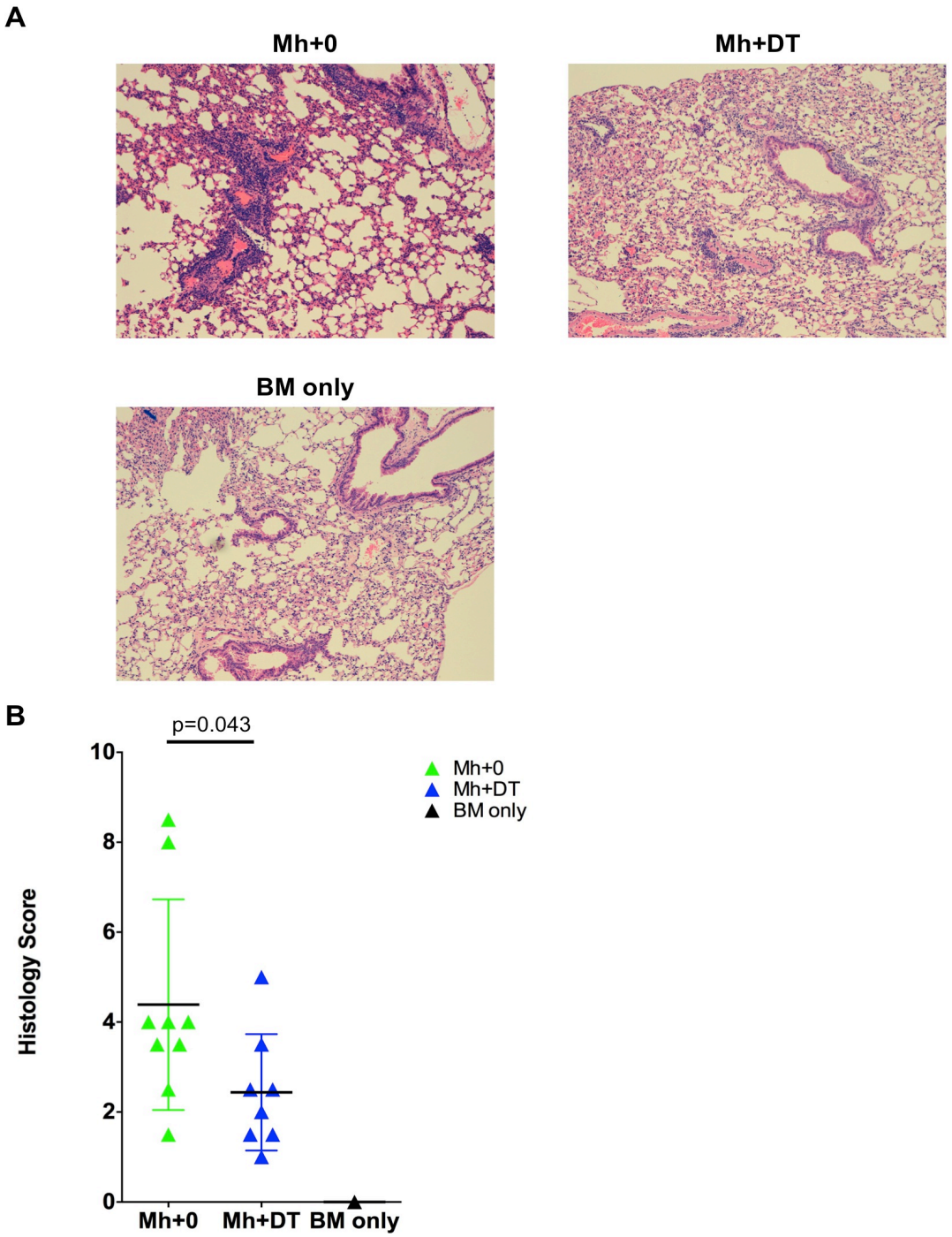

Figure 65: The depletion of host Langerhans cells had no effect on the severity of GVHD in the lung. A. Histological sections of the lung taken from Langerin-DTR recipeints 26 days after transplant. Only host LC were depleted in DT treated samples. Images captured at X20 magnification using a Leica DMD108 light microscope. **B.** Summary data of histological GVHD score as evaluated single blind (n=1-9, data pooled from 3 independent experiments, analysed using a Mann-Whitney test, the mean ±SD is indicated by the horizontal bars.). There was a significant reduction in the severity of GVHD in the lung when host LC were depleted. However, the magnitude of the difference was lower than that seen in the skin.

4.2.6 Mh T cells accumulate in the skin 6 days after transplant

In all allogeneic BMT experiments involving Mh T cells to date, the earliest time point investigated post transplant was 7 days. This was sufficient for Mh T cells to have markedly expanded in the lymphoid tissues and also to infiltrate tissues commonly affected by GVHD such as the skin, liver, lung and LP+PP.

To investigate the kinetics of Mh T cell infiltration in the aforementioned tissues, Langerin-DTR recipients, treated with or without DT 20 days before transplant to deplete host LC, were culled 3, 4, 5 and 6 days after transplant and the frequency of Mh T cells in each organ analysed.

In the liver, lung and LP+PP, Mh T cells were gated using the strategy outlined in Figure 66. Mh T cells were detected in all three tissues 3 days after transplant, although the frequency of cells in the LP+PP at this time point was very low. The frequency of Mh T cells in each tissue increased steadily until day 6 post transplant. However, 26 days after transplant, the frequency of MataHari T cells was markedly decreased in all 3 tissues versus day 6 (Figure 68).

In the skin, a different pattern was observed (Figure 67). In the epidermis, no Mh T cells were detected until day 6 post transplant and there was a significant reduction in the frequency of Mh T cells in the absence of host LC at this timepoint. In contrast to the liver, lung and LP+PP, the frequency of Mh T cells increased from day 6 to day 26 post transplant. In the dermis, a very low frequency of Mh T cells was detected by day 5 post transplant, which increased steadily by day 6. There was no difference in the accumulation of Mh T cells in the dermis in the absence of host LC by day 6. The frequency of Mh T cells also increased in the dermis between day 6 and day 26. Taken together, these data highlights the site-specific differences of a T cell response targeting the same antigen between tissues, and was the first step at identifying the mechanism of the phenotype mediated by host LC.

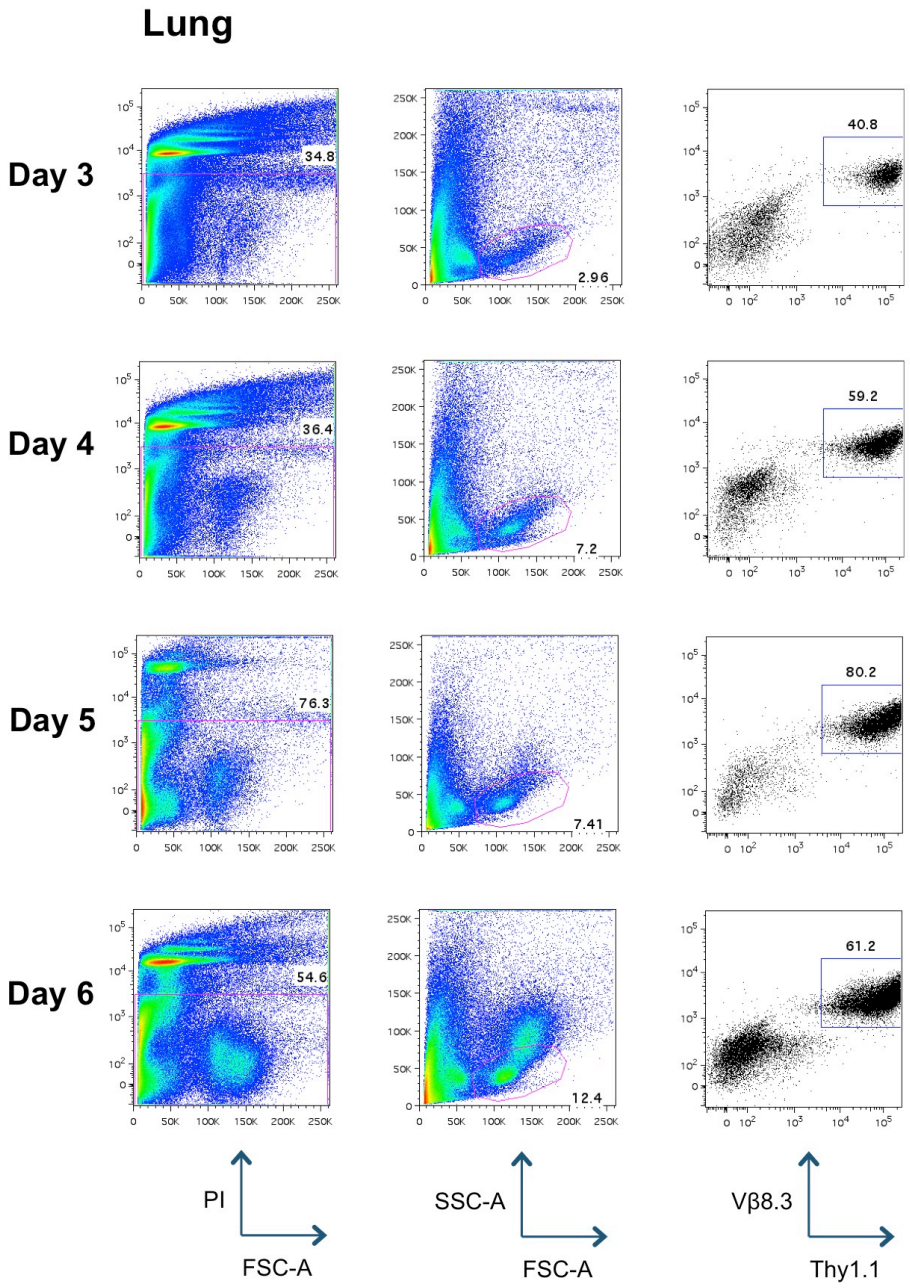

Figure 66: MataHari T cells have infiltrated the lung by day 3 post-transplant. Representative dot plots of the lung taken from Langerin-DTR recipients 3, 4, 5 and 6 days after transplant with Mh T cells. After a PI^- gate followed by a lymphocyte gate, Mh T cells were identified based on their expression of Vβ8.3 and Thy1.1. This gating strategy was used for liver and LP+PP samples. Mh T cells had infiltrated the lung 3 days after transplant, with the frequency of cells in the lung increasing over the next few days.

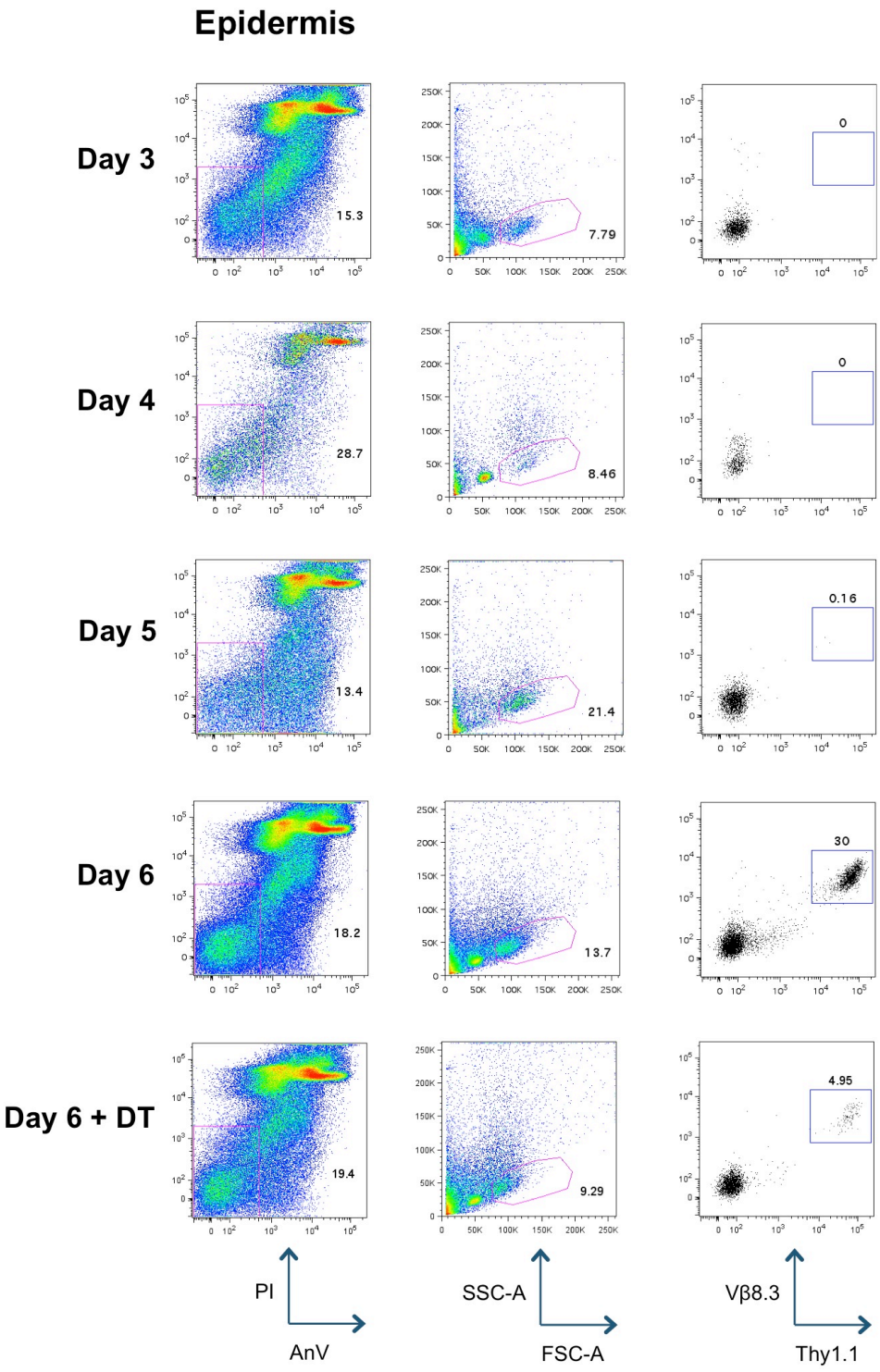

Figure 67: MataHari T cells infiltrate the epidermis by day 6 post-transplant. Representative dot plots of the epidermis taken from Langerin-DTR recipients 3, 4, 5 and 6 days after transplant with Mh T cells. After a PI^- AnV^- gate, to eliminate dead and apoptotic cells, followed by a lymphocyte gate, Mh T cells were identified based on their expression of Vβ8.3 and Thy1.1. Interestingly, no Mh T cells were detected in the epidermis 3, 4 and 5 days post transplant. On day 6, Mh T cells accumulated in the epidermis. In recipients depleted of host LC, there was a reduction in the frequency of Mh T cells detected.

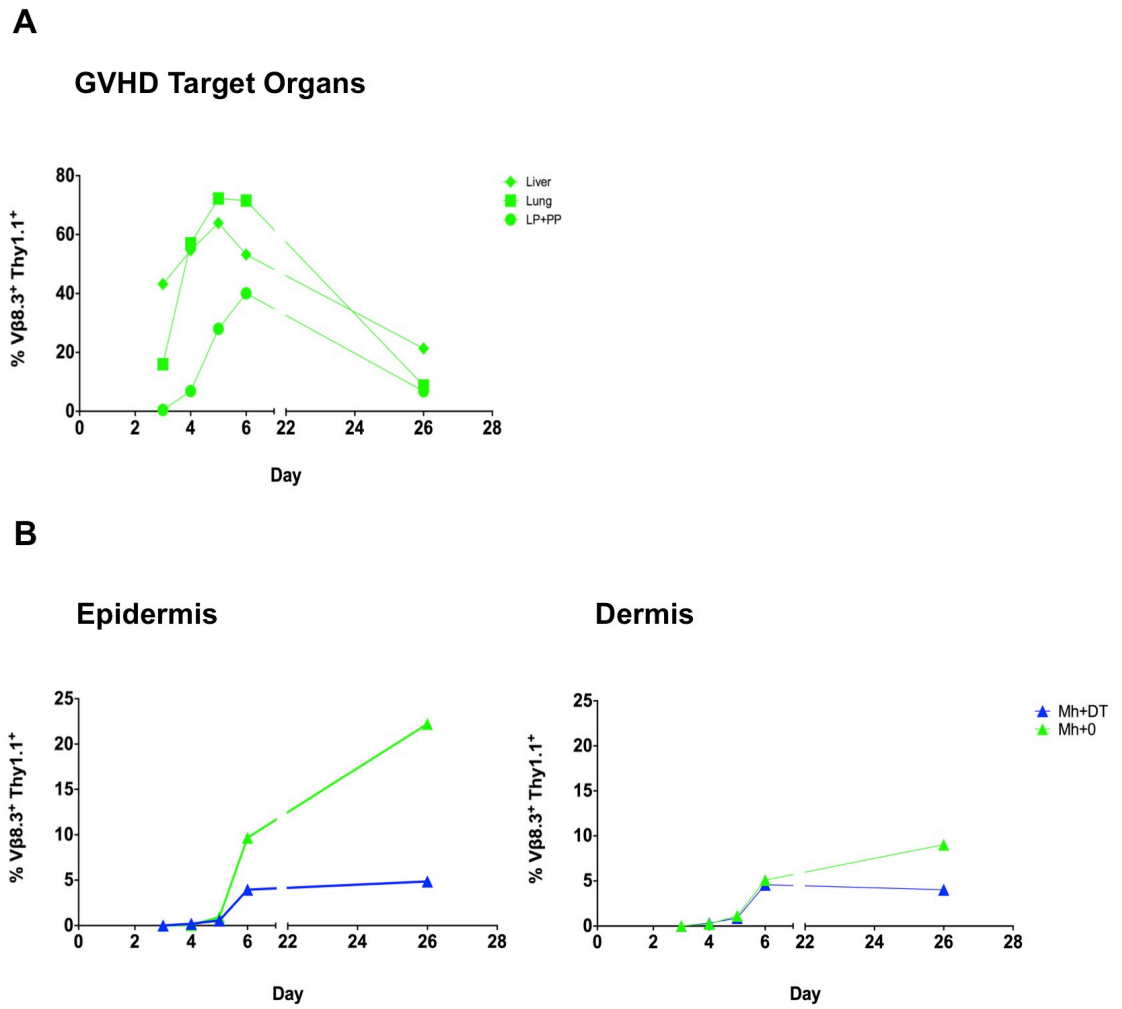

Figure 68: The infiltration of Mh T cells into the skin is distinct from other GVHD target organs. A. Summary data showing the frequency of Vβ8.3$^+$ Thy1.1$^+$ Mh T cells as a percentage the initial lymphocyte gate versus time after transplant in tissues indicated (day 3: n=1, day 4: n=2, day 5: n=5, day 6: n=6, day 26: n=6, data pooled from 1-4 independent experiments, horizontal lines represent the mean). Mh T cells accumulated the liver and lung by day 3 post transplant. Mh T cells were detected on day 3 at very low frequencies, but increased steadily in the days afterwards. In all 3 tissues, there was a reduction in the frequency of Mh T cells at day 26 versus day 6. **B.** *Top*- Summary data showing the frequency of Vβ8.3$^+$ Thy1.1$^+$ Mh T cells as a percentage the initial lymphocyte gate versus time after transplant in the epidermis (day 3: n=1, day 4: n=2, day 5: n=5, day 6: n=6, day 26: n=9, data pooled from 1-4 independent experiments, horizontal lines represent the mean). Unlike other tissues affected by GVHD, Mh T cells were not detected in the epidermis until day 6 post transplant. The frequency of Mh T cells in the epidermis was lower on day 6 when host LC were depleted. The frequency of Mh T cells also increased between day 6 and day 26, unlike other tissues investigated. *Bottom*- Summary data showing the frequency of Vβ8.3$^+$ Thy1.1$^+$ Mh T cells as a percentage the initial lymphocyte gate versus time after transplant in the dermis (day 3: n=1, day 4: n=2, day 5: n=5, day 6: n=6, day 26: n=9, data pooled from 1-4 independent experiments, horizontal lines represent the mean). In contrast to the epidermis, a very small frequency of Mh T cell was detected in the dermis by day 6 post transplant. The depletion of host LC had no effect on the frequency of Mh T cells by day 6. The frequency of Mh T cells also increased between day 6 and day 26.

4.3 Discussion

4.3.1 MHC-matched, minor H mismatch model of acute GVHD

In the previous chapter, the role of host Langerin$^+$ dDC was explored using an MHC-mismatched model of localised cutaneous GVHD. Previous work in our lab using this model has shown a role for host LC in the development of cutaneous GVHD. However, the MC model is a highly reductionist system that has no clear clinical correlate.

To further explore the role of host LC and Langerin$^+$ dDC in the development of cutaneous GVHD, I developed a more clinically relevant model of acute systemic GVHD, where either host LC or Langerin$^+$ dDC could be conditionally depleted. In the clinic, male recipients of female BM (F→M) are at a greater risk of developing GVHD and show H-Y specific alloresponses[306]. Adapting this observation to mice, I developed a F→M, MHC-matched, minor H mismatch model of acute GVHD using Mh Tg CD8 T cells, which bear a TCR specific for a ubiquitous male antigen, to initiate GVHD.

This model had a number of advantages over the MC model. Firstly, MHC-matched, minor H antigen mismatched models represent transplants in the clinic more closely than MHC-mismatched models, as MHC-mismatched transplants are not commonly performed in humans. Secondly, the GVHD that developed in this model was systemic. Histopathological GVHD developed in both the skin and gut 7 days after transplant with Mh T cells, organs that are commonly affected by acute GVHD in the clinic. Thirdly, the inflammation in this model is also generated by the conditioning regime, which more closely resembles the type of inflammation that initiates acute GVHD in the clinic rather than the application of the TLR agonist Imiquimod in the MC model.

Using a monoclonal Tg T cell population to initiate GVHD also had advantages. A major limitation of MHC-matched, minor H antigen mismatched models that use polyclonal T cells is the difficultly in determining which alloantigens donor T cells are responding to. Differences in the TCR-repertoire may also have a significant influence

on the development of GVHD in a particular tissue. Using monoclonal Mh T cells, the dose of alloreactive T cells can be tightly controlled and easily traced *in vivo* using Vβ8.3 and Thy1.1, making the model highly tractable. The TCR is also 'fixed' and recognises the same antigen at every site, thus any changes in the development of GVHD in the skin when Langerin^{+} DC are depleted are TCR-repertoire independent.

To initiate GVHD, I initially infused lethally irradiated BL/6 male mice with 1 x10^6 Mh T cells from the spleen of female Mh donors and 5 x10^6 BM cells derived from female BL/6 donor 4 h after the final dose of irradiation. This dosage was sufficient for Mh T cells to engraft and rapidly expand *in vivo*. By day 7 post transplant, Mh T cells had expanded in the spleen, with the majority of cells exhibiting a CD44^{high} CD62L^{low} effector phenotype. This dosage was also sufficient for Mh T cells to infiltrate and accumulate in the skin 7 days after transplant.

The addition of polyclonal CD4 T cells from a female donor appeared to enhance the Mh T cell response *in vivo*. There was an increase in both the absolute number of Mh T cells in the spleen and the frequency of infiltrating cells in the epidermis 7 days after transplant. In addition, recipients that received both Mh and CD4 T cells developed slightly more severe clinical GVHD, as evidenced by an increased weight loss and higher clinical scores, key indicators of GVHD. This was not unexpected, as the addition of CD4 'help' has been shown to enhance the CD8 T cells response in other MHC-matched, minor H mismatch models[193]. Therefore, a dose of 2 x10^6 polyclonal CD4 T cells derived from the spleen of female WT BL/6 donors was added to the transplant mixture in all future experiments. This was sufficient to induce acute and systemic GVHD as evidenced by the development of histopathological GVHD in both the skin and gut 7 days after transplant, pathology that was absent in recipients that received BM alone.

In the skin, the expression of CD8 in Mh T cells was inconsistent, with a large frequency of cells infiltrating the epidermis negative for CD8. This was unexpected and indicated that either Mh T cells were downregulating their expression of CD8 or an enzymatic step during processing was interfering with staining. To test the latter hypothesis, I incubated SC harvested from male BL/6 recipients 7 days after transplant with donor Mh T cells with 2.5 mg/ml Dispase II for 0, 30, 60 and 90 min at 37°C. This had a profound effect on the expression of both CD8α and CD8β on VB8.3 and Thy1.1 Mh T cells in line with a previously published report on the effects of Dispase II[308]. Therefore, the use of anti-CD8 antibodies to detect Mh T cells in the skin was discontinued in future experiments.

4.3.2 The depletion of host LC, but not Langerin$^+$ dDC, significantly reduces the severity of cutaneous GVHD

To evaluate the role host Langerin$^+$ DC in the development of acute GVHD, male Langerin-DTR mice were used as recipients in the MataHari minor H mismatch model I developed at the beginning of the chapter. To deplete both host LC and Langerin$^+$ dDC, Langerin-DTR recipients were injected on day -2, 1, 4 and 7 days post transplant with 400 ng of DT. This was sufficient to deplete both host LC and Langerin$^+$ dDC during the initiation phase of acute GVHD and was based on the premise that the majority of infused donor Mh T cells would be primed by day 7 post transplant. As a control for any potential side effects associated with repeated i.p. injections, another cohort of Langerin-DTR recipients were treated with a similar volume PBS in parallel. This was important due to the frequency of injections at such an early stage after lethal irradiation, as it may have increased morbidity and mortality.

Langerin-DTR recipients were subsequently tracked for 7 weeks after transplant for changes in survival and clinical GVHD. Langerin-DTR recipients that received Mh T cells developed moderate to severe clinical GVHD, with over 50% of recipients in both cohorts sacrificed for humane reasons before 7 weeks. This contrasted recipients that were transplanted with BM alone, which had a 100% survival rate. Langerin-DTR recipients of Mh T cells lost weight, appeared hunched, showed reduced activity and fur ruffling (key indicators of clinical GVHD in mice). The depletion of host Langerin$^+$ DC had no significant effect on the survival, degree of weight loss and clinical score compared to PBS treated controls. Thus, host Langerin$^+$ DC are not required for the initiation of acute GVHD in this model. The severity of GVHD that developed in this model appeared to be less severe than that published by another group using a similar dose of Mh T cells. However, it is well established in the field that differences in protocols and environmental pathogens between labs can significantly influence the degree of GVHD that develops[181]. For instance, in our model we add the antibiotic

Baytril to the drinking water a week before transplant, which may account for some of the differences observed between models.

Focusing on the degree of weight loss in recipients, a double dip pattern emerged where recipients rapidly lost weight immediately after transplant before subsequently recovering for a few days, followed by another period of rapid weight loss, which was associated with the highest rate of mortality. This is a pattern commonly seen in other pre-clinical models, where mice initially lose weight due to the 'cytokine storm' associated with the conditioning regime before rapidly losing again due to the effector functions of alloreactive donor T cells. To assess the donor T cell response *in vivo*, Langerin-DTR recipients were culled at day 7 and 26 post transplant, where clinical GVHD appeared to peak in recipients around day 26.

The depletion of host Langerin^{+} DC had no effect on the activation or expansion of donor Mh or CD4 T cells in the lymphoid tissue at day 7 or day 26 post transplant. In the spleen, the absolute number and frequency of effector CD44^{high} CD62L^{low} Mh and CD4 T cells was similar in both cohorts. However, the absolute number of Mh T cells was significantly reduced in both cohorts by day 26 compared to day 7. This may be a result of either trafficking or activation induced cell death. The function of Mh T cells derived from the spleen of Langerin-DTR recipients 7 days after transplant was also assessed using an *in vitro* restimulation assay. There was no significant difference in the expression of IFN-γ in Mh T cells derived from Langerin-DTR recipients depleted of host Langerin^{+} DC compared to PBS treated controls.

In the skin draining lymph nodes, which in this project refer to the inguinal, axial, brachial and cervical lymph nodes, a similar pattern emerged. The depletion of host Langerin^{+} DC had no effect on the activation or expansion of donor Mh T cells in the skin draining lymph nodes at day 7 or day 26 post transplant. The activation and expansion of donor CD4 T cells was not assessed on day 7 post transplant due to

efforts to stain T cells with E-selectin ligand, which were unsuccessfully due to technical reasons. However, there was no significant difference in the activation and expansion of donor CD4 T cells between cohorts after 26 days. The frequency of circulating donor Mh T cells was also assessed by tail bleed 14 days after transplant and there was also no difference in the frequency or activation profile between cohorts.

Taken together, the survival data and T cell response *in vivo* demonstrates that host Langerin$^+$ DC are not required for the initiation of acute GVHD in this model. The depletion of host Langerin$^+$ DC also had no effect on the severity of systemic GVHD that developed. This was not unexpected, as several reports published during the course of these experiments challenged the role of host haematopoietic APC in the development of acute GVHD[125,129,310]. In both MHC-matched, minor H mismatched models of CD8- and CD4- mediated acute GVHD, both donor haematopoietic and host non-haematopoietic APC were found to be sufficient to initiate GVHD. In this model, host LC and Langerin$^+$ dDC in the skin are depleted. Many other host DC populations capable of priming alloresponses will remain in DT treated recipients. Thus, the lack of a systemic effect on the development of acute GVHD was not surprising.

However, when the skin was assessed, the depletion of host Langerin$^+$ DC did have a profound effect on the development of GVHD. Initial experiments depleting both host LC and Langerin$^+$ dDC demonstrated a significant reduction in the accumulation of Mh T cells in the epidermis at day 7 and day 26 post transplant. The effect on CD4 T cells was not as pronounced, with a significant difference in the accumulation only observed in the epidermis by day 26. To delineate whether host LC or Langerin$^+$ dDC were responsible for this reduction in the accumulation of T cells, two experimental approaches were developed. Taking advantage of the repopulation kinetics of Langerin$^+$ dDC, which fully reconstitute its dermal niche 7 days after acute depletion, Langerin-DTR recipients were injected with DT 20 days before transplant to deplete host LC but not Langerin$^+$ dDC. This proved remarkably effective. 20 days after a

single i.p. injection of 400 ng DT, LC remained depleted but host Langerin$^+$ dDC has fully reconstituted the dermis, in line with previously published data. Adopting the same gating strategy used to analyse the skin when both host LC and Langerin+ dDC were depleted, a similar reduction in the accumulation of Mh T cells in both the epidermis and dermis was observed when only host LC but not Langerin$^+$ dDC were depleted.

To deplete host Langerin$^+$ dDC but not LC, I developed a different approach. Using male BL/6 mice as recipients, I generated [Langerin-DTR → BL/6] chimeras where host Langerin$^+$ dDC were susceptible to DT mediated depletion but not LC. I confirmed that host LC were not depleted 7 days after transplant. However, I was unable to directly confirm depletion of host Langerin$^+$ dDC due to inflammation and cellular infiltrate rendering the detection of Langerin$^+$ dDC found at relatively low frequencies technically difficult. Due to time constraints, I was unable to generate a cohort of [Langerin-DTR → BL/6] chimeras to specifically test the chimerism and depletion of Langerin$^+$ dDC. However, in the previous chapter, I established that host Langerin$^+$ dDC were radiosensitive and in MC were derived entirely from donor cells. Thus, host Langerin$^+$ dDC will be depleted in this model. Interestingly, adopting the same gating strategy used to analyse the skin when both host LC and Langerin+ dDC were depleted, the reduction in the accumulation of Mh T cells in both the epidermis and dermis was abrogated when Langerin$^+$ dDC but not LC were depleted.

Taken together, these data demonstrates that host LC but not Langerin$^+$ dDC are responsible for a reduction in the accumulation of Mh T cells in the skin. This reduction was also skin specific, as the depletion of either host LC or Langerin$^+$ dDC had no effect on the accumulation of Mh and CD4 T cells in the liver, lung and LP+PP.

To evaluate whether this reduction in Mh T cells in the skin correlated with a reduction in the development of cutaneous GVHD, histopathological sections of the skin, liver, lung and colon were taken from Langerin-DTR recipients 26 days after transplant when

host LC but not Langerin$^+$ dDC were depleted and scored single blind for evidence of GVHD. Remarkably, the depletion of host LC resulted in a highly significant reduction in the severity of GVHD that developed. The depletion of host LC had no effect on the development of GVHD in the liver or colon. However, there was a reduction in the development of GVHD in the lung in the absence of host LC although the reduction was relatively minor.

To investigate the mechanism underpinning the reduction in cutaneous GVHD in the absence of LC, the kinetics of Mh T cell infiltration was analysed. In the liver, lung and LP+PP, Mh T cells were detected in all three tissues 3 days after transplant and steadily increased in frequency. Interestingly, in the skin, a different pattern emerged, no Mh T cells were detected until day 6 after transplant and highlighted the site-specific differences of a T cell response targeting the same antigen between tissues. In addition, there was a significant difference in the accumulation of Mh T cells in the epidermis in absence of host LC at this early stage.

Interestingly, the frequency of Mh T cells in the epidermis and magnitude of the difference in the absence of host LC increased from day 6 to day 26. However, by day 26 the majority of host LC had been depleted, yet the response and magnitude of the difference was still maintained *in situ*. The presence of host LC during the initiation stage of acute GVHD appears to be sufficient to drive the response observed. It is also noteworthy that the repopulation kinetics of DC into the epidermis was influenced by the depletion of host Langerin$^+$ DC. By day 26, there were significantly more MHCII$^+$ CD11b$^+$ in the skin of PBS controls than recipients treated with DT, despite the majority of cells in PBS controls being donor derived. However, this increase may be a result of the immunostimulatory cytokines and chemokines released due to the increased pathology associated with the presence of host LC, promoting the migration of inflammatory monocyte derived DC into the epidermis[259].

5 Langerhans cells are required *in situ* for full effector function of donor CD8 T cells

In the previous chapter, I established that the depletion of host LC, but not Langerin^{+} dDC, significantly reduced the severity of cutaneous GVHD in the skin in a model of acute GVHD. However, whether this reduction was the result of a difference in T cell priming or homing in the skin draining lymph node or an extrinsic signal mediated by host LC *in situ* remained to be determined.

To investigate whether host LC influence the severity of cutaneous GVHD *in situ*, I initially developed a localised model of cutaneous GVHD where alloreactive donor T cells were injected directly into skin. This proved unsuccessful so two alternative experimental approaches were developed. One involved the secondary transfer of primed alloreactive Mh T cells into Langerin-DTR recipients, while the other focused on the localised depletion of host LC *in situ*.

In the final part of my project, I flow sorted Mh T cells from the epidermis and skin draining lymph nodes of Langerin-DTR recipients 7 days after transplant and investigated the effect of host LC depletion on the transcriptional profile of Mh T cells. In addition, host LC were sorted from the epidermis of allogeneic (F→M) and syngeneic (F→F) recipients of BMT with Mh T cells. Mh T cells do not infiltrate the epidermis in syngeneic recipient. Thus, I was able to investigate the effects of infiltrating Mh T cells on the transcriptional profile of host LC.

5.1 A model of GVHD using antigen exposed MataHari T cells

5.1.1 A dose of 0.1 x10^6 AEMTs is insufficient for Mh T cells to accumulate in the skin

To establish whether host LC are required *in situ* to regulate cutaneous GVHD, I developed a new model of GVHD where antigen exposed MataHari T cells (AEMTs) taken from skin draining lymph nodes, along with BM and CD4 T cells from a female WT BL/6 donor, were injected i.v. into lethally irradiated male BL/6 recipients. The assumption in this experiment is that the majority of AEMTs, which had been exposed to antigen for 5 days *in vivo* in a lethally irradiated BL/6 male recipient, would be already primed against male antigen and ready to initiate GVHD. Therefore, any differences in the ability of these T cells to accumulate in the skin in the absence of host LC would provide strong evidence that LC are required *in situ* in the skin.

Adapting the already established MataHari minor mismatch model of GVHD, an irradiated male BL/6 recipient was transplanted with 5 x10^6 BM and 2 x10^6 polyclonal CD4 T cells from a female BL/6 donor. However, the Mh T cell dose administered was increased from 1 x10^6 to 2 x10^6 cells (Figure 69, A). 5 days later, the male BL/6 recipient was culled and skin draining lymph nodes harvested. This time point was chosen based on the kinetics data from the previous chapter where Mh T cells were found to accumulate in the skin from day 6 post transplant. The skin draining lymph node cell suspension was then passed through 0.5 g nylon wool to enrich lymphocytes. The majority of cells in the skin draining LN at this time point node were found to be donor Mh CD8 T cells (Figure 69, B). 0.1 x10^6 of these AEMTs were then transplanted into a lethally irradiated male Langerin-DTR mouse along with 5 x10^6 bone marrow and 2 x10^6 CD4 T cells obtained from a female BL/6 donor (Figure 69C). AEMTs were tracked *in vivo* based on the expression of their expression of Vβ8.3, Thy1.1.

7 day after transplant, the male Langerin-DTR recipient was culled. AEMTs were found to have accumulated and expanded in the spleen and skin draining lymph nodes

(Figure 70). The absolute number of AEMTs found in the spleen and skin draining lymph nodes was 128,064 and 56,532 respectively. AEMTs were also found to have infiltrated and accumulated in organs commonly affected by GVHD such as the liver, lung and LP+PP (Figure 70). However, in the skin no AEMTs were found to have accumulated in the epidermis by day 7 and few were found to have accumulated in the dermis compared to frequencies typically observed using 1 $x10^6$ naïve Mh T cells (Figure 71).

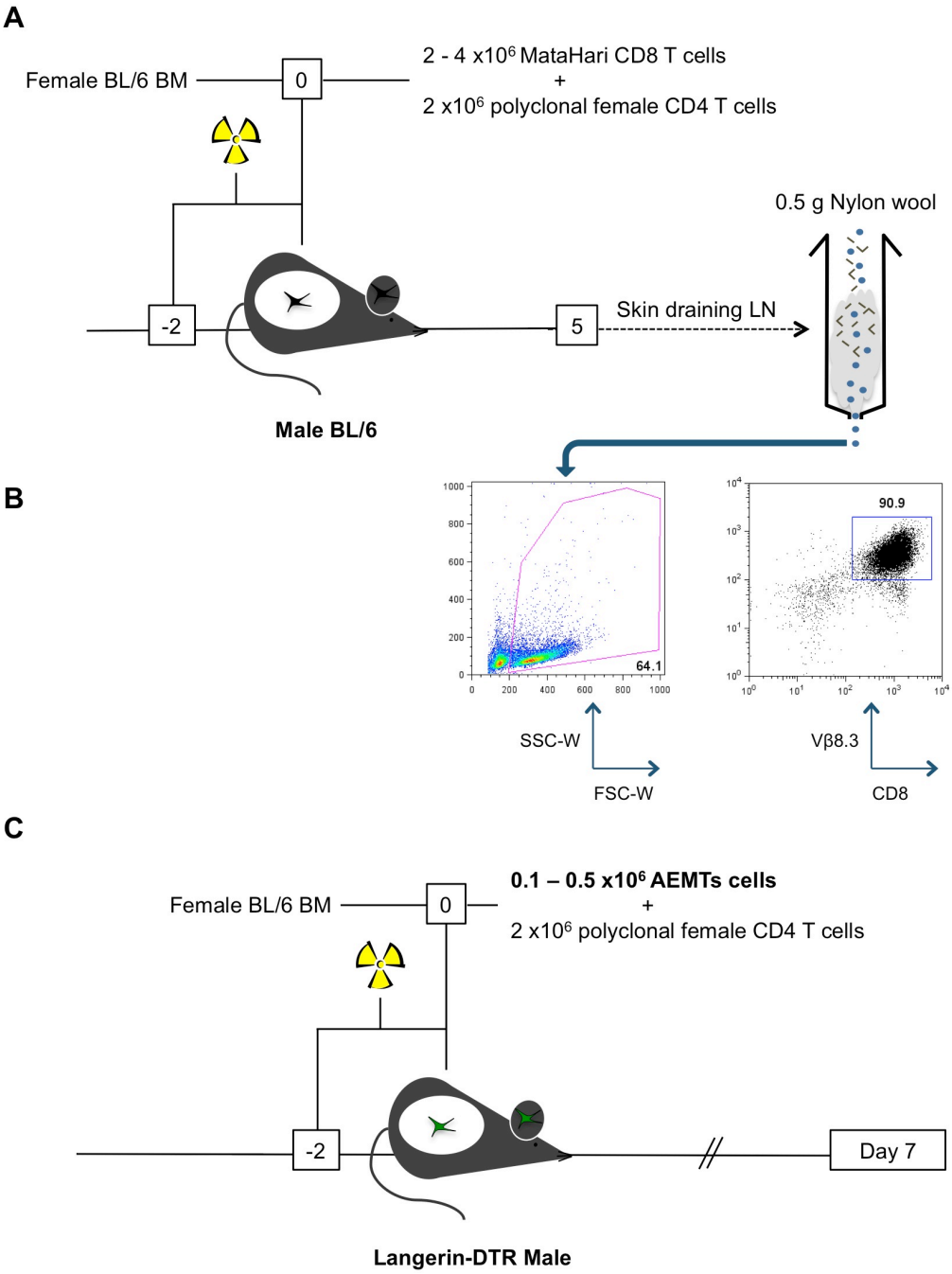

Figure 69: Initiating systemic GVHD using AEMTs. A. Male BL/6 mice were lethally irradiated with a split dose of 11 GY and reconstituted of 5 x10^6 BM and 2 x10^6 SC from a female BL/6 donor. 2-4 x10^6 MataHari T cells were also transplanted to initiate systemic GVHD. On day 5 post transplant recipient male BL/6 mice were culled and the skin draining lymph nodes harvested. The skin draining lymph node cell suspension was then passed through 0.5 g nylon wool to enrich lymphocytes. **B.** Representative dot plots of a skin draining lymph node cell suspension that had been passed through nylon wool. The majority of cells in the lymph node at this time point were MataHari CD8 T cells. After an initial anti-apoptotic gate, MataHari CD8 T cells were identified based on their expression of Vβ8.3 and CD8. **C** Male Langerin-DTR were lethally irradiated with a split dose of 11 GY and reconstituted with a mixture of 5 x10^6 bone marrow and 2 x10^6 CD4 T cells obtained from a female BL/6 donor. 0.1-0.5 x10^6 AEMTs were also transplanted to initiate systemic GVHD.

0.1 x 10^6 MataHari T cells (5 days)

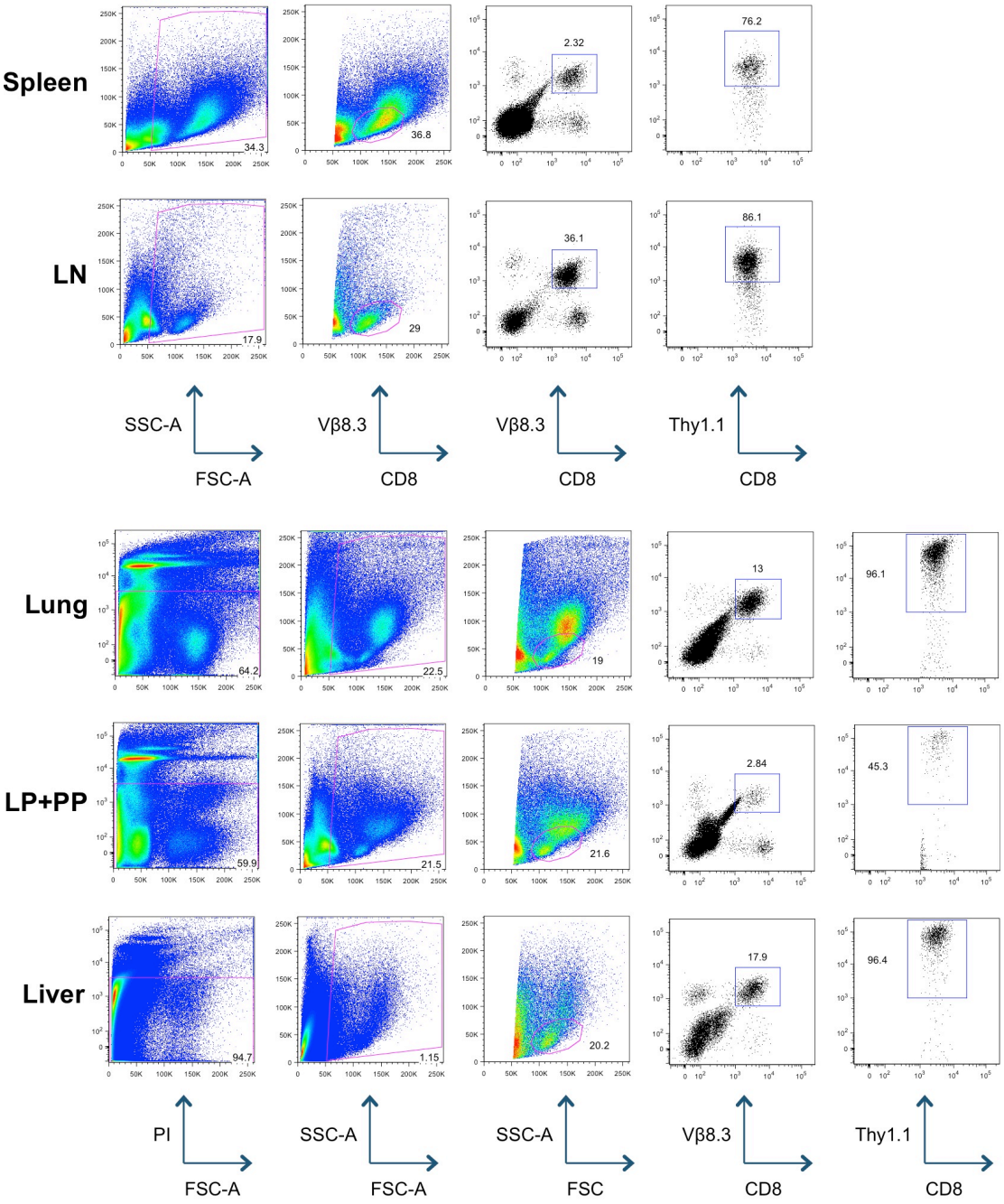

Figure 70: A dose of 0.1 x10^6 AEMTs is sufficient for MataHari T cells to expand and accumulate in GVHD target organs. Dot plots of the spleen, skin draining lymph nodes, lung, LP+PP and liver from a male Langerin-DTR recipient 7 days after transplant with 0.1 x10^6 AEMTs. In the spleen and skin draining lymph nodes, after an initial anti-apoptotic gate followed by a lymphocyte gate, MataHari T cells were identified based on their expression of Vβ8.3, Thy1.1 and CD8. The lung, LP+PP and liver were additionally stained with PI and cells that were PI^- were gated the same as the spleen and skin draining lymph nodes. AEMTs, which had previously been exposed to antigen in vivo for 5 days, were found to have successfully engrafted into the secondary recipient.

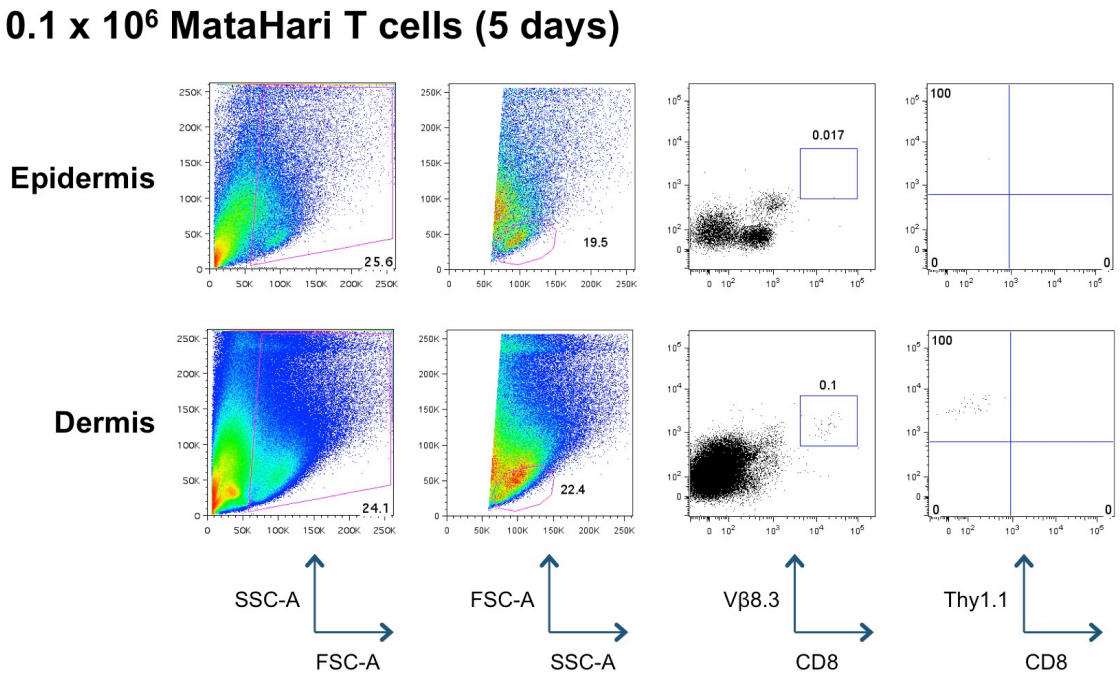

Figure 71: A dose of 0.1 x10^6 AEMTs was insufficient for AEMTs to accumulate in the skin. Dot plots of the epidermis and dermis from a male Langerin-DTR recipient 7 days after transplant with 0.1 x10^6 AEMTs. After an initial anti-apoptotic gate followed by a lymphocyte gate, MataHari T cells were identified based on their expression of Vβ8.3, Thy1.1 and CD8. In contrast to the liver, lung and LP+PP, transplanting 0.1 x10^6 AEMTs was insufficient for MataHari T cells to accumulate in the skin.

5.1.2 Increasing the dose to 0.5 x10^6 AEMTs had no effect on the ability of Mh T cells to accumulate in the skin

The experiment was repeated, increasing the dose of AEMTs to investigate whether the failure of Mh T cells to infiltrate the skin in the previous experiment was dose dependent. WT male BL/6 mice were irradiated with a split dose of 11 GY and transplanted with a mixture of 5 x10^6 bone marrow and 2 x10^6 CD4 T cells from female BL/6 donors along with 4 x 10^6 Vβ8.3$^+$, Thy1.1$^+$ Mh T cells. The number of MataHari T cells transplanted was increased from 2 x10^6 to 4 x10^6 to increase the number of AEMTs harvested (Figure 69A). 5 days after transplant, the skin draining lymph nodes were harvested and lymphocytes enriched as before.

This time the dose of AEMTs transplanted was increased from 0.1 x10^6 to 0.5 x10^6 (Figure 69B). 0.5 x10^6 AEMTs were injected into male Langerin-DTR recipients, along with bone marrow and CD4 T cells from female BL/6 donors as before. As a control, one male Langerin-DTR recipient received female BL/6 bone marrow only. To test the role of host Langerhans cells when Mh T cells have already been exposed and primed against male antigen, Langerin-DTR recipients were also treated with either 400 ng of DT (n=3) or PBS (n=3) i.p. 20 days before transplant.

In the lung, LP+PP and liver, Mh T cells accumulated in all recipients that received AEMTs and the depletion of host LC had no effect on the accumulation of Mh T cells in these organs (Figure 72).

In the skin, there was no evidence of Mh T cell accumulation in either the epidermis or dermis in the presence or absence of host LC (Figure 73). Increasing the dose to 0.5 x10^6 cells had no effect on the accumulation of donor AEMTs in the skin at this time point.

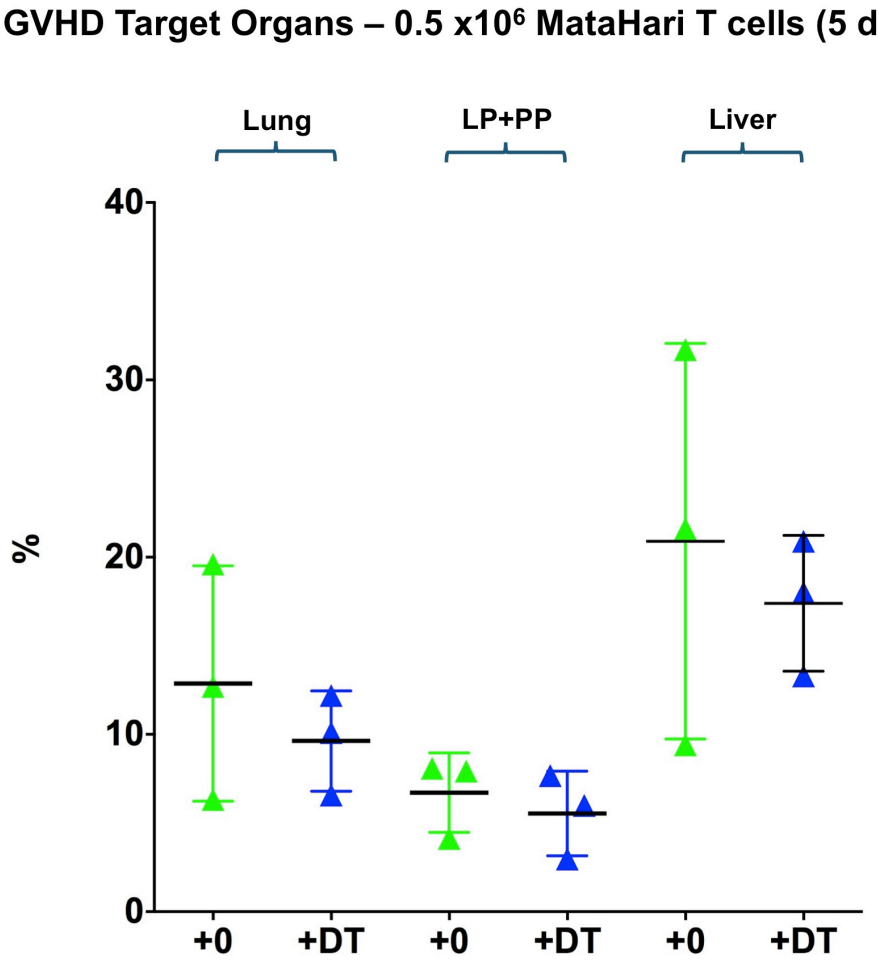

Figure 72: The depletion of host Langerhans cells had no effect on the accumulation of AEMTs in the lung, LP+PP and liver. Summary data showing the accumulation of Vβ8.3^{+}, Thy1.1^{+}, CD8^{+} AEMTs as a percentage of the FSC-A, SSC-A lymphocyte gate in Langerin-DTR recipients transplanted 7 days previously (n=3, data representative of 1 experiment, the mean ±SD is indicated by the horizontal bars). There was no difference in the accumulation of AEMTs in the lung, LP+PP and liver in the presence or absences of host LC.

Skin – 0.5 x10^6 MataHari T cells (5 days)

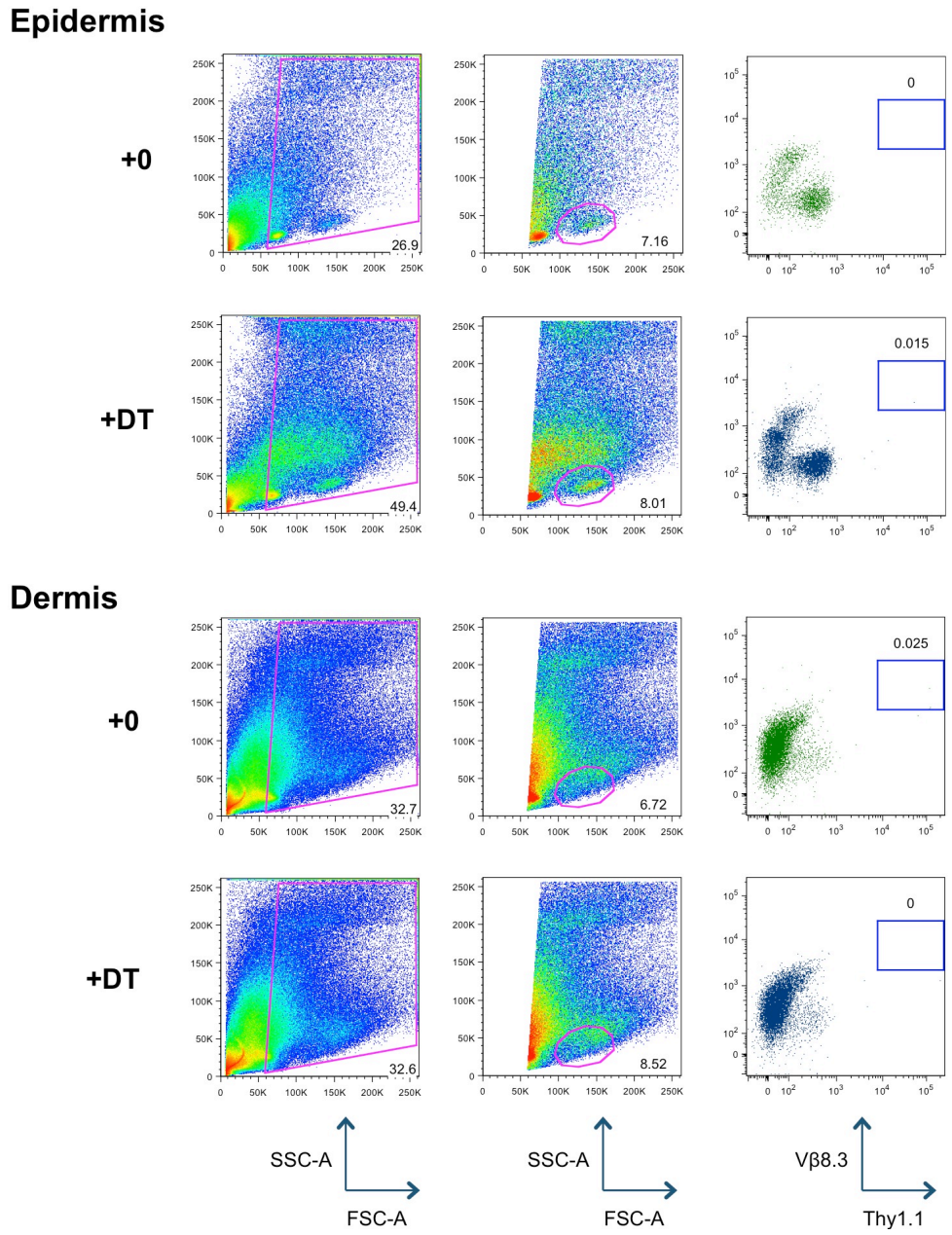

Figure 73: A dose of 0.5 x 10^6 AEMTs was insufficient for AEMTs to accumulate in the skin. Representative dot plots of the epidermis and dermis from a Langerin-DTR mouse transplanted with 0.5 x10^6 AEMTs 7 days previously. After an initial anti-apoptotic gate followed by a lymphocyte gate, samples were examined for the expression of Vβ8.3 and Thy1.1. There was no evidence of AEMTs accumulating in either the epidermis or dermis in any of the samples tested (PBS/DT: n=3).

5.1.3 Reducing the time Mh T cells are exposed to antigen *in vivo* increases their ability to accumulate in the skin

Increasing the dose of AEMTs transplanted from 0.1 x10^6 to 0.5 x10^6 had no effect on the accumulation of Mh T cells in the skin. To investigate whether the length of time donor Mh T cells were exposed to antigen *in vivo* affected their ability to accumulate in the skin, MataHari T cells exposed to antigen for 3, 4 and 5 days were mixed together at a 1:1:1 ratio and transplanted into male BL/6 recipients (Figure 74). The Mh T cells exposed to antigen for 3, 4 and 5 days could be tracked *in vivo* due to their differential expression of the congenic markers, CD45.1 and CD45.2 (Figure 75).

0.75 x10^6 AEMTs from BL/6 recipients culled 3, 4 and 5 days after transplant, mixed at a 1:1:1 ratio were injected into male BL/6 recipients along with BM and CD4 T cells derived from a female BL/6 donor. To verify that infiltration into the skin was not dose dependant, another cohort of male BL/6 recipients were injected with 1 x10^6 Mh T cells exposed to antigen for 4 days, a similar number used in the naïve model.

In the lung, LP+PP and liver, three distinct populations of MataHari T cells could be identified 7 days after transplant (Figure 76). In the cohort that received 1 x10^6 AEMTs, only one population of Mh T cells could be identified (Figure 76). AEMTs exposed to antigen for 4 days accumulated at higher frequencies than any other AEMTs in the lung, LP+PP and liver (Figure 78).

Interestingly, in the skin a different pattern emerged. Only Mh T cells exposed to antigen for 3 and 4 days were identified in both the epidermis and dermis in all samples, accumulating in similar frequencies (Figure 77). AEMTs exposed to antigen for 5 days accumulated infrequently in the skin and were undetectable in a number of samples (Figure 78). In the cohort that received 1 x10^6 AEMTs, Mh T cells exposed to antigen for 4 days accumulated in the epidermis and dermis in all recipients (n=3, Figure 77). However, the average frequency at which the AEMTs accumulated in the

epidermis and dermis was much lower than the frequencies observed transplanting 1 x10^6 naïve MataHari T cells.

These data indicates that the length of time Mh T cells are exposed to antigen *in vivo* influences their ability to accumulate in the skin. Due to the development of a more robust model and issues yet to be resolved in this model, further work using AEMTs to initiate GVHD was discontinued.

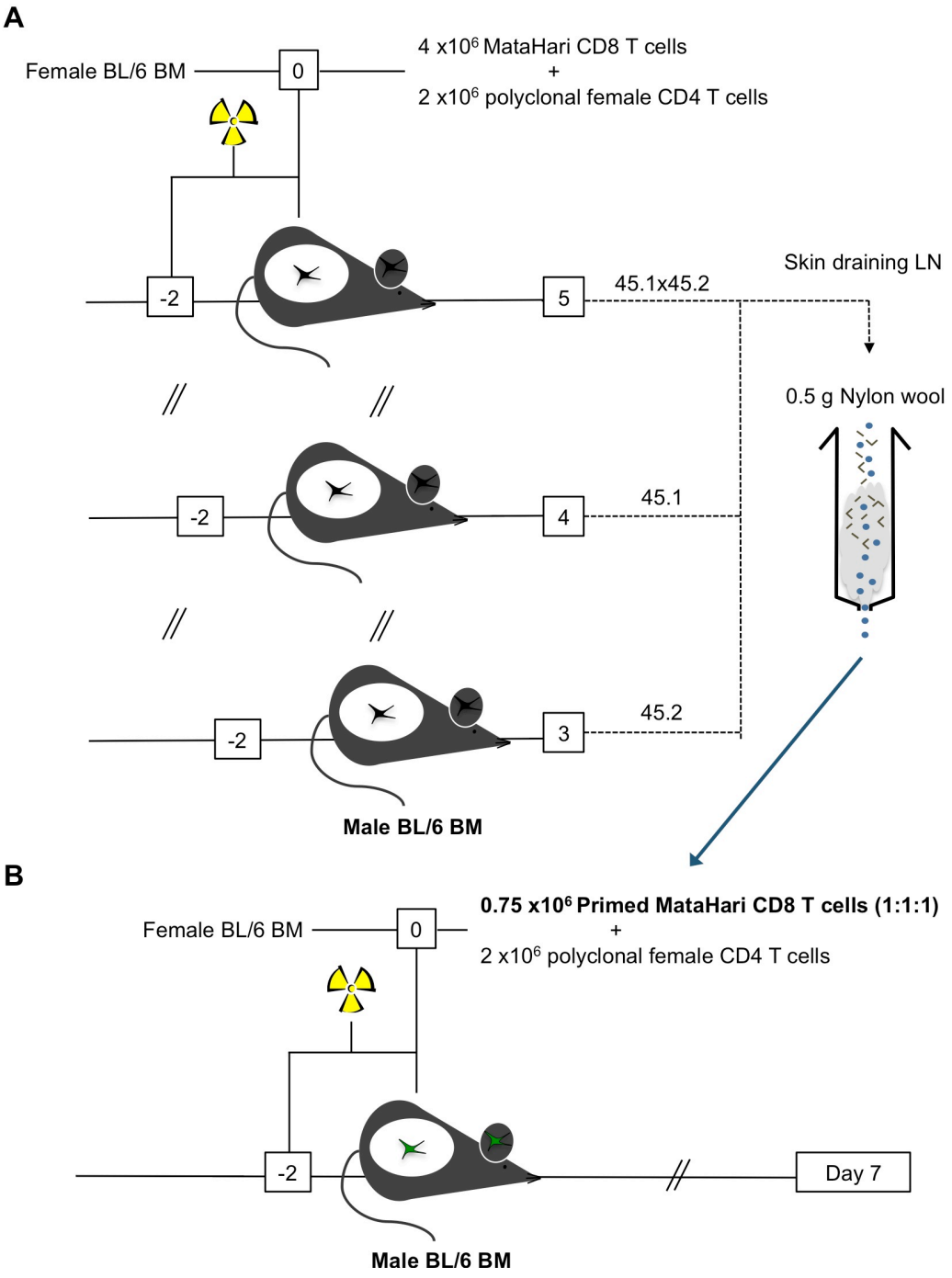

Figure 74: Initiating systemic GVHD using a combination of AEMTs. A. Three cohorts of male BL/6 mice were lethally irradiated with a split dose of 11 GY and reconstituted of 5 x10^6 BM and 2 x10^6 SC from a female BL/6 donor. 4 x10^6 MataHari T cells were also transplanted to initiate systemic GVHD. On days 3, 4 and 5 post transplant recipient male BL/6 mice were culled and the skin draining lymph nodes harvested. The skin draining lymph node cell suspension was then passed through 0.5 g nylon wool to enrich lymphocytes. **B.** Male BL/6 mice were lethally irradiated with a split dose of 11 GY and reconstituted with a mixture of 5 x10^6 bone marrow and 2 x10^6 CD4 T cells obtained from a female BL/6 donor. To initiate GVHD, 0.75 x10^6 AEMTs from BL/6 recipients culled 3, 4 and 5 days post transplant mixed at a ratio of 1:1:1 were also transplanted. This was possible as AEMTs from each time point could be separated based on their differential expression of the congenic markers CD45.1 and CD45.2.

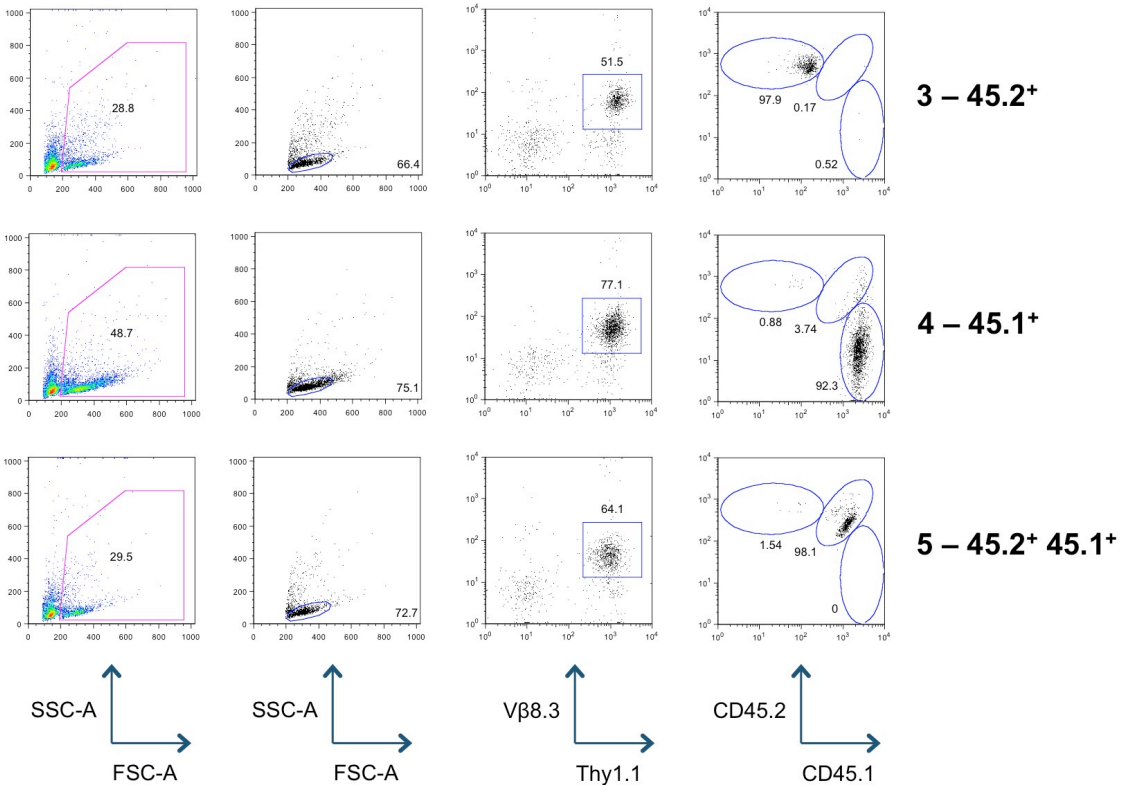

Figure 75: AEMTs from BL/6 recipients culled 3, 4 and 5 days post transplant could be identified based on their expression of the congenic markers CD45.1 and CD45.2. Dot plots from skin draining lymph node cell suspensions from BL/6 mice 3, 4 and 5 days post transplant that had been passed through nylon wool. After an initial anti-apoptotic gate, MataHari CD8 T cells were identified based on their expression of Vβ8.3, Thy1.1, CD45.1 and CD45.2. MataHari T cells from BL/6 recipients culled 3, 4 and 5 days post transplant based on their differential expression of the congenic markers CD45.1 and CD45.2.

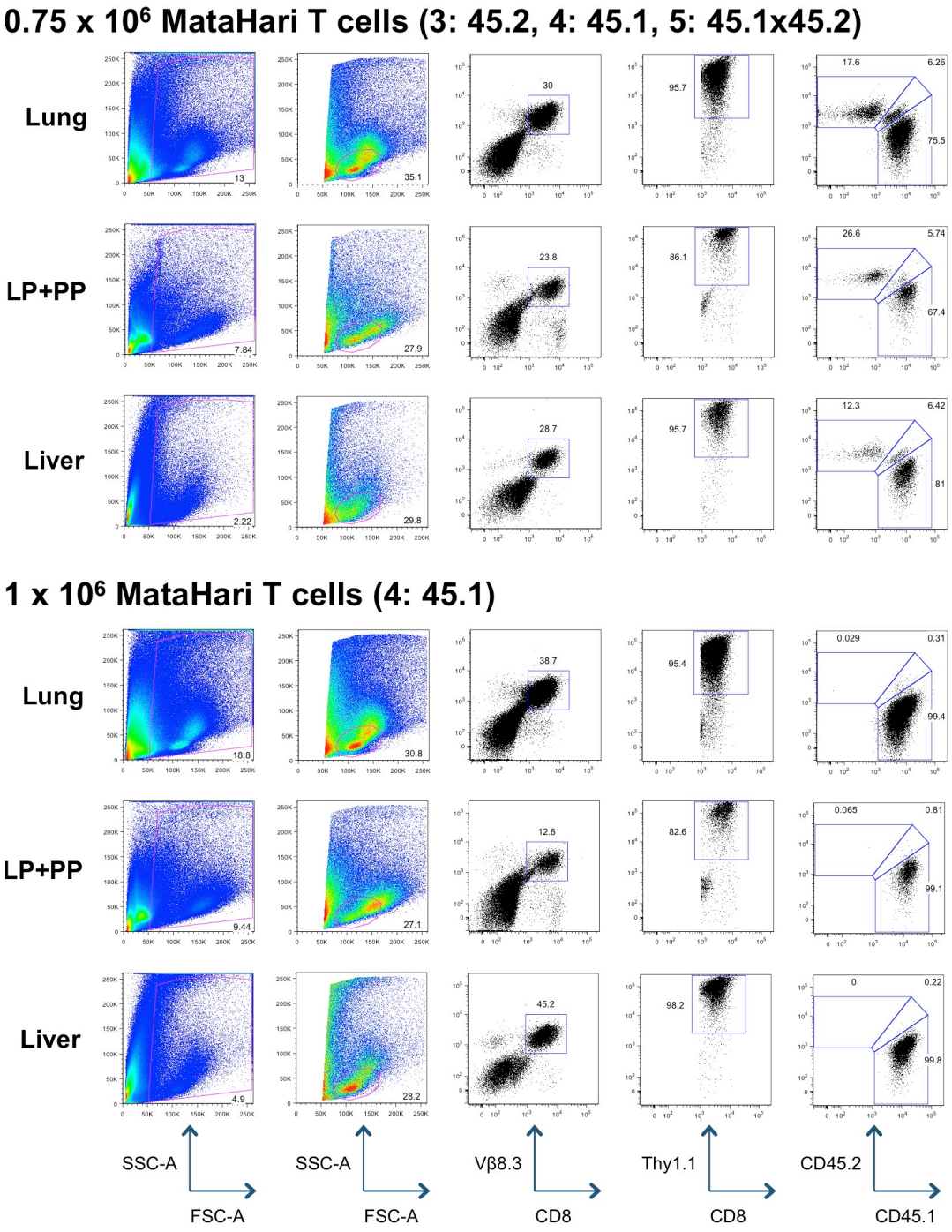

Figure 76: MataHari T cells exposed to antigen for 4 days accumulate in higher frequencies in GVHD target organs than MataHari T cells exposed to antigen for 3 and 5 days. Representative dot plots from the lung, LP+PP and liver from male BL/6 recipients culled 7 days after transplant with AEMTs. After an initial anti-apoptotic gate followed by a lymphocyte gate, samples were examined for the expression of Vβ8.3, Thy1.1, CD8, CD45.1 and CD45.2. *Top*- In BL/6 recipients that received 0.75 x 10^6 AEMTs, from BL/6 recipients culled 3, 4 and 5 days post transplant mixed at a 1:1:1 ratio, AEMTs exposed to antigen for 4 days accumulated in higher frequencies in the lung, LP+PP and liver than other AEMTs. *Bottom*- Another cohort of BL/6 recipients were transplanted with 1 x10^6 AEMTs exposed to antigen for 4 days. AEMTs from this time point and dose accumulated in the lung, LP+PP and liver.

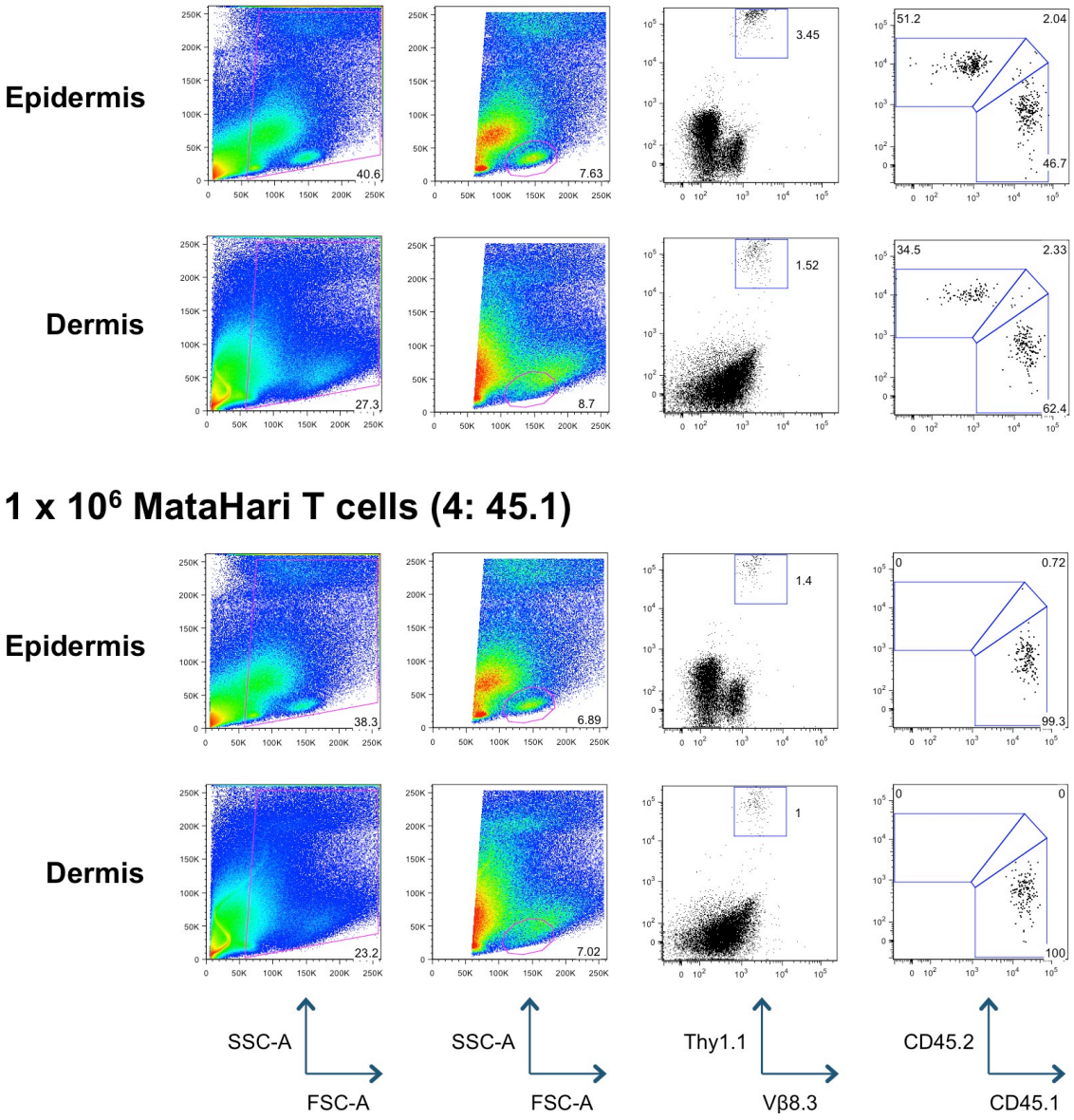

Figure 77: MataHari T cells exposed to antigen for 3 and 4 days accumulate in higher frequencies in the skin than MataHari T cells exposed to antigen for 5 days. Representative dot plots from the epidermis and dermis from male BL/6 recipients culled 7 days after transplant with AEMTs. After an initial anti-apoptotic gate followed by a lymphocyte gate, samples were examined for the expression of Vβ8.3, Thy1.1, CD45.1 and CD45.2. *Top*- In BL/6 recipients that received 0.75 x 10^6 AEMTs, from BL/6 recipients culled 3, 4 and 5 days post transplant mixed at a 1:1:1 ratio, AEMTs exposed to antigen for 3 and 4 days accumulated in higher frequencies in epidermis and dermis than AEMTs exposed to antigen for 5 days. *Bottom*- In BL/6 recipients transplanted with 1 x10^6 AEMTs exposed to antigen for 4 days, AEMTs accumulated in the both the epidermis and dermis.

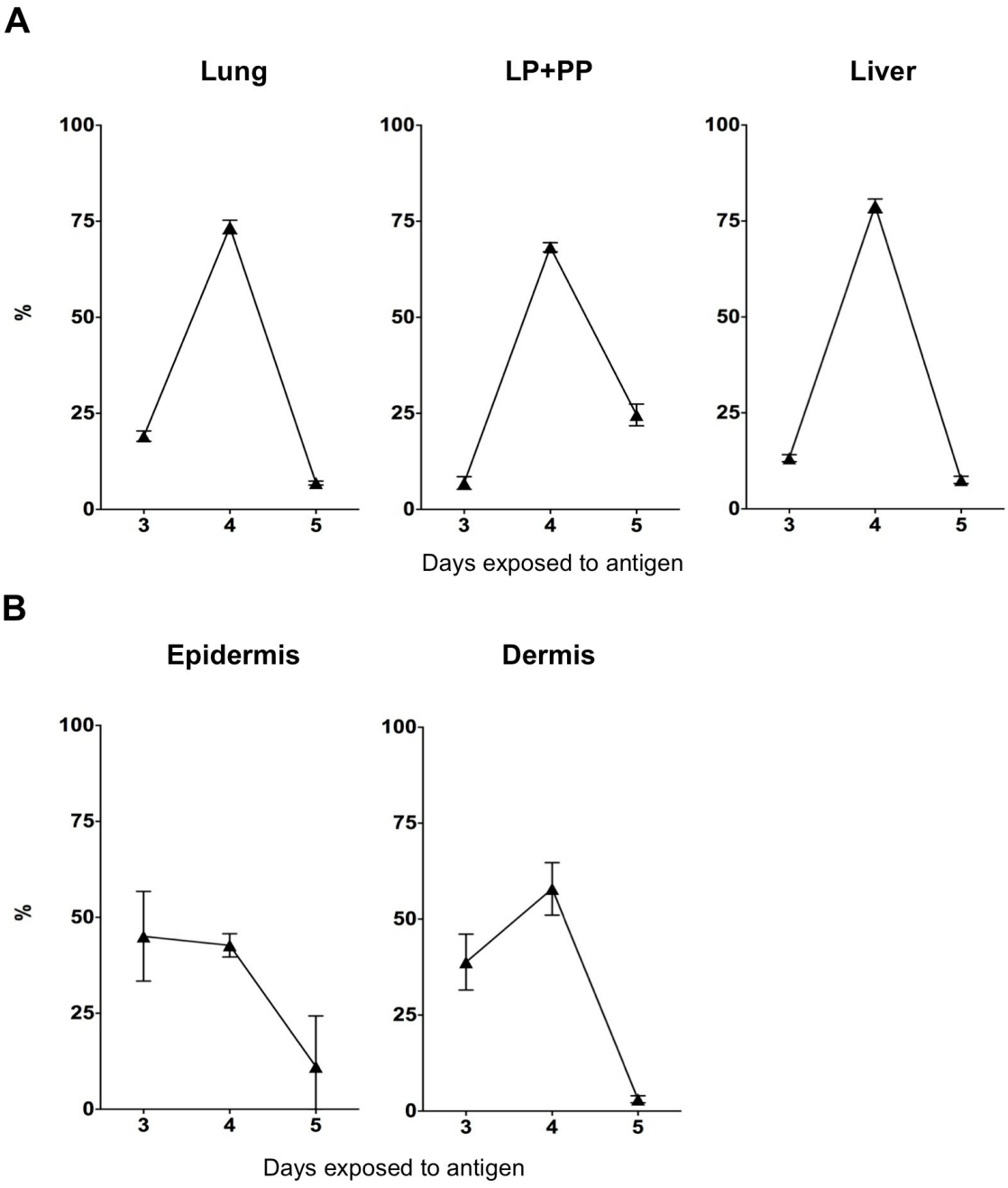

Figure 78: In contrast to other GVHD target organs, MataHari T cells exposed to antigen for 3 days accumulate in high frequencies in the skin. Summary data showing the accumulation of Vβ8.3$^+$ Thy1.1$^+$ MataHari T cells exposed to antigen for 3, 4 and 5 days as a percentage of the total MataHari T cells gated in BL/6 recipients culled after 7 days (n=3, data representative of one experiment, horizontal lines represent the mean ±SD). **A.** In the liver, LP+PP and liver, when MataHari T cells exposed to antigen for 3, 4 and 5 days were mixed together and transplanted into male BL/6 recipients, AEMTs exposed to antigen for 4 days accumulated at the highest frequencies. **B.** In the skin, AEMTs exposed to antigen for 3 and 4 days accumulated in the skin at similar frequencies with AEMTs exposed to antigen for 5 days accumulating at much lower frequencies.

5.2 The localised depletion of Langerhans cells reduced cutaneous GVHD

5.2.1.1 Injecting 50 ng i.d. is sufficient to locally deplete LC in Langerin-DTR mice

Previous experiments to determine whether host LC *in situ* are required for cutaneous GVHD had focused on either changing the site of T cell injection (intravenous → skin) or phenotype of the donor alloreactive T cells (naïve → primed) themselves. Focusing on the skin itself, a new experimental approach was developed where DT was injected directly into the skin of Langerin-DTR mice to locally deplete LC *in situ*.

To locally deplete LC, male Langerin-DTR mice were injected with 25 ng of DT in 20 μl i.d. into the dorsal and ventral side of the left ear (Figure 79, A). The right ear remained untreated and acted as an internal control. The mice were then allowed to recover for 9 days before being transplanted with naive Mh T cells to initiate GVHD in accordance with the model developed in the previous chapter (Figure 79, B). This allowed Langerin$^+$ dDC but not LC to recover in recipients before transplant[275].

The injection of 50 ng of DT was sufficient to locally deplete LC in Langerin-DTR mice. After an initial anti-apoptotic gate followed by a DC gate, host LC were characterised as being GFP$^+$, MHCII$^+$, CD45.2$^+$, CD207$^+$ and CD11b$^+$ (Figure 80). Host LC were depleted in the left ears (treated) but not the right ears (untreated) of Langerin-DTR recipients that received DT 7 days after transplant (Figure 80). There were significantly more host LC in the right ears compared to the left ears of DT treated Langerin-DTR recipients (Figure 81). Localised LC depletion was also confirmed in epidermal sheets stained with MHCII, where LC were depleted in the left but not the right ear in mice that received DT 9 days earlier (Figure 79A). The i.d. injection of PBS in controls had no effect on the frequency of LC in the epidermis (Figure 80). However, there was a significant reduction in the frequency of host LC in the right ears of mice treated with DT versus PBS controls indicating some systemic depletion associated with DT (Figure 81).

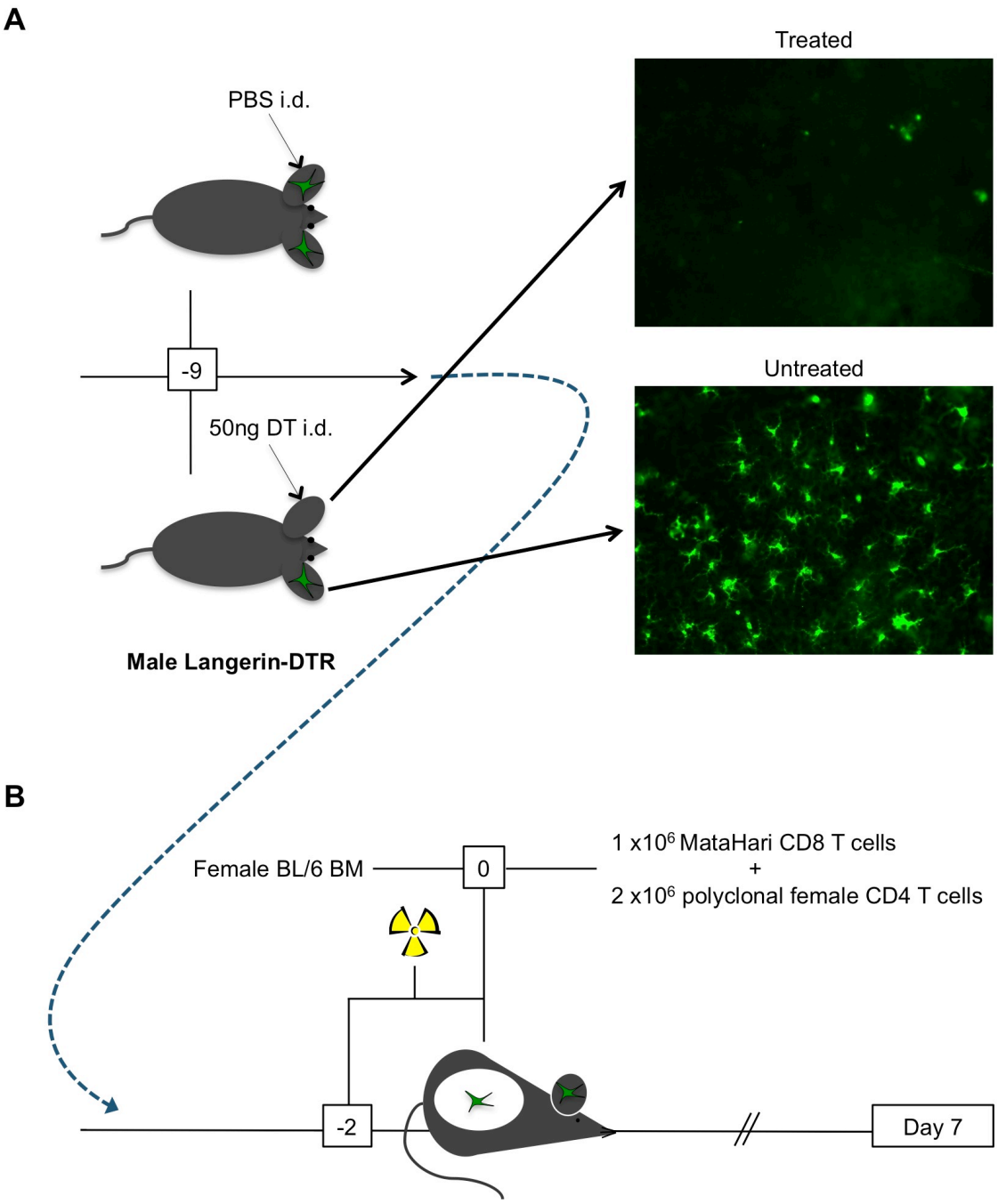

Figure 79: Depleting Langerhans cells *in situ* in the MataHari minor H mismatch model of acute GVHD. A. *Left*- Male Langerin-DTR mice were injected i.d. with either 50 ng of DT or PBS in the left ear 9 days before transplant. This was sufficient to locally deplete LC in that ear. *Right*- Fluorescent images of the epidermis taken from the left and right ear of a Langerin-DTR mouse treated i.d. with DT 9 days earlier. LC were visualised staining MHCII with Alexa Fluor 488. Images obtained at x20 magnification on a Zeiss Axio Scope A1 fluorescence microscope. In the left ear (DT treated), $MHCII^+$ LC were depleted. However, in the right ear (untreated), a dense interlacing network of LC was observed. **B.** Male Langerin-DTR mice, which were treated with DT or PBS i.d., are irradiated with a split dose of 11 GY and transplanted with a mixture of 5 $x10^6$ BM and 2 $x10^6$ CD4 T cells from a female BL/6 donor and 1 $x10^6$ MataHari CD8 T cells.

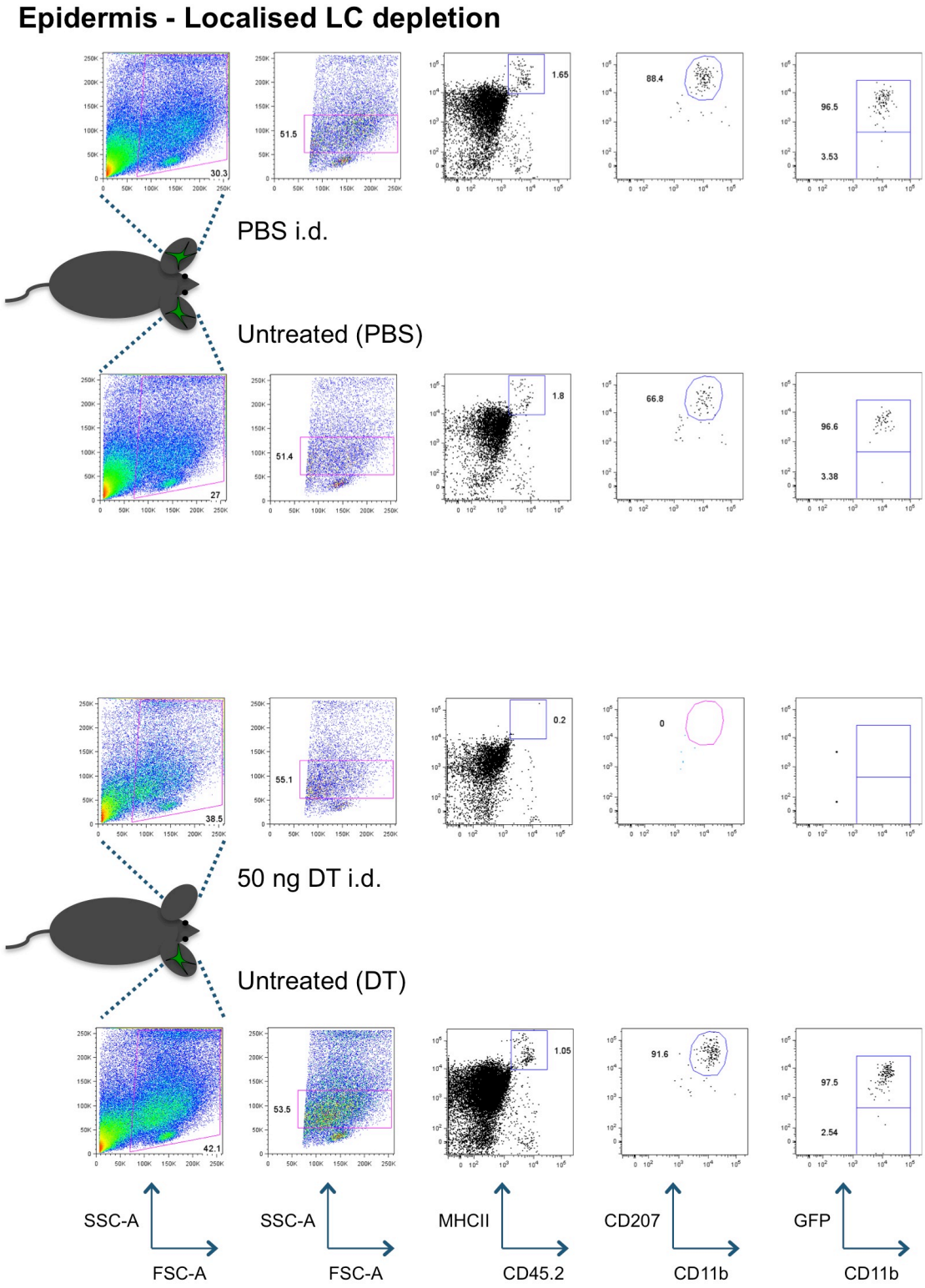

Figure 80: The injection of DT but not PBS i.d. is sufficient to locally deplete Langerhans cells in Langerin-DTR mice. Representative dot plots of the epidermis from Langerin-DTR mice that received 50 ng of DT or PBS i.d. 16 days previously. After an initial live gate followed by a DC gate, host LC were identified based on their expression of MHCII, CD45.2, CD207, CD11b and GFP. *Top*- The injection of PBS i.d. into the left ear of Langerin-DTR mice had no effect on LC. *Bottom*- The injection of 50 ng of DT i.d. into the left ear of Langerin-DTR mice was sufficient to locally deplete LC; LC remained in the untreated right ear.

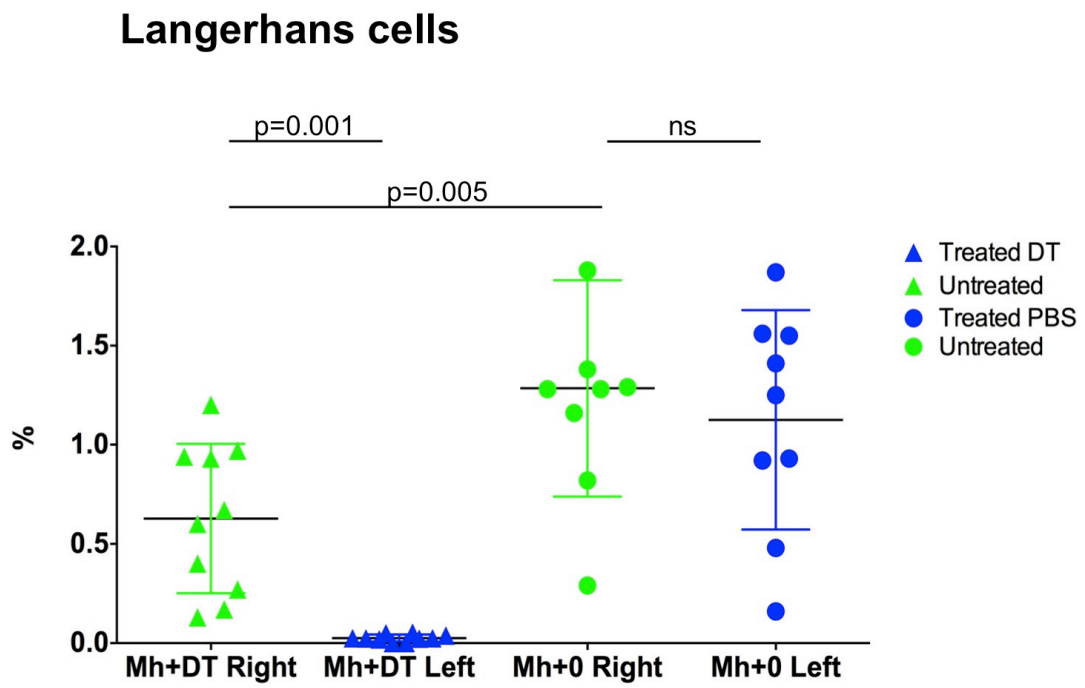

Figure 81: 50 ng of DT injected i.d. is sufficient to locally deplete Langerhans cells in Langerin-DTR mice. Summary data showing the frequency of host LC in the epidermis as a percentage of the initial DC gate based on FSC-A, SSC-A 7 days after transplant (n=9-10, data pooled from 4 independent experiments, analysed using a Mann-Whitney test, the mean ±SD is indicated by the horizontal bars.). In Langerin-DTR recipients treated with DT i.d. in the left ear, host LC were significantly depleted in the left (treated) versus the right (untreated) ear. In Langerin-DTR recipients treated with PBS i.d. in the left ear, there was no difference in the frequency of host LC between the left (treated) and right (untreated) ears. However, there was a significant reduction in the frequency of host LC in the right ears (untreated) of recipients that received DT versus PBS controls.

5.2.2 Localised depletion of LC had no effect on the systemic expansion of MataHari T cells

The Langerin-DTR recipients were culled 7 days after transplant. In the spleen, after an initial anti-apoptotic gate followed by a lymphocyte gate, Mh CD8 T cells were again identified by their expression of the TCR Vβ8.3 and congenic marker Thy1.1 (Figure 82, A). In addition, Mh T cells were also analysed for their expression of the T cell memory markers CD44 and CD62L (Figure 82, A).

The localised depletion of host LC had no significant effect on either the expansion or activation profile of Mh T cells in the spleen. The absolute number and frequency of effector Mh T cells ($CD44^{high}$ $CD62L^{low}$) was similar in the presence or absence of host LC in the left ear (Figure 82, B).

In the skin draining lymph nodes, a similar pattern was observed. Adopting a similar gating strategy used to analyse the spleen (Figure 83, A), the localised depletion of host LC had no effect on either the absolute number or frequency of effector Mh T cells ($CD44^{high}$ $CD62L^{low}$) in the skin draining lymph nodes (Figure 83, B).

Taken together, these data shows that the localised depletion of host LC had no effect on the systemic expansion and activation of Mh T cells. This corresponds with the data from the systemic depletion of host LC in the previous chapter.

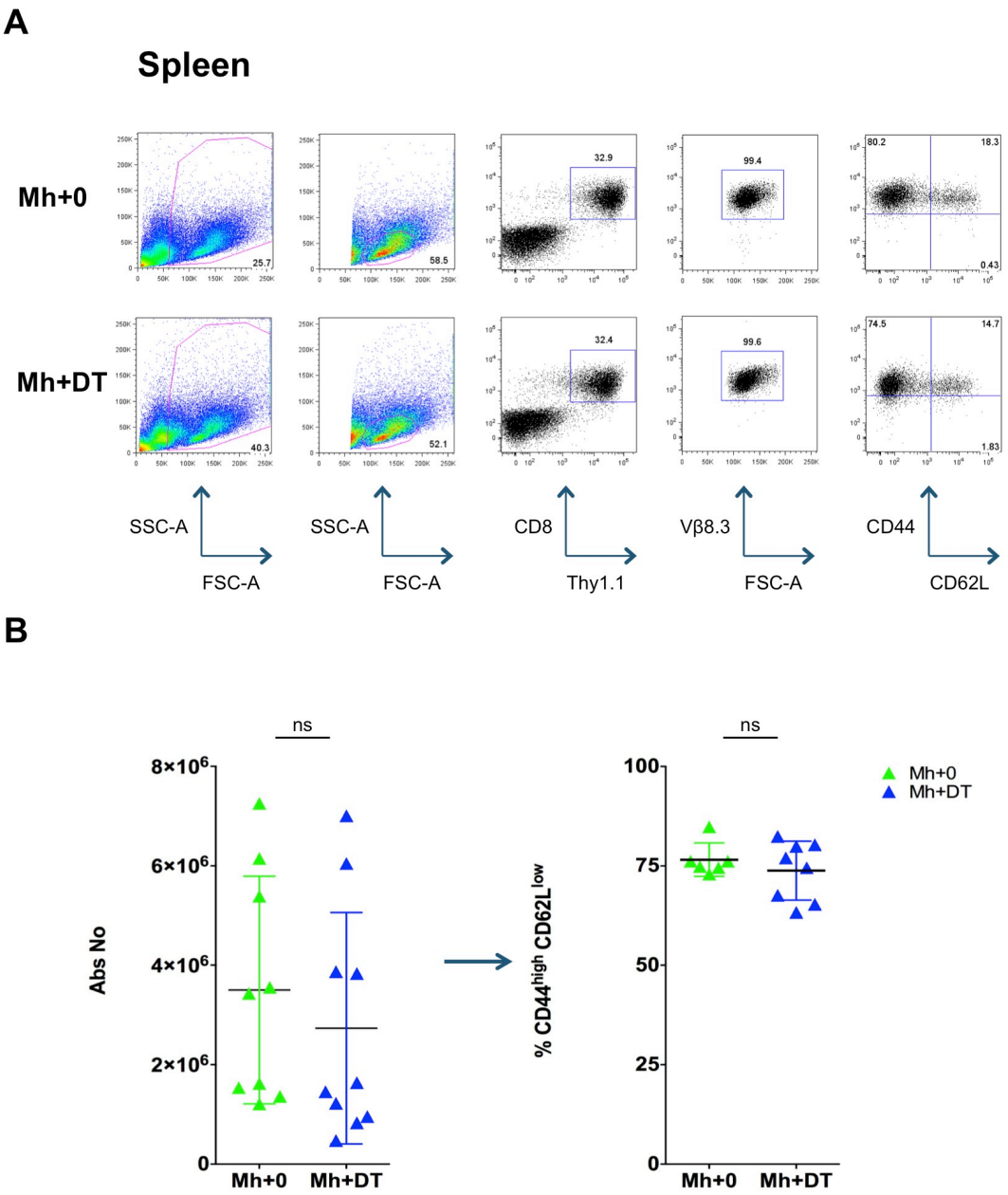

Figure 82: The localised depletion of host Langerhans cells had no effect on the expansion and activation of MataHari T cells in the spleen. A. Representative dot plots of splenocytes taken from Langerin-DTR recipients, treated with either DT or PBS i.d., 7 days after transplant. After an initial anti-apoptotic gate followed by a lymphocyte gate, MataHari T cells were identified based on their expression of Vβ8.3, Thy1.1 and CD8. **B.** *Left*- Summary data showing the absolute number of donor Vβ8.3^{+} Thy1.1^{+} MataHari T cells in the spleen (n=9-10, data pooled from 4 independent experiments, analysed using a Mann-Whitney test, the mean ±SD is indicated by the horizontal bars.). There was no difference in the expansion of donor MataHari T cells when host LC were depleted *in situ*. *Right*- Summary data showing the percentage of donor Vβ8.3+ Thy1.1^{+} MataHari T cells that are CD44^{high} CD62L^{low} (n=9-10, data pooled from 4 independent experiments, analysed using a Mann-Whitney test, the mean ±SD is indicated by the horizontal bars.). There was no difference in the activation profile of donor MataHari T cells when host LC were depleted *in situ*.

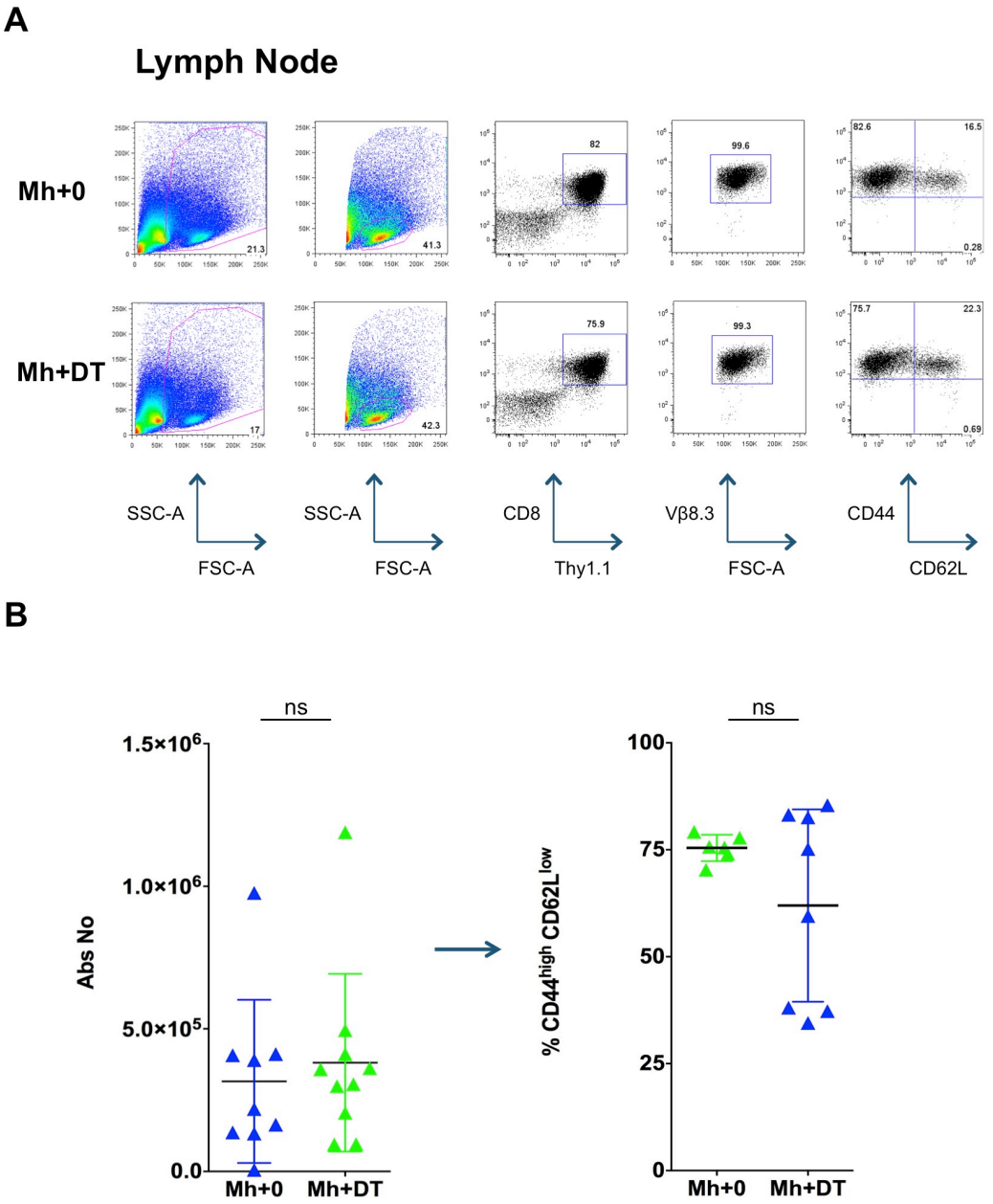

Figure 83: The localised depletion of host Langerhans cells had no effect on the expansion and activation of MataHari T cells in the skin draining lymph nodes. A. Representative dot plots of skin draining LN samples taken from Langerin-DTR recipients, treated with either DT or PBS i.d., 7 days after transplant. After an initial anti-apoptotic gate followed by a lymphocyte gate, MataHari T cells were identified based on their expression of Vβ8.3, Thy1.1 and CD8. **B.** *Left*- Summary data showing the absolute number of donor Vβ8.3^{+} Thy1.1^{+} MataHari T cells in the skin draining LN (n=9-10, data pooled from 4 independent experiments, analysed using a Mann-Whitney test, the mean ±SD is indicated by the horizontal bars.). There was no difference in the expansion of donor MataHari T cells when host LC were depleted *in situ*. *Right*- Summary data showing the percentage of donor Vβ8.3^{+} Thy1.1^{+} MataHari T cells that are CD44^{high} CD62L^{low} (n=9-10, data pooled from 4 independent experiments, analysed using a Mann-Whitney test, the mean ±SD is indicated by the horizontal bars.). There was no difference in the activation profile of donor MataHari T cells when host LC were depleted *in situ*.

5.2.3 Host LC are required *in situ* for CD8-mediated GVHD

In accordance with previous findings, Mh T cells were found to have accumulated in the skin 7 days after transplant. After an initial anti-apoptotic cell gate followed by a lymphocyte gate, Mh T cells were identified based on their expression of Vβ8.3, Thy1.1, and the congenic markers CD45.1 and CD45.2 (Figure 84).

The localised depletion of host LC in the left ear had a significant effect on the ability of Mh T cells to accumulate in the skin (Figure 84). There was a significant reduction in the frequency of Mh T cells in the epidermis between the left (treated) and right (untreated) ears of DT treated Langerin-DTR recipients (Figure 85). In PBS treated controls, there was no difference in the accumulation of Mh T cells in the epidermis between the left and right ears of recipients (Figure 85). However, there was a significant reduction in the frequency of Mh T cells in the epidermis of the right ears of DT versus PBS mice (Figure 85).

These data, in parallel with the data from the systemic depletion of host LC in the previous chapter, shows that host LC are in fact required *in situ* in the skin for cutaneous GVHD.

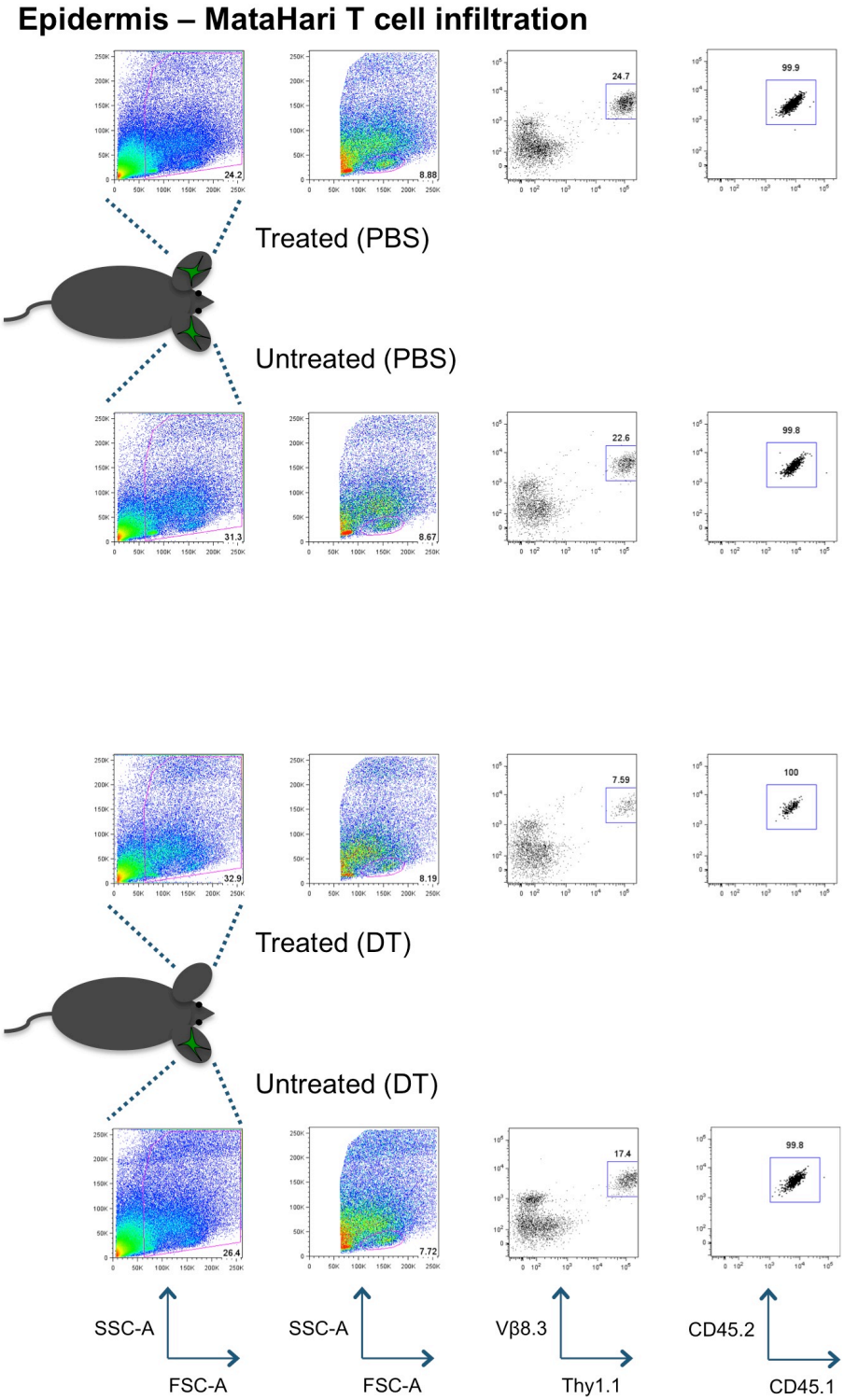

Figure 84: When Langerhans cells are depleted *in situ*, the accumulation of donor MataHari T cells is reduced. Representative dot plots of the epidermis from Langerin-DTR mice 7 days after transplant. After an initial anti-apoptotic gate followed by a lymphocyte gate, donor MataHari T cells were identified based on their expression of Vβ8.3, Thy1.1, CD45.1 and CD45.2. *Top*- There was no difference in the accumulation of donor MataHari T cells in the epidermis of Langerin-DTR recipients treated with PBS. *Bottom*- In the absence of host LC in the left ear, there was a reduction in the accumulation of donor MataHari T cells between the left and right ear of the same recipient.

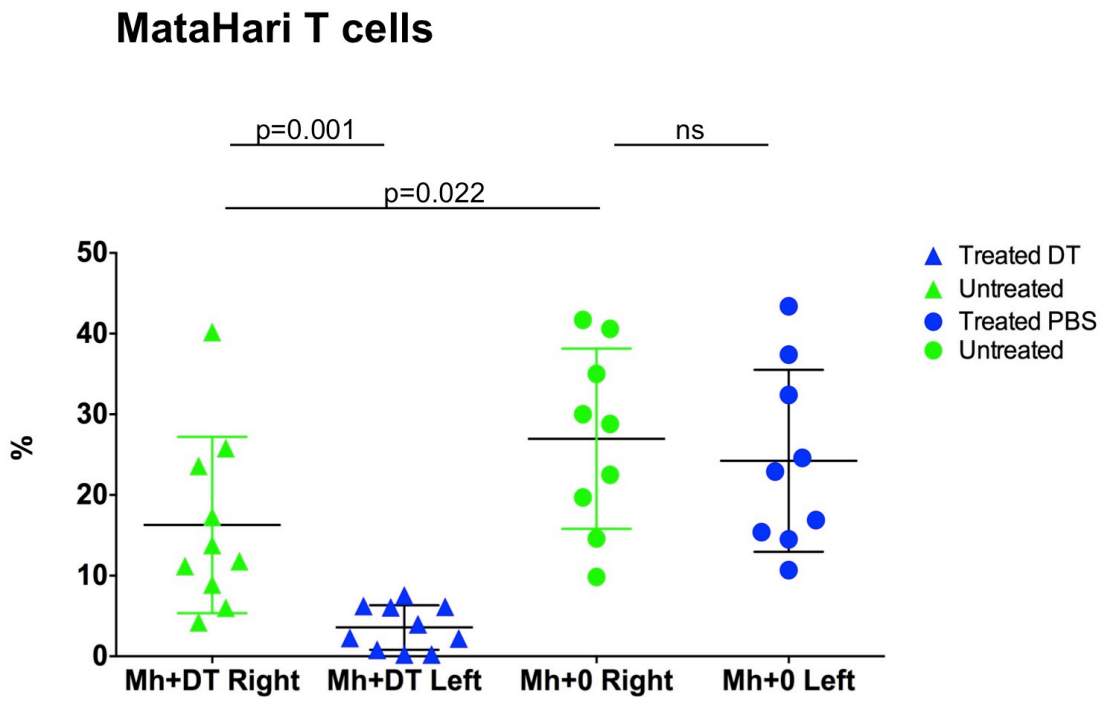

Figure 85: Host Langerhans cells are required *in situ* for cutaneous GVHD. Summary data showing the accumulation of donor Vβ8.3^{+} Thy1.1^{+} MataHari T cells in the epidermis as a percentage of the initial lymphocyte gate based on FSC-A, SSC-A (n=9-10, data pooled from 4 independent experiments, analysed using a Mann-Whitney test, the mean ±SD is indicated by the horizontal bars.). In Langerin-DTR recipients treated with DT, there was a significant reduction in the accumulation of donor MataHari T cells in the left (treated) versus the right (untreated) ear. In PBS controls, there was no difference in the accumulation of donor MataHari T cells between the left (treated) and right (untreated) ears. However, there was a significant reduction in the accumulation of donor MataHari T cells in the right ears (untreated) of recipients that received DT versus PBS controls.

5.3 Gene expression analysis of MataHari T cells and Langerhans cells

5.3.1 Host LC are required for full effector function and proliferation of MataHari T cells in the epidermis

To investigate whether there was functional difference between Mh T cells in the skin of mice depleted of host Langerin$^+$ DC versus controls, Vβ8.3$^+$ Thy1.1$^+$ Mh T cells were sorted by fluorescence-activated cell sorting (FACS) from the epidermis and dermis of Langerin-DTR recipients 7 days after transplant.

This proved technically challenging with the number of Vβ8.3$^+$ Thy1.1$^+$ Mh T cells sorted from the epidermis (Mh+0: median 2.3 x10^3, range 0.4-5.7 x10^3; Mh+DT: median 0.9 x10^3, range 0.4-1.5 x10^6) and dermis (Mh+0: median 3 x10^3, range 1.5-3.8 x10^3; Mh+DT: median 2 x10^3, range 1.4-3.1 x10^3) were very low and not appropriate to directly evaluate protein expression or direct CTL function *in vitro*. Instead, Mh T cells were sorted directly into RLT lysis buffer containing 1μM β-mercaptoethanol (to denature RNases) and the mRNA isolated for quantitative PCR of molecules associated with effector CTL function. A full list of the molecules analysed is outlined in the Materials and Methods.

To deplete host Langerin$^+$ DC (LC and Langerin$^+$ dDC), Langerin-DTR recipients were treated with 400 ng of DT i.p. on day's -1, 2, 4 and 7 post-transplant. In parallel, male Langerin-DTR were treated with a similar volume of PBS i.p. as a control. Before each sort, the depletion of host LC was verified by flow cytometry (Figure 86, A). Mh T cells were sorted using the following gating strategy. Firstly, after an anti-apoptotic gate, doublets were eliminated based on FSC-W and FSC-A. Then a very broad lymphocyte gate was taken and Mh cells sorted based on their expression of Vβ8.3 and Thy1.1 (Figure 86, B). This resulted in sort purity ≥95%, when cells were sorted into FACS buffer instead of lysis buffer and checked via flow cytometry (Figure 86, B).

As shown in Figure 87, Mh T cells in the epidermis showed a significant reduction in the expression of mRNA transcripts for a number of key effector molecules including IFN-γ, TNF-α, Granzyme B, TRAIL and the pro-survival molecule Bcl-xL in the absence of host Langerin$^+$ DC. Attempts to stain Mh T cells in the epidermis with antibodies for some of the molecules was not pursued as the number of events was very small.

A similar pattern was not observed in the dermis. There was no significant difference in the expression of any mRNA transcript investigated by Mh T cells in the dermis in the absence of host Langerin$^+$ DC (Figure 87). These data, along with the reduction in the accumulation of Mh T cells in by day 7, suggests that there is a significant reduction in the function of Mh T cells in the absence host Langerin$^+$ DC.

To further characterise the reduction in effector function of Mh T cells in the epidermis, a whole-transcriptome microarray analysis was carried out on Mh T cells when host LC, but not Langerin$^+$ dDC, were depleted. To deplete host LC, male Langerin-DTR recipients were treated with 400 ng of DT i.p. 20 days before transplant as described in the previous chapter. In parallel, male Langerin-DTR were treated with PBS i.p. as a control.

Vβ8.3$^+$ Thy1.1$^+$ Mh T cells were sorted by FACS directly into RLT lysis buffer containing 1μM β-mercaptoethanol from the epidermis and skin draining lymph nodes of Langerin-DTR recipients 7 days after transplant using the same gating strategy described before (Figure 86, B). For the epidermis, the samples from different recipients were pooled if necessary so that a minimum of 5 x10^3 Mh T cells was collected per biological replicate with sort purity ≥95%. For the skin draining lymph node, a minimum of 100 x10^3 Mh T cells was collected per biological replicate with sort purity ≥90%. The RNA was then purified and amplified for whole-transcriptome microarray analysis using the Affymetrix GeneChip Mouse Gene 2.0 ST Array. The microarray dataset was kindly analysed by Dr Pedro Sousa in our lab using the

Affymetrix Expression Console Software (v1.3.1.187), applying the RMA algorithm for probe-level normalisation and background correction.

To initially explore any potential differences in the gene expression profile between Mh T cells in the skin draining lymph nodes and the epidermis, we used a PVCA. PVCA is a statistical technique that reduces the number of dimensions in a dataset in order to simplify the analysis. This is accomplished by performing covariance analysis between the factors which identifies directions (principal components) along which the variation in the dataset is maximal. This enables both a two- and three-dimensional scatter plot to be constructed that allows similarities or differences between datasets to be visualised, where each symbol represents the gene expression profile derived from T cells within a replicate.

The PVCA on Mh T cells derived from the skin draining lymph nodes and epidermis of PBS and DT treated Langerin-DTR recipients demonstrated a striking divergence in the transcriptional profile of Mh T cells between the skin draining lymph nodes and epidermis (Figure 88, A). Interestingly, the principal components of effector Mh T cells derived from the epidermis when host LC were both present (PBS controls) and absent (DT treated) differed significantly from Mh T cells in the skin draining lymph node. In addition, there was a divergence in the transcriptional profile between effector Mh T cells in the epidermis when host LC were present or absent, although they did not form a cluster. However, the depletion of host LC had no effect on the transcriptional profile of Mh T cells in the skin draining lymph nodes, with both populations clustering together according to principal components 1 and 2.

To investigate the change in the transcriptional profile between the skin draining lymph nodes and epidermis, a gene set enrichment analysis (GSEA) was performed between Mh T cells from the skin draining lymph nodes of control mice versus Mh T cells from the epidermis of control mice using the Molecular Signature Database Collection 2.

This was based on the assumption that by day 7 post-transplant, the majority of Mh T cells in the skin draining lymph nodes were primed. GSEA is an analytical technique that focuses on the change in gene expression at the level of gene sets between two biological states. These gene sets have been defined based on prior biological knowledge, obtained from studies published in the literature (e.g. co-expression of genes in certain disease states, the expression profile in an immune response to a particular pathogen). By detecting modest but coordinated changes in gene expression within a specified set of a related genes, variations in the activity of biologically significant pathways can be identified by GSEA that may otherwise be missed by focusing on a single gene that showed a 10-fold increase in expression.

Comparing the transcription profile of effector Mh T cells from the epidermis where host LC were present versus Mh T cells from the skin draining lymph node, 63 biological pathways were active in effector Mh T cells in the epidermis. The majority of these pathways were involved in the cell cycle, metabolism, transcription and signal transduction, indicating that effector Mh T cells are undergoing a proliferative burst in the epidermis (Figure 89). Remarkably, when the transcription profile of effector Mh T cells from the epidermis when host LC were depleted was compared to Mh T cells from the skin draining lymph node, all of the active biological pathways identified when host LC were present were lost, with the exception of one that is involved in T cell apoptosis (Figure 89).

Focusing on the skin, a heat map was generated from an unsupervised agglomerative clustering analysis of Mh T cells in the epidermis and revealed a noticeable difference in the expression of a number of genes in effector Mh T cells when host LC were depleted (Figure 88, B). A gene level differential expression analysis was then performed on Mh T cells in the epidermis in the presence versus the absence of host LC, using an absolute log fold change (LFC) $\geq \pm 2$ and an ANOVA p-value ≤ 0.05 as the chosen cut off. Following this analysis, 94 genes were upregulated and 16 genes were

downregulated in effector Mh T cells in the epidermis in the presence versus the absence of host LC (Table 8 and Table 9). Interestingly, a number of key T cell effector molecules were upregulated in the presence of host LC, including Granzyme C, IFN-γ, TNF and TNFSF14 (LIGHT). This corresponds with earlier findings from initial qPCR experiments. Thus, in the absence of host LC, there is a significant reduction in the effector function of Mh T cells in the epidermis.

In addition, the majority of genes that were upregulated in Mh T cells in the presence of host LC were indicative of pathway that favours proliferation (e.g. transcription, translation, cell cycle, signal transduction), with genes such as the transcription factor *Myc* and serine/threonine protein kinase *Plk2* being significantly upregulated.

The transcriptional profile of Mh T cells in the epidermis in the presence versus the absence of host LC was further scrutinised using a GSEA. 220 biological pathways were upregulated in Mh T cells in the presence of host LC. Interestingly, 14 out of the top 20 of these pathways, as determined by their FDR p-value, were involved the cell cycle (Table 10). Pathways related to the effector T cells response were also found to be upregulated in the presence of host LC. Taken together, the depletion of host LC has a significant effect on both the effector function and proliferation of effector Mh T cells in the epidermis.

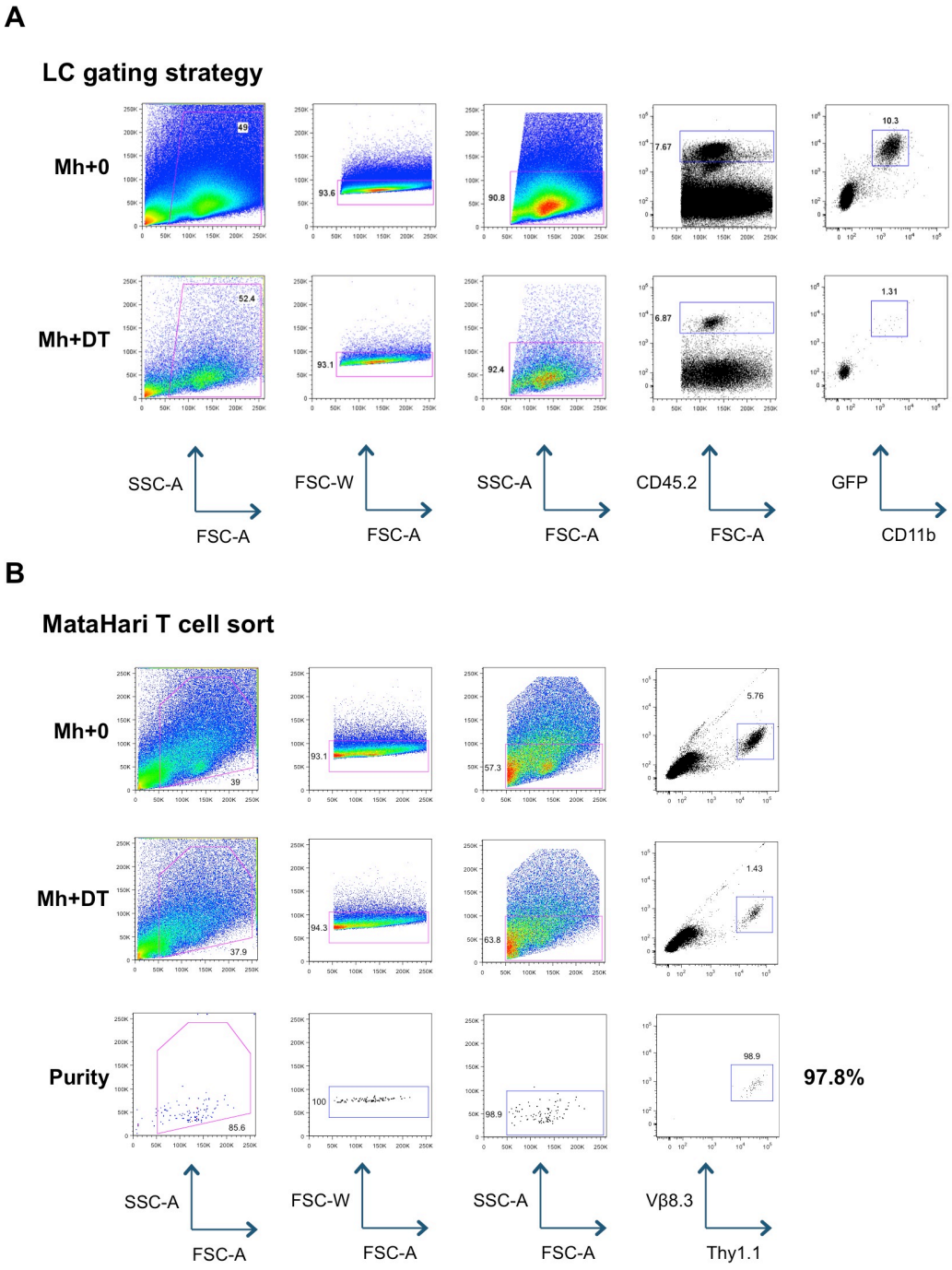

Figure 86: Gating strategy used to sort LC and Mh T cells through flow cytometry. A. Representative dot plots of the epidermis from Langerin-DTR recipients 7 days after transplant. After an initial live cell gate followed by a FSC-W, FSC-A gate, to eliminate doublets, and a lymphocyte/DC gate, host LC cells were identified based on their expression of CD45.2, CD11b and GFP. LC were efficiently depleted in DT treated recipients 7 days after transplant. When sorts were performed using BL/6 recipients, CD24 was used instead of GFP. **B.** Representative dot plots of the epidermis from Langerin-DTR recipients 7 days after transplant. After an initial live cell gate doublets were eliminated based on a FSC-W, FSC-A gate. A broad lymphocyte gate was then gated and Mh T cells were sorted within this based on their expression of Vβ8.3 and Thy1.1. The purity of Mh T cells sorted remained >90%.

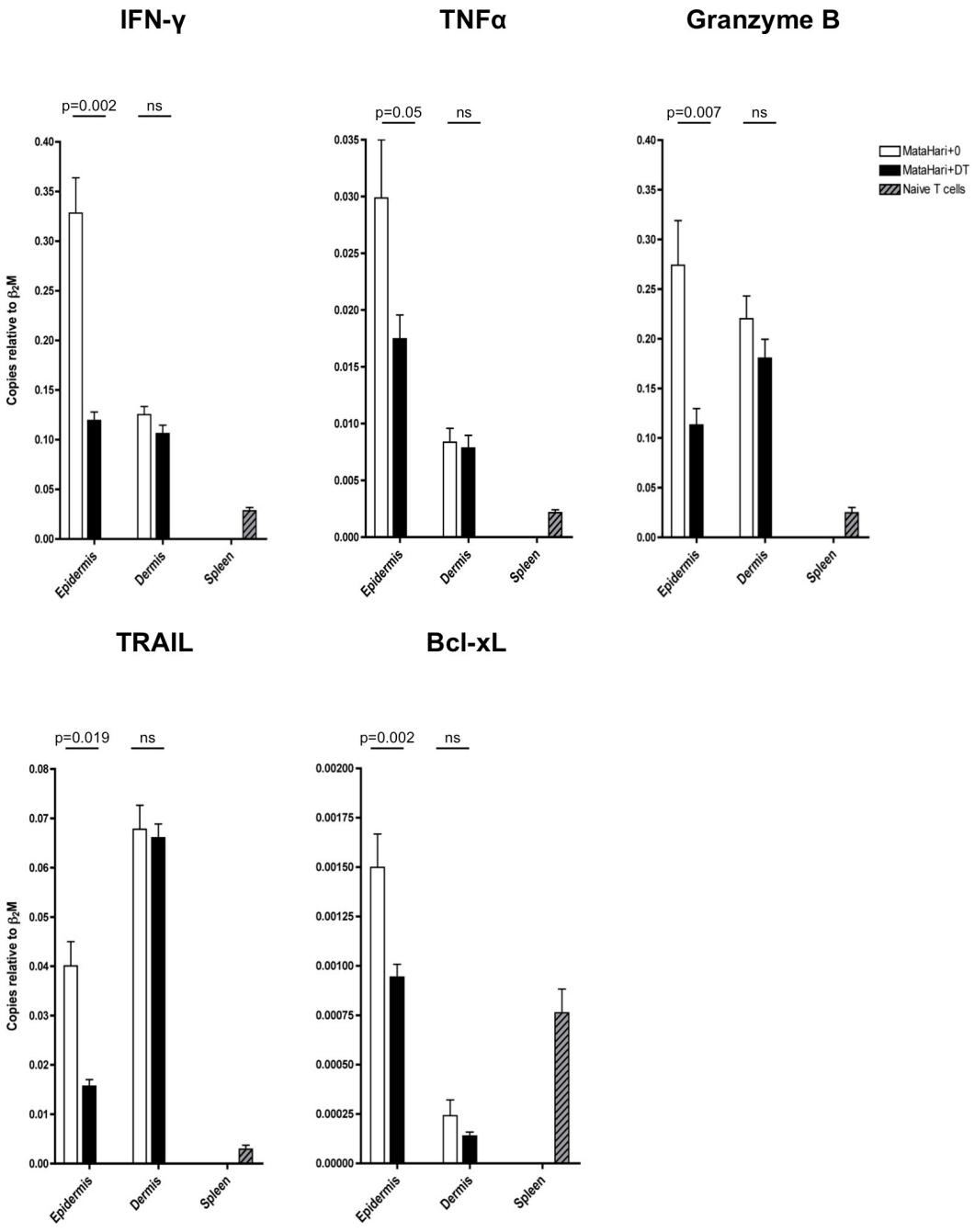

Figure 87: In the absence of host Langerin$^+$ DC, MataHari T cells reduced their expression of a number of key effector molecules in the epidermis. Graphs represent the mean±SD mRNA quantification for each transcript relative to β_2M from Vβ8.3$^+$ Thy1.1$^+$ Mh T cells flow sorted from the epidermis and dermis from Langerin-DTR recipients treated with either DT or PBS 7 days after transplant. Mh T cells from the spleen were from naïve MataHari mice and acted as a control (n=4-6, data pooled from 2 independent experiments, data analysed using a Mann-Whitney test). In the epidermis, Mh T cells significantly reduced their expression of IFN-γ, TNF-α, Granzyme B, TRAIL and the pro-survival molecule Bcl-xL in the absence of host Langerin$^+$ DC. In the dermis, there was no difference in the expression of these transcripts by Mh T cells.

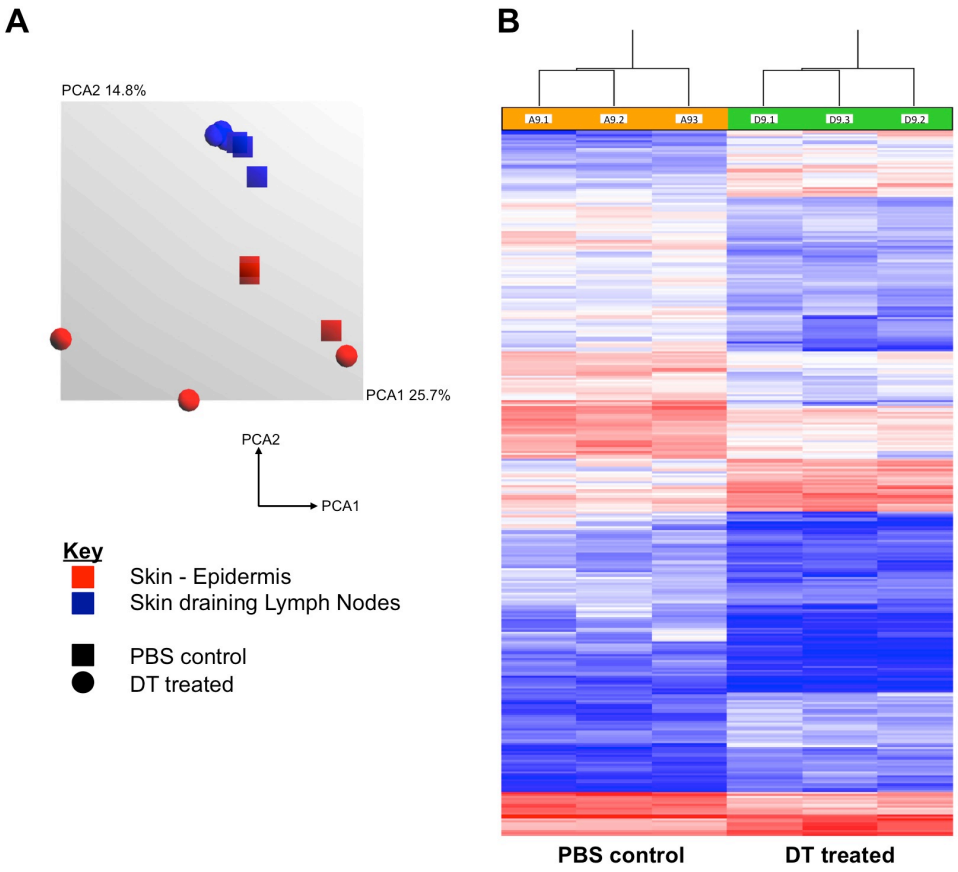

Figure 88: The depletion of host Langerhans cells significantly alters the transcriptional profile of MataHari T cells that infiltrate the epidermis. A. PVCA of microarray data plotting the transcriptional profile of Mh T cells derived from the epidermis and skin draining lymph nodes from host LC depleted (DT treated) recipients *versus* the control (PBS). The gene expression profile was determined using the Affymetrix GeneChip 2.0 Mouse Gene 2.0 ST Array. **B.** Heat map depicting the unsupervised agglomerative hierarchical clustering analysis of Mh T cells from the epidermis of host LC depleted (DT treated) and control (PBS) recipients (Each biological replicate represents pooled RNA, n=3-10 from 1-2 independent experiments).

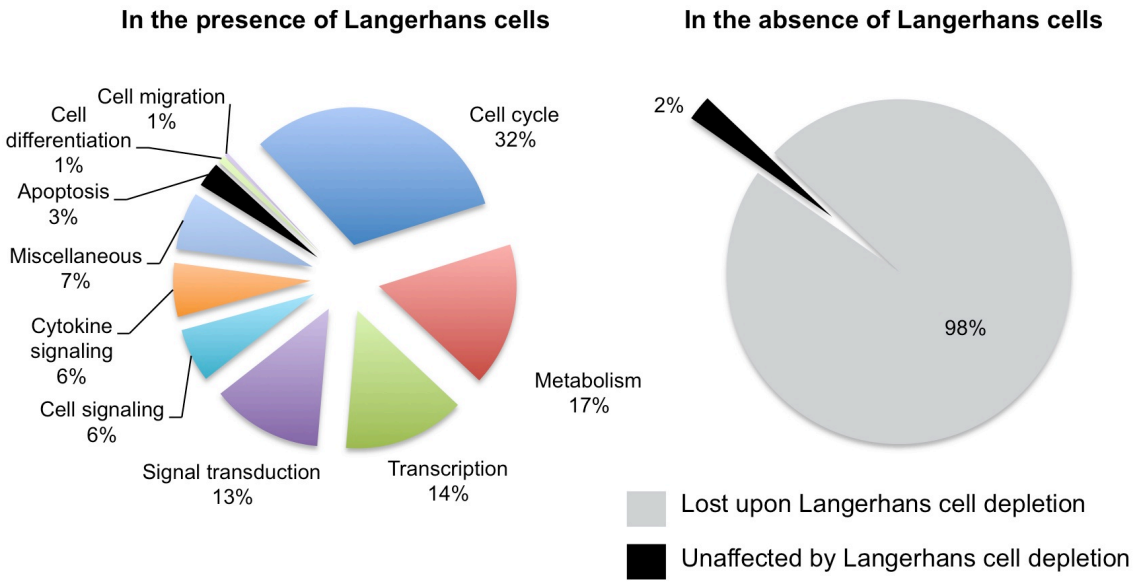

Figure 89: In the absence of host Langerhans cells the majority of biological pathways upregulated by effector MataHari T cells in the epidermis are lost. GSEA comparing Mh T cells from the skin draining lymph nodes to those derived from the epidermis in the presence or absence of host LC (Molecular Signatures Database Collection 2 – Canonical Pathways; FDR p-value ≤ 0.25). This led to the identification of 63 biological pathways that are active in Mh T cells in the presence of host LC. Remarkably, all but one of these biological pathways are lost in the absence of host LC.

Genes over-expressed in Mh T cells from the epidermis in PBS vs DT treated recipients		
Gene	**Description**	**LFC**
Cytokine/Chemokine		
Gzmc	Granzyme C	3.00
Tnf	Tumor necrosis factor	2.75
Ifng	Interferon gamma	2.38
Tnfsf14	Tumor necrosis factor (ligand) superfamily, member 14 (Light)	2.11
Transcription regulation		
Mir467f	microRNA 467f	13.47
Mir1927	microRNA 1927	9.73
Mir3096	microRNA 3096	5.17
Znhit6	Zinc finger, HIT type 6	4.18
Nolc1	Zinc finger protein 119b	3.35
Taf1d	TATA box binding protein (Tbp)-associated factor	3.04
Snhg3	Small nucleolar RNA host gene 3	2.93
Zbtb41	Zinc finger and BTB domain containing 41 homolog	2.53
Polr1a	Polymerase (RNA) I polypeptide A	2.51
Ttll4	Tubulin tyrosine ligase-like family, member 4	2.50
Nolc1	Nucleolar and coiled-body phosphoprotein 1	2.32
Epas1	Endothelial PAS domain protein 1	2.12
Atf7	Activating transcription factor 7	2.07
Tnip2	TNFAIP3 interacting protein 2	2.03
Translation regulation		
Snord16a	Small nucleolar RNA, C/D box 16A	5.52
Snora69	Small nucleolar RNA, H/ACA box 69	3.17
Trit1	tRNA isopentenyltransferase 1	2.85
Exosc2	Exosome component 2	2.51
Mir343	microRNA 343	2.71
Myc	Myelocytomatosis oncogene	2.23
Snord87	Small nucleolar RNA, C/D box 87	2.13
Gnl2	Guanine nucleotide binding protein-like 2 (nucleolar)	2.11
Utp20	UTP20, small subunit (SSU) processome component	2.10
Parp8	Poly (ADP-ribose) polymerase family, member 8	2.05
Dkc1	Dyskeratosis congenita 1, dyskerin	2.03
Trmt5	TRM5 tRNA methyltransferase 5	2.02
Regulation of cell cycle		
Plk2	Polo-like kinase 2	3.01
Cenpi	Centromere protein I	2.46
Gnl3	Guanine nucleotide binding protein-like 3 (nucleolar)	2.39
Nup43	Nucleoporin 43	2.43
Usp33	Ubiquitin specific peptidase 33	2.32
Hist3h2a	Histone cluster 3, H2a	2.30
Fancd2	Fanconi anemia, complementation group D2	2.05
Mpg	N-methylpurine-DNA glycosylase	2.00
Signal transduction		
Gbp5	Guanylate binding protein 5	5.11
Sdr39u1	Short chain dehydrogenase/reductase family 39U	3.62
Slc15a3	Solute carrier family 15, member 3	3.56
Serpine2	Serine (or cysteine) peptidase inhibitor, clade E, member 2	3.52
Cish	Cytokine inducible SH2-containing protein	3.02
Gbp5	Guanylate binding protein 5	2.92
Skap2	Src family associated phosphoprotein 2	2.87
Casd1	CAS1 domain containing 1	2.4
Ric8b	Resistance to inhibitors of cholinesterase 8 homolog B	2.28
Atg7	Autophagy related 7	2.28
Tmem64	Transmembrane protein 64	2.26
Prkcd	Protein kinase C, delta	2.20
Nle1	Notchless homolog 1 (Drosophila)	2.18
Stk3	Serine/threonine kinase 3	2.09
Frmd6	FERM domain containing 6	2.02

Ctsc	Cathespin C	2.01
Proteasome		
Ublcp1	Ubiquitin-like domain containing CTD phosphatase 1	6.81
Psmd3	Proteasome 26S subunit	2.47
T cell receptor		
Traj53	T cell receptor alpha joining 53	3.40
Trav6-6	T cell receptor alpha variable 6-6	2.36
Nucleotide metabolism		
Uprt	Uracil phosphoribosyltransferase (FUR1) homolog	3.16
Membrane transport		
Pla2g15	Phospholipase A2, group XV	2.82
Chac2	ChaC, cation transport regulator 2	2.23
Slc7a6	Solute carrier family 7, member 6	2.04
Metabolism		
Fasn	Fatty acid synthase	2.40
Enoph1	Enolase-phosphatase 1	2.24
Tm9sf4	Transmembrane 9 superfamily protein member 4	2.13
Atad3a	ATPase family, AAA domain containing 3A	2.00
Protein transport		
Slc35e3	Peroxisome proliferative activated receptor 1	2.39
Cpd	HemK methyltransferase family member 1	2.27
DNA Repair		
Brca1	Breast cancer 1	2.30
Tonsl	Tonsoku-like, DNA repair protein	2.20
Xrcc2	X-ray repair complementing defective repair 2	2.19
Peptidase inhibitor		
Serpina3f	Serine (or cysteine) peptidase inhibitor, clade A, member 3F	2.18
Apoptosis		
Smpd2	Sphingomyelin phosphodiesterase 2, neutral	2.50
Mitochondria biogenesis		
Pprc1	Peroxisome proliferative activated receptor 1	2.17
Hemk1	HemK methyltransferase family member 1	2.00
Glycoprotein synthesis		
St3gal2	ST3 beta-galactoside alpha-2,3-sialyltransferase 2	2.10
Chst14	Carbohydrate (N-acetylgalactosamine 4-0) sulfotransferase 14	2.07
Lipid transport		
Stard7	START domain containing 7	2.06
Nuclear Envelope		
Tmem43	Transmembrane protein 43	2.12
Uncharacterised		
1110038B12Rik	RIKEN cDNA 1110038B12Rik gene	3.17
Gm4129	Predicted gene 4129	3.12
4930549G23Rik	RIKEN cDNA 1110038B12Rik gene	2.83
Ccdc90b	Coiled-coil domain containing 90B	2.72
n-R5s64	Nuclear encoded rRNA 5S 64	2.72
Fundc2	FUN14 domain containing 2	2.69
C230052I12Rik	RIKEN cDNA C230052I12 gene	2.61
Gm15764	Predicted gene 15764	2.60
1110008L16Rik	RIKEN cDNA 1110008L16 gene	2.57
LOC100505155	Uncharacterised LOC100505155	2.52
D430020J02Rik	RIKEN cDNA D430020J02 gene	2.48
Gm10688	RIKEN cDNA A730077B16 gene	2.34
Gm11110	Predicted gene 11110	2.32

Gm2046	Predicted gene 2046	2.21
Rasl11b	RAS-like, family 11, member B	2.21
Nudcd2	NudC domain containing 2	2.19
Nnat	Neuronatin	2.12
Wdr53	WD repeat domain 53	2.11
Gm17041	Predicted gene 17041	2.10
Heatr3	HEAT repeat containing 3	2.10
Cnih4	Cornichon homolog 4 (Drosophila)	2.09
Gm12316	Predicted gene 12316	2.07
Gm13008	Predicted gene 13008	2.07
Tmem8	Transmembrane protein 8 (five membrane-spanning domains)	2.05
Ldlrad4	Low density lipoprotein receptor class A domain containing 4	2.05
Gm19412	Predicted gene 19412	2.04
Fam212a	family with sequence similarity 212, member A	2.02

Table 8: Genes upregulated in MataHari T cells derived from the epidermis in the presence *versus* the absence of host Langerhans cells. Mh T cells obtained from the epidermis of PBS and DT treated Langerin-DTR recipients 7 days after transplant. Dataset kindly analysed by Dr Pedro Sousa using Affymetrix transcriptome analysis console software. A linear fold change (LFC) ≥2 and ANOVA p-value ≤0.05 was chosen as the cut off.

Genes under-expressed in Mh T cells from the epidermis in PBS versus DT treated recipients		
Gene	**Description**	**LFC**
Signal transduction		
Dcaf12	DDB1 and CUL4 associated factor 12	-4.67
Serpinb1a	Serine peptidase inhibitor, clade B, member 1a	-2.40
CD7	CD7 antigen	-2.40
Klhl20	Kelch-like 20	-2.03
Tumor suppressor		
Dear1	Dual endothelin 1/angiotensin II receptor 1	-2.51
Trp53cor1	Tumor protein p53 pathway corepressor 1	-2.17
T cell receptor		
Traj29	T cell receptor alpha joining 29	-2.44
Metabolism		
Hba-a1	Hemoglobin alpha, adult chain 1	-2.27
Translation regulation		
Mir139	microRNA 139	-2.09
Uncharacterised		
9430037G07Rik	RIKEN cDNA 9430037G07 gene	-3.23
1700056E22Rik	RIKEN cDNA 1700056E22 gene	-2.72
Klk1b5	Kallikrein 1-related peptidase b5	-2.40
Gm10552	Predicted gene 10552	-2.34
Gm17106	Predicted gene 17106	-2.28
A130066N16Rik	RIKEN cDNA A130066N16 gene	-2.18
Tmem167b	Transmembrane protein 167B	-2.02

Table 9: Genes downregulated in MataHari T cells derived from the epidermis in the presence *versus* the absence of host Langerhans cells. Mh T cells obtained from the epidermis of PBS and DT treated Langerin-DTR recipients 7 days after transplant. Dataset kindly analysed by Dr Pedro Sousa using Affymetrix transcriptome analysis console software. A linear fold change (LFC) ≥2 and ANOVA p-value ≤0.05 was chosen as the cut off.

Biological pathways upregulated in Mh T cells in PBS vs DT treated recipients	FDR p-value
Top 20 pathways as determined by FDR p-value	
Assembly of the pre-replicative complex	0.00001
Cell cycle	0.00001
Cell cycle checkpoints	0.00001
Cell cycle mitotic	0.00001
DNA replication	0.00001
M G1 Transition	0.00001
Mitotic M M G1 phases	0.00001
Regulation of mRNA stability by proteins that bind AU rich elements	0.00001
Synthesis of DNA	0.00001
Transport of mature transcript to cytoplasm	0.00001
Orc1 removal from chromatin	0.00002
Processing of capped intron containing pre mRNA	0.00002
CDT1 association with the CDC6 orc origin complex	0.00002
S phase	0.00002
Activation of ATR in response to replication stress	0.00002
G1 S transition	0.00003
mRNA processing	0.00003
Cytosolic tRNA aminoacylation	0.00004
CDH1 targeted proteins in late mitosis early G1	0.00005
ER phagosome pathway	0.00005
Pathways related to effector T cell function	
IL3, IL5 and GM CSF signalling	0.04708
Cytokine signalling in the immune system	0.05983
Immune system	0.09002
Adaptive immune system	0.09885
IL2 signalling	0.12634
Interferon signalling	0.16782
IL1 signalling	0.19632

Table 10: GSEA comparing MataHari T cells derived from the epidermis in the presence *versus* the absence of host Langerhans cells. 220 biological pathways were active in Mh T cells in the presence versus the absence of host LC. The top 20 pathways were determined based on the FDR p-value. Dataset kindly analysed by Dr Pedro Sousa using the Molecular Signatures Database Collection 2 – Canonical Pathways. A FDR p-value ≤0.25 was chosen as the cut off.

5.3.2 Langerhans cells upregulate multiple genes and biological pathways in allogeneic versus syngeneic BMT with MataHari T cells

To investigate the role of host LC in the development of acute GVHD, host LC were sorted by FACS directly into RLT lysis buffer containing 1μM β-mercaptoethanol from the epidermis of male Langerin-DTR (allogeneic) and female BL/6 (syngeneic) recipients 7 days after transplant with female BM, MataHari T cells and polyclonal CD4 T cells. In addition, host LC were also collected from WT male BL/6 mice as a control for inflammation associated with the conditioning regime.

The gating strategy used to sort these cells is described in Figure 86A. Samples from different recipients were pooled if necessary so that a minimum of 8 $x10^3$ LC were collected per biological replicate with sort purity ≥95%. The RNA was then purified and amplified for whole-transcriptome microarray analysis using the Affymetrix GeneChip Mouse Gene 2.0 ST Array. The microarray dataset was then analysed by Dr Pedro Sousa in our lab using the same software and statistical techniques described in the previous sections.

In contrast to allogeneic (F→M) recipients, no $V\beta8.3^+$ $Thy1.1^+$ Mh T cells were detected in the epidermis of syngeneic (F→F) recipients 7 days after transplant. Female recipients lack the requisite HY antigen (UTY) Mh T cells are reactive to and are not exposed to antigen in syngeneic recipients (Figure 90). By directly comparing the gene expression of profile of host LC in the epidermis of allogeneic (F→M) recipients versus syngeneic (F→F) recipients of BMT at this timepoint, we were able to investigate the change in gene expression in host LC when alloreactive donor Mh T cells were either present or absent in the epidermis.

Following an unsupervised agglomerative clustering analysis and PVCA of host LC in the epidermis, there was a noticeable divergence in the transcriptional profiles between all three sets of host LC (Figure 91). A gene level differential expression analysis of

host LC in the epidermis identified 57 genes that were upregulated and 24 genes that were downregulated in allogeneic versus syngeneic recipients of BMT (Table 11 and Table 12). Interestingly, the IFN-γ inducible chemokine CXCL9, which has been linked to the pathogenesis of GVHD, was significantly upregulated in host LC from allogeneic recipients. Comparing the transcriptional profiles of host LC from allogeneic versus syngeneic recipients of BMT through a GSEA, it was evident that host LC upregulate multiple biological pathways involved in chemoattraction, cell migration and co-stimulation in response to signalling associated by type I and type II IFN (Table 13). Taken together, it appears that the presence of effector Mh T cells in the epidermis increases the immunostimulatory capacity of host LC.

Epidermis: MataHari T cell infiltration in allogeneic vs syngeneic recipients

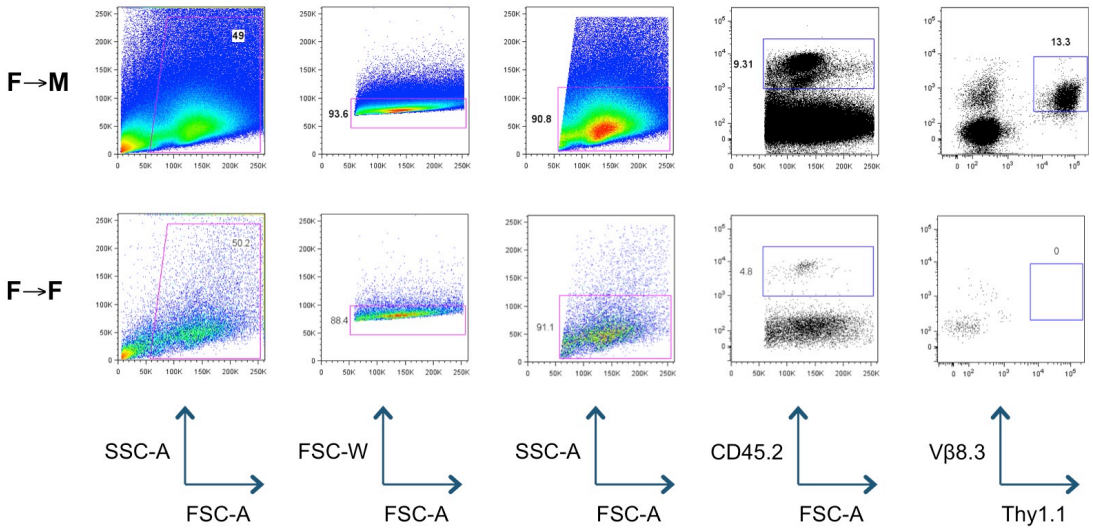

Figure 90: In contrast to allogeneic (F→M) recipients of BMT, MataHari T cells do not infiltrate the epidermis in syngeneic (F→F) recipients of BMT 7 days after transplant. Representative dot plots of the epidermis from male Langerin-DTR and female C57BL/6 recipients of BMT 7 days after transplant. After an initial live cell gate doublets were eliminated based on a FSC-W, FSC-A gate. A broad lymphocyte gate was then gated and Mh T cells were identified within this based on their expression of Vβ8.3, Thy1.1 and CD45.2. In male Langerin-DTR recipients of allogeneic (F→M) BMT, Mh T cells had infiltrated the epidermis by day 7 as previously described. In female C57BL/6 recipients of syngeneic (F→F) BMT, Mh T cells did not infiltrate the epidermis by day 7.

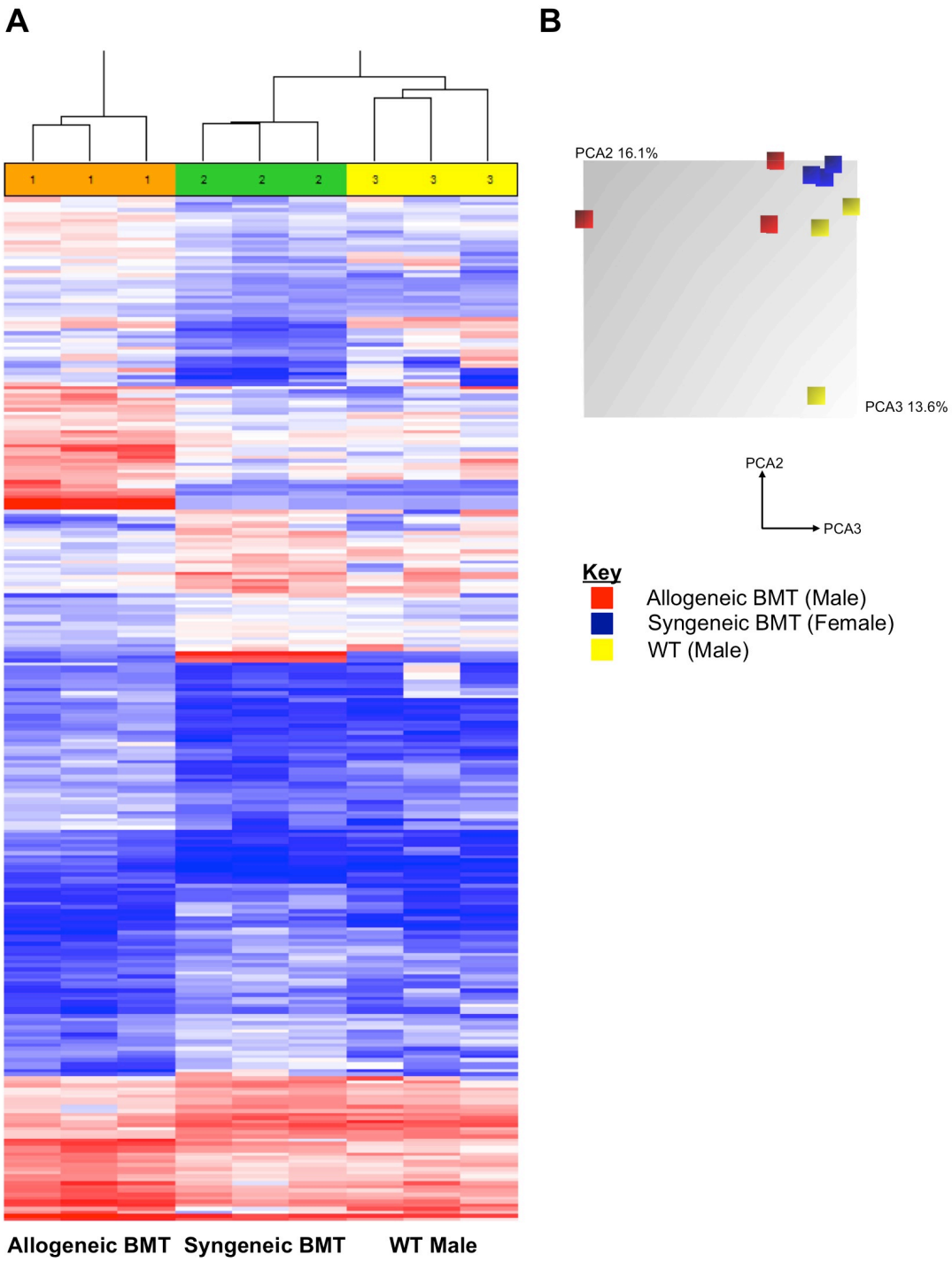

Figure 91: Heat map and principal variance component analysis of Langerhans cells from the epidermis. A. Heat map depicting the unsupervised agglomerative hierarchical clustering analysis of Langerhans cells from the epidermis of allogeneic and syngeneic recipients of BMT with Mh T cells and WT male Langerin-DTR mice according to the gene expression profile determined using the Affymetrix GeneChip 2.0 Mouse Gene 2.0 ST Array (Each biological replicate represents pooled RNA, n=3-9 from 1-2 independent experiments). **B.** Principal variance component analysis of LC samples according to the gene expression profile determined using the Affymetrix GeneChip 2.0 Mouse Gene 2.0 ST Array. There is a divergence in the transcriptional profile of LC in all 3 groups.

Genes over-expressed in Langerhans cells in allogeneic versus syngeneic recipients		
Gene	**Description**	**LFC**
Translation regulation		
Ddx3y	DEAD (Asp-Glu-Ala-Asp) box polypeptide 3, Y-linked	28.35
Eif2s3y	Eukaryotic translation initiation factor 2, subunit 3, structural gene	17.64
Cytokine/Chemokine		
Cxcl9	Chemokine (C-X-C motif) ligand 9	20.76
Signal transduction		
Gbp2	Guanylate binding protein 2	9.89
Cish	Cytokine inducible SH2-containing protein	8.36
Kmo	Kynurenine 3-monooxygenase (kynurenine 3-hydroxylase)	6.85
CD209c	CD209c antigen	3.59
Stat1	Signal transducer and activator of transcription 1	3.46
Nlrc5	NLR family, CARD domain containing 5	3.1
CD33	CD33 antigen	2.82
CD274	CD274 antigen	2.79
Klrb1b	Killer cell lectin-like receptor subfamily B member 1b	2.72
Pram1	PML-RAR alpha-regulated adaptor molecule 1	2.68
Olfr99	Olfactory receptor 99	2.65
Gpr171	G protein-coupled receptor 171	2.61
Irf8	Interferon regulatory factor 8	2.56
Il2rg	Interleukin 2 receptor, gamma chain	2.5
Tbc1d8	TBC1 domain family, member 8	2.46
Gnb4	Guanine nucleotide binding protein (G protein), beta 4	2.36
Gbp7	Guanylate binding protein 7	2.28
Zbp1	Z-DNA binding protein 1	2.05
Clec2d	C-type lectin domain family 2, member d	2.04
Ly6e	Lymphocyte antigen 6 complex, locus E	2.03
Adcy6	Adenylate cyclase 6	2.02
Cell adhesion		
Cd97	CD97 antigen	6.54
Slamf7	SLAM family member 7	2.97
Vcl	Vinculin	2.17
Epigenetic regulation		
Uty	Ubiquitously transcribed tetratricopeptide repeat gene	6.02
Kdm5d	Lysine (K)-specific demethylase 5D	4.32
Inflammasome		
Gbp5	Guanylate binding protein 5	5.11
Zinc metabolism		
Mt4	Metallothionein 4	4.12
Antigen presentation		
H2-Q10	Histocompatibility 2, Q region locus 10	4.11
Apoptosis		
Dnase1l3	Deoxyribonuclease 1-like 3	3.15
Bcl2	B cell leukemia/lymphoma 2	3.05
Bcl2l11	BCL2-like 11 (Apoptosis facilitator)	2.34
Tmem173	Transmembrane protein 173	2.2
Transcription regulation		
Mir18	MicroRNA 18	3.14
Arid5b	AT rich interactive domain 5B (MRF1-like)	2.42
1810022K09Rik	RIKEN cDNA 1810022K09 gene	2.18
Apopbec3	Apolipoprotein B mRNA editing enzyme, catalytic polypeptide 3	2.17
Mir186	MicroRNA 186	2.14
Ahcy	S-adenosylhomocysteine hydrolase	2

Membrane Transport		
Mfsd2a	Major facilitator superfamily domain containing 2A	2.75
Clcn7	Chloride channel 7	2.63
Cytoskeleton		
Coro2a	Coronin, actin binding protein 2A	2.53
Lipid metabolism		
Dgat2	Diacylglycerol O-acyltransferase 2	2.4
Protein transport		
Ehd1	EH-domain containing 1	2.32
Regulation of cell cycle		
Suv39h1	Suppressor of variegation 3-9 homolog 1	2.06
Flavin metabolism		
Rfk	Riboflavin kinase	2.01
Uncharacterised		
Gm19951	Predicted gene, 19951	17.32
1600029D21Rik	RIKEN cDNA 1600029D21 gene	6
Gm19763	Predicted gene, 19763	3.26
AU020206	Expressed sequence AU020206	2.73
Sectm1a	Secreted and transmembrane 1A	2.68
2310030G06Rik	RIKEN cDNA 2310030G06 gene	2.6
A130040M12Rik	RIKEN cDNA A130040M12 gene	2.25
Aim1	Absent in melanoma 1	2.06

Table 11: Genes upregulated in Langerhans cells from the epidermis of allogeneic *versus* syngeneic recipients of BMT. Dataset kindly analysed by Dr Pedro Sousa using Affymetrix transcriptome analysis console software. A linear fold change (LFC) ≥2 and ANOVA p-value ≤0.05 was chosen as the cut off.

Genes under-expressed in Langerhans cells in allogeneic versus syngeneic recipients		
Gene	**Description**	**LFC**
Translation regulation		
Xist	Inactive X specific transcripts	-72.91
Mir146	microRNA 146	-3.52
Trim27	tripartite motif-containing 27	-3.05
Kansl2	KAT8 regulatory NSL complex subunit 2	-2.80
Churc1	Churchill domain containing 1	-2.07
Signal transduction		
Emr4	EGF-like module, hormone receptor-like sequence 4	-3.04
Hax1	HCLS1 associated X-1	-2.19
Itga8	Integrin alpha 8	-2.18
Cell differentiation		
Pid1	Phosphotyrosine interaction domain containing 1	-2.63
Oxidation/Reduction metabolism		
Higd1a	HIG1 domain family, member 1A	-2.44
Acot6	Acyl-CoA thioesterase 6	-2.39
Transmembrane transport		
Slc36a	Solute carrier family 36, member 2	-2.40
Regulation of cell cycle		
Ninl	Ninein-like	-2.35
Cell adhesion		
St8sia4	ST8 alpha-N-acetyl-neuraminide alpha-2,8	-2.15
Itgame	Integrin alpha M	-2.09
Cytoskeleton		
Cript	Cysteine-rich PDZ-binding protein	-2.13
Uncharacterised		
1600010M07Rik	Riken cDNA 1600010M07 gene	-3.02
1110005A03Rik	Riken cDNA 1110005A03 gene	-2.59
Zfp958	Zinc finger protein 958	-2.28
Lrp2bp, Ankrd37	Lrp2 binding protein, ankyrin repeat domain	-2.16
4930447A16Rik	Riken cDNA 4930447A16 gene	-2.09
4930522L14Rik	Riken cDNA 4930522L14 gene	-2.09
1600002H07Rik	Riken cDNA 1600002H07 gene	-2.05

Table 12: Genes downregulated in Langerhans cells from the epidermis of allogeneic versus syngeneic recipients. Dataset kindly analysed by Dr Pedro Sousa using Affymetrix transcriptome analysis console software. A linear fold change (LFC) ≥-2 and ANOVA p-value ≤0.05 was chosen as the cut off.

Biological pathways upregulated in Langerhans cells in allogeneic versus syngeneic recipients	FDR p-value
Cytokine signalling in immune system	0.001
Interferon gamma signalling	0.001
Interferon signalling	0.001
Growth hormone receptor signalling	0.002
Interferon alpha beta signalling	0.008
Regulation of IFNG signalling	0.030
Interleukin 6 signalling	0.059
Apoptotic cleavage of cell adhesion proteins	0.068
Signalling by ILS	0.084
NEF mediated downregulation of MHC Class I complex cell surface expression	0.158
P2Y receptors	0.168
Smooth muscle contraction	0.171
Regulation of IFNA signalling	0.177
P38MAPK events	0.182
CTLA4 inhibitory signalling	0.182
Immune system	0.185
Extrinsic pathway for apoptosis	0.202
Interleukin 7 signalling	0.224
Antigen presentation: folding, assembly and peptide loading of MHC Class I	0.224
Chemokine receptors bind chemokines	0.227
Antiviral mechanism by IFN stimulated genes	0.227
GPVI mediated activation cascade	0.227
PI metabolism	0.230
Nucleotide-like purinergic receptors	0.230
Amine compound SLC transporters	0.230
Double-strand break repair	0.244

Table 13: GSEA comparing Langerhans cells from the epidermis of allogeneic (F→M) versus syngeneic (F→F) recipients of BMT. Dataset kindly analysed by Dr Pedro Sousa using the Molecular Signatures Database Collection 2 – Canonical Pathways. A FDR p-value ≤0.25 was chosen as the cut off.

5.4 Discussion

5.4.1 LC are required *in situ*

The majority of studies investigating the role of donor and host APC in the development of GVHD have focused on these cell populations in priming the T cell response. In the previous chapter, I established a role for host LC in the development of cutaneous GVHD. However, the severity of acute systemic GVHD that developed was unaffected. The activation and expansion profile of Mh T cells in the lymphoid tissue was also unaffected as well as the capacity of Mh T cells to infiltrate other peripheral tissues such as the liver, lung and gut. This indicated that the depletion of host LC had no effect on the initiation or priming of acute systemic GVHD in this model. However, mature host LC that migrate to the secondary lymphoid tissue may have an important 'cellular' or 'humoral' interaction with T cells in the lymph node that effects their capacity to initiate cutaneous GVHD. To investigate whether host LC were required *in situ* to peripherally regulate alloreactive donor T cell responses, I developed three experimental approaches.

I initially developed a model of cutaneous GVHD where alloreactive donor T cells were injected directly into the skin. This was based on a protocol adapted from a published study where OT-1 T cells directly injected into the dermis of K14-OVA mice, where keratinocytes express OVA in the epidermis, were sufficient to induce cutaneous GVHD[311]. Adapting this model, two MHC-mismatched strains, Langerin-DTR (H-2b) and DBA/2 (H-2d) mice, were mated to create the Langerin-DTR x DBA/2 (H-2db) strain. To generate alloreactive T cells for i.d. injection, Langerin-DTR x DBA/2 mice were lethally irradiated with a split dose of 11 GY and reconstituted with a mixture of 5 $x10^6$ BM and 20 $x10^6$ SC from a WT BL/6 donor. This Primary→F1 MHC-mismatch was sufficient to induce severe systemic GVHD[283]. After 4 days, 0.5 $x10^6$ of these primed $CD8^+$ T cells were then injected i.d. in 50 μl into the ears of Langerin-DTR x DBA/2 mice, which had been treated with 4 mg of Imiquimod and either 400 ng of DT or PBS.

The ears were subsequently harvested 3 days later and examined for histopathological signs of GVHD.

The assumption in this experiment was that if host LC were required *in situ*, then there would be a significant reduction in the severity of cutaneous GVHD that developed when host LC were depleted. However, controls treated with Imiquimod alone developed an observable pathology. The volume of liquid injected also added to background noise, with observable pathology developing in ears injected with 50 μl of PBS. Due to the high levels of background noise in control, it was difficult to discern any meaningful observations and further work using this approach was discontinued.

Due to the technical issues associated with directly injecting cell into the ear, I developed a secondary transfer model of GVHD where Mh T cells exposed to antigen *in vivo* were infused back into lethally irradiated male BL/6 recipients. The assumption in this experiment is that the majority of AEMTs, which had been exposed to antigen for *in vivo* in another lethally irradiated BL/6 male recipient, would be already primed against male antigen and ready to initiate GVHD. Thus, any differences in the ability of these T cells to accumulate in the skin in the absence of host LC would provide strong evidence that LC are required *in situ*. Adapting the already established MataHari minor mismatch model of GVHD, an irradiated male BL/6 recipient was transplanted with Mh T cells. After 3, 4, or 5 days, the Mh T cells were harvested from the skin draining lymph nodes and enriched before secondary transfer into lethally irradiated male Langerin-DTR recipients treated with either 400 ng of PBS or DT. Initially, Mh T cells that were primed for 5 days were used due to kinetics data from the previous chapter where Mh T cells infiltrated the skin by day 6.

Interestingly, the transfer of 0.1-0.5 $x10^6$ Mh T cells exposed to antigen for 5 days was sufficient for Mh T cells to infiltrate the liver, lungs and LP+PP but not the skin. To investigate whether the length of time donor Mh T cells were exposed to antigen *in vivo*

effected their ability to accumulate in the skin, Mh T cells exposed to antigen for 3, 4 and 5 days were mixed together at a 1:1:1 ratio and transplanted into male BL/6 recipients. In the lung, LP+PP and liver, three distinct populations of Mh T cells could be identified 7 days after transplant with Mh T cells exposed to antigen for 4 days accumulating at higher frequencies than any other AEMTs. Interestingly, in the skin a different pattern emerged. Only Mh T cells exposed to antigen for 3 and 4 days were identified in both the epidermis and dermis in all samples. However, the average frequency at which the AEMTs accumulated in the epidermis and dermis was much lower than the frequencies observed transplanting 1 $x10^6$ naïve Mh T cells even when 1 $x10^6$ AEMTs primed for 4 days were transferred into secondary recipients.

These data indicate that early effectors migrate more efficiently to peripheral tissues. Although the precise mechanism for this observation is unclear, a similar observation has also been made in lymphocytic choriomeningitis (LCMV) infection model in mice, where CD8 T cells isolated 7 days after LCMV infection lost their ability to migrate to the gut epithelium in contrast to early effectors transferred after 4.5 days[312]. Without further experimental evidence it is difficult to speculate what caused this phenomenon. The frequency of infiltrating cells is decreased even when 1 $x10^6$ AEMTs were transferred into secondary recipients. It could be that T cells primed for 5 days may be more sensitive to treatment *ex vivo* during harvesting, which effects their ability to initiate GVHD *in vivo*. Alternatively, primed T cells may require a secondary 'licensing' signal in a peripheral tissue in order to proliferate and survive, by the time the T cell infiltrates the skin it may be too late. Due to the time constraints on the project and the artificial nature of the experiment in the context of acute GVHD, further work on this model was discontinued.

Previous experimental approaches to investigate a role for LC *in situ* had focused on the injection of antigen exposed donor T cells intravenously or directly into the skin. Focusing on the skin itself, a new experimental approach was developed where DT

was injected i.d. into the left ear of Langerin-DTR mice to locally deplete LC *in situ*. The premise is that host LC that remain in untreated skin are capable of migrating to skin draining lymph nodes and interacting with donor CD8 T cells upon activation. Thus, if there was no difference in the accumulation and function of donor CD8 T cells in the area of the skin where host LC had been locally depleted, this would provide strong evidence that host LC are required *in situ* to regulate the T cell response in the periphery.

Taking into account data from the T cell injection model, the volume used was reduced from the 50 μl to 20 μl to reduce any potential inflammatory side effects. The injection of 25 ng into the dorsal and ventral side of the ear was sufficient to host LC in the treated left ear, but not the untreated right ear in the same mouse. There was a slight reduction in the frequency in the untreated ear of a mouse receiving DT versus the untreated ear of a mouse receiving PBS, indication some systemic effects of DT. However, there was a significant reduction in the frequency of LC between the left (treated) versus the right (untreated) ear in DT treated mice. This was also confirmed by immunofluorescence microscopy of epidermal sheets, where LC were absent in the left (treated) ear but present in the right (untreated) ear. The mice were then allowed to recover for 9 days to allow Langerin^{+} dDC to reconstitute before being transplanted with naïve Mh T cells using the model described in the previous chapter.

Remarkably, the localised depletion of host LC in the left ear had a significant effect on the ability of Mh T cells to accumulate in the skin 7 days after transplant. This reduction was specific for host LC, as a similar volume of PBS injected into Langerin-DTR had no effect on either the frequency of host LC *in situ* or Mh T cells infiltrating into the epidermis after transplant. Interestingly, there was a significant difference in the accumulation of Mh T cells in the right (untreated) ear of DT treated recipients versus the right (untreated) ear of PBS treated recipients hinting that the relationship between host LC and the T cell response may initially be dependant on the number of LC.

However, when the corresponding frequencies of host LC and Mh T cells were directly compared from all experiments involving the MataHari minor H mismatch model a relationship was difficult to interpret.

These data, in parallel with the data from the systemic depletion of host LC in the previous chapter, demonstrate a critical role for host LC *in situ* in peripheral regulation of CD8 T cell responses in the skin during acute GVHD.

5.4.2 Gene expression analysis of MataHari T cells and LC

To investigate whether there was functional difference between Mh T cells in the skin of mice in the presence versus the absence of host LC, the transcriptional profile of Mh T cells derived from the epidermis, dermis and skin draining lymph nodes was examined. This proved technically challenging and required a high number of replicates to sort relatively low numbers of cells for the microarray study; 5 $x10^3$ epidermal Mh T cells, 100 $x10^3$ lymph node Mh T cells and 8 $x10^3$ host LC. However, using the NuGEN Ovation Pico WTA System V2, which can reliably amplify cDNA from as little as 500 pg of RNA, the study was feasible.

Initially, the expression of effector molecules associated with CTL function was analysed in flow sorted Mh T cells derived from the epidermis and dermis by qPCR, which was kindly performed by Dr Terry Means at Massachusetts General Hospital. Mh T cells in the epidermis showed a significant reduction in the expression of mRNA transcripts for a number of key effector molecules including IFN-γ, TNF-α, Granzyme B, TRAIL and the pro-survival molecule Bcl-xL, demonstrating a significant reduction in effector function of Mh T cells in the absence of host LC.

In the final part of my PhD, I analysed the transcriptional profile of Mh T cells from the epidermis and skin draining lymph nodes using a microarray. From the dataset, it was clear that the transcriptional profile of Mh T cells changes substantially after cells infiltrate the epidermis, with several pathways favouring proliferation and survival upregulated. Remarkably, when host LC were depleted all of these biological pathways were lost, with the exception of one that is involved in T cell apoptosis.

This was also apparent when gene expression profile of Mh T cells in the epidermis in the presence *versus* the absence of host LC was analysed. Over 220 biological pathways were upregulated in the presence of host LC. The vast majority of these pathways favoured cell proliferation, exemplified by the observation that 14 out of the

top 20 of these pathways were involved the cell cycle. The expression of *Myc* was significantly upregulated in Mh T cells in the presence of host LC. *Myc* is a marker of cell activation and plays a key role in the metabolic switch that favours T cell growth. In addition, the expression of the T cell co-stimulatory molecule TNFS14 (LIGHT), which promotes T cell expansion in a T:T cell dependent manner, was significantly upregulated in the presence of host LC[313]. A number of key T cell effector molecules were also upregulated in the presence of host LC, including Granzyme C, IFN-γ and TNF-α, thus, demonstrating a critical role for host LC in 'licensing' CD8 T cells to become fully competent effector cells in the skin, similar to our observations in the MHC-mismatched MC model.

The transcriptional profile of host LC in the epidermis was then analysed to evaluate their role in the development of cutaneous GVHD. By directly comparing the gene expression profile of host LC in allogeneic (F→M) versus syngeneic (F→F) recipients of BMT, I was able to investigate the effect of infiltrating Mh T cells on the transcriptional profile of host LC, while controlling for the immunomodulatory effects of damage associated with the conditioning regime. However, it should be noted that the up- and downregulation of some genes in host LC in allogeneic (F→M) versus syngeneic (F→F) recipients is a result of the sex-mismatch between the recipients. For instance, the most highly downregulated gene in host LC in allogeneic versus syngeneic recipients is *Xist*, which is major effector of the X chromosome inactivation process in females.

Through GSEA, it appears that type I- and type II IFN signalling is important to the activity of host LC in the epidermis. In the secondary lymphoid tissue, type-I interferons have been shown to augment CTL function, directly enhancing their expansion and differentiation, and indirectly by enhancing cross-presentation by APC and promoting DC maturation[314–316]. The role of type-II interferons in the development of acute GVHD remains controversial as it can have both immunosuppressive and pathogenic

effects[316]. However, in the presence of host LC, Mh T cell significantly upregulate their expression of IFN-γ and the most striking observation from the LC microarray data was the significant upregulation of the chemokine CXCL9, a chemokine induced by IFN-γ. CXCL9 is a potent chemokine involved in the migration of immune effector cells to sites of inflammation through its cognate receptor CXCR3. Several studies have already shown that CXCR3 is important in the pathogenesis of acute GVHD, with a recent study by Villarroel et al. demonstrating a critical role for CXCR3 in the skin-specific recruitment of effector CD8 T cells in a model cutaneous GVHD[146,317,318].

6 Discussion

The role of host haematopoietic APC in the development of acute GVHD remains controversial. In MHC-mismatched models of GVHD, host haematopoietic APC are important during the initiation phase of acute GVHD. A role for host DC in these models is not surprising, as a high frequency of donor T cell precursors will be alloreactive against host MHC, molecules that are ubiquitously expressed by DC. However, in MHC-matched, minor H mismatched models of acute GVHD, the role of host haematopoietic APC is less clear. Using Mh T cells to induce GVHD, Toubai et al. generated [BL/6 $2M^{-/-}$→BL/6] chimeras where antigen presentation is restricted to host non-haematopoietic APC. GVHD was induced when [BL/6 $\beta2M^{-/-}$→BL/6] chimeras were reirradiated and transplanted with female BL/6 $\beta2M^{-/-}$ BM and Mh T cells, indicating that antigen presentation by host non-haematopoietic APC alone was sufficient to initiate GVHD[130]. Similarly, in CD4-mediated models of acute GVHD using B6.H2-$Ab1^{-/-}$ mice, which are MHC Class II deficient, Koyama et al. demonstrated that antigen presentation by host non-haematopoietic was sufficient to induce severe and lethal GVHD when antigen presentation was restricted in both donor and host haematopoietic cells[129]. Thus, a wide array of cells are capable of stimulating naïve donor T cells and the likelihood that one particular subset of APC has a non-redundant role in the initiation of this response seems improbable.

An area less well investigated is the role of tissue-resident APC populations in the regulation of alloreactive donor T cell responses *in situ* after T cell priming. It is becoming increasingly clear that APC, such as DC, are important at not only priming immune responses in secondary lymphoid tissues but also in modulating their responses *in situ*. A role for DC in the peripheral regulation of T cells *in situ* has been particularly well characterised in the lung, where direct DC:T cell interactions are required after priming for the clearance of influenza. The existence of such a secondary

'licensing' signal makes evolutionary sense, as dysregulated immune responses can mediate tissue injury that far exceeds that caused by the pathogen it was intended to clear.

In this project, I demonstrate for the first time a critical role for host LC *in situ* in the peripheral regulation of donor CD8 T cells that infiltrate the skin during acute GVHD. The depletion of host LC, but not Langerin$^+$ dDC was associated with a significant reduction in the accumulation and function of donor CD8 T cells in the epidermis, that resulted in a substantial decrease in the severity of pathology that developed in this skin. This phenotype also appears to be CD8 dependant. In a MHC-matched, minor H mismatch model of CD4-mediated GVHD using Tg Marilyn CD4 T cells, which bear a TCR specific for male H-Y antigen (derived from *Dby* gene)[319], the depletion of host LC had no significant effect on the accumulation of Marilyn T cells in the epidermis although there was a trend towards a lower frequency in the absence of host LC (data not shown).

Interestingly, two studies published during my project directly ruled out a role for LC in MHC-matched, minor H mismatch models of CD8-mediated GVHD. Using Langerin-DTA mice, which specifically lack LC due to the expression of the diphtheria toxin A chain, Li et al. demonstrated that host LC were dispensable in a C3H.SW → BL/6 model of acute GVHD[126]. In fact, the absence of host LC slightly exacerbated the severity of cutaneous GVHD in this model. Similarly, using CD11c-DTA mice, which constitutively lack CD11c$^+$ cDC, LC and most plasmacytoid DC, Li et al. demonstrated that host cDC, LC and pDC were dispensable for the induction of acute GVHD in the C3H.SW → BL/6 model[125]. Considering these observations against the profound immunostimulatory role of LC in my model of GVHD, it is hard to ignore that Langerhans cells are constitutively depleted from the skin in both the Langerin-DTA and CD11c-DTA mouse model. This constitutive absence during development may have a significant effect on the immune microenvironment that develops within the

epidermis, which may account for the disparity between the two models. However, it would be interesting to see if a similar phenotype was observed if these recipients were transplanted Mh T cells.

The key question that remains to be answered is why do host LC, which only persist for a short time after transplant, mediate such a potent immunostimulatory signal to CD8 T cells. Other APC subsets in the skin, such as Langerin^{+} dDC, are capable of presenting antigen while epithelial cells, such as keratinocytes, can express pro-inflammatory cytokines and chemokines in response to tissue damage associated with the conditioning regime. Keratinocytes are equipped with a variety of TLRs, NOD-like receptors (NLR) and RIG-I-like receptors (RLR) that makes them particularly adept at sensing and responding to a variety of PAMPs and DAMPs, producing cytokines and chemokines such as CXCL9, CXCL10, CXCL11, TNF, IL-1, IL-6 and IL-10[320]. LC on the other hand appear to favour the induction of tolerance, promoting the formation of Tregs, and are widely considered dispensable for the induction of CD8 T cell immunity in the skin[263,321]. Interestingly, the epidermis contains a large population of memory CD8^{+} T cells that persist for long periods of time and are largely sequestered from the wider circulation[322]. Commonly referred to as T resident memory (Trm) cells, they compete with epidermal $\gamma\delta$ T cells for survival signals and can be rapidly reactivated *in situ* upon reinfection[323]. It may be that LC have a key role in the expansion and homeostasis of this population *in situ* and in the context of tissue damage associated with the conditioning regime promote the induction of a dysregulated response, which can persist long after host LC are depleted. Recent data in our lab has hinted at this possibility, with Mh T cells in the epidermis increasing their expression of CD103 and CD69, molecules associated with the formation of Trm cells[324].

However, the mechanism by which host LC mediate this potent immunostimulatory effect on alloreactive donor CD8 T cells remains elusive. It may involve a direct *cis* interaction between host LC and effector CD8 T cells in the epidermis or it could

involve a *trans* interaction via the secretion of a 'humoral' effector. In addition, host LC could indirectly stimulate donor T cells by interacting with other infiltrating immune effectors, such as NK cells or neutrophils, resident immune effectors (γδ T cells) or stromal cells (keratinocytes).

From the microarray data, it appears that type I- and II-IFN signalling is important during the development of cutaneous GVHD in this model. One hypothesis we propose is that damage associated with the conditioning regime leads to the secretion of type I IFN by innate cells such as plasmacytoid DC or stromal cells such keratinocytes. In response to these activation signals LC stimulate infiltrating CD8 T cells to produce IFN-γ which in turn promotes the production of cytokines and chemokines such as CXCL9 by LC which further augments the infiltration and accumulation of immune effectors in the skin, thus, perpetuating cutaneous GVHD.

In the lung, a direct MHC Class I mediated interaction between pulmonary DC and infiltrating CTL induces a proliferative burst in T cells upon entry that is necessary for the clearance of influenza. Similar to the lung, the most striking observation from the T cell array data was the significant increase in expression of genes and biological pathways associated with proliferation when Mh T cells transitioned from the skin draining lymph nodes to the epidermis, a transcriptional signature that was lost in the absence of host LC. Whether a similar MHC Class I mediated interaction between host LC and donor CD8 T cells in the epidermis is critical for the downstream effector function of T cells remains to be determined. Based on observations in the MC model, it is tempting to speculate that a direct MHC Class I mediated interaction between host LC and donor CD8 T cells is responsible for the phenotype observed, although I was unable to definitely show this. In the context of our MHC-mismatched MC model of localised cutaneous inflammation ([BL/6+BALB/c] → Langerin-DTR), the unexpected finding of donor LC derived from MHC-mismatched BALB/c donor BM is important to consider. In [BL/6+BALB/c] → Langerin-DTR MC, two populations of LC were present

in the epidermis, LC derived from the host (Langerin-DTR, H-2b) and LC derived from MHC-mismatched donor BM (BALB/c, H-2d). However, after topical application of the TLR 7-8 agonist Imiquimod and DLI using donor splenocytes derived from MHC-mismatched BALB/s donors, the depletion of host LC (Langerin-DTR, H-2b) significantly reduced the effector function of alloreactive donor CD8 T cells in the epidermis despite the presence of donor LC (BALB/c, H-2d)[229]. This indicates that a direct interaction of host LC with alloreactive donor CD8 T cells or another immunomodulatory cell type that interacts donor CD8 T cells is important. Inflammation mediated by the TLR 7-8 agonist Imiquimod would have the same effect on donor and host derived LC in the epidermis. The cytokines and/or chemokines released by LC in response to Imiquimod could be compensated for by BALB/c derived LC when host LC have been depleted using DT. However, it is also important to consider that BALB/c derived LC in this model are derived from bone marrow progenitors in contrast to host LC which are derived from yolk sac derived precursors and fetal liver monocytes. This may affect their response upon stimulation although no differences between LC populations derived from long-term bone marrow progenitors, yolk sac derived precursors and fetal liver monocytes has been reported in the literature.

To investigate whether host LC are required to directly interact with Mh T cells via MHC Class I, the ideal model would have LC deficient in MHC Class I when all other host haematopoietic and non-haematopoietic cells express MHC Class I. One way to achieve this is the use of Cre-lox mouse models. Kaplan et al. have created Langerin-Cre mice where Cre recombinase inserted into a human Langerin gene is selectively expressed in LC[325]. FVB $D^{b\text{-}LoxP}$ transgenic mice have recently been created, inserting LoxP sites that flank the transmembrane exon of the D^b class I gene (exon 5)[326]. Mating Langerin-Cre with FVB $D^{b\text{-}LoxP}$ mice, the expression of MHC Class I could be selectively depleted in host LC. Adopting this mouse to the MataHari minor H mismatch model, any deficiency in the accumulation and activation of Mh T cells in epidermis

would provide strong evidence supporting a direct *cis* interaction between host LC and donor CD8 T cells.

Alternatively, the infiltration of Mh T cells into the skin could be visualised using intravital two-photon microscopy, a fluorescence imaging technique that permits live cell imaging up to 1 mm[327]. Mh T cells infiltrate the epidermis by day 6 post transplant and in the absence of host LC there is already a significant reduction in the accumulation of Mh T cells in the epidermis at this timepoint. Imaging the infiltration of Mh T cells into the epidermis in the presence or absence of host LC at this timepoint would give us a greater insight into the behaviour of these cells *in vivo*.

The role of host LC may also be independent of an interaction with an immune effector cell. A recent study by Moussion and Girad has proposed an unexpected new function for DC *in vivo*. Using the CD11c-DTR model, they noted that the continued depletion of DC over a one-week period reduced both the size and cellularity of peripheral and mucosal lymph nodes[328]. In the absence of DC, high endothelial venules, which regulate the recruitment of lymphocytes, reverted from a mature phenotype to an immature neonatal phenotype preventing the entry of lymphocytes into the lymph node. In the skin, a role for LC in vasodilation has been described in response to the antidyslipidemic drug nicotinic acid[329]. Nicotinic acid induced the expression of prostanoid synthases in LC, which are required for the formation of vasodilators prostaglandin E2 and prostaglandin D2. Using the Langerin-DTR mouse model, the depletion of LC abrogated nicotinic acid induced skin flushing. In the context of cutaneous GVHD, vasodilators produced by LC may help increase the frequency of Mh T cells that infiltrate into the epidermis, which in turn promotes tissue damage and inflammation that further augments the severity of cutaneous GVHD. To test this hypothesis, Langerin-DTR recipients could be injected 3, 4 or 5 days post transplant before Mh T cells infiltrate the epidermis. The assumption in this experiment is that LC would mediate a vasodilatory effect before T cells infiltrate the skin. If there was no

difference in the accumulation of Mh T cells in the epidermis when LC were depleted at any one of these timepoints then at the very least the requirement for a direct cell:cell contact between host LC and Mh T cells could be ruled out.

Taking these data forward, the importance of host LC will need to be verified in a polyclonal T cell model of acute GVHD. Although LC had a role in the development of cutaneous GVHD in a model of localised cutaneous inflammation using polyclonal T cells, the majority of the work in my project has used monoclonal Mh CD8 T cells. This is not representative of GVHD in the clinic, where alloreactive donor polyclonal T cells respond to a multitude of different minor histocompatibility antigens, and will need to be addressed[330]. In addition, care needs to be taken when interpreting the results from a translational point of view, as substantial differences can exist between mice and humans. In the skin, epidermal $\gamma\delta$ T cells are abundant in mice but absent in humans.

To conclude, it is clear that host LC can mediate a potent immunostimulatory role *in vivo*. The precise role of LC remains enigmatic, but it appears they may have a 'sentinel' like role in the epidermis. In the presence of the appropriate stimulus, in this study tissue damage associated with the conditioning regime, LC are capable of promoting potent immune responses. Similarly, they are equally capable of downregulating immune responses to promote tolerance. Dissecting the nature of these LC:T cell interaction *in situ* could lead to the identification of a novel mechanism to both control and promote CD8 T cell immune responses in the skin. In the context of GVHD, controlling the response locally at the site of inflammation is an attractive therapeutic strategy, as the beneficial anti-neoplastic effects of systemic GVL may be maintained.

7 References

1. Pasquini, M. C. & Wang, Z. Current use and outcome of hematopoietic stem cell transplantation. *CIBMTR Summ. Slides* (2013). at <http://www.cibmtr.org/ReferenceCenter/SlidesReports/SummarySlides/pages/index.aspx>

2. Barriga, F., Ramírez, P., Wietstruck, A. & Rojas, N. Hematopoietic stem cell transplantation: clinical use and perspectives. *Biol. Res.* **45,** 307–16 (2012).

3. Thomas, E. D., Lochte, H. L., Lu, W. C. & Ferrebee, J. W. Intravenous Infusion of Bone Marrow in Patients Receiving Radiation and Chemotherapy. *N Engl J Med* **257,** 491–496 (1957).

4. Shlomchik, W. D. Graft-versus-host disease. *Nat. Rev. Immunol.* **7,** 340–52 (2007).

5. Bacigalupo, A. Matched and mismatched unrelated donor transplantation: is the outcome the same as for matched sibling donor transplantation? *Hematology Am. Soc. Hematol. Educ. Program* **2012,** 223–9 (2012).

6. Gratwohl, A. & Niederwieser, D. History of hematopoietic stem cell transplantation: evolution and perspectives. *Curr. Probl. Dermatol.* **43,** 81–90 (2012).

7. Jacobson, L. O., Marks, E. K., Robson, M. J., Gaston, E. & Zirkle, R. E. The effect of spleen protection on mortality following x-irradiation. *J. Lab. Clin. Med.* **34,** 1538–1543 (1949).

8. Jacobson, L. O., Simmons, E. L., Marks, E. K. & Eldredge, J. H. Recovery from Radiation Injury. *Science (80-.).* **113,** 510–511 (1951).

9. Jacobson, L. O. Modification of radiation injury. *Bull. N. Y. Acad. Med.* **30,** 675–92 (1954).

10. Lorenz, E., Congdon, C. & Uphoff, D. Modification of Acute Irradiation Injury in Mice and Guinea-Pigs by Bone Marrow Injections. (1952). at <http://pubs.rsna.org/doi/abs/10.1148/58.6.863?journalCode=radiology>

11. Main, J. M. & Prehn, R. T. Successful skin homografts after the administration of high dosage X radiation and homologous bone marrow. *J. Natl. Cancer Inst.* **15,** 1023–9 (1955).

12. Ford, C. E., Hamerton, J. L., Barnes, D. W. & Loutit, J. F. Cytological identification of radiation-chimaeras. *Nature* **177,** 452–4 (1956).

13. Barnes, D. W. H., Ford, C. E., Ilbery, P. L. T., Koller, P. C. & Loutit, J. F. Tissue transplantation in the radiation chimera. *J. Cell. Comp. Physiol.* **50,** 123–138 (1957).

14. Thomas, E. D. in *Thomas' Hematop. Cell Transplant. Stem Cell Transplantation, Fourth Ed.* (eds. Appelbaum, F. R., Forman, S. J., Negrin, R. & Blume, K. G.) (Wiley-Blackwell, 2009). doi:10.1002/9781444303537.ch1

15. Thomas, E. D., Lochte, H. L., Cannon, J. H., Sahler, O. D. & Ferrebee, J. W. Supralethal whole body irradiation and isologous marrow transplantation in man. *J. Clin. Invest.* **38,** 1709–16 (1959).

16. McGovern, J. J., Russell, P. S., Atkins, L. & Webster, E. W. Treatment of terminal leukemic relapse by total-body irradiation and intravenous infusion of stored autologous bone marrow obtained during remission. *N Engl J Med* **260,** 675–83 (1959).

17. Mathé, G., Amiel, J. L., Schwarzenberg, L., Cattan, A. & Schneider, M. Adoptive immunotherapy of acute leukemia: experimental and clinical results. *Cancer Res.* **25,** 1525–31 (1965).

18. Barnes, D. W. H. & Loutit, J. F. Treatment of Murine Leukaemia with X-Rays and Homologous Bone Marrow: II. *Br. J. Haematol.* **3,** 241–252 (1957).

19. Van Bekkum, D. W. The Selective Eliomination Of Immunologically Competent Cells From Bone Marrow And Lymphatic Cell Mixtures. *Transplantation* **2,** 393–404 (1964).

20. Baron, F., Storb, R. & Little, M.-T. Hematopoietic cell transplantation: five decades of progress. *Arch. Med. Res.* **34,** 528–44 (2004).

21. Bekkum, D. W. & Vries, M. J. de. *Radiation chimaeras*. 277 (Logos Press, 1967). at <http://books.google.com/books?id=Iw06AAAAMAAJ&pgis=1>

22. Bortin, M. M. A compendium of reported human bone marrow transplants. *Transplantation* **9,** 571–87 (1970).

23. Little, M.-T. & Storb, R. History of haematopoietic stem-cell transplantation. *Nat. Rev. Cancer* **2,** 231–8 (2002).

24. De la Morena, M. T. & Gatti, R. A. A history of bone marrow transplantation. *Hematol. Oncol. Clin. North Am.* **25,** 1–15 (2011).

25. Uphoff, D. E. Genetic factors influencing irradiation protection by bone marrow. I. The F1 hybrid effect. *J. Natl. Cancer Inst.* **19,** 123–30 (1957).

26. Snell, G. D. Studies in histocompatibility. *Science* **213,** 172–8 (1981).

27. Lupu, M. & Storb, R. Five decades of progress in haematopoietic cell transplantation based on the preclinical canine model. *Vet. Comp. Oncol.* **5,** 14–30 (2007).

28. Epstein, R. B., Storb, R., Ragde, H. & Thomas, E. D. Cytotoxic typing antisera for marrow grafting in littermate dogs. *Transplantation* **6,** 45–58 (1968).

29. Storb, R., Rudolph, R. H. & Thomas, E. D. Marrow grafts between canine siblings matched by serotyping and mixed leukocyte culture. *J. Clin. Invest.* **50,** 1272–5 (1971).

30. Lochte, H. L., Levy, A. S., Guenther, D. M., Thomas, E. D. & Ferrebee, J. W. Prevention of Delayed Foreign Marrow Reaction in Lethally Irradiated Mice by Early Administration of Methotrexate. *Nature* **196,** 1110–1111 (1962).

31. Storb, R., Epstein, R. B., Graham, T. C. & Thomas, E. D. Methotrexate regimens for control of graft-versus-host disease in dogs with allogeneic marrow grafts. *Transplantation* **9,** 240–6 (1970).

32. Thomas, E. D., Collins, J. A., Herman, E. C. & Ferrebee, J. W. Marrow transplants in lethally irradiated dogs given methotrexate. *Blood* **19,** 217–28 (1962).

33. Epstein, R. B., Storb, R., Clift, R. A. & Thomas, E. D. Autologous bone marrow grafts in dogs treated with lethal doses of cyclophosphamide. *Cancer Res.* **29,** 1072–5 (1969).

34. Storb, R., Epstein, R. B., Rudolph, R. H. & Thomas, E. D. Allogeneic canine bone marrow transplantation following cyclophosphamide. *Transplantation* **7,** 378–86 (1969).

35. Santos, G. W. & Owens, A. H. Allogeneic marrow transplants in cyclophosphamide treated mice. *Transplant. Proc.* **1,** 44–6 (1969).

36. Dausset, J. Iso-leuco-anticorps. *Acta Haematol.* **20,** 156–166 (1958).

37. Mickelson, E. M. *et al.* Evaluation of the mixed lymphocyte culture (MLC) assay as a method for selecting unrelated donors for marrow transplantation. *Tissue Antigens* **47,** 27–36 (1996).

38. Thomas, E. D. *et al.* Bone-Marrow Transplantation. *N Engl J Med* **295,** 832–843 (1975).

39. Thomas, E. D. *et al.* One hundred patients with acute leukemia treated by chemotherapy, total body irradiation, and allogeneic marrow transplantation. *Blood* **49,** 511–33 (1977).

40. Thomas, E. D. *et al.* Marrow transplantation for patients with acute lymphoblastic leukemia in remission. *Blood* **54,** 468–476 (1979).

41. Thomas, E. D. *et al.* Marrow transplantation for acute nonlymphoblastic leukemia in first remission. *N. Engl. J. Med.* **301,** 597–9 (1979).

42. Thomas, E. D. *et al.* Marrow transplantation for the treatment of chronic myelogenous leukemia. *Ann. Intern. Med.* **104,** 155–63 (1986).

43. Storb, R. *et al.* Marrow transplantation for severe aplastic anemia: methotrexate alone compared with a combination of methotrexate and cyclosporine for prevention of acute graft-versus-host disease. *Blood* **68,** 119–25 (1986).

44. Storb, R. *et al.* Methotrexate and cyclosporine compared with cyclosporine alone for prophylaxis of acute graft versus host disease after marrow transplantation for leukemia. *N. Engl. J. Med.* **314,** 729–35 (1986).

45. Weiden, P. L. *et al.* Antileukemic effect of graft-versus-host disease in human recipients of allogeneic-marrow grafts. *N. Engl. J. Med.* **300,** 1068–73 (1979).

46. Horowitz, M. M. *et al.* Graft-versus-leukemia reactions after bone marrow transplantation. *Blood* **75,** 555–62 (1990).

47. Marmont, A. M. *et al.* T-cell depletion of HLA-identical transplants in leukemia. *Blood* **78,** 2120–30 (1991).

48. Petersdorf, E. W. *et al.* Major-histocompatibility-complex class I alleles and antigens in hematopoietic-cell transplantation. *N. Engl. J. Med.* **345,** 1794–800 (2001).

49. Ezzone, S. A. History of hematopoietic stem cell transplantation. *Semin. Oncol. Nurs.* **25,** 95–9 (2009).

50. Jenq, R. R. & van den Brink, M. R. M. Allogeneic haematopoietic stem cell transplantation: individualized stem cell and immune therapy of cancer. *Nat. Rev. Cancer* **10,** 213–21 (2010).

51. Appelbaum, F. R. Hematopoietic-Cell Transplantation at 50. *N Engl J Med* 1472–1475 (2007). at <http://www.nejm.org/doi/full/10.1056/NEJMp078166>

52. Gooley, T. A. *et al.* Reduced mortality after allogeneic hematopoietic-cell transplantation. *N. Engl. J. Med.* **363,** 2091–101 (2010).

53. Billingham, R. E. The biology of graft-versus-host reactions. *Harvey Lect.* **62,** 21–78 (1966).

54. Kernan, N. A. *et al.* Clonable T lymphocytes in T cell-depleted bone marrow transplants correlate with development of graft-v-host disease. *Blood* **68,** 770–3 (1986).

55. Shlomchik, W. D. Prevention of Graft Versus Host Disease by Inactivation of Host Antigen-Presenting Cells. *Science (80-.).* **285,** 412–415 (1999).

56. Ferrara, J. L. M., Levine, J. E., Reddy, P. & Holler, E. Graft-versus-host disease. *Lancet* **373,** 1550–61 (2009).

57. Flomenberg, N. *et al.* Impact of HLA class I and class II high-resolution matching on outcomes of unrelated donor bone marrow transplantation: HLA-C mismatching is associated with a strong adverse effect on transplantation outcome. *Blood* **104,** 1923–30 (2004).

58. Lee, S. J. *et al.* High-resolution donor-recipient HLA matching contributes to the success of unrelated donor marrow transplantation. *Blood* **110,** 4576–83 (2007).

59. Kawase, T. *et al.* High-risk HLA allele mismatch combinations responsible for severe acute graft-versus-host disease and implication for its molecular mechanism. *Blood* **110,** 2235–41 (2007).

60. Brickner, A. G. *et al.* The immunogenicity of a new human minor histocompatibility antigen results from differential antigen processing. *J. Exp. Med.* **193,** 195–206 (2001).

61. Yadav, R. *et al.* The H4b minor histocompatibility antigen is caused by a combination of genetically determined and posttranslational modifications. *J. Immunol.* **170,** 5133–42 (2003).

62. Den Haan, J. M. The Minor Histocompatibility Antigen HA-1: A Diallelic Gene with a Single Amino Acid Polymorphism. *Science (80-.).* **279,** 1054–1057 (1998).

63. Murata, M., Warren, E. H. & Riddell, S. R. A human minor histocompatibility antigen resulting from differential expression due to a gene deletion. *J. Exp. Med.* **197,** 1279–89 (2003).

64. Dzierzak-Mietla, M. *et al.* Occurrence and Impact of Minor Histocompatibility Antigens' Disparities on Outcomes of Hematopoietic Stem Cell Transplantation from HLA-Matched Sibling Donors. *Bone Marrow Res.* **2012,** 257086 (2012).

65. Vogt, M. H. J. *et al.* The DBY gene codes for an HLA-DQ5-restricted human male-specific minor histocompatibility antigen involved in graft-versus-host disease. *Blood* **99,** 3027–32 (2002).

66. Randolph, S. S. B., Gooley, T. A., Warren, E. H., Appelbaum, F. R. & Riddell, S. R. Female donors contribute to a selective graft-versus-leukemia effect in male recipients of HLA-matched, related hematopoietic stem cell transplants. *Blood* **103,** 347–52 (2004).

67. Goulmy, E. *et al.* Mismatches of minor histocompatibility antigens between HLA-identical donors and recipients and the development of graft-versus-host disease after bone marrow transplantation. *N. Engl. J. Med.* **334,** 281–5 (1996).

68. Marijt, W. A. E. *et al.* Hematopoiesis-restricted minor histocompatibility antigens HA-1- or HA-2-specific T cells can induce complete remissions of relapsed leukemia. *Proc. Natl. Acad. Sci. U. S. A.* **100,** 2742–7 (2003).

69. Wysocki, C. A. & Shlomchik, W. D. in *Immune Biol. Allogeneic Hematop. Stem Cell Transplant. Model. Discov. Transl.* (eds. Socié, G. & Blazar, B. R.) 173–194 (Academic Press, 2012). at <http://books.google.com/books?id=R6PhnYnkDzUC&pgis=1>

70. Sherman, L. A. & Chattopadhyay, S. The molecular basis of allorecognition. *Annu. Rev. Immunol.* **11,** 385–402 (1993).

71. Filipovich, A. H. *et al.* National Institutes of Health consensus development project on criteria for clinical trials in chronic graft-versus-host disease: I. Diagnosis and staging working group report. *Biol. Blood Marrow Transplant.* **11,** 945–56 (2005).

72. Sullivan, K. M. in *Thomas' Hematop. Cell Transplant.* (eds. Blume, K. G., Forman, S. J. & Appelbaum, F. R.) (Blackwell Publishing Ltd, 2003). doi:10.1002/9780470987070

73. Hahn, T. *et al.* Risk factors for acute graft-versus-host disease after human leukocyte antigen-identical sibling transplants for adults with leukemia. *J. Clin. Oncol.* **26,** 5728–34 (2008).

74. Jagasia, M. *et al.* Risk factors for acute GVHD and survival after hematopoietic cell transplantation. *Blood* **119,** 296–307 (2012).

75. Martin, P. J. *et al.* A retrospective analysis of therapy for acute graft-versus-host disease: initial treatment. *Blood* **76,** 1464–72 (1990).

76. Ziemer, M. Graft-versus-host disease of the skin and adjacent mucous membranes. *J. Dtsch. Dermatol. Ges.* **11,** 477–95 (2013).

77. Ball, L. M. & Egeler, R. M. Acute GvHD: pathogenesis and classification. *Bone Marrow Transplant.* **41 Suppl 2,** S58–64 (2008).

78. Martin, P. J. *et al.* Increasingly frequent diagnosis of acute gastrointestinal graft-versus-host disease after allogeneic hematopoietic cell transplantation. *Biol. Blood Marrow Transplant.* **10,** 320–7 (2004).

79. Nevo, S. *et al.* Acute bleeding after allogeneic bone marrow transplantation: association with graft versus host disease and effect on survival. *Transplantation* **67,** 681–9 (1999).

80. Snover, D. C., Weisdorf, S. A., Ramsay, N. K., McGlave, P. & Kersey, J. H. Hepatic graft versus host disease: a study of the predictive value of liver biopsy in diagnosis. *Hepatology* **4,** 123–30 (1984).

81. McDonald, G. B. Review article: management of hepatic disease following haematopoietic cell transplant. *Aliment. Pharmacol. Ther.* **24,** 441–52 (2006).

82. Dignan, F. L. *et al.* Diagnosis and management of acute graft-versus-host disease. *Br. J. Haematol.* **158,** 30–45 (2012).

83. Przepiorka, D. *et al.* 1994 Consensus Conference on Acute GVHD Grading. *Bone Marrow Transplant.* **15,** 825–8 (1995).

84. Cahn, J.-Y. *et al.* Prospective evaluation of 2 acute graft-versus-host (GVHD) grading systems: a joint Société Française de Greffe de Moëlle et Thérapie Cellulaire (SFGM-TC), Dana Farber Cancer Institute (DFCI), and International Bone Marrow Transplant Registry (IBMTR) pros. *Blood* **106,** 1495–500 (2005).

85. MacMillan, M. L. *et al.* Response of 443 patients to steroids as primary therapy for acute graft-versus-host disease: comparison of grading systems. *Biol. Blood Marrow Transplant.* **8,** 387–94 (2002).

86. Holtan, S. G., Pasquini, M. & Weisdorf, D. J. Acute GVHD: a bench to bedside update. *Blood* **124,** 363–373 (2014).

87. Ferrara, J. L. M. & Reddy, P. Pathophysiology of graft-versus-host disease. *Semin. Hematol.* **43,** 3–10 (2006).

88. Wysocki, C. A., Panoskaltsis-Mortari, A., Blazar, B. R. & Serody, J. S. Leukocyte migration and graft-versus-host disease. *Blood* **105,** 4191–9 (2005).

89. Heidegger, S., van den Brink, M. R. M., Haas, T. & Poeck, H. The role of pattern-recognition receptors in graft-versus-host disease and graft-versus-leukemia after allogeneic stem cell transplantation. *Front. Immunol.* **5,** 337 (2014).

90. Hill, G. R. & Ferrara, J. L. The primacy of the gastrointestinal tract as a target organ of acute graft-versus-host disease: rationale for the use of cytokine shields in allogeneic bone marrow transplantation. *Blood* **95,** 2754–9 (2000).

91. Reddy, P. & Ferrara, J. L. M. in *Stembook* (Harvard Stem Cell Institute, 2009). at <http://www.ncbi.nlm.nih.gov/books/NBK27033/>

92. Chen, X. *et al.* Blockade of interleukin-6 signaling augments regulatory T-cell reconstitution and attenuates the severity of graft-versus-host disease. *Blood* **114,** 891–900 (2009).

93. Banchereau, J. & Steinman, R. M. Dendritic cells and the control of immunity. *Nature* **392,** 245–52 (1998).

94. Wilhelm, K. *et al.* Graft-versus-host disease is enhanced by extracellular ATP activating P2X7R. *Nat. Med.* **16,** 1434–8 (2010).

95. Zeiser, R., Penack, O., Holler, E. & Idzko, M. Danger signals activating innate immunity in graft-versus-host disease. *J. Mol. Med. (Berl).* **89,** 833–45 (2011).

96. Ferrari, D. *et al.* The P2X7 receptor: a key player in IL-1 processing and release. *J. Immunol.* **176,** 3877–83 (2006).

97. Jankovic, D. *et al.* The Nlrp3 inflammasome regulates acute graft-versus-host disease. *J. Exp. Med.* **210,** 1899–910 (2013).

98. Ozawa, H., Nakagawa, S., Tagami, H. & Aiba, S. Interleukin-1 beta and granulocyte-macrophage colony-stimulating factor mediate Langerhans cell maturation differently. *J. Invest. Dermatol.* **106,** 441–5 (1996).

99. Sims, J. E. & Smith, D. E. The IL-1 family: regulators of immunity. *Nat. Rev. Immunol.* **10,** 89–102 (2010).

100. Elliott, M. R. *et al.* Nucleotides released by apoptotic cells act as a find-me signal to promote phagocytic clearance. *Nature* **461,** 282–6 (2009).

101. La Sala, A. *et al.* Dendritic cells exposed to extracellular adenosine triphosphate acquire the migratory properties of mature cells and show a reduced capacity to attract type 1 T lymphocytes. *Blood* **99,** 1715–22 (2002).

102. Maeda, Y. Pathogenesis of graft-versus-host disease: innate immunity amplifying acute alloimmune responses. *Int. J. Hematol.* **98,** 293–9 (2013).

103. Van Bekkum, D. W. & Knaan, S. Role of bacterial microflora in development of intestinal lesions from graft-versus-host reaction. *J. Natl. Cancer Inst.* **58,** 787–90 (1977).

104. Beelen, D. W. *et al.* Evidence that sustained growth suppression of intestinal anaerobic bacteria reduces the risk of acute graft-versus-host disease after sibling marrow transplantation. *Blood* **80,** 2668–76 (1992).

105. Cooke, K. R. *et al.* LPS antagonism reduces graft-versus-host disease and preserves graft-versus-leukemia activity after experimental bone marrow transplantation. *J. Clin. Invest.* **107,** 1581–9 (2001).

106. Cohen, J. *et al.* Antibody titres to a rough-mutant strain of Escherichia coli in patients undergoing allogeneic bone-marrow transplantation. Evidence of a protective effect against graft-versus-host disease. *Lancet* **1,** 8–11 (1987).

107. Bayston, K., Baumgartner, J. D., Clark, P. & Cohen, J. Anti-endotoxin antibody for prevention of acute GVHD. *Bone Marrow Transplant.* **8,** 426–7 (1991).

108. Cooke, K. R. *et al.* Tumor necrosis factor- alpha production to lipopolysaccharide stimulation by donor cells predicts the severity of experimental acute graft-versus-host disease. *J. Clin. Invest.* **102,** 1882–91 (1998).

109. Markey, K. A., MacDonald, K. P. A. & Hill, G. R. The biology of graft-versus-host disease: experimental systems instructing clinical practice. *Blood* blood–2014–02–514745– (2014). doi:10.1182/blood-2014-02-514745

110. Toubai, T. *et al.* Siglec-G-CD24 axis controls the severity of graft-versus-host disease in mice. *Blood* **123,** 3512–23 (2014).

111. Beilhack, A. *et al.* Prevention of acute graft-versus-host disease by blocking T-cell entry to secondary lymphoid organs. *Blood* **111,** 2919–28 (2008).

112. Blazar, B. R., Murphy, W. J. & Abedi, M. Advances in graft-versus-host disease biology and therapy. *Nat. Rev. Immunol.* **12,** 443–58 (2012).

113. Sprent, J., Schaefer, M., Lo, D. & Korngold, R. Properties of purified T cell subsets. II. In vivo responses to class I vs. class II H-2 differences. *J. Exp. Med.* **163,** 998–1011 (1986).

114. Wakim, L. M. & Bevan, M. J. Cross-dressed dendritic cells drive memory CD8+ T-cell activation after viral infection. *Nature* **471,** 629–32 (2011).

115. Sprent, J., Miller, J. F. & Mitchell, G. F. Antigen-induced selective recruitment of circulating lymphocytes. *Cell. Immunol.* **2,** 171–81 (1971).

116. Ruggeri, L. *et al.* Effectiveness of donor natural killer cell alloreactivity in mismatched hematopoietic transplants. *Science* **295,** 2097–100 (2002).

117. Teshima, T. *et al.* Acute graft-versus-host disease does not require alloantigen expression on host epithelium. *Nat. Med.* **8,** 575–81 (2002).

118. Smyth, L. A., Herrera, O. B., Golshayan, D., Lombardi, G. & Lechler, R. I. A novel pathway of antigen presentation by dendritic and endothelial cells: Implications for allorecognition and infectious diseases. *Transplantation* **82,** S15–8 (2006).

119. Markey, K. A. *et al.* Cross-dressing by donor dendritic cells after allogeneic bone marrow transplantation contributes to formation of the immunological synapse and maximizes responses to indirectly presented antigen. *J. Immunol.* **192,** 5426–33 (2014).

120. Shlomchik, W. D. *et al.* Prevention of graft versus host disease by inactivation of host antigen-presenting cells. *Science* **285,** 412–5 (1999).

121. Matte, C. C. *et al.* Donor APCs are required for maximal GVHD but not for GVL. *Nat. Med.* **10,** 987–92 (2004).

122. Wang, X. *et al.* Mechanisms of antigen presentation to T cells in murine graft-versus-host disease: cross-presentation and the appearance of cross-presentation. *Blood* **118,** 6426–37 (2011).

123. Duffner, U. A. *et al.* Host Dendritic Cells Alone Are Sufficient to Initiate Acute Graft-versus-Host Disease. *J. Immunol.* **172,** 7393–7398 (2004).

124. Anderson, B. E. *et al.* Distinct roles for donor- and host-derived antigen-presenting cells and costimulatory molecules in murine chronic graft-versus-host disease: requirements depend on target organ. *Blood* **105,** 2227–34 (2005).

125. Li, H. *et al.* Profound depletion of host conventional dendritic cells, plasmacytoid dendritic cells, and B cells does not prevent graft-versus-host disease induction. *J. Immunol.* **188,** 3804–11 (2012).

126. Li, H. *et al.* Langerhans cells are not required for graft-versus-host disease. *Blood* **117,** 697–707 (2011).

127. Matte-Martone, C. *et al.* Recipient B cells are not required for graft-versus-host disease induction. *Biol. Blood Marrow Transplant.* **16,** 1222–30 (2010).

128. Hashimoto, D. *et al.* Pretransplant CSF-1 therapy expands recipient macrophages and ameliorates GVHD after allogeneic hematopoietic cell transplantation. *J. Exp. Med.* **208,** 1069–82 (2011).

129. Koyama, M. *et al.* Recipient nonhematopoietic antigen-presenting cells are sufficient to induce lethal acute graft-versus-host disease. *Nat. Med.* **18,** 135–42 (2012).

130. Toubai, T. *et al.* Induction of acute GVHD by sex-mismatched H-Y antigens in the absence of functional radiosensitive host hematopoietic-derived antigen-presenting cells. *Blood* **119,** 3844–53 (2012).

131. Appleman, L. J. & Boussiotis, V. A. T cell anergy and costimulation. *Immunol. Rev.* **192,** 161–80 (2003).

132. Greenwald, R. J., Freeman, G. J. & Sharpe, A. H. The B7 family revisited. *Annu. Rev. Immunol.* **23,** 515–48 (2005).

133. Blazar, B. R., Taylor, P. A., Linsley, P. S. & Vallera, D. A. In vivo blockade of CD28/CTLA4: B7/BB1 interaction with CTLA4-Ig reduces lethal murine graft-versus-host disease across the major histocompatibility complex barrier in mice. *Blood* **83,** 3815–25 (1994).

134. Blazar, B. R. *et al.* Blockade of CD40 ligand-CD40 interaction impairs CD4+ T cell-mediated alloreactivity by inhibiting mature donor T cell expansion and function after bone marrow transplantation. *J. Immunol.* **158,** 29–39 (1997).

135. Blazar, B. R. *et al.* Blockade of programmed death-1 engagement accelerates graft-versus-host disease lethality by an IFN-gamma-dependent mechanism. *J. Immunol.* **171,** 1272–7 (2003).

136. Paczesny, S., Hanauer, D., Sun, Y. & Reddy, P. New perspectives on the biology of acute GVHD. *Bone Marrow Transplant.* **45,** 1–11 (2010).

137. Wu, C. J. & Ritz, J. *Cancer Immunotherapy*. *Adv. Immunol.* **90,** 133–73 (Elsevier, 2006).

138. Yi, T. *et al.* Reciprocal differentiation and tissue-specific pathogenesis of Th1, Th2, and Th17 cells in graft-versus-host disease. *Blood* **114,** 3101–12 (2009).

139. Brown, G. R., Lee, E. L., El-Hayek, J., Kintner, K. & Luck, C. IL-12-independent LIGHT signaling enhances MHC class II disparate CD4+ T cell alloproliferation, IFN-gamma responses, and intestinal graft-versus-host disease. *J. Immunol.* **174,** 4688–95 (2005).

140. Chen, B. J., Cui, X., Sempowski, G. D., Liu, C. & Chao, N. J. Transfer of allogeneic CD62L- memory T cells without graft-versus-host disease. *Blood* **103,** 1534–41 (2004).

141. Anderson, B. E. *et al.* Effects of donor T-cell trafficking and priming site on graft-versus-host disease induction by naive and memory phenotype CD4 T cells. *Blood* **111,** 5242–51 (2008).

142. Sung, A. D. & Chao, N. J. Concise review: acute graft-versus-host disease: immunobiology, prevention, and treatment. *Stem Cells Transl. Med.* **2,** 25–32 (2013).

143. Nolz, J. C., Starbeck-Miller, G. R. & Harty, J. T. Naive, effector and memory CD8 T-cell trafficking: parallels and distinctions. *Immunotherapy* **3,** 1223–33 (2011).

144. Dudda, J. C., Simon, J. C. & Martin, S. Dendritic cell immunization route determines CD8+ T cell trafficking to inflamed skin: role for tissue microenvironment and dendritic cells in establishment of T cell-homing subsets. *J. Immunol.* **172,** 857–63 (2004).

145. Mora, J. R. *et al.* Reciprocal and dynamic control of CD8 T cell homing by dendritic cells from skin- and gut-associated lymphoid tissues. *J. Exp. Med.* **201,** 303–16 (2005).

146. Villarroel, V. A., Okiyama, N., Tsuji, G., Linton, J. T. & Katz, S. I. CXCR3-mediated skin homing of autoreactive CD8 T cells is a key determinant in murine graft-versus-host disease. *J. Invest. Dermatol.* **134,** 1552–60 (2014).

147. Kägi, D. *et al.* Fas and perforin pathways as major mechanisms of T cell-mediated cytotoxicity. *Science* **265,** 528–30 (1994).

148. Van den Brink, M. R. M. & Burakoff, S. J. Cytolytic pathways in haematopoietic stem-cell transplantation. *Nat. Rev. Immunol.* **2,** 273–81 (2002).

149. Maeda, Y. *et al.* Both perforin and Fas ligand are required for the regulation of alloreactive CD8+ T cells during acute graft-versus-host disease. *Blood* **105,** 2023–7 (2005).

150. Trapani, J. A. & Smyth, M. J. Functional significance of the perforin/granzyme cell death pathway. *Nat. Rev. Immunol.* **2,** 735–47 (2002).

151. Kischkel, F. C. *et al.* Cytotoxicity-dependent APO-1 (Fas/CD95)-associated proteins form a death-inducing signaling complex (DISC) with the receptor. *EMBO J.* **14,** 5579–88 (1995).

152. Krammer, P. H. CD95's deadly mission in the immune system. *Nature* **407,** 789–95 (2000).

153. Via, C. S., Nguyen, P., Shustov, A., Drappa, J. & Elkon, K. B. A major role for the Fas pathway in acute graft-versus-host disease. *J. Immunol.* **157,** 5387–93 (1996).

154. Graubert, T. A., DiPersio, J. F., Russell, J. H. & Ley, T. J. Perforin/granzyme-dependent and independent mechanisms are both important for the development of graft-versus-host disease after murine bone marrow transplantation. *J. Clin. Invest.* **100,** 904–11 (1997).

155. Welniak, L. A., Blazar, B. R. & Murphy, W. J. Immunobiology of allogeneic hematopoietic stem cell transplantation. *Annu. Rev. Immunol.* **25,** 139–70 (2007).

156. Baker, M. B., Altman, N. H., Podack, E. R. & Levy, R. B. The role of cell-mediated cytotoxicity in acute GVHD after MHC-matched allogeneic bone marrow transplantation in mice. *J. Exp. Med.* **183,** 2645–56 (1996).

157. Zeng, D. *et al.* Bone marrow NK1.1(-) and NK1.1(+) T cells reciprocally regulate acute graft versus host disease. *J. Exp. Med.* **189,** 1073–81 (1999).

158. Marks, L., Altman, N. H., Podack, E. R. & Levy, R. B. Donor T cells lacking Fas ligand and perforin retain the capacity to induce severe GvHD in minor histocompatibility antigen mismatched bone-marrow transplantation recipients. *Transplantation* **77,** 804–12 (2004).

159. Piguet, P. F., Grau, G. E., Allet, B. & Vassalli, P. Tumor necrosis factor/cachectin is an effector of skin and gut lesions of the acute phase of graft-vs.-host disease. *J. Exp. Med.* **166,** 1280–9 (1987).

160. Xun, C. Q., Thompson, J. S., Jennings, C. D., Brown, S. A. & Widmer, M. B. Effect of total body irradiation, busulfan-cyclophosphamide, or cyclophosphamide conditioning on inflammatory cytokine release and development of acute and chronic graft-versus-host disease in H-2-incompatible transplanted SCID mice. *Blood* **83,** 2360–7 (1994).

161. Hill, G. R. *et al.* The p55 TNF-alpha receptor plays a critical role in T cell alloreactivity. *J. Immunol.* **164,** 656–63 (2000).

162. Wilson, A. G., Symons, J. A., McDowell, T. L., McDevitt, H. O. & Duff, G. W. Effects of a polymorphism in the human tumor necrosis factor alpha promoter on transcriptional activation. *Proc. Natl. Acad. Sci. U. S. A.* **94,** 3195–9 (1997).

163. Mullighan, C. *et al.* Non-HLA immunogenetic polymorphisms and the risk of complications after allogeneic hemopoietic stem-cell transplantation. *Transplantation* **77,** 587–96 (2004).

164. Steinman, R. M. & Banchereau, J. Taking dendritic cells into medicine. *Nature* **449,** 419–26 (2007).

165. Lin, Y. *et al.* Tumor necrosis factor-induced nonapoptotic cell death requires receptor-interacting protein-mediated cellular reactive oxygen species accumulation. *J. Biol. Chem.* **279,** 10822–8 (2004).

166. Lu, Y. & Waller, E. K. Dichotomous role of interferon-gamma in allogeneic bone marrow transplant. *Biol. Blood Marrow Transplant.* **15,** 1347–53 (2009).

167. Wang, H. & Yang, Y.-G. The complex and central role of interferon-γ in graft-versus-host disease and graft-versus-tumor activity. *Immunol. Rev.* **258,** 30–44 (2014).

168. Sykes, M., Szot, G. L., Nguyen, P. L. & Pearson, D. A. Interleukin-12 inhibits murine graft-versus-host disease. *Blood* **86,** 2429–38 (1995).

169. Brok, H. P., Vossen, J. M. & Heidt, P. J. IFN-gamma-mediated prevention of graft-versus-host disease: pharmacodynamic studies and influence on proliferative capacity of chimeric spleen cells. *Bone Marrow Transplant.* **22,** 1005–10 (1998).

170. Murphy, W. J. *et al.* Differential effects of the absence of interferon-gamma and IL-4 in acute graft-versus-host disease after allogeneic bone marrow transplantation in mice. *J. Clin. Invest.* **102,** 1742–8 (1998).

171. Yang, Y. G., Dey, B. R., Sergio, J. J., Pearson, D. A. & Sykes, M. Donor-derived interferon gamma is required for inhibition of acute graft-versus-host disease by interleukin 12. *J. Clin. Invest.* **102,** 2126–35 (1998).

172. Nestel, F. P., Greene, R. N., Kichian, K., Ponka, P. & Lapp, W. S. Activation of macrophage cytostatic effector mechanisms during acute graft-versus-host disease: release of intracellular iron and nitric oxide-mediated cytostasis. *Blood* **96,** 1836–43 (2000).

173. Ferrara, J. L., Levy, R. & Chao, N. J. Pathophysiologic mechanisms of acute graft-vs.-host disease. *Biol. Blood Marrow Transplant.* **5,** 347–56 (1999).

174. Lo, J. W. S. *et al.* Macrophage migratory inhibitory factor (MIF) expression in acute graft-versus-host disease (GVHD) in allogeneic hemopoietic stem cell transplant recipients. *Bone Marrow Transplant.* **30,** 375–80 (2002).

175. Schwab, L. *et al.* Neutrophil granulocytes recruited upon translocation of intestinal bacteria enhance graft-versus-host disease via tissue damage. *Nat. Med.* **20,** 648–54 (2014).

176. Snell, G. D. The Genetics of Transplantation. *Ann. N. Y. Acad. Sci.* **69,** 555–560 (1957).

177. Korngold, R. & Sprent, J. Lethal graft-versus-host disease after bone marrow transplantation across minor histocompatibility barriers in mice. Prevention by removing mature T cells from marrow. *J. Exp. Med.* **148,** 1687–98 (1978).

178. Korngold, R. & Sprent, J. Selection of cytotoxic T-cell precursors specific for minor histocompatibility determinants. I. Negative selection across H-2 barriers induced with disrupted cells but not with glutaraldehyde-treated cells: evidence for antigen processing. *J. Exp. Med.* **151,** 314–27 (1980).

179. Korngold, R. & Sprent, J. Negative selection of T cells causing lethal graft-versus-host disease across minor histocompatibility barriers. Role of the H-2 complex. *J. Exp. Med.* **151,** 1114–24 (1980).

180. Arber, C., Brenner, M. K. & Reddy, P. Mouse models in bone marrow transplantation and adoptive cellular therapy. *Semin. Hematol.* **50,** 131–44 (2013).

181. Schroeder, M. A. & DiPersio, J. F. Mouse models of graft-versus-host disease: advances and limitations. *Dis. Model. Mech.* **4,** 318–33 (2011).

182. Garnett, C., Apperley, J. F. & Pavlů, J. Treatment and management of graft-versus-host disease: improving response and survival. *Ther. Adv. Hematol.* **4,** 366–78 (2013).

183. Mestas, J. & Hughes, C. C. W. Of Mice and Not Men: Differences between Mouse and Human Immunology. *J. Immunol.* **172,** 2731–2738 (2004).

184. Choo, J. K. *et al.* Species differences in the expression of major histocompatibility complex class II antigens on coronary artery endothelium: implications for cell-mediated xenoreactivity. *Transplantation* **64,** 1315–22 (1997).

185. Van Leeuwen, L., Guiffre, A., Atkinson, K., Rainer, S. P. & Sewell, W. A. A two-phase pathogenesis of graft-versus-host disease in mice. *Bone Marrow Transplant.* **29,** 151–8 (2002).

186. Sprent, J., Schaefer, M. & Korngold, R. Role of T cell subsets in lethal graft-versus-host disease (GVHD) directed to class I versus class II H-2 differences.

II. Protective effects of L3T4+ cells in anti-class II GVHD. *J. Immunol.* **144,** 2946–54 (1990).

187. Sha, W. C. *et al.* Selective expression of an antigen receptor on CD8-bearing T lymphocytes in transgenic mice. *Nature* **335,** 271–4 (1988).

188. Yu, X.-Z., Albert, M. H. & Anasetti, C. Alloantigen Affinity and CD4 Help Determine Severity of Graft-versus-Host Disease Mediated by CD8 Donor T Cells. *J. Immunol.* **176,** 3383–3390 (2006).

189. Valujskikh, A., Lantz, O., Celli, S., Matzinger, P. & Heeger, P. S. Cross-primed CD8(+) T cells mediate graft rejection via a distinct effector pathway. *Nat. Immunol.* **3,** 844–51 (2002).

190. Miyagawa, F., Gutermuth, J., Zhang, H. & Katz, S. I. The use of mouse models to better understand mechanisms of autoimmunity and tolerance. *J. Autoimmun.* **35,** 192–8 (2010).

191. Hill, G. R. *et al.* Total body irradiation and acute graft-versus-host disease: the role of gastrointestinal damage and inflammatory cytokines. *Blood* **90,** 3204–13 (1997).

192. Schwarte, S. & Hoffmann, M. W. Influence of radiation protocols on graft-vs-host disease incidence after bone-marrow transplantation in experimental models. *Methods Mol. Med.* **109,** 445–58 (2005).

193. Korngold, R. Lethal graft-versus-host disease in mice directed to multiple minor histocompatibility antigens: features of CD8+ and CD4+ T cell responses. *Bone Marrow Transplant.* **9,** 355–64 (1992).

194. Anderson, B. E. *et al.* Memory CD4+ T cells do not induce graft-versus-host disease. *J. Clin. Invest.* **112,** 101–8 (2003).

195. Edinger, M. *et al.* CD4+CD25+ regulatory T cells preserve graft-versus-tumor activity while inhibiting graft-versus-host disease after bone marrow transplantation. *Nat. Med.* **9,** 1144–50 (2003).

196. Vossen, J. M. & Heidt, P. J. in *Graft-Versus-Host-Disease Immunol. Pathophysiol. Treat.* (eds. Burakoff, S. J., Deeg, H. J., Ferrara, J. L. M. & Atkinson, K.) 403–413 (Marcel Dekker, 1990).

197. Nestel, F. P., Price, K. S., Seemayer, T. A. & Lapp, W. S. Macrophage priming and lipopolysaccharide-triggered release of tumor necrosis factor alpha during graft-versus-host disease. *J. Exp. Med.* **175,** 405–13 (1992).

198. Masopust, D. & Schenkel, J. M. The integration of T cell migration, differentiation and function. *Nat. Rev. Immunol.* **13,** 309–20 (2013).

199. Sprent, J. Antigen-Presenting Cells: Professionals and amateurs. *Curr. Biol.* **5,** 1095–1097 (1995).

200. Rescigno, M. Functional specialization of antigen presenting cells in the gastrointestinal tract. *Curr. Opin. Immunol.* **22,** 131–6 (2010).

201. Hershberg, R. M. *et al.* Highly polarized HLA class II antigen processing and presentation by human intestinal epithelial cells. *J. Clin. Invest.* **102,** 792–803 (1998).

202. Hershberg, R. M. & Mayer, L. F. Antigen processing and presentation by intestinal epithelial cells - polarity and complexity. *Immunol. Today* **21,** 123–8 (2000).

203. Steinman, R. M. & Cohn, Z. A. Identification of a novel cell type in peripheral lymphoid organs of mice. I. Morphology, quantitation, tissue distribution. *J. Exp. Med.* **137,** 1142–62 (1973).

204. Jung, S. *et al.* In vivo depletion of CD11c+ dendritic cells abrogates priming of CD8+ T cells by exogenous cell-associated antigens. *Immunity* **17,** 211–20 (2002).

205. Tian, T., Woodworth, J., Sköld, M. & Behar, S. M. In vivo depletion of CD11c+ cells delays the CD4+ T cell response to Mycobacterium tuberculosis and exacerbates the outcome of infection. *J. Immunol.* **175,** 3268–72 (2005).

206. Kassim, S. H., Rajasagi, N. K., Zhao, X., Chervenak, R. & Jennings, S. R. In vivo ablation of CD11c-positive dendritic cells increases susceptibility to herpes simplex virus type 1 infection and diminishes NK and T-cell responses. *J. Virol.* **80,** 3985–93 (2006).

207. Sertl, K. *et al.* Dendritic cells with antigen-presenting capability reside in airway epithelium, lung parenchyma, and visceral pleura. *J. Exp. Med.* **163,** 436–51 (1986).

208. Mora, J. R. *et al.* Selective imprinting of gut-homing T cells by Peyer's patch dendritic cells. *Nature* **424,** 88–93 (2003).

209. Pasparakis, M., Haase, I. & Nestle, F. O. Mechanisms regulating skin immunity and inflammation. *Nat. Rev. Immunol.* **14,** 289–301 (2014).

210. Trombetta, E. S. & Mellman, I. Cell biology of antigen processing in vitro and in vivo. *Annu. Rev. Immunol.* **23,** 975–1028 (2005).

211. Blum, J. S., Wearsch, P. A. & Cresswell, P. Pathways of antigen processing. *Annu. Rev. Immunol.* **31,** 443–73 (2013).

212. Mellman, I. & Steinman, R. M. Dendritic Cells. *Cell* **106,** 255–258 (2001).

213. Bevan, M. J. Cross-priming for a secondary cytotoxic response to minor H antigens with H-2 congenic cells which do not cross-react in the cytotoxic assay. *J. Exp. Med.* **143,** 1283–8 (1976).

214. Hoeffel, G. *et al.* Antigen crosspresentation by human plasmacytoid dendritic cells. *Immunity* **27,** 481–92 (2007).

215. Platzer, B., Stout, M. & Fiebiger, E. Antigen cross-presentation of immune complexes. *Front. Immunol.* **5,** 140 (2014).

216. Savina, A. *et al.* NOX2 controls phagosomal pH to regulate antigen processing during crosspresentation by dendritic cells. *Cell* **126,** 205–18 (2006).

217. Savina, A. *et al.* The small GTPase Rac2 controls phagosomal alkalinization and antigen crosspresentation selectively in CD8(+) dendritic cells. *Immunity* **30,** 544–55 (2009).

218. Nierkens, S., Tel, J., Janssen, E. & Adema, G. J. Antigen cross-presentation by dendritic cell subsets: one general or all sergeants? *Trends Immunol.* **34,** 361–70 (2013).

219. Janeway, C. A. & Medzhitov, R. Innate immune recognition. *Annu. Rev. Immunol.* **20,** 197–216 (2002).

220. Hawiger, D. *et al.* Dendritic cells induce peripheral T cell unresponsiveness under steady state conditions in vivo. *J. Exp. Med.* **194,** 769–79 (2001).

221. Dalod, M. *et al.* Interferon alpha/beta and interleukin 12 responses to viral infections: pathways regulating dendritic cell cytokine expression in vivo. *J. Exp. Med.* **195,** 517–28 (2002).

222. Maldonado, R. A. & von Andrian, U. H. How tolerogenic dendritic cells induce regulatory T cells. *Adv. Immunol.* **108,** 111–65 (2010).

223. Förster, R., Braun, A. & Worbs, T. Lymph node homing of T cells and dendritic cells via afferent lymphatics. *Trends Immunol.* **33,** 271–80 (2012).

224. Tang, A., Amagai, M., Granger, L. G., Stanley, J. R. & Udey, M. C. Adhesion of epidermal Langerhans cells to keratinocytes mediated by E-cadherin. *Nature* **361,** 82–5 (1993).

225. Jiang, A. *et al.* Disruption of E-cadherin-mediated adhesion induces a functionally distinct pathway of dendritic cell maturation. *Immunity* **27,** 610–24 (2007).

226. Hemann, E. A. & Legge, K. L. Peripheral regulation of T cells by dendritic cells during infection. *Immunol. Res.* **59,** 66–72 (2014).

227. Bennett, C. L. & Chakraverty, R. Dendritic cells in tissues: in situ stimulation of immunity and immunopathology. *Trends Immunol.* **33,** 8–13 (2012).

228. Legge, K. L. & Braciale, T. J. Accelerated migration of respiratory dendritic cells to the regional lymph nodes is limited to the early phase of pulmonary infection. *Immunity* **18,** 265–77 (2003).

229. Bennett, C. L. *et al.* Langerhans cells regulate cutaneous injury by licensing CD8 effector cells recruited to the skin. *Blood* **117,** 7063–7069 (2011).

230. Eidsmo, L. *et al.* Differential migration of epidermal and dermal dendritic cells during skin infection. *J. Immunol.* **182,** 3165–72 (2009).

231. GeurtsvanKessel, C. H. *et al.* Clearance of influenza virus from the lung depends on migratory langerin+CD11b- but not plasmacytoid dendritic cells. *J. Exp. Med.* **205,** 1621–34 (2008).

232. Mitamura, T. *et al.* Structure-function analysis of the diphtheria toxin receptor toxin binding site by site-directed mutagenesis. *J. Biol. Chem.* **272,** 27084–90 (1997).

233. Saito, M. *et al.* Diphtheria toxin receptor-mediated conditional and targeted cell ablation in transgenic mice. *Nat. Biotechnol.* **19,** 746–50 (2001).

234. McGill, J. & Legge, K. L. Cutting edge: contribution of lung-resident T cell proliferation to the overall magnitude of the antigen-specific CD8 T cell response in the lungs following murine influenza virus infection. *J. Immunol.* **183,** 4177–81 (2009).

235. Roberts, A. D. & Woodland, D. L. Cutting edge: effector memory CD8+ T cells play a prominent role in recall responses to secondary viral infection in the lung. *J. Immunol.* **172,** 6533–7 (2004).

236. Moyron-Quiroz, J. E. *et al.* Persistence and responsiveness of immunologic memory in the absence of secondary lymphoid organs. *Immunity* **25,** 643–54 (2006).

237. McGill, J., Van Rooijen, N. & Legge, K. L. IL-15 trans-presentation by pulmonary dendritic cells promotes effector CD8 T cell survival during influenza virus infection. *J. Exp. Med.* **207,** 521–34 (2010).

238. McGill, J., Van Rooijen, N. & Legge, K. L. Protective influenza-specific CD8 T cell responses require interactions with dendritic cells in the lungs. *J. Exp. Med.* **205,** 1635–46 (2008).

239. Dolfi, D. V *et al.* Dendritic cells and CD28 costimulation are required to sustain virus-specific CD8+ T cell responses during the effector phase in vivo. *J. Immunol.* **186,** 4599–608 (2011).

240. Iijima, N., Mattei, L. M. & Iwasaki, A. Recruited inflammatory monocytes stimulate antiviral Th1 immunity in infected tissue. *Proc. Natl. Acad. Sci. U. S. A.* **108,** 284–9 (2011).

241. Weber, C. *et al.* CCL17-expressing dendritic cells drive atherosclerosis by restraining regulatory T cell homeostasis in mice. *J. Clin. Invest.* **121,** 2898–910 (2011).

242. Huang, L.-R. *et al.* Intrahepatic myeloid-cell aggregates enable local proliferation of CD8(+) T cells and successful immunotherapy against chronic viral liver infection. *Nat. Immunol.* **14,** 574–83 (2013).

243. Heymann, F. *et al.* Kidney dendritic cell activation is required for progression of renal disease in a mouse model of glomerular injury. *J. Clin. Invest.* **119,** 1286–97 (2009).

244. McLachlan, J. B., Catron, D. M., Moon, J. J. & Jenkins, M. K. Dendritic cell antigen presentation drives simultaneous cytokine production by effector and regulatory T cells in inflamed skin. *Immunity* **30,** 277–88 (2009).

245. Bennett, C. L. & Chakraverty, R. Dendritic cells in tissues: in situ stimulation of immunity and immunopathology. *Trends Immunol.* **33,** 8–13 (2012).

246. Nestle, F. O., Di Meglio, P., Qin, J.-Z. & Nickoloff, B. J. Skin immune sentinels in health and disease. *Nat. Rev. Immunol.* **9,** 679–91 (2009).

247. Kupper, T. S. & Fuhlbrigge, R. C. Immune surveillance in the skin: mechanisms and clinical consequences. *Nat. Rev. Immunol.* **4,** 211–22 (2004).

248. Kadunce, D. P. & Krueger, G. G. Pathogenesis of psoriasis. *Dermatol. Clin.* **13,** 723–37 (1995).

249. Galli, E. *et al.* Atopic dermatitis: molecular mechanisms, clinical aspects and new therapeutical approaches. *Curr. Mol. Med.* **3,** 127–38 (2003).

250. Ganguly, D., Haak, S., Sisirak, V. & Reizis, B. The role of dendritic cells in autoimmunity. *Nat. Rev. Immunol.* **13,** 566–77 (2013).

251. Lowes, M. A. *et al.* Increase in TNF-alpha and inducible nitric oxide synthase-expressing dendritic cells in psoriasis and reduction with efalizumab (anti-CD11a). *Proc. Natl. Acad. Sci. U. S. A.* **102,** 19057–62 (2005).

252. Zaba, L. C. *et al.* Amelioration of epidermal hyperplasia by TNF inhibition is associated with reduced Th17 responses. *J. Exp. Med.* **204,** 3183–94 (2007).

253. Romani, N., Brunner, P. M. & Stingl, G. Changing views of the role of Langerhans cells. *J. Invest. Dermatol.* **132,** 872–81 (2012).

254. Merad, M., Ginhoux, F. & Collin, M. Origin, homeostasis and function of Langerhans cells and other langerin-expressing dendritic cells. *Nat. Rev. Immunol.* **8,** 935–47 (2008).

255. Hoeffel, G. *et al.* Adult Langerhans cells derive predominantly from embryonic fetal liver monocytes with a minor contribution of yolk sac-derived macrophages. *J. Exp. Med.* **209,** 1167–81 (2012).

256. Wang, Y. *et al.* IL-34 is a tissue-restricted ligand of CSF1R required for the development of Langerhans cells and microglia. *Nat. Immunol.* **13,** 753–60 (2012).

257. Merad, M. & Manz, M. G. Dendritic cell homeostasis. *Blood* **113,** 3418–27 (2009).

258. Merad, M. *et al.* Langerhans cells renew in the skin throughout life under steady-state conditions. *Nat. Immunol.* **3,** 1135–41 (2002).

259. Malissen, B., Tamoutounour, S. & Henri, S. The origins and functions of dendritic cells and macrophages in the skin. *Nat. Rev. Immunol.* **14,** 417–28 (2014).

260. Bennett, C., Rijn, E. Van & Jung, S. Inducible ablation of mouse Langerhans cells diminishes but fails to abrogate contact hypersensitivity. *J. cell …* **169,** 569–576 (2005).

261. Schuler, G. & Steinman, R. M. Murine epidermal Langerhans cells mature into potent immunostimulatory dendritic cells in vitro. *J. Exp. Med.* **161,** 526–46 (1985).

262. Hunger, R. E. *et al.* Langerhans cells utilize CD1a and langerin to efficiently present nonpeptide antigens to T cells. *J. Clin. Invest.* **113,** 701–8 (2004).

263. Allan, R. S. *et al.* Epidermal viral immunity induced by CD8alpha+ dendritic cells but not by Langerhans cells. *Science* **301,** 1925–8 (2003).

264. Ritter, U., Meissner, A., Scheidig, C. & Körner, H. CD8 alpha- and Langerin-negative dendritic cells, but not Langerhans cells, act as principal antigen-presenting cells in leishmaniasis. *Eur. J. Immunol.* **34,** 1542–50 (2004).

265. Bobr, A. *et al.* Acute ablation of Langerhans cells enhances skin immune responses. *J. Immunol.* **185,** 4724–8 (2010).

266. Kautz-Neu, K. *et al.* Langerhans cells are negative regulators of the anti-Leishmania response. *J. Exp. Med.* **208,** 885–91 (2011).

267. Gomez de Agüero, M. *et al.* Langerhans cells protect from allergic contact dermatitis in mice by tolerizing CD8(+) T cells and activating Foxp3(+) regulatory T cells. *J. Clin. Invest.* **122,** 1700–11 (2012).

268. Igyártó, B. Z. *et al.* Skin-resident murine dendritic cell subsets promote distinct and opposing antigen-specific T helper cell responses. *Immunity* **35,** 260–72 (2011).

269. Ouchi, T. *et al.* Langerhans cell antigen capture through tight junctions confers preemptive immunity in experimental staphylococcal scalded skin syndrome. *J. Exp. Med.* **208,** 2607–13 (2011).

270. Bennett, C. L. & Clausen, B. E. DC ablation in mice: promises, pitfalls, and challenges. *Trends Immunol.* **28,** 525–31 (2007).

271. Geissmann, F. *et al.* Development of monocytes, macrophages, and dendritic cells. *Science* **327,** 656–61 (2010).

272. Bursch, L. S. *et al.* Identification of a novel population of Langerin+ dendritic cells. *J. Exp. Med.* **204,** 3147–56 (2007).

273. Ginhoux, F. *et al.* Blood-derived dermal langerin+ dendritic cells survey the skin in the steady state. *J. Exp. Med.* **204,** 3133–46 (2007).

274. Poulin, L. F. *et al.* The dermis contains langerin+ dendritic cells that develop and function independently of epidermal Langerhans cells. *J. Exp. Med.* **204,** 3119–31 (2007).

275. Nagao, K. *et al.* Murine epidermal Langerhans cells and langerin-expressing dermal dendritic cells are unrelated and exhibit distinct functions. *Proc. Natl. Acad. Sci. U. S. A.* **106,** 3312–7 (2009).

276. Henri, S. *et al.* CD207+ CD103+ dermal dendritic cells cross-present keratinocyte-derived antigens irrespective of the presence of Langerhans cells. *J. Exp. Med.* **207,** 189–206 (2010).

277. Bedoui, S. *et al.* Cross-presentation of viral and self antigens by skin-derived CD103+ dendritic cells. *Nat. Immunol.* **10,** 488–95 (2009).

278. Stoitzner, P. *et al.* Langerhans cells cross-present antigen derived from skin. *Proc. Natl. Acad. Sci. U. S. A.* **103,** 7783–8 (2006).

279. Sung, S.-S. J. *et al.* A major lung CD103 (alphaE)-beta7 integrin-positive epithelial dendritic cell population expressing Langerin and tight junction proteins. *J. Immunol.* **176,** 2161–72 (2006).

280. Haniffa, M. *et al.* Human tissues contain CD141hi cross-presenting dendritic cells with functional homology to mouse CD103+ nonlymphoid dendritic cells. *Immunity* **37,** 60–73 (2012).

281. Mielcarek, M. *et al.* Langerhans Cell Homeostasis and Turnover After Nonmyeloablative and Myeloablative Allogeneic Hematopoietic Cell Transplantation. *Transplantation* (2014). doi:10.1097/TP.0000000000000097

282. Merad, M. *et al.* Depletion of host Langerhans cells before transplantation of donor alloreactive T cells prevents skin graft-versus-host disease. *Nat. Med.* **10,** 510–7 (2004).

283. Chakraverty, R. *et al.* An inflammatory checkpoint regulates recruitment of graft-versus-host reactive T cells to peripheral tissues. *J. Exp. Med.* **203,** 2021–31 (2006).

284. Stern, M. *et al.* Influence of donor/recipient sex matching on outcome of allogeneic hematopoietic stem cell transplantation for aplastic anemia. *Transplantation* **82,** 218–26 (2006).

285. Sykes, M., Bukhari, Z. & Sachs, D. H. Graft-versus-leukemia effect using mixed allogeneic bone marrow transplantation. *Bone Marrow Transplant.* **4,** 465–74 (1989).

286. Flutter, B. *et al.* Nonhematopoietic antigen blocks memory programming of alloreactive CD8+ T cells and drives their eventual exhaustion in mouse models of bone marrow transplantation. *J. Clin. Invest.* **120,** 3855–68 (2010).

287. Gunzer, M., Weishaupt, C., Planelles, L. & Grabbe, S. Two-step negative enrichment of CD4+ and CD8+ T cells from murine spleen via nylon wool adherence and an optimized antibody cocktail. *J. Immunol. Methods* **258,** 55–63 (2001).

288. Truett, G. E. *et al.* Preparation of PCR-quality mouse genomic DNA with hot sodium hydroxide and tris (HotSHOT). *Biotechniques* **29,** 52, 54 (2000).

289. Abdi, R., Means, T. K. & Luster, A. D. Chemokines in islet allograft rejection. *Diabetes. Metab. Res. Rev.* **19,** 186–90

290. Chakraverty, R. *et al.* The host environment regulates the function of CD8+ graft-versus-host-reactive effector cells. *J. Immunol.* **181,** 6820–8 (2008).

291. Reich, M. *et al.* GenePattern 2.0. *Nat. Genet.* **38,** 500–1 (2006).

292. Subramanian, A. *et al.* Gene set enrichment analysis: a knowledge-based approach for interpreting genome-wide expression profiles. *Proc. Natl. Acad. Sci. U. S. A.* **102,** 15545–50 (2005).

293. Helft, J. & Merad, M. Isolation of cutaneous dendritic cells. *Methods Mol. Biol. Clift. Nj* **595,** 231–233 (2010).

294. Kitano, Y. & Okada, N. Separation of the epidermal sheet by dispase. *Br. J. Dermatol.* **108,** 555–60 (1983).

295. Stutte, S., Jux, B., Esser, C. & Förster, I. CD24a expression levels discriminate Langerhans cells from dermal dendritic cells in murine skin and lymph nodes. *J. Invest. Dermatol.* **128,** 1470–5 (2008).

296. Koopman, G. *et al.* Annexin V for flow cytometric detection of phosphatidylserine expression on B cells undergoing apoptosis. *Blood* **84,** 1415–20 (1994).

297. Schön, M. P. & Schön, M. Imiquimod: mode of action. *Br. J. Dermatol.* **157 Suppl ,** 8–13 (2007).

298. Chow, A., Toomre, D., Garrett, W. & Mellman, I. Dendritic cell maturation triggers retrograde MHC class II transport from lysosomes to the plasma membrane. *Nature* **418,** 988–94 (2002).

299. Chorro, L. *et al.* Langerhans cell (LC) proliferation mediates neonatal development, homeostasis, and inflammation-associated expansion of the epidermal LC network. *J. Exp. Med.* **206,** 3089–100 (2009).

300. Gorczyca, W. *et al.* Immunophenotypic pattern of myeloid populations by flow cytometry analysis. *Methods Cell Biol.* **103,** 221–66 (2011).

301. Mayerova, D., Parke, E. A., Bursch, L. S., Odumade, O. A. & Hogquist, K. A. Langerhans cells activate naive self-antigen-specific CD8 T cells in the steady state. *Immunity* **21,** 391–400 (2004).

302. Strid, J. *et al.* Acute upregulation of an NKG2D ligand promotes rapid reorganization of a local immune compartment with pleiotropic effects on carcinogenesis. *Nat. Immunol.* **9,** 146–54 (2008).

303. Vantourout, P. & Hayday, A. Six-of-the-best: unique contributions of γδ T cells to immunology. *Nat. Rev. Immunol.* **13,** 88–100 (2013).

304. Henri, S. *et al.* Disentangling the complexity of the skin dendritic cell network. *Immunol. Cell Biol.* **88,** 366–75 (2010).

305. Wang, W. *et al.* Human H-Y: a male-specific histocompatibility antigen derived from the SMCY protein. *Science (80-.).* **269,** 1588–1590 (1995).

306. Miklos, D. B. *et al.* Antibody responses to H-Y minor histocompatibility antigens correlate with chronic graft-versus-host disease and disease remission. *Blood* **105,** 2973–8 (2005).

307. Chakraverty, R., Eom, H. & Sachs, J. MHC class II+ antigen-presenting cells and CD4 cells are required for CD8-mediated graft-versus-leukemia responses following delayed donor leukocyte infusions. *Blood* **108,** 2106–2113 (2006).

308. Abuzakouk, M., Feighery, C. & O'Farrelly, C. Collagenase and Dispase enzymes disrupt lymphocyte surface molecules. *J. Immunol. Methods* **194,** 211–216 (1996).

309. Yang, Y.-G., Wang, H., Asavaroengchai, W. & Dey, B. R. Role of Interferon-gamma in GVHD and GVL. *Cell. Mol. Immunol.* **2,** 323–9 (2005).

310. Toubai, T., Mathewson, N. & Reddy, P. The role of dendritic cells in graft-versus-tumor effect. *Front. Immunol.* **5,** 66 (2014).

311. Kim, B. S. *et al.* Keratinocytes function as accessory cells for presentation of endogenous antigen expressed in the epidermis. *J. Invest. Dermatol.* **129,** 2805–17 (2009).

312. Masopust, D. *et al.* Dynamic T cell migration program provides resident memory within intestinal epithelium. *J. Exp. Med.* **207,** 553–64 (2010).

313. Wang, J. & Fu, Y.-X. The role of LIGHT in T cell-mediated immunity. *Immunol. Res.* **30,** 201–14 (2004).

314. Le Bon, A. *et al.* Cross-priming of CD8+ T cells stimulated by virus-induced type I interferon. *Nat. Immunol.* **4,** 1009–15 (2003).

315. Fuertes, M. B. *et al.* Host type I IFN signals are required for antitumor CD8+ T cell responses through CD8{alpha}+ dendritic cells. *J. Exp. Med.* **208,** 2005–16 (2011).

316. Robb, R. J. & Hill, G. R. The interferon-dependent orchestration of innate and adaptive immunity after transplantation. *Blood* **119,** 5351–8 (2012).

317. Duffner, U. *et al.* Role of CXCR3-induced donor T-cell migration in acute GVHD. *Exp. Hematol.* **31,** 897–902 (2003).

318. Croudace, J. E. *et al.* Chemokine-mediated tissue recruitment of CXCR3+ CD4+ T cells plays a major role in the pathogenesis of chronic GVHD. *Blood* **120,** 4246–55 (2012).

319. Lantz, O., Grandjean, I., Matzinger, P. & Di Santo, J. P. Gamma chain required for naïve CD4+ T cell survival but not for antigen proliferation. *Nat. Immunol.* **1,** 54–8 (2000).

320. Heath, W. R. & Carbone, F. R. The skin-resident and migratory immune system in steady state and memory: innate lymphocytes, dendritic cells and T cells. *Nat. Immunol.* **14,** 978–85 (2013).

321. Shklovskaya, E. *et al.* Langerhans cells are precommitted to immune tolerance induction. *Proc. Natl. Acad. Sci. U. S. A.* **108,** 18049–54 (2011).

322. Gebhardt, T. *et al.* Memory T cells in nonlymphoid tissue that provide enhanced local immunity during infection with herpes simplex virus. *Nat. Immunol.* **10,** 524–30 (2009).

323. Wakim, L. M., Waithman, J., van Rooijen, N., Heath, W. R. & Carbone, F. R. Dendritic cell-induced memory T cell activation in nonlymphoid tissues. *Science* **319,** 198–202 (2008).

324. Mackay, L. K. *et al.* The developmental pathway for CD103(+)CD8+ tissue-resident memory T cells of skin. *Nat. Immunol.* **14,** 1294–301 (2013).

325. Kaplan, D. H., Jenison, M. C., Saeland, S., Shlomchik, W. D. & Shlomchik, M. J. Epidermal langerhans cell-deficient mice develop enhanced contact hypersensitivity. *Immunity* **23,** 611–20 (2005).

326. Pavelko, K. D. *et al.* Nonequivalence of classical MHC class I loci in ability to direct effective antiviral immunity. *PLoS Pathog.* **8,** e1002541 (2012).

327. Benechet, A. P., Menon, M. & Khanna, K. M. Visualizing T Cell Migration in situ. *Front. Immunol.* **5,** 363 (2014).

328. Moussion, C. & Girard, J.-P. Dendritic cells control lymphocyte entry to lymph nodes through high endothelial venules. *Nature* **479,** 542–6 (2011).

329. Benyó, Z., Gille, A., Bennett, C. L., Clausen, B. E. & Offermanns, S. Nicotinic acid-induced flushing is mediated by activation of epidermal langerhans cells. *Mol. Pharmacol.* **70,** 1844–9 (2006).

330. Mori, S., El-Baki, H. & Mullen, C. A. Analysis of immunodominance among minor histocompatibility antigens in allogeneic hematopoietic stem cell transplantation. *Bone Marrow Transplant.* **31,** 865–75 (2003).